

**Non-viral Gene Delivery of BMP-2 Plasmid from Collagen Based Scaffolds  
for Bone Regeneration Therapy**

by  
Eleni Tsekoura

A thesis submitted in partial fulfillment of the requirements for the degree of  
Doctor of Philosophy  
in  
Chemical Engineering

Department of Chemical & Materials Engineering  
University of Alberta

©Eleni Tsekoura,2020

## Abstract

Significant progress in the field of bone regeneration therapy has been achieved in the last two decades. While regeneration therapies with autogenous, allografts and exogenous grafts are remaining the preferred treatments, the outcomes remained are usually sub-optimal. Gene therapy holds a great promise for bone regeneration, since the therapeutic genes can be delivered with a plasmid DNA (pDNA) that can be designed to promote bone regeneration, or to suppress mediators that inhibit bone formation. Since the delivery of free pDNA will likely be degraded in biological fluids and may not enter the cells on its own, a delivery agent or carrier will be needed in order to secure the entry of nucleic acids into the cells. Viral and non-viral carriers are the two main categories of gene delivery systems. Although, viral vectors are still the most successful one in gene therapy, the safety concerns are eliminating their clinical applications. On the other hand, non-viral vectors like cationic polymers (Polyethylenimine (PEI)) are less like to induce immune response but are not able to enhance transfection efficiency. Herein, we explored the potential and operational conditions of using low molecular weight polyethylenimines (PEIs) substituted with lipidic moieties carriers for the delivery of pDNA to bone-related cells *in vitro*. Among the modified PEIs synthesized in our lab, thioester-linked linoleic acid (PEI-tLA) with different levels of substitution has been the most successful candidate for pDNA delivery. We first showed that PEI1.2-tLA2 efficiently delivered pDNA to primary periosteum-derived cells (PDCs) and calvarial bone-derived cells (BDCs). After validating the delivery conditions, the delivery of BMP-2 plasmid from PEI1.2-tLA2 to PDCs and BDCs successfully promoted the calcium deposition by the cells. We then explored the possibility of improving the transfection efficiency of PEI1.2-tLA carriers by supplementing the complexation with a polyaspartic acid (pASP) additive. For this exploration, we used C2C12 and MC-3T3 cells which are well characterized osteogenic cell

models. We found that PEI1.2-tLA10 was the most successful candidate for the delivery of pDNA to both cell lines and secondly that the pASP improved the transfection efficiency significantly for both cell models, but optimal conditions for the proposed delivery system differed between the cells.

The loading of complexes into scaffolds by physical adsorption, electrospinning, chemical immobilization etc. may provide not only the needed signals for bone regeneration but also the physical support for tissue growth. The incorporation of the optimized complexes for both cell lines into three different collagen-based scaffolds (uncrosslinked (native), crosslinked and 3D mineralized collagen scaffolds) showed that 3D mineralized scaffolds carrying BMP-2 plasmid/PEI-tLA10-pASP complexes, induced the ALP activity in C2C12 cells, while the collagen scaffolds carrying the optimal complexes for MC-3T3 cells where the ones that enhanced the ALP activity. Finally, the investigated the incorporation and release of the optimized complexes from mono-layer and double-layer collagen and gelatin based electrospun nanofiber mats. The delivery of complexes from mono-layered fibers with high collagen concentration to C2C12 and MC-3T3 cells had a negative impact on encapsulation and transfection efficiency, while the fabrication of double-layered scaffolds that had collagen mat as a first layer and separated from the complexes was able to induce ALP activity in C2C12 cells. Overall, we concluded that complexes containing low molecular weight modified PEI with thioester-linked linoleic acid (PEI-tLA) and pASP as an additive can effectively deliver pBMP-2 to osteogenic cells and induce desired osteogenic features in 2D cultures. In addition, the design of 3D bioactive scaffolds can further improve the osteogenic activity of the cells, so these proposed therapeutic formulations could be further used for bone regeneration applications.

## Preface

All chapters presented in this thesis have been conceptualized, researched and written by me under the supervision of Dr. Hasan Uludag. Parts of the literature and research presented in this thesis have been previously published.

**Chapter 1** contains a portion of the literature review paper published earlier, *Biomaterials to Facilitate Delivery of RNA Agents in Bone Regeneration and Repair*: Eleni K. Tsekoura, Remant Bahadur K.C. and Hasan Uludag, ACS Biomaterials Science and Engineering, 2017, vol. 3, 1195-1206. As the primary author, I was responsible for the literature review, analysis and discussion of the manuscript. Remant Bahadur K.C. contributed specifically in the section of Biomaterials carriers in intracellular RNA delivery. Some sections of Chapter 1 were also published as “*Current State of Fabrication Technologies and Materials for Bone Tissue Engineering*”, Abiy Wubneh, Eleni K. Tsekoura, Remant Bahadur K.C., Cagri Ayranci and Hasan Uludag, Acta Biomaterialia, 2018, vol. 80, 1-30. As a co-author, I contributed the section mainly related to osteogenesis and the incorporation of bioactive factors into scaffolds during fabrication in this review paper. In both cases, I included in my thesis only the sections that I wrote myself.

**Chapter 2** contains studies with periosteum and bone derived rat cells and will serve as a future manuscript. Dr. Harmanpreet Kaur (University of Alberta) helped with harvesting of the cells. Polymers were synthesized by Dr. Remant Bahadur K.C. I designed, performed, collected and analyzed the data and wrote the chapter thesis. I used a small portion of the published paper, “*Hydrophobe-substituted bPEI Derivatives: Boosting Transfection on Primary Vascular Cells*”, Danielle Pezzoli, Eleni K. Tsekoura, Remant Bahadur K.C, Gabriele Candiani, Diego Mantovani

and Hasan Uludag, Science China Materials, 2017, 60, 529-542, in this chapter. The section transferred involved size and  $\zeta$ -potential of the polyplexes.

**Chapter 3** is a research paper that will be submitted for publication in the future. The collagen scaffolds used in this chapter was part of the research collaboration with Professor Eli D. Sone from University of Toronto. Training for scaffolds synthesis and production was provided by Dr. Alex Lausch and the synthesis of additional scaffolds by Lucy Luo from University of Toronto and by me. Polymers used in this Chapter were synthesized by Dr. Remant Bahadur K.C. Aysha Ansari (PhD student in Uludag Lab) performed the RT-PCR analysis in this Chapter under my supervision. As the lead researcher, I designed, performed, analyzed and wrote the chapter thesis.

**Chapter 4** contains unpublished studies on the delivery of complexes via electrospun mats. Training on the mat fabrication via electrospinning was provided by Dr. Porntipa Pankongadisak (visiting PhD student from University of Mae Fah Luang, Thailand). This work is a continuation (no overlap) from the published work “*Electrospun Gelatin Matrices with Bioactive pDNA Complexes*”, Porntipa Pankongadisak, Eleni K.Tsekoura, Orawan Suwantong and Hasan Uludag, International Journal of Biological Macromolecules, 2020, vol.149, 296-308. Polymers used in this Chapter were synthesized by Dr. Remant Bahadur K.C. Teo Dick (PhD student in Uludag Lab) performed the SEM analysis. As the lead researcher, I contributed to the design, performance, analysis and writing of this chapter thesis.

**Chapter 5** contains unpublished literature review, overall conclusions and future studies learnt through my PhD studies. This section was conceptualized and written by myself.

## **Dedication**

**To the future me, I am looking forward to meeting you**

*Life must be lived as a play-Plato*

## Acknowledgments

My latest journey started 10 years ago when I left Greece and moved to Sweden for my Master's Degree then I moved to Ireland to work as a Research Assistant and now my adventure is coming to an end here in Canada. Completing this PhD is only the beginning of my new expedition. I can only be grateful for all the people I have met along this journey and I would like to thank each one of them for their unwavering support. I couldn't have been the person that I am today without you.

First, to my main PhD supervisor, Prof. Hasan Uludag, I am incredibly grateful for having invited me to become a member of your group and work by your side. I still remember your question during one of our first Skype calls, "Are you sure that you can survive the Canadian winter?" "Of course! I can survive anywhere!" and I survived not only the winters but also several rough times. Thank you so much for all your support and understanding.

To my supervisor committee members, I am very glad that I had you by my side, guiding me through these years. I would like to extend my thanks to all the funding agencies that have supported me during my doctoral studies, particularly NSERC CREATE Program for granting two years of my Graduate Studentship.

To my previous supervisors that supported my decision to move to Canada and for helping me during my first years in this field, Dr. K. Welch (Uppsala University) and Dr. D. Zeugolis (NUI Galway), you were great mentors.

To my lab mates (former and present): First, my two amazing ladies: Deniz and Juli, thank you so much girls for all your support and friendship (and your partners of course) all these years. I miss you so much but at the same time, I am so happy for where life brought you. Then, there is my

dear Cezy followed by Remant, Bindu, Anyeld, Teo, Amp, Affy, Beste, Haiming, Yousef, Herman, Aysha, Mahsa, Manoj and Daniel. Guys, thank you for everything. I wouldn't have asked for better lab mates and friends. Wishing each one of you a happy life.

To all of my U of A colleagues and TA mates of the MATE 202 course, thank you all for the great collaborations all these years. You made my PhD student life more exciting.

To all my friends around the world, Angeliki & George, Spiro & Aranza, (Sweden), Dani (Italy), Alexandra (USA), Ayelen, Ermi, Silvia & Panos S. (UK), Vasso, Panos K., Argiroula, Anta, Georgia & Katerina (Greece), and of course, my best friend Panagiotis Ntaikos, thank you all for your friendship all these years. I know I am so far away from one another and we don't talk very often but I've never forgotten our moments together. I hope at some point, life will bring us closer and if not then let's continue to make it work.

To my family in Greece: Μπαμπά & Μαμά μου, δεν θα μπορούσα να σας ξεχωρίσω, γιατί για μένα είσατε αυτοί οι δύο ξεχωριστοί άνθρωποι που αποκαλώ γονείς. Δεν ξέρω πως να εκφράσω με λόγια την αγάπη μου για εσάς. Σας αγαπώ πολύ με τον δικό μου μοναδικό τρόπο. Δεν ήταν εύκολο αυτό το ταξίδι αλλά με τον έναν ή με τον άλλον τρόπο, ήσασταν εδώ όταν σας χρειαζόμουν. Σας ευχαριστώ πάρα πολύ για όλα. Ηλία μου, αδελφούλη μου, δυστυχώς, δεν έχουμε ζήσει πολλές στιγμές μαζί. Σ' ευχαριστώ όμως που βρίσκεσαι δίπλα στο πλευρό της μαμάς και της γιαγιάς. Γιαγιά μου Μαρία, δεν ξέρω πως να σε ευχαριστήσω για όλα όσα μου έχεις προσφέρει όλα αυτά τα χρόνια και είναι πολλά. Δυστυχώς, Γιαγιά μου Ελένη, έφυγες από την ζωή λίγο πριν με δεις να παίρνω το πτυχίο μου. Δεν ξέρω πως να εκφράσω το πόσο πολύ μου λείπεις και πόσο θα ήθελα να σε ξαναδώ. Θα είσαι πάντα μέσα στην καρδιά μου. Στην καρδιά μου είσαι και εσύ Κώστα μου, που δυστυχώς μας άφησες νωρίς αλλά θέλω να πιστεύω πως ίσως με βλέπεις από εκεί ψηλά. Χρηστάκο μου, ξαδερφάκι μου, πάντα βρίσκεις έναν τρόπο να βρισκόμαστε.

Περιμένω να κανονίσουμε το επόμενο ταξίδι μας. Τέλος, Θεία Λιλή και Παρή μου, σας ευχαριστώ που απλά ομορφαίνετε την ζωή μου. Όλους εσάς και όσους δεν ανέφερα, σας ευχαριστώ που είστε οικογένεια μου. Σας αγαπώ.

Finally, to my friends and family in Edmonton: Edmonton would never have felt like home if I didn't have all of you in my life. First, a big thank you to my roommate Mamie. You are my first and last roommate, lady. Thank you for everything. Thank you for taking care of me, may be more than I did sometimes. Thank you for being you. You are an amazing person. Do not stop dreaming. Natasa & Zinon, I can not express with words my appreciation for whatever you have done for me all these years. You made me feel like a member of your family from the very first moment. Jo mou, my crazy British-Greek friend, who would have thought that back in 2015 when you were looking for Venus, you would have found a friend for life. Thank you for being you, with your own unique way. Angeliki mou, distance brought us closer. Thank you for being my best friend these last couple of years, I miss you so much fili mou. Thank you for listening to me, for your support and non-stop chats over the phone. I wish you all the best in Norway, you deserve it. Last but definitely not least, Kosta mou. How can words describe how I feel about you? Our lives brought us close to each other more than once but finally Edmonton was meant to be our meeting point. I never expected to meet a person who can love with no limits, a person who loves life as you do. Our friendship is like a roller coaster with lots of laughs and cries. I am embracing every moment, feeling and looking forward to seeing what life will bring to us (#alwaysbyyourside). To all of you, you are not just my friends, you are my family.

Thank you all- Σας ευχαριστώ όλους

## Table of Contents

Chapter 1- The process of bone regeneration and the current therapies in the bone tissue engineering field .....	1
1.1 Background.....	2
1.2 Cellular Component of Bone .....	3
1.2.1. Mesenchymal Stem Cells (MSCs) .....	3
1.2.2 Osteoblasts .....	4
1.2.3 Osteocytes .....	7
1.2.4 Osteoclasts .....	8
1.3 Extracellular Matrix (ECM) Component of Bone .....	10
1.3.1 Marrow stroma.....	10
1.3.2 Endosteum.....	11
1.3.3 Periosteum.....	11
1.4 Main Growth Factors Involved in Bone Physiology.....	11
1.4.1 The transforming growth factor-beta family (TGF- $\beta$ ) .....	12
1.4.2 Bone morphogenetic proteins (BMPs).....	12
1.4.3 Fibroblast Growth Factors (FGFs).....	14
1.4.4 Vascular Endothelial Growth Factor (VEGF).....	15
1.4.5 Insulin-like Growth Factors (IGF) .....	15
1.4.6 Platelet-Derived Growth Factors (PDGF).....	16
1.5 Osteogenesis .....	16
1.6 Bone Fracture Healing .....	19
1.7 Technology of Current Therapies for Bone Regeneration and Emerging Gene Therapy.....	20
1.7.1 Incorporation of GFs into Scaffolds.....	31
1.7.2 Biomaterial Carriers in Intracellular DNA Delivery.....	22
1.8 Scaffolds in Bone Regeneration.....	34
1.8.1 Collagen as the Foundation of a Biomimetic Scaffold .....	35
1.8.2 Fabrication of Collagen Scaffolds.....	42
1.8.3 Chemical Crosslinking of Collagen Scaffolds .....	37
1.8.4 Presence of Hydroxyapatite .....	44
1.8.5 Mechanical Properties of Scaffolds .....	45

1.8.6	Recombinant Collagen as a Replacement for Purified Collagen .....	47
	Thesis Scope .....	48
	Chapter 2- In Vitro Modification of Rat Skull Periosteum and Bone Derived Cells Using Non-Viral Polyplexes .....	52
2.1	Introduction.....	53
2.2	Materials and Methods.....	55
2.2.1	Materials .....	55
2.2.2	Isolation of Cells and Cell Culture.....	55
2.2.3	Polymeric Carriers .....	56
2.2.4	Physicochemical Characterization .....	56
2.2.5	Carrier Screening for Transfection of Cells and Quantitative Analysis of Transfection .....	56
2.2.6	Cytotoxicity Assay.....	57
2.2.7	Osteogenic Activity of Transfected Cells .....	58
2.2.8	Statistical Analysis.....	59
2.3	Results.....	59
2.3.1	Initial Screening of Polymers.....	59
2.3.2	Cytotoxicity of Polymer/pDNA Complexes .....	62
2.3.3	Transfection Efficiency of Plasmid/Polymer Complexes .....	63
2.3.4	ALP Activity of BMP-2 and PDGF Treated Cells.....	64
2.3.5	Calcification of BMP-2 and PDGF Treated Cells.....	65
2.4	Discussion.....	66
2.5	Conclusions.....	69
	Chapter 3- pDNA Delivery using Polyaspartic Acid Supplemented Low MW PEI Polyplexes via Collagen Scaffolds .....	70
3.1	Introduction.....	71
3.2	Materials & Methods .....	74
3.2.1	Materials .....	74
3.2.2	Cell Culture.....	74
3.2.3	Library Screen for Polymeric Carriers.....	75
3.2.4	Transfection Experiments on Tissue Culture Plastic .....	75
3.2.5	Cytotoxicity Assay.....	76

3.2.6	Alkaline Phosphatase (ALP) Activity.....	76
3.2.7	Polymerase Chain Reaction (RT-qPCR) Analysis.....	77
3.2.8	Delivery of Polyplexes from Collagen Scaffolds.....	78
3.2.8.1	Scaffolds preparation.....	78
3.2.8.2	Evaluation of Cell Growth in Collagen scaffolds.....	78
3.2.8.3	Observation genes in Collagen scaffolds.....	79
3.2.8.4	Transfection with Gene-activated Collagen Scaffolds.....	79
3.2.8.5	Osteogenic Activity from Gene Activated Collagen Scaffolds.....	80
3.2.9	Statistical Analysis.....	81
3.3	Results.....	81
3.3.1	Polymer Screening.....	81
3.3.2	Effect of Polymer:pDNA Ratio and pASP on Polyplex Size and Zeta-potential.....	84
3.3.3	Transfection Efficiency with C2C12 & MC-3TC cells.....	85
3.3.4	Assessment of Cytotoxicity of Complexes.....	92
3.3.5	ALP Activity on Tissue Culture Polystyrene.....	94
3.3.6	qPCR for Osteogenic Markers in MC-3T3.....	98
3.3.7	Growth of cells in mineralized collagen scaffolds.....	98
3.3.7.1	Observation of genes in Collagen scaffolds.....	99
3.3.7.2	Transfection efficiency in gene-activated scaffolds.....	101
3.3.7.3	ALP activity in gene activated scaffolds.....	102
3.4	Discussion.....	104
3.5	Conclusions.....	108
Chapter 4- Delivery of particles via collagen/gelatin fibers in C2C12 and MC-3T3 cells.....		110
4.1	Introduction.....	111
4.2	Materials & Methods.....	113
4.2.1	Materials.....	113
4.2.2	Preparation of complexes.....	114
4.2.3	Fabrication of gene-activated electrospun mats.....	114
4.2.3.1	Monolayer mats.....	114
4.2.3.2	Double-layered mats.....	115
4.2.4	Characterization of gene-activated electrospun mats.....	115
4.2.5	Cell culture.....	116

4.2.6	Transfection efficiency of gene activated matrices.....	116
4.2.7	Delivery of BMP-2 plasmid from gene activated matrices.....	117
4.3.1	SEM imaging of gene-activated matrices .....	119
4.3.2	Delivery of Cy3 loaded complexes via mats.....	121
4.3.3	Particle size and charge analysis.....	121
4.3.4	Transfection efficiency .....	122
4.3.5	Double-layer vs. Monolayer Mats .....	125
4.4.	Discussion.....	130
4.5.	Conclusions.....	135
Chapter 5-	Overall Conclusions and Future Considerations.....	136
5.1	Overall Thesis Conclusions and Discussion .....	137
5.2	Further Discussion and Future Considerations .....	147
5.2.1	Enhanced osteogenic activity of primary cells through a 3D system .....	147
5.2.2	Treatment of bone defects in animal models .....	149
5.2.3	RNA delivery as an alternative to pDNA therapy for bone regeneration .....	149
References.....		152
Appendix.....		170
Supplementary information for Chapter 4 .....		171
Supplementary information for Chapter 5 .....		173

## List of Tables

### Chapter 1

Table 1.1. Specific miRNAs involved in osteogenesis <i>in vitro</i> . .....	24
Table 1.2. Specific miRNAs involved in bone repair <i>in vivo</i> . .....	25
Table 1.3. Specific siRNA targets involved in osteogenesis <i>in vitro</i> . .....	26
Table 1.4. Specific siRNA targets employed for bone repair in animal models. ....	26
Table 1.5. Various processing conditions used for generating functional collagen-based scaffolds. ....	39

### Chapter 2

Table 2.1. Summary of the transfection efficiency of various polymers on PDCs and BDCs. ....	60
--	----

### Chapter 3

Table 3.1. Size and $\zeta$ -potential of pDNA/PEI1.2-tLA10 complexes with and without pASP additive. ....	84
--	----

### Chapter 4

Table 4.1. Average fiber diameters and bead size of electrospun mats without and with pDNA complexes. ....	120
Table 4.2. Size and $\zeta$ -potential of original free particles and particles released from the different Gel-Col-PEG mats. ....	122

### Chapter 5

Table 5.1. Delivery of gene therapeutics via viral carriers in animal models in the last 5 years. ....	138
Table 5.2. Delivery of gene therapeutics via non-viral carriers <i>in vitro</i> in the last 5 years. ....	140
Table 5.3. Delivery of gene therapeutics via non-viral carriers in animal models. ....	142

## List of Schemes

### Chapter 2

Scheme 2.1. Reaction scheme for the synthesis of PEI1.2 and PEI2 derivatives substituted with StA, LA, $\alpha$ LA, PrA and tLA. ....	60
---	----

### Chapter 3

Scheme 3.1. (A) Reaction scheme for the synthesis of lipid-substituted PEIs. ....	82
---	----

# List of Figures

## Chapter 1

Figure 1.1. Cell signaling pathways (Wnt, BMP-2 and TGF- $\beta$ ) activated in osteogenic differentiation of MSCs into osteoblasts.....	5
Figure 1.2. Chemical structure of cationic lipids and schematic of targeted NP preparation of described in this review. ....	29
Figure 1.3. miRNA concentrations (nM in horizontal axis) delivered by non-viral carriers <i>in vitro</i> and <i>in vivo</i> . ....	31

## Chapter 2

Figure 2.1. Size and $\zeta$ -potential of synthesized complexes at different polymer/pDNA ratios....	61
Figure 2.2. Cell toxicity of complexes in PDCs (left) and BDCs (right) at different polymer/pDNA ratios as assessed by the MTT assay.....	62
Figure 2.3. Transfection efficiency of the complexes in PDCs (Ai-Aii) and BDCs (Bi-Bii) as determined by flowcytometry.....	64
Figure 2.4. Effect of BMP-2 and PDGF complexes with PEI1.2-tLA2 on osteogenic differentiation.....	65
Figure 2.5. Calcium content of PDCs (left) and BDCs (right) following treatment with gWIZ, BMP-2, PDGF or BMP-2/PDGF complexes formed with PEI1.2-tLA2.....	66

## Chapter 3

Figure 3.1. Polymer library screening for GFP transfection.....	83
Figure 3.2. The mean fluorescence intensity/cell (i) and GFP-positive population (ii) in C2C12 as analyzed 48 h post-transfection. ....	88
Figure 3.3. The mean fluorescence intensity per cell (i) and GFP-positive population (ii) in MC-3T3 as analyzed 48 h post transfection. ....	91
Figure 3.4. Viability of C2C12 cells incubated with complexes containing different pDNA concentrations. ....	92
Figure 3.5. Viability of MC-3TC incubated with complexes containing different DNA concentrations. ....	93
Figure 3.6. Osteogenic activity (ALP induction) in C2C12 cells after delivery of gWIZ and gWIZ-BMP-2 complexes.....	95
Figure 3.7. ALP induction in MC-3T3 cells after delivery of gWIZ and gWIZ-BMP-2 complexes. ....	96
Figure 3.8. 'Net' ALP induction in MC-3T3 cells after delivery of gWIZ and gWIZ-BMP-2 complexes. ....	97
Figure 3.9. The expression levels of osteogenic marker genes in MC-3T3 was analyzed by PCR. ....	98
Figure 3.10. The viability of C2C12 (A) and MC-3T3 (B) cells cultured on mineralized collagen scaffolds. ....	99
Figure 3.11. The presence of complexes in collagen, X-linked collagen and 3d mineralized scaffolds was determined with SEM (scale bars 10 and 1 $\mu$ m). ....	100
Figure 3.12. Transfection efficiency of PEI 1.2-tLA10-pGFP delivered to C2C12 cells via collagen, X-linked collagen and 3d mineralized scaffolds. ....	101

Figure 3.13. The ALP activity was evaluated by delivering pBMP-2 to C2C12 (A) and MC-3T3 (B) cells via collagen, X-linked collagen and 3d mineralized scaffolds for 1, 2 and 3 weeks. .. 103

#### Chapter 4

Figure 4.1. SEM images of different volume ratio Gel-Col-PEG electrospun fibers with and without complexes (scale bars 10 and 1 $\mu\text{m}$ ). .....	121
Figure 4.2. Fluorescence microscopy images of mats with Cy3 labeled pDNA complexes. ....	121
Figure 4.3. Delivery of gWIZ-GFP complexes via different volume ratio Gel-Col-PEG mats to C2C12 (A) and MC-3T3 (B) cells. ....	123
Figure 4.4. The GFP-positive population and mean fluorescence intensity/cell in C2C12 (Ai-ii) and MC3T3 (Bi-ii) cells analyzed 48 h post-transfection by flow cytometry. ....	125
Figure 4.5. Experimentally observed the morphology of double layered fibers and the delivery of Cy3 and GFP labeled DNAs by them. ....	127
Figure 4.6. ALP induction in C2C12 cells (A) and in MC3T3-E1 (B) cells after delivery of gWIZ-BMP-2 complexes from different Gel-Col-PEG monolayer mats and double-layered mats 7 days post transfection. ....	129

#### Chapter 5

Figure 5.1. Schematic diagram of non-viral delivery of pDNA related to bone formation and the concentrations ( $\mu\text{g}/\text{scaffold}$ in horizontal axis) that have been used in the <i>in vitro</i> (A) and <i>in vivo</i> (B) studies. ....	143
--	-----

#### Appendix

Figure 3.S 1. SEM images of 3 days and 6 days intrafibrillar mineralized scaffolds.....	170
Figure 4.S 1. Correlation function and size distribution of particles released from different volume ratio Gel-Col-PEG mats (A-D) in comparison to mats without particles.....	172
Figure 5.S1. The expression levels of osteogenic genes in MC-3T3 and hBMSCs were analyzed by PCR.....	173
Figure 5.S2. ‘Net’ ALP induction in MC-3T3 (A) and hBMSCs (B) cells after delivery of gWIZ and gWIZ-BMP-2 complexes. ....	174

## List of Abbreviations

AMP	2-amino-2-methyl-propan-1-ol
ACAN	Aggrecan
ADSC	Adipose Derived Stem Cells
ALP	Alcaline Phosphatase assay
aLA	alpha Linoleic Acid
Arg	Arginine
AA	Ascorbic Acid
Asp	Aspartic Acid
AD-MSCs	Autologous adipose tissue Derived MSCs (AD-MSCs)
bFGF	Basic fibroblast growth factor
$\beta$ -TCP	Beta-tricalcium phosphate
BDCs	Bone Derived Cells
BM	Bone Marrow
BMP-2	Bone Morphogenetic Protein-2
BMSCs	Bone Marrow Stem Cells
cmRNA	chemically modified RiboNucleic Acids
COL	Collagen
COL1A1	Collagen type 1
CAD	Computer Aided Design
CT	Computer Tomography
CTRP3	C1q TNF Related Protein 3
Cx	Connexin
X-linked	Crosslinked
CD	Cyclodextrin
DHT	Dehydrothermal Treatment
DNA	DeoxyriboNucleic Acid
DEX	Dexamethasone
DMSO	Dimethyl Sulfoxide

DDR1 & 2	Discoidin Domain Receptor 1 &2
DMEM	Dulbecco's Modified Eagles Medium
EC	Endothelial Cells
ECM	Extracellular Matrix
FBS	Fetal Bovine Serum
FDA	Food and Drug Administration
FGF	Fibroblast Growth Factors
Fz	Frizzled receptor
GAM	Gene Activated Matrices
GAPDH	Glyceraldehyde 3-phosphate dehydrogenase
GP	Glycerolphosphate
Gly	Glycine
GSK-3 $\beta$	Glycogen Synthase Kinase-3 beta
GAG	Glycosaminoglycan
GM-SCF	Granulocyte-Macrophage Colony-Stimulating Factor
GDFs	Growth Differentiation Factors
GF	Growth Factor
GFP	Green Fluorescence Protein
HBSS	Hank's Balanced Salt Solution
HGF	Hepatocyte Growth Factor
HFP	1,1,1,3,3,3-HexaFluoro-2-Propanol
HDIM	Hexamethylene Diisocyanate
HCL	Hydrochloric Acid
H-NMR	Hydrogen -Proton nuclear magnetic resonance
HPH	High Pressure Homogenization
hASCs	Human Adipose Stem Cells
HCECs	Human Corneal Epithelial Cells
hPDLSCs	Human Periodontal Ligament Stem Ce
HA	Hyaluronic Acid
HA	Hydroxyapatite
Hyp	Hydroxyproline

IGF	Insulin Growth Factors
IL	Interleukins
LIF	Leukemia Inhibitory Factor
LA	Linoleic Acid
LRP5	Lipoprotein Receptor-related Protein 5
M-CSF	Macrophage Colony Stimulating Factor
MRI	Magnetic Resonance imaging
miRNA	micro RNA
MP	Matricellular Protein
MTT	3-(4,5-Dimethylthiazol-2-yl)-2,5-diphenyltetrazolium bromide
MW	Molecular Weight
NP	Nanoparticle
NEAA	Non-Essential Amino Acid
NFATc1	Nuclear Factor of Activated T-cells cytoplasmic-1
OCN	Osteocalcin
OPN	Osteopontin
Osx	Osterix
PDCs	Periosteum Derived Cells
Phe	Phenylalanine
PDGF	Platelet-Derived Growth Factor
pDNA	Plasmid DNA
PA	Polyacrylic Acid
pAsp	Polyaspartic Acid
PCL	Polycaprolactone
PDLLA	Poly (DL-lactide)
PEG	Polyethylene glycol
PEI	Polyethylenimine
PLGA	Poly (lactic-co-glycolic acid)
PLLA	Poly (L-lactic acid)
PLLACL	Poly(L-lactide-co-caprolactone)
Poly(LLA-co-CL)	Poly(lactide-co- $\epsilon$ -caprolactone)

Pro	Proline
PrA	Propionic Acid
RT-PCR	Real Time
RANLK	Receptor Activator of Nuclear Factor Kappa-B Ligand
rhBMP-2	recombinant human Bone Morphogenetic Protein-2
RNA	Ribonucleic Acid
RT	Room Temperature
RUNX2	Runt-related transcription factor-2
p-NPP	p-nitrophenol phosphate
PDGF	Platelet-Derived Growth Factors
SEM	Scanning Electron Microscopy
siRNA	short interfering RNAs
SD	Standard Deviation
StA	Stearic Acid
SCF	Stem Cell Factor
TRAP	Tartrate Resistant Acid Phosphatase
tLA	thioester Linoleic Acid
$\alpha$ -LA	thioester $\alpha$ -Linoleic acid
3D	Three Dimensions
TGF- $\beta$	Transforming Growth Factor-beta
TCP	1,2,3-Trichloropropane
TFE	2,2,2-Trifluoroethanol
TNF- $\alpha$	Tumor Necrosis Factor-alpha
2D	Two Dimensions
UV	Ultraviolet irradiation
VEGF	Vascular Endothelial Growth Factor
VSMCs	Vascular Smooth Muscle cells

# **Chapter 1- The process of bone regeneration and the current therapies in the bone tissue engineering field**

## **Parts from this chapter were published in:**

- i) Biomaterials to Facilitate Delivery of RNA Agents in Bone Regeneration and Repair, **Eleni K. Tsekoura**, Remant Bahadur K.C and Hasan Uludag, ACS Biomaterials Science and Engineering, 2017, 3, 1195-1206
- ii) Current state of the fabrication technologies and materials for bone tissue engineering, Abiy Wubneh, **Eleni Tsekoura**, Cagri Ayranci and Hasan Uludag, Acta Biomaterialia, 2018, 80, 1-30

## 1.1 Background

Bone healing after a traumatic injury or pathological diseases remains an important world-wide problem as well as a clinical goal. Each year approximately 6.2 million bone fractured cases are recorded in the United States, where 5 to 10% result in non-union or delayed union (1,2). Throughout life, bone tissue possesses the ability of modelling and remodelling of damaged skeleton via intra-membraneous pathway (where flat bones such as skull and clavicle are derived) and endochondral pathway (where long bones of the axial and appendicular skeleton are derived) without leaving a scar tissue (3,4). In situations of bone lost due to trauma or musculoskeletal disease where self-repair is not achievable, the use of bone grafting is the preferred treatment. It has been recorded that over 2.2 million bone grafting procedures are performed world-wide annually in orthopaedics field and dentistry (5). The treatment of the defect with an autogenous bone grafting is the current gold standard procedure; during the treatment, the host bone is removed from another site (typically from patient's iliac crest or other locations like distal femur, proximal tibia, ribs and intramedullary canal) and used to fill a bone defect (6). Autogenous grafts offer no immunological rejection and provide the best osteoconductive (scaffold), osteogenic (cellular) and osteoinductive (growth factor, GF) properties that constitute the three essential elements of bone regeneration (7). However, transplantation with autogenous grafts have shown as high as 30% complication rates such as excess haematoma formation, blood loss, increased risk of deep infection and sometimes chronic pain and morbidity at the donor site. Other reasonable options are the use of allografts coming from a donor's cadavers or xenografts coming from a non-human source. In both cases, the possibilities of disease transmission, infection and host rejection have restrict their use (8). These limitations of bone grafts have led the scientists to alternative therapies, including the delivery of osteoinductive GFs, using direct protein delivery or gene therapy, as well

as combination of the protein/gene therapies with osteoconductive scaffolds in order to promote bone regeneration. Relying on synthetic approaches, and using agents derived from biotechnology or pharmaceutical industry facilitates development of safe and disease-free agents.

Below I first describe the main constituents of bone (cellular components and extracellular matrix), the basics of bone biology as relevant to regeneration and bone repair, and the class of biomolecules, namely growth factors, involved in stimulation of bone repair. Then, I summarize various approaches and critical issues relevant to the current interventions to stimulate and assure bone healing. The design and key considerations for creating scaffolds, i.e., extracellular mimics for bone regeneration, are especially emphasized given their indispensable role in any attempt for bone repair. I emphasize collagen-based scaffolds in my Introduction section since I will use collagen scaffolds for delivery of genes and cell culture.

## **1.2 Cellular Component of Bone**

### **1.2.1. Mesenchymal Stem Cells (MSCs)**

The term ‘stem cell’ characterizes cells that have the ability to self-replicate and give rise to daughter cells which undergo irreversible, terminal differentiation process. Mesenchymal stem cells (MSCs) are multipotent cells that maintain homeostasis in the human body by regeneration and repair of damaged tissues. In addition to bone marrow, which is the most abundant source of MSCs, MSCs have been isolated from almost all body compartments, including tendons, periosteum, trabecular bone, adipose tissue, synovial membrane and muscle. They are capable of differentiating into several mesodermal cell lineages including osteoblasts, chondrocytes, adipocytes, tenocytes and myoblasts. Their main function is to create a tissue framework that will provide mechanical support to the hematopoietic cell system. MSCs can secrete a number of

extracellular matrix (ECM) proteins like fibronectin, laminin, collagen and proteoglycans. In addition, they secrete interleukins (ILs) such as IL-1a, IL-1b, IL-6, IL-7, IL-8, IL-11, IL-14 and IL-15, macrophage colony-stimulating factor, granulocyte-macrophage colony-stimulating factor (GM-CSF), leukemia inhibitory factor (LIF), stem cell factor (SCF), fetal liver tyrosine kinase-3, thrombopoietin and hepatocyte growth factor (HGF).

In the last decade, the therapeutic potential of MSCs has been extensively investigated *in vitro* and in preclinical settings, as well as at clinical level for their ability to enhance orthopaedic healing such as osteoarthritis, chondral lesion and bone non-union/delayed unions. Osteoarthritis is the most common form of arthritis that cause pain, stiffness, and decreases function. Jo et al. studied the intra-articular injection of autologous adipose tissue derived MSCs (AD-MSCs) in 18 patients for the treatment of the knee osteoarthritis. The results showed that injection of  $10^8$  AD-MSCs improved function and pain of the knee joint without side effects. In addition, it reduced cartilage defects by regeneration of hyaline-like articular cartilage.

### **1.2.2 Osteoblasts**

Osteoblasts are derived from MSCs and are responsible for bone matrix deposition and mineralization. Osteogenic differentiation of MSCs into osteoblasts is mainly driven by Runx2, which regulates the expression levels of osteogenic genes including alkaline phosphatase (ALP), osteopontin, type I collagen, osteocalcin, and osterix. There are several other signalling pathways including bone morphogenetic protein (BMP), transforming growth factor beta (TGF- $\beta$ ), and Wnt/ $\beta$ -catenin signalling that are involved in osteogenic differentiation (Fig 1.1) (9). Mainly osteoblastogenesis is under the control of the Wnt protein and the Bone Morphogenetic Proteins (BMPs) pathway (10). The Wnt signalling plays an important role in the development and

maintenance of bone since Wnt signal can regulate cell growth, differentiation, function and death. The activation of the canonical Wnt/ $\beta$ -catenin pathway is particularly important for bone biology that occurs upon binding of Wnt to the 7-transmembrane domain-spanning frizzled receptor (Frz) and the low-density lipoprotein receptor-related protein LRP5 or 6 coreceptors. The binding of Wnt to the receptor results in the inhibition of Glycogen Synthase Kinase-3 beta (GSK-3 $\beta$ ) activity which prevents the phosphorylation of  $\beta$ -catenin, leading to the accumulation of  $\beta$ -catenin in the cytoplasm. When  $\beta$ -catenin reaches a certain concentration level, it translocates to the nucleus where it associates with the LEF1/TCF7 family of transcription factors to regulate the expression of canonical Wnt target genes. Upregulated canonical Wnt signalling stimulates osteoblastogenesis when inhibits the differentiation of MSCs to chondrocytes and adipocytes.

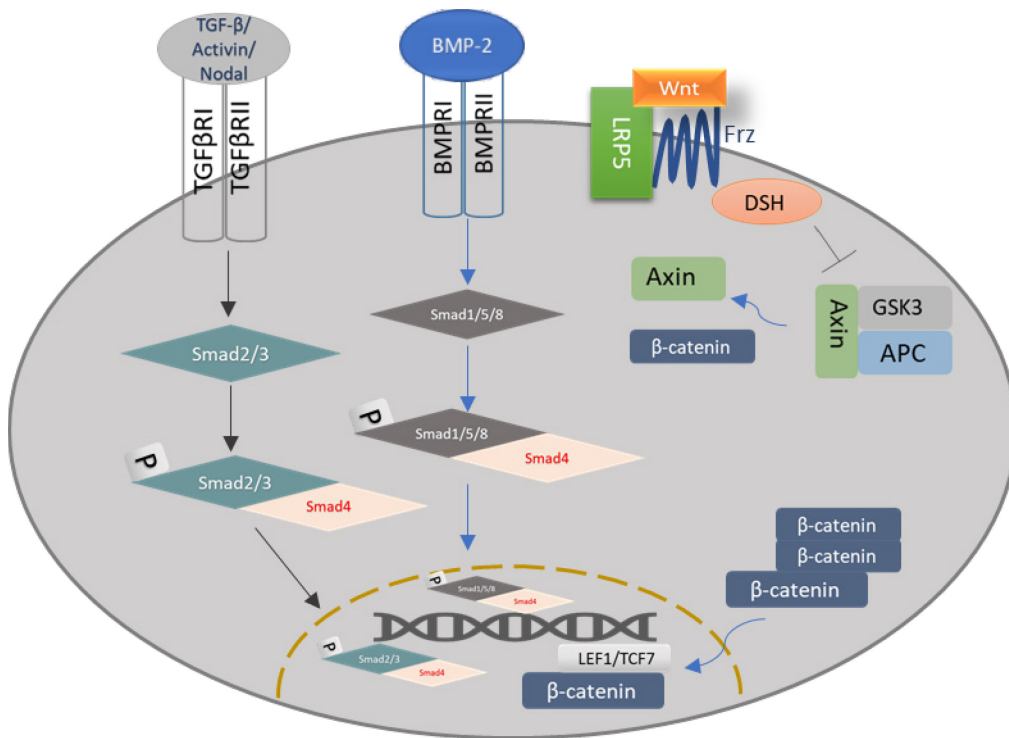


**Figure 1.1. Cell signaling pathways (Wnt, BMP-2 and TGF- $\beta$ ) activated in osteogenic differentiation of MSCs into osteoblasts.**

Osteoblasts are divided into four categories a) active osteoblast b) bone lining cells or inactive osteoblasts and c) osteocytes. Active osteoblasts are mononuclear cuboidal shaped cells which produce a complex combination of extracellular proteins, including osteocalcin, ALP and a large amount of type I collagen. The ECM during the first deposition of Type I collagen is called osteoid which is an un-mineralized form of collagen (11). The deposited collagen is subsequently mineralized through accumulation of calcium phosphate in the form of hydroxyapatite. The deposition of collagen from the osteoblasts can lead to two basic confirmations of bone: i) woven bone where the collagen fibrils are randomly oriented in the bone tissue and ii) lamellar bone where the fibrils are clustered in parallel arrays in the bone tissue. Woven bone is usually found in early stage of bone development, remodelling or fracture healing. It is mineralized but has less biomechanical strength. On the other hand, the collagen fibers of lamellar bone are parallel to each other but their direction differs from layer to layer, which provides a tensile strength in more than one direction (12). The replacement of woven bone from lamellar is a process that can take many years. Bone-lining cells or inactive osteoblasts are found lining on the surface of the bone and have the ability of becoming active osteoblasts. Finally, osteocytes are mature osteoblasts which are embedded in bone. Their activity will be further analysed in the next session.

Failure of collagen deposition by osteoblasts is called osteogenesis imperfecta or brittle bone disease. It is a genetic disorder resulting in most cases (> 85%) from mutations in one of the genes that encode collagen type I chains (COL1A1 and COL1A2). The most common structural disorder occurs when glycines in the collagen fibril are replaced by a larger amino acid, which disrupts the folding process of the collagen into a triple helical structure (13,14).

### 1.2.3 Osteocytes

Osteocytes represent the terminal differentiated form of osteoblasts. They are the most abundant cell type in bone and are regularly spaced throughout the matrix. They are communicating between each other and with other cells on the bone surface (e.g osteoblasts) via gap junction channels which are formed by six molecules of connexin (Cx) which are arranged on the cell membrane and recognized by the adjacent cell membrane hexamer. Connexin 43 (CX43) is the primary integral cellular protein expressed by bone cells and allows the maturation, activity, and survival of osteocytes. During osteoblasts differentiation to osteocytes, the shape of osteoblasts changes from polygonal to a more stellate shape. The matrix production slows down and are embedded more into the matrix. During embedding of osteocytes within the mineralized matrix (Lacunae) numerous cellular projections (dendritic processes) are formed and elongated in a polarized manner toward the mineralizing front and then are extended toward the vascular space or bone surface. Once embedded, osteocytes maintain their polarity in the direction of the dendrimers and the direction of mineral deposition.

Osteocytes have been characterized as mechanosensors due to the absorption of mechanical strain and translating the strain into biochemical signals like hormone secretion (estrogen and glucocorticoids) that can affect bone formation and resorption. Therefore, a possible network disruption can have negative consequences on bone health such as to increase bone fragility (15–17).

### 1.2.4 Osteoclasts

Osteoclasts are hematopoietic-origin progenitor cells that are formed by fusion of small precursor cells, but mainly from bone marrow monocyte-macrophage precursor cells, into large, highly active cells with many nuclei (containing up to 50 nuclei). Osteoclasts formation and maturation is controlled by Receptor Activator of Nuclear Factor Kappa-B Ligand (RANKL) and Macrophages Colony Stimulating Factor (M-CSF) cytokines, which are both produced mainly by marrow stromal cells and osteoblasts as membrane-bound and soluble forms. The binding between RANKL and RANK receptor on the surface of osteoclast induces osteoclast activation. The process can be inhibited by osteoprotegerin (OPG) which competitively binds to RANKL on the surface of osteoblasts or stroma cells.

Osteoclasts are responsible for the dissolution of bone mineral and for the degradation of the organic matrix. Their size can reach a diameter of 20-100 micron that enables the resorbing of a large tissue area. During degradation, osteoclasts bind to bone matrix *via* integrin which is expressed on their surface. The  $\beta 1$  integrin in osteoclasts bind to collagen, fibronectin and laminin. The integrin that mainly facilitates on bone resorption is the  $\alpha_v\beta_3$  integrin, which binds to osteopontin and bone sialoprotein (18). Bone resorption process by osteoclasts involves first the degradation of the mineral matrix by local acidification and then the protease-mediated degradation (secreted by osteoclast) of the organic matrix. Secretion of  $H^+$  especially vacuolar (V-type) electrogenic  $H^+$ -ATPase from the ruffled border of cell membrane can acidify the 'resorbing lacuna' beneath the osteoclasts (a local pH of  $\sim 4.5$  is typical). The dissolving of the minerals allows proteases especially cathepsin K to freely digest the proteinaceous matrix of bone, which is mostly composed by Type I collagen (15,19). Then, the osteoclasts transfer the fragments of the degraded matrix into the interstitial space by transcytosis and the osteoblasts filled the resorption area with

a new bone matrix. Osteoblasts and osteoclasts are able to communicate between each other in order to guarantee bone homeostasis. An imbalance activity between deposition and resorption will lead to various skeletal diseases, either due to excessive resorption (e.g., osteoporosis) or excessive deposition (e.g., hypertrophic osteoarthropathy) (20). Osteoporosis is the most common skeletal disease and it is characterized by low bone mass with a high susceptibility to fractures. The bone becomes porous and light, with the spongy bone of the spine being most vulnerable. Primary osteoporosis is a disease of older people and it's divided into two main categories: a) postmenopausal (type I) and senile osteoporosis (type II). Type I osteoporosis affects mainly the trabecular bone of women vertebral artery and hip. As mentioned above, binding of RANKL with its receptor RANK in osteoclasts stimulates their differentiation and prevents osteoclasts apoptosis. Expression of estrogens and TGF- $\beta$  by osteoblasts as well as mechanical forces can inhibit RANKL expression that will affect osteoclast cell formation and differentiation and finally will decrease bone resorption. On the other hand, type II osteoporosis is mainly affecting cortical bone of elderly patients. Possible changes in hormone levels as well as vitamin D levels can enhance osteoclastic bone resorption.

### **1.3 Extracellular Matrix (ECM) Component of Bone**

The ECM of the bone is produced by osteoblasts that are responsible for producing most of the dry weight of the bone. The bone remodelling involves two important steps, bone resorption followed by new bone formation. The mechanical properties of the skeleton are related to the composition and organization of ECM. Bone is composed by an organic and inorganic (mineralized) phase. The organic phase is mainly composed of Type I collagen, and over 100 ECM non-collagenous proteins such as osteocalcin, osteopontin, osteonectin, fibronectin and GFs. The inorganic phase is mainly composed of calcium phosphate ions in the form of hydroxyapatite (15,21,22). During the early stages of mineralization, the host matrix allows limited crystal growth and keeps the crystals separate from each other, at least along the length of the fibril. Growth of crystals results in collagens triple-helical molecules compression and eventually crystals conjunction and formation of extended crystal sheets. Eventually, the mechanical properties of the collagen fibrils change considerably under such conditions. In addition to the mineralized bone ECM, other unique unmineralized tissue types exist in association with the bone, including, a) marrow, b) endosteum and c) periosteum.

#### **1.3.1 Marrow stroma**

It is a loose connective tissue that supports hematopoiesis as well as MSC and osteoclasts precursor cells. Bone marrow (BM) microenvironment is an extraordinarily heterogeneous and dynamic system which is generated by the functional relationship of different cells found in the bone marrow that are producing soluble factors that allow autocrine, paracrine and endocrine activities (23).

### **1.3.2 Endosteum**

It is a highly vascular membrane lining the inner surface of cortical bone and is composed of bone lining cells which are mostly osteoblasts-lineage cells, with a specialized type of macrophage- OsteoMacs. The OsteoMacs play a regulatory role in bone formation and resorption and during these processes can form a remodelling ‘canopy’. The osteoblast-lineage derived from bone-lining cells can differentiate to become functional (bone-forming) osteoblasts. The primary matrix component is the osteoid, which is the unmineralized matrix secreted and assembled by the osteoblasts. Osteoid will be mineralized under condition of normal bone maturation (22,24).

### **1.3.3 Periosteum**

It is a vascular membrane that lines the outer surface of bone and is attached to the bone by collagen fibers (Sharpey’s fibers). It contains two layers, an outer fibrous layer containing fibroblasts dispersed in between collagen fibers and a cambium layer that contains skeletal progenitor cells and osteoblasts. Periosteum is highly vascularized and innervated. Progenitor cells in the cambium layer give rise to osteoblasts to produce bone. This process is believed to play a crucial role especially in bone regeneration and fracture repair. The carboxylated matricellular protein (MP) is a key ECM protein presented in periosteum. The presence of longitudinal Haversian canals and transversal Volkmann canals allows a continuous connection between periosteum and endosteum (25–27).

## **1.4 Main Growth Factors Involved in Bone Physiology**

Proper bone formation and homeostasis involves the group work of cells, cytokines and GFs. GFs are polypeptides that can act as autocrine, paracrine or endocrine. Autocrines are the

GFs that influence the cell of its origin or cell with the same phenotype when paracrine GFs influence neighbouring cells with a different phenotype and finally endocrine GFs are acting on cells located at a remote anatomical site after systemic distribution (28). Multiple GFs are involved in controlling different phases of the bone regeneration process. Some of these GFs have been already mentioned in the sections related to cellular composition and extracellular matrix of the bone above. Nevertheless, I again provide a short synopsis below on the most important GFs involved in bone regeneration.

#### **1.4.1 The transforming growth factor-beta family (TGF- $\beta$ )**

It is a large family of growth and differentiation factors including BMPs, transforming growth factor-beta (TGF- $\beta$ ), growth differentiation factors (GDFs), activins, inhibins and the Mullerian inhibiting substance. They are activated by proteolytic enzymes and act on serine/threonine kinase membrane receptor on target cells (29). TGF- $\beta$  is a pleiotropic GF initially released by the degranulating platelets in the hematoma and by the bone extracellular matrix at the fracture site (30,31).

#### **1.4.2 Bone morphogenetic proteins (BMPs)**

They are members of the TGF- $\beta$  family. Different BMPs are activated and deactivated during different phases of skeletal homeostasis and prevent undesirable effects like heterotopic bone formation. BMP-2, 4 and 7 were found to play a critical role in bone healing due to their ability to stimulate the differentiation of MSCs to an osteochondroblastic lineage. In bone, BMPs are produced by a variety of cells like endothelial cells, osteoblasts and chondrocytes. BMP ligands are synthesized as large dimers that contain a secretion signal peptide in the N-terminus

domain (called prodomain) and a cysteine-knot domain in the C-terminus. The binding of BMPs to specific receptors on the cell surface involves the interaction and formation of heterodimers between two transmembrane distinct serine/threonine kinase receptors known as type I (BMPR-I) and type II receptors (BMPR-II). Some of the BMPs have been shown to have higher affinity for certain type I receptors like BMP-4 which binds to ALK3 and ALK6 when BMP-7 preferentially bind first to type II receptors followed by phosphorylation of the type I receptor on its cytoplasmic domain which is rich in glycine and serine residues. Afterwards, the BMP signal is transmitted to the nucleus via canonical *Caenorhabditis elegans* protein (sma) and mothers against decapentaplegic (Smad) and /or non-canonical Smad-independent pathways (e.g MARK and Akt pathways). The activated R-smads form a protein complex with the Co-smad named Smad-4 which translocates toward the nucleus. The R-smad/Smad-4 complex enters the nucleus to activate Runx 2 (runx-relates transcription factor 2) and Osterix (Osx) genes. Osteoblast differentiation and bone metabolism is mainly induced by overexpression of Runx2 and Osx. Also, the BMP/Smad signalling pathway can be regulated by a family of secreted extracellular antagonists like Noggin, chordin and gremlin that can directly bind to the BMP ligand and prevent their interaction with the BMP receptors. Noggin is a secreted polypeptide which binds and inactivates BMP-2, 4 and 7. It is able to inhibit BMP signalling by blocking the interfaces of the binding epitopes for both type I and II BMP receptors.

Direct delivery of BMPs has received great attention due to their promising preclinical and clinical results to induce or accelerate bone healing process (28). To date, the U.S Food and Drug Administration (FDA) approved the use of BMP-2 and BMP-7 (rhOP-1) for select clinical applications and other BMPs are currently undergoing clinical trials (32–34). Despite the fact, there is concern that non-local and focal delivery of the single dose, the high amount of protein

needed (evident in preclinical studies and early clinical trials) as well as the short in situ residence time of the protein will not be beneficial (30,35). However, studies have shown that their direct delivery has resulted in undesirable tissue responses, like bone resorption and local inflammation (36,37). The use of high protein dose has been questioned due to the post –treatment side effects. Effects like swelling, ectopic bone formation, tumour formation, seroma have been recorded after the use of BMP-2 in spinal fusion therapy (38,39). Others have also questioned the economics of BMP treatment since a single dose of BMP costs approximately US\$5,000. Several economic analyses suggest that the treatment is only cost-effective when used in high-grade open fractures and in high-risk patients such as smokers.

### **1.4.3 Fibroblast Growth Factors (FGFs)**

They are playing a significant role during angiogenesis and mitogenesis of various MSCs including fibroblasts, chondrocytes and osteoblasts. Multiple FGFs and FGF receptors have been dynamically expressed during fracture healing. FGFs are mainly produced by macrophages, monocytes, MSCs, chondrocytes, osteoblasts and endothelial cells. Several animal and clinical studies have demonstrated the positive potential of FGF-2 for bone regeneration; however, the exact mechanism behind their beneficial effect is not well understood (angiogenesis vs. mitogenesis). An in vivo study by van Gaestel et al, explored the delivery of FGF-2 to periosteal cells. The implantation of FGF-2 primed cells in a large bone defect in mice resulted in complete healing (40).

#### **1.4.4 Vascular Endothelial Growth Factor (VEGF)**

It is the key regulator of vascular regeneration, which is critical for bone regeneration. The family of VEGF proteins (-A, -B, -C, -D and -E) are produced by endothelial cells, macrophages, fibroblasts, smooth muscle cells, osteoblasts and hypertrophic chondrocytes (41,42). Neovascularization of damaged tissue is crucial to successful bone healing since it provides oxygen and delivering progenitor cells from systemic circulation. The loss of vascular integrity produces hypoxic conditions that induce chondrogenesis. During fracture healing, the VEGF-A, VEGF-C and VEGF-D isoforms are present that can stimulate the proliferation and migration of endothelial cells, resulting in the formation of tubular blood vessels. In addition, VEGF plays a crucial role during bone regeneration by promoting the recruitment, survival and activity of bone forming cells. VEGFs and especially VEGF-A are the first isoforms that appear in the bone regeneration process, lead to coordinated angiogenesis and bone regeneration (43).

#### **1.4.5 Insulin-like Growth Factors (IGF)**

They are mainly produced by osteoblasts, chondrocytes, hepatocytes and endothelial cells. IGF-I (or somatomedin-C) promotes bone matrix formation by fully differentiated osteoblasts when IGF-II (or skeletal growth factor) acts during endochondral bone formation and stimulates Type I collagen production, cartilage matrix synthesis and cellular proliferation (29,30).

#### 1.4.6 Platelet-Derived Growth Factors (PDGF)

It has various isoforms like PDGF-AA,-AB, -BB, -CC and -DD which signal through two distinct receptors ( $\alpha$  and  $\beta$ ) with different binding affinities. PDGFs are mainly released by platelets (as originally discovered), but also secreted by osteoblasts, endothelial cells, monocytes and macrophages. PDGF is released by platelets in the early phase of structure healing and it is a potent chemotactic stimulator for inflammatory cells and the main stimulator for proliferation and migration of MSCs and osteoblasts (30). Recently, studies on PDGF-BB showed that could function as a central connector between the cellular components and contributors of the osteoblasts differentiation program. In addition, supports angiogenesis since could function at sites of injury to mobilize and promote the proliferation of MSCs, progenitor osteoblasts and pericytes. Several *in vivo* studies support the beneficial effect to heal critical side defects by delivering PDFG when other studies failed to show any effect on bone regeneration. For example, the study of Kaipel et al. showed that rats that have been treated with fibrin bound rhPDGF-BB and rhVEGF-165 failed to increase bone healing in comparison to rhBMP-2 in delayed- union rat model. On the other hand Hollinger et al. , study was able to enhance tibial fracture healing in geriatric osteoporotic rats via the delivery of rhPDGF-BB in an injectable beta-tricalcium phosphate/collagen matrix (44,45).

### 1.5 Osteogenesis

*Osteogenesis (bone formation)* is a natural biological process that starts early in the fetus developmental and continues throughout life. There are two distinct modes of bone formation, namely *endochondral ossification* and *intramembranous ossification*. Both modes of osteogenesis start with condensed specialized MSC aggregated in the shape of the future bone. MSCs can secrete several different proteins that can regulate inflammation and stimulate tissue regeneration.

Their differentiation plays a critical role in the regeneration effect, and part of this can be influenced by the microenvironment, cell-cell communication, physical factors and cell structure. MSCs are capable to differentiate along the osteogenic, chondrogenic, adipogenic and marrow stromal lineages (46). Transcription factors such as SOX9, Runx2 and Osterix have essential roles in the cell-fate decision process by which MSCs become chondrocytes or osteoblasts, through activation of cell type-specific genes. In addition, the microenvironment can influence this process by the presence of different proteins like BMPs, and other GFs and cytokines (47), some of which have been articulated above.

Endochondral ossification involves recruitment, proliferation and differentiation of undifferentiated MSCs into cartilage, which then is replaced by bone. It is responsible for the development and growth of most bones in the human body, such as the long bones of the limbs and ribs while the intramembranous ossification involves differentiation of the MSC condensate directly into osteoblast cells without the formation of cartilage intermediate (48). Most flat bones, collarbones, cranial, and facial bones are examples of this process. Endochondral ossification starts with the differentiation of the condensed MSC into chondrocytes, resulting in the formation of cartilaginous tissue with a distinctive extracellular matrix (ECM) (49,50). This intermediate cartilage formation is unique to this mode of bone formation. The chondrocytes later differentiate into a terminal state known as hypertrophic chondrocytes. When engulfed by specialized cells (osteoblast progenitors and osteoclasts) and blood vessels, the hypertrophic cartilage goes through resorption and get replaced by bone marrow. The resorption and mineralization within the cartilage leads to the formation of the primary and secondary ossification centers. This is followed by the differentiation of the osteoblast progenitors into osteoblast cells which are producing a combination of extracellular proteins, including osteocalcin, alkaline phosphatases and a large

amount of type I collagen. The extracellular matrix during the first deposition of type I collagen is called osteoid which is a non-mineralized form of collagen (12). Afterwards, the collagen-proteoglycan in osteoid is mineralized through accumulation of calcium phosphates in the form of hydroxyapatite (organic and inorganic phase) (49,51,52). Finally, the osteoblast cells find themselves trapped in or encapsulated by the layers of the osteoid matrix and the outer calcified shell, leading to formation of *osteocyte* cells (49,51,53).

With the establishment of mature bone tissue, the integrity of the tissue is maintained by the dynamic process of *bone remodeling* that cover the lifecycles of bone cells (54). It includes both the *osteogenesis* stage discussed above and the removal of old mineralized tissue at the end of its useful life (resorption). While osteoblasts are responsible for building new bone tissue, the resorption of old bone matrix is undertaken by the specialized multi-nucleated osteoclasts (55). The main function of osteoclasts is to breakdown the old tissue and collagen matrix, and free up the essential minerals and ions in the making the new bone tissue. Osteoblasts and osteoclasts are able to cross-communicate in order to maintain bone homeostasis (56).

The continues remodeling helps to maintain the proper mechanical properties (strength and elasticity) of local tissue; hormonal imbalance (as in estrogen depletion) or pharmacological intervention (as in bisphosphonate administration) can severely affect the remodeling process and can alter the normally robust regenerative capability of bone tissue. In case the integrity of bone is comprised upon sudden impact, such as the case of bone fracture, a distinct process kicks in to establish the original contours of the tissue. Bone fracture not only disturbs the skeletal integrity from a mechanical perspective, but also the normal vascular structures and nutrients flow at the fracture site. The degree of fracture communication and displacement affects the extent of bone cell death, disruption of the local blood supply and the extent of periosteal stripping (affects the

cortical blood supply and removes cambial layer of cells from the bone surface). The healing time depends on the blood supply to the bone, the amount of force producing the fracture and the conditions of the soft tissues. In addition, other general factors affecting the period of healing involve the type of the fracture, the age of the patient, bone pathology, and type of bone to name few (57,58).

## **1.6 Bone Fracture Healing**

Fracture healing is a multistep process which involves specific cellular and molecular activity in concert with the appropriate ECM. The process involves four phases: an inflammatory phase, two repair phases consisting of soft and hard callus formation and remodeling. The presence of inflammatory cells, vascular cells, osteochondral progenitors, and osteoclasts as well as the presence of pro-inflammatory cytokines, GFs, angiogenic and pro-osteogenic factors that are secreted by the digested bone matrix and cells at the site of injury can control cellular activity responsible for healing. These include cellular migration to the wound site, cell proliferation and differentiation into osteogenic phenotype, osteoid deposition and angiogenesis (58,59). Angiogenesis is an essential process since the formation of new blood vessels is required for supplying the cells with nutrients, oxygen, hormones, cytokines (60,61). At the site of injury, the environment gradually become hypoxic and the surrounding tissues start to degrade since the damaged vessels fail to provide sufficient oxygen and nutrients (62). Lack or inhibition of angiogenesis in distraction osteogenesis, prevents normal osteogenesis during healing process and has been reported as one of the main reasons of non-union or delayed union of the bone (60,63,64). During the initial inflammation phase, inflammatory cells (macrophages, de-granulating platelets, granulocytes, lymphocytes and monocytes) infiltrate the fracture and secrete inflammatory

cytokines such as tumor necrosis factor- $\alpha$  (TNF- $\alpha$ ) and interleukins (IL-1a, IL-1b, and IL-6, -11, -18) as well as several GFs like BMPs (BMP-2,-3,-4 and -7), TGF- $\beta$ , FGF-2, VEGF, PDGF, and macrophage colony stimulating factor (M-CSF). The GFs are responsible for controlling the previous mentioned cellular activities at the repair site and their controlled concentration, timing and spatial location at the site of the defect has an essential role during the healing process (59,63,65). Afterwards the formation of soft callus provides temporally mechanical support to the fracture, as well as an outline for the hard callus formation after mineralization. The hard callus stage is characterized as the most active period of osteogenesis and includes high level activity of osteoblasts and the formation of mineralized bone matrix by mature osteoblasts. Finally, in the remodeling phase, the hard callus is replaced by secondary bone or lamellar bone. Eventually, the size and shape of the bone is reinstated, as well as the mechanical strength and stability despite the fact that the remodeling phase continues for several years (66). It is believed that a similar process takes place in case of large bone defects, except the migration of cells need to take over longer distances and greater mass of tissue need to be induced and reorganized to fill the defects.

## **1.7 Technology of Current Therapies for Bone Regeneration and Emerging Gene Therapy**

Direct delivery of GFs in bone regeneration has been received great attention which makes them natural candidates for therapeutic agents due to their promising preclinical and clinical results that throughout appropriate signalling they may induce or accelerate the healing process (28). Their ability to deliver particular messages to the cells varies with the target cell type, type of receptor on the cells and the intracellular signal transduction subsequent to GF binding. The US Food and Drug Administration has already approved BMP-2 and BMP-7 (rhOP-1) for selected

clinical applications and other GFs have undergone or are currently undergoing clinical trials (32–34). However, there are concerns with localization of GFs and high protein doses needed (evident in preclinical studies and early clinical trials) as well as their short *in situ* residence time (30,35). Conventional delivery of GFs may result in undesirable tissue responses, such as bone resorption and local inflammation (36,37). High doses have been a concern due to the post-treatment side effects such as swelling, ectopic bone formation, tumour formation and seroma after BMP-2 in spinal fusion therapy (38,39). The cost of the treatment is also concerning in the case of GF therapies (67).

Gene therapy can be an alternative approach to avoid the limitations associated with protein therapy. Genes are commonly delivered within a plasmid DNA (pDNA) that can be designed to promote a signalling mechanism supportive of regeneration, or to suppress mediators inhibiting bone formation. Several regenerative genes have been explored to-date, mainly based on GFs (e.g., BMPs, PDGF and FGFs) and transcription factors associated with bone/cartilage formation Runx2/Cbfa1 and Osterix (68). Gene delivery has the flexibility to express proteins locally, focally and intracellularly, as needed. It eliminates any issues related to contamination of a protein preparation with incorrectly-folded and possibly antigenic species. An additional advantage is the ability to sustain protein production *in situ* for a longer time. Gene delivery is likely to result in lower levels of therapeutic proteins so that it may reduce protein exposure to the body (lower undesirable side effects) as well as reduced cost (69,70). The use of pDNA is now well established for bone repair, with promising preclinical studies elucidating the factors responsible for its successful application (71).

Below I summarize the key concepts related to the use of GFs to stimulate bone repair. Various approaches for incorporation of GFs into three dimensional scaffolds intended to replace

bone tissue are articulated. Afterwards, I present the role of biomaterial carriers in delivery of pDNA based nucleic acids.

### **1.7.1 Biomaterial Carriers in Intracellular DNA Delivery**

Successful use of nucleic acids requires carriers that facilitate cellular entry of nucleic acids into target cells. In the absence of a carrier, the nucleic acid is likely to be degraded in biological fluids by nucleases before it reaches surface of target cells. It will also have a low chance of undergoing cellular uptake due to electrostatic repulsion at the cell membrane. A number of viral (*i.e.* retroviruses, lentiviruses, adenovirus and adeno-associated virus) and non-viral carriers (*i.e.* polymers, cationic lipids, chitosan) have been investigated to increase the intracellular bioavailability of nucleic acids. The size of the carriers should be small enough for their uptake by the cells or contain either targeting moieties or excess positive charge to enhance the binding to the cell membrane. Moreover, these carriers should provide intermediate stability since robust transfer and dissociation of the genes to the target site is required. In the case of viral carriers, the genome of the virus must be deleted (or replaced to some extent) in order to be replaced by the therapeutic gene (72–74). Gene transfer using a virus origin carrier is called transduction and is achieved when the carrier attaches to a target cell receptor and then enters the cell along with the cargo. In spite of their high efficiency, clinical application of viral expression systems (vectors) is limited due to toxicity and immunogenicity issues. Naturally derived and synthetic biomaterials, when combined with nucleic acids, can create nanoparticles (NPs) suitable for cellular uptake, which could be further aided by presence of targeting moieties or excess cationic charge for binding to cell membrane. The expression of genes via non-viral carrier is known as transfection.

Being synthetic, non-viral carriers offer excellent molecular tunability (facile chemistry), large scale production, stability for long-term storage and reconstitution (75,76). Non-viral carriers can also provide optimal unpacking for robust transfer and dissociation of the genes as required. While cytotoxicity on host cells is an important concern, lack of long-term immune response or little chance of oncogenic transformation are the key reasons for their pursuit for clinical applications. There have been two types of nucleic acids explored for bone repair, one based on DNA based expression systems (mainly pDNA) and one based on RNA based regulatory agents. With pDNA delivery, access to the nucleus is paramount and complexes have to overcome the passage of nuclear membrane. With RNA, effective delivery faces less challenge since these molecules are acting in cytoplasm and there is no need to actively deliver them to the nucleus. Two types of RNA molecules are now actively explored to modulate bone repair, micro-RNAs (miRNA) and short interfering RNAs (siRNA). Mature miRNAs are non-protein coding small (20-24 nucleotide) RNAs that bind to RNA-Induced Silencing Complex (RISC), which then bind miRNA at the 3' untranslated region to reduce or inhibit the translation (77–79). Several studies suggest a strong connection between the presence of specific miRNAs and regulation of various osteogenesis steps, acting as both inhibitors of osteogenesis and promoters of osteoblast differentiation. **Table 1.1** provides a brief summary of miRNAs currently explored for stimulation of *in vitro* osteogenic differentiation. The importance of miRNAs have been initially identified from cell culture and mutagenesis models (80,81), but recent activity is beginning to validate their therapeutic utility in preclinical animal models (**Table 1.2**). The latter includes studies where specific miRNAs were directly delivered to a bone repair site to modulate cell fate at the site, or when cells modified with specific miRNAs are implanted in bone repair models. A more detailed list of miRNAs are provided in (82); I present this list to provide a glimpse of non-viral carriers and scaffolds explored

for delivery of this emerging nucleic acid. It has been possible to identify both inhibitory and stimulatory miRNAs on osteogenesis and even silence inhibitory miRNAs to obtain a stimulation of bone induction (83). While one can envision direct delivery of RNA-based agents to modulate cell fate, one can also deliver pDNA expression vectors for *in situ* synthesis of miRNAs or anti-miRNAs.

<b>miRNA</b>	<b>Study outcome</b>	<b>Carrier</b>	<b>Scaffold</b>	<b>Ref.</b>
<b>miRNA-20a</b>	Sustained and controlled release from the hydrogels over a period of 3-6 weeks. Osteogenic differentiation was enhanced.	PEI 25	PEG hydrogel	(84)
<b>miRNA-133a</b>	Enhance of Runx2 and osteocalcin expression. Increase of ALP and calcium deposition.	nHA particles	COL/nHA scaffold	(85)
<b>miRNA-148b</b>	MSCs become susceptible to osteogenic factors. Rapid and robust induction of bone related markers.	Human MSC Nucleofection kit	PEG-NB hydrogel	(86)
<b>miRNA-489</b>	MSCs are becoming susceptible to osteogenic factors. Rapid and robust induction of bone related markers.	Human MSC Nucleofection kit	PEG-NB hydrogel	(86)

**Table 1.1. Specific miRNAs involved in osteogenesis *in vitro*.**

The data are derived from cell culture studies where a specific miRNA was delivered with a non-viral carrier or nucleofection. The cells that were tested were MSC and the type of scaffold used is also indicated.

miRNA	Study outcome	Carrier	Scaffold	<i>In vivo</i> model	Ref.
miRNA-26a	Improves vascularization & bone regeneration. HP-HA-PEG system improves miRNA-26a expression.	siPORT NeoFX	HP-HA-PEG hydrogel	Calvarial bone defect in mouse	(87)
	Actions through targeting Gsk-3 $\beta$ to increase osteoblastic activity. Long-term delivery for higher expression of multiple osteogenic genes.	PLGA microspheres	PLLA scaffold	Subcutaneously in mouse	(88)
antimiRNA-31	Increase in the expression of osteogenic genes <i>in vitro</i> . Robust new bone formation <i>in vivo</i> . The miRNA-scaffold system improved (~60%) <i>in vivo</i> bone formation.	Lentiviral	Poly(glycerol sebacate) scaffold	Cranium bone defect in rat	(89)
miRNA-34a	Modulator of osteoblastic differentiation of MSCs. Targets JAG1-ligand for Notch 1. Controls both hMSCs proliferation and osteoblast differentiation.	Lipofectamine	3D-spheroid HA/TCP scaffold	Heterotopic model in mouse	(90)
miRNA-135	Upregulation during osteogenesis of rat ADSCs. Overexpression promotes bone formation.	Lipofectamine	Poly(sebacoyl diglyceride)	Calvarial bone defect in rat	(91)
miRNA-148b	miRNA-148b & -196a showed more osteoinductive effects. Co-transduction of hASCs with miRNA-148b accelerates bone formation <i>in vivo</i> in 12 weeks.	Baculovirus	PLGA scaffolds	Calvarial bone defect in mouse	(92)
miRNA-196a					
miRNA-29b					
miRNA-26a					
miRNA-216a	Promotes osteogenic differentiation of hASCs <i>in vitro</i> and bone formation <i>in vivo</i> .	Lipofectamine	HA/TCP scaffold	Subcutaneously in mouse	(93)

**Table 1.2. Specific miRNAs involved in bone repair *in vivo*.**

The data are derived from animal models where a specific miRNA was delivered into a bone defect with a non-viral carrier and a scaffold.

Double-stranded siRNAs, on the other hand, are synthetic entities that can target specific mRNAs and inhibit their translation after binding by pair-specificity on mRNA. **Table 1.3** and **Table 1.4** summarize, respectively, recent siRNA targets employed for *in vitro* stimulation of osteogenic differentiation and bone repair in animal models. The early activity on siRNA delivery in animal studies, which involved specific siRNA against Plekho1 (casein kinase-2 interacting protein-1), GNAS1 and PDH2 combination(71), were recently expanded with siRNAs against numerous new protein targets. Representative non-viral delivery agents and scaffolds used for osteogenesis are provided in the Tables 1-4.

siRNA	Study outcome	Carrier	Scaffold	Ref.
Noggin	Sustained and controlled release from the hydrogels over a period of 3-6 weeks. Enhance of osteogenic differentiation.	PEI 25	PEG hydrogel	(84)
	Over 98% intracellular uptake of MC3T3-E1 cells after 48h. Reduction in the use of rhBMP-2 by knockdown BMP-2 antagonists.	Lipofectamine	Fibrin hydrogel	(94)
	Stimulation of BMP signalling by downregulate Noggin. Promotion of osteogenesis.	Lentiviral particles	Chitosan/Chondroitin sulfate (Apatite-coated) scaffold	(95)
VEGF	Hypoxic conditions can stimulate cell proliferative response. Activation of PI3K/Akt plays a vital role in inducing proliferation, osteogenesis and angiogenesis.	Lipofectamine	Natural bone-derived scaffold	(96)

**Table 1.3. Specific siRNA targets involved in osteogenesis *in vitro*.**

The data are derived from cell culture studies where siRNA against specific targets was delivered with a non-viral carrier.

siRNA	Role/Study outcome	Carrier	Scaffold	<i>In vivo</i> model	Ref.
Noggin	Efficient gene knockdown with minimal toxicity. Osteogenesis promotion <i>in vitro</i> and bone regeneration promotion <i>in vivo</i> .	Stereosomes Lipofectamine	Methacrylated glycol chitosan hydrogel	Calvarial defect in mouse	(97)
Cbfa-1	The NPs easily enters the hMSCs <i>in vitro</i> and can differentiate into chondrocytes. High markers expression in mature chondrocytes.	PLGA-PEI particles	NO	Subcutaneous injection in mouse	(98)
Plekho 1p	The presence of CH6 improves <i>in vitro</i> osteoblast-selective uptake of the siRNA. Promotion of bone regeneration <i>in vivo</i> .	CH6-Lipid nanoparticles	NO	Injection to ovariectomized rat	(99)
siCkip-1 siFlt-1	Upregulation of osteogenic and angiogenic genes. Promotion of bone regeneration <i>in vivo</i> .	Lipofectamine	Chitosan sponge	Calvarial defect in rat	(100)
CTRP3	CTRP3 is a negative regulator of RANKL. Acts as an inhibitor of NFATc1 activation through the AMPK pathway.	Lipofectamine	NO	Calvarial defect in mouse	(101)

**Table 1.4. Specific siRNA targets employed for bone repair in animal models.**

**1.7.1.1 Cationic Polymers as pDNA Carriers.** Cationic polymers like polyethylenimine (PEI), polyamidoamine, cationic polycarbonates and polyamino acid based polymers are the most studied material in non-viral gene delivery due to their facile chemistry, cost-effectiveness and safety profiles (74,102). Multivalent electrostatic interaction between cationic amino groups of polymers and anionic phosphate groups of DNA molecules forms condensed polyionic complexes

(polyplexes). These complexes enhance cellular uptake via interaction with anionic cell surface proteoglycans and increase nucleic acid half-life in cytoplasm.

So far, polyethyleneimine (PEI) is the most commonly used chemical carriers for both *in vitro* and *in vivo* applications. The starting monomer for PEI synthesis, aziridine, is a three-membered ring which in the presence of a catalyst is converted into a highly bonded polymer that contains primary, secondary and tertiary amine groups. The amine groups makes it possible to go under hydrophobic modification while maintaining its buffering capacity. The high positive surface charge of PEI facilitates formation of complexes (polyplexes) with the negatively charged DNA molecules. PEI has the ability to act as a “proton sponge” which can escape from endosomes (103). Studies confirmed that high molecular weight (MW) PEI’s (25kDa) led to polyplexes with high transfection efficiency and high toxicity (104). The toxicity is related with the strong positively charged surface of the polymer which leads to strong interaction between the polymer and the cell surface.

On the other hand, by lowering the PEI molecular weight (1.2-2 kDa), the complexes are less cytotoxic but can be less effective due to weak polymer-DNA binding and low protection of transfecting DNA from the nucleases (105). To address such critical challenges studies have shown that chemical modification of different substituents, overall hydrophobic-hydrophilic balance of the conjugates and chemical structure of the hydrophobic segments may improve the transfection efficiency by improving the interaction between polyplexes and cell membrane (106,107). In particular, hydrophobic modification of PEI1.2 and PEI2 with long or short aliphatic chains and different degrees of unsaturation and substitution has shown some promising approaches to improve transfection efficiency in endothelial (ECs) and vascular smooth muscle cells (VSMCs) (108).

**1.7.1.2 Other Carriers for Nucleic Acid Delivery.** Cationic lipids were the earliest materials explored in gene delivery (109). They are composed of three structural domains; a cationic head group, a hydrophobic tail and a linker between these domains. Cationic head group is the specific component that interacts with nucleic acids, forming nano-sized 'lipoplexes' or cationic liposomes. These complexes are usually small enough (~100 nm) for cellular uptake and resilient enough to protect the payload against digestion (110,111). Main cationic lipids used in therapeutic delivery and bone tissue engineering are shown in **Figure 1.1** (99,112). As an example of comprehensive approach, Zhang et al. reported a sophisticated formulation for a bone-targeting liposomal system (AspSerSer)<sub>6</sub>-DOTAP encapsulated with a siRNA specific for PleKho1(112). (AspSerSer)<sub>6</sub> specifically target to osteogenic-lineage of the cells, the osteoblasts at tissue level. As another example of recently emerging delivery system, Liang et al. reported aptamer-functionalized lipid NPs for osteogenic siRNA delivery. The integration of aptamer onto lipid NPs is to facilitate endocytic uptake (99). Systemic delivery of these carrier in an animal model selectively accumulated siRNA in osteogenic/osteoblast cells and subsequently depleted PleKho1, resulting in enhanced bone micro-architecture and tissue mass. Lipoplexes were also utilized to promote bone regeneration with the 'cell-sheet' technology, where regenerative repair is achieved with a dense sheet of cells with abundant endogenous ECM (113). Yan et al. reported on the *in vitro* osteogenic differentiation of BMSC-sheet after transfection with antimiR-138 using Lipofectamine<sup>TM</sup> 2000 (114). The latter is a commonly used transfection reagent that is derived from cationic lipids (exact formulation not disclosed by the manufacturer) and is recommended for cell culture studies, but not preclinical (animal) studies. The antimiR-138 delivery, by down-regulating endogenous miRNA-138 and activating extracellular signal-regulated kinases

pathways, enhanced the expression of runt-related transcription factor-2 (RUNX2), osterix, osteocalcin and BMP-2 at miRNA and protein levels. *In vivo* results from these BMSC sheets were also exciting in immunocompromised mice for bone regeneration. Lipofectamine has been also used to enable RNAi knockdown of specific inhibitors of BMPs (115). Lipofectamine mediated siRNA delivery to preosteoblast MC3T3-E1 cells through hydrogel surfaces substantially down-regulated inhibitory noggin miRNAs (94). The Lipofectamine-based cationic liposomes were also incorporated into scaffolds that maintained the integrity of siRNAs for longer period. In a recent study, Jia et al. reported a porous chitosan scaffolds bearing Lipofectamine™ 2000/siRNA (siCkip-1 and siFlt-1) complexes (100). The bioactivity of these scaffolds was studied by growing bone marrow MSCs; the loaded siRNAs remained intact for 2 weeks. The target genes were significantly silenced and upregulation of ALP activities, VEGF and osteocalcin were clearly observed in MSCs as a result of siRNA delivery.

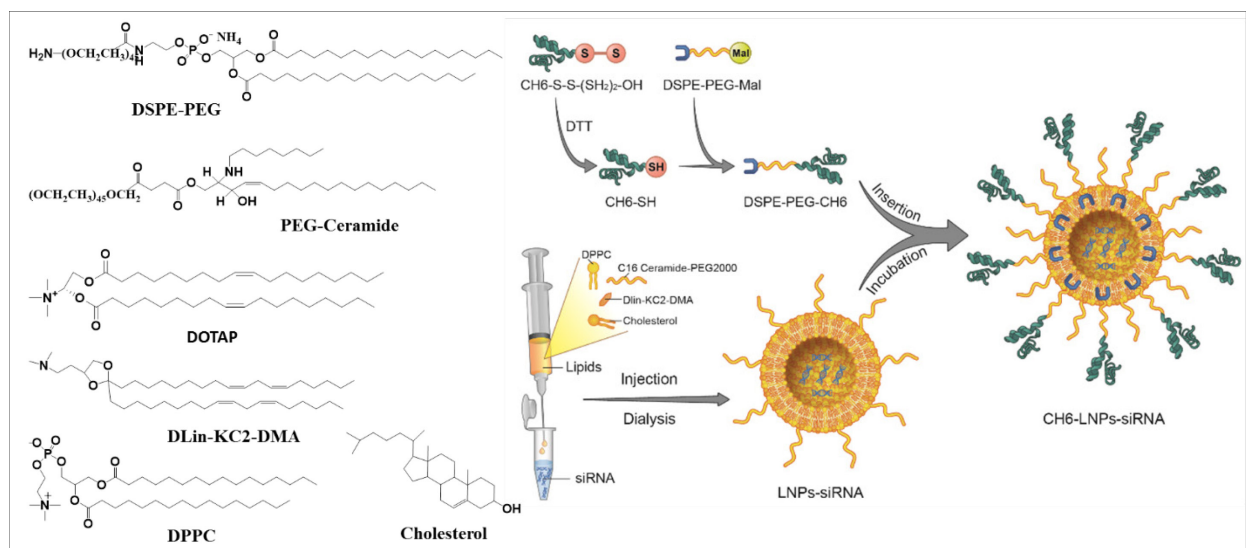


**Figure 1.2. Chemical structure of cationic lipids and schematic of targeted NP preparation of described in this review.**

DSPE-PEG: 1,2-distearoyl-sn-glycero-3-phosphoethanolamine-N-[amino(polyethylene glycol)],  
 PEG-Ceramide: N-palmitoyl-sphingosine-1-succinyl[methoxy(polyethyleneglycol)], DOTAP:  
 1,2-Dioleoyl-3-trimethylammonium-propane, DLin-KC2-DMA: 2,2-Dilinoley-4-(2-

Dimethylaminoethyl)- [1,3]-Dioxolane, DPPC: 1,2-Dipalmitoyl-sn-glycero-3-phosphocholine. The schematic of NP formulation was adopted from reference (99).

Inorganic nanomaterials have been used as gene carriers due to unique features such as light scattering, localized surface plasmon resonance effect and photothermal effect (116,117). In recent studies, mesoporous bioactive glass nanospheres and silica NPs were explored for siRNA delivery due to their unique bone-binding activity and degradability (118,119), with specific application for treatment of osteoporosis (120,121). The survival of mature osteoclasts, bone resorption and expression osteoclast-specific genes is primarily driven by the interaction of cytokines RANKL and its receptor RANK, present on the surface of osteoclast precursors (122,123). To this end, Kim et al. has reported mesoporous bioactive glass as a potential RANK-siRNA carrier to macrophage RAW264.7 cells (121). These NP sustained the release of the payload over a period of ~4 days and exhibit knockdown of osteoclastogenesis-related gene, including c-fos, cathepsin-K, tartrate-resistant acid phosphatase (TRAP) and nuclear factor of activated T-cells cytoplasmic-1 (NFATc1). Gold NPs is another unique carrier for gene delivery (117). Tunable size and optical properties based on the size along with outstanding biocompatibility makes gold NPs a good choice for diagnostic and therapeutic application (124). Zhao et al. has reported on delivery of LSD1-siRNA and consequent impact in differentiation of hMSCs with gold NPs (125). LSD1 maintains the pluripotency in embryonic and other stem cells (such as neural and leukemic stem cells) so that silencing of LSD1 can down-regulate stemless and up-regulate differentiation genes (126). LSAD1-siRNA was successfully grafted onto gold NPs by coating with poly(sodium 4-styrenesulfonate) and poly-allylamine hydrochloride (125). The delivery of LSD1-siRNA to hMSCs significantly induced the differentiation of hMSCs into a hepatocyte lineage.

Numerous 20 miRNAs have been described the last years to be involved in osteogenesis, where the majority of the studies examined the therapeutic applications of the new miRNAs. Most studies were reported with a single miRNA concentration (typically 50 nM, **Figure 1.4**) and this raises questions about the actual effectiveness of the miRNA since a dose-response relationship is paramount to fully assess the outcome of the therapy. Only limited number of studies had used scaffolds as miRNA reservoir and only one study used <50 nM miRNA dose.

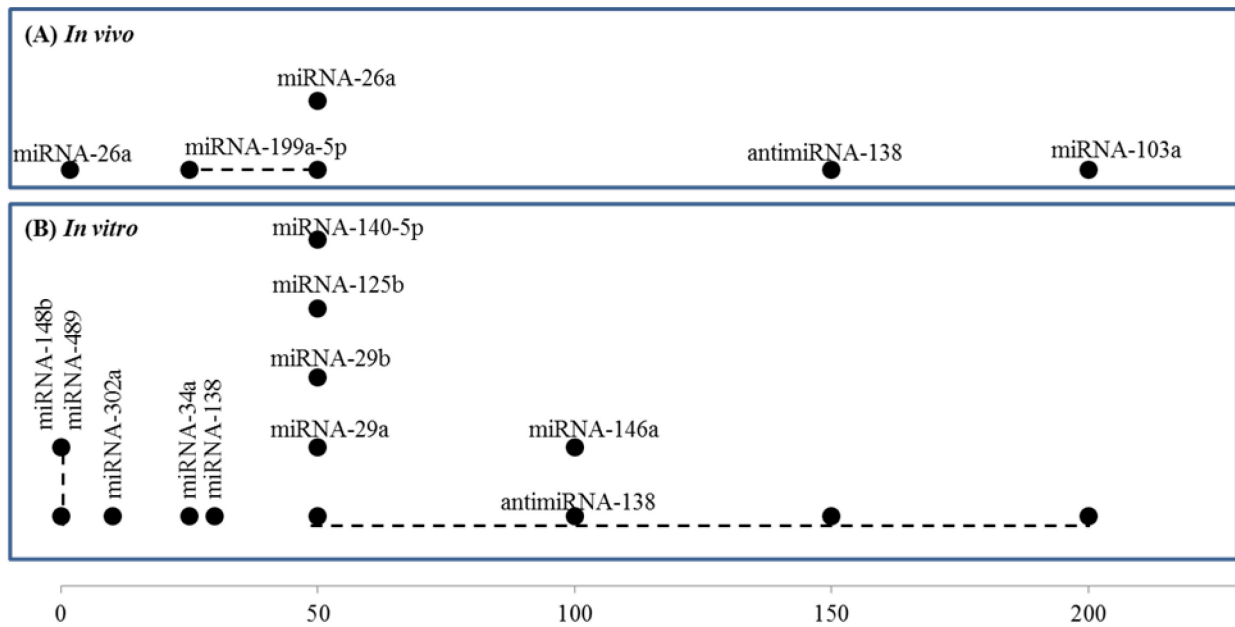


**Figure 1.3. miRNA concentrations (nM in horizontal axis) delivered by non-viral carriers *in vitro* and *in vivo*.**

The dash line between points indicates the test of different concentrations in the same study.

### 1.7.2 Incorporation of GFs into Scaffolds

Indeed, three dimensional (3D) scaffolds should be a bridge between the *in vitro* (2D) and *in vivo* (3D) environment. But while the design of the scaffold can influence tissue formation, the addition of biomolecular agents like GFs or genes can promote the desired cellular response needed to accelerate the formation of new tissue. Studies have shown that the release of pDNA from 3D scaffold which closely imitates the natural *in vivo* condition of cells has resulted in greater

encoded protein expression than a similar amount of pDNA delivered through 2D cell culture system (127,128) . As we have seen above, numerous fabrication methods have been proposed for development of new scaffolds that will closely imitate the natural tissue and regulate cellular activity appropriately. However, the scaffold itself has limited capacity to induce differentiation of the surrounding cells. Incorporation of GFs that are involved in regulating different phases of bone regeneration into scaffolds can not only control cellular responses but also accelerate the formation of new tissue. Strategies for incorporation of micro-or nanoparticles into the scaffolds can be either non-covalent (such as surface absorption, physical encapsulation) or covalent (chemical conjugation), the right method depends on scaffolds physicochemical properties as well as the interaction between the GFs and the scaffold. Absorption of GFs on the surface of the scaffold as well as physical encapsulation of factors, covalent or non-covalent binding (including layer-by-layer assembly) to the scaffolds and the use of micro- or nanoparticles as factors reservoirs have been examined as strategies for the incorporation of GFs within the scaffold matrix(129). In the design of scaffolds, the main goal is to display effective release levels for prolonged periods of time and protect the factors from physiological degradation that could reduce their therapeutic efficacy. In general, low affinity interactions between the agents and scaffold will increase the release rates, while by increasing the affinity, the delivery rate can decrease, and the agents will remain in the scaffold.

**1.7.2.1 Absorption of GFs on Scaffolds Surface.** Absorption of GFs on the surface has attracted much attention since it is easy to achieve under physical room conditions. Absorption requires the GFs to be loaded after scaffolds fabrication; however, this method is leading to uncontrolled delivery. For example, the delivery of recombinant human BMPs (rhBMPs) by absorbable collagen scaffolds has been approved by FDA for clinical uses due to promising results that have been obtained in the field of spinal fusion. However, as rhBMPs has a very short half-life and collagen scaffolds have low natural affinity, resulting in burst release of the proteins, a large dose is required in order to be effective (1.5 mg/ml) what may cause adverse side effects (130,131).

**1.7.2.2 Physical Encapsulation of GFs.** Physical encapsulation of GFs involves the blending of the factors within the polymer's solution prior to scaffolds fabrication. The method of direct encapsulation has the advantage that during the scaffold's fabrication the optimized properties and the factors bioactivity are not affected by the process. On the other hand, the low binding between the molecules and the scaffold may lead to the 'burst' (initial uncontrolled rapid) release of the molecules prior to tissue regeneration. The incorporation of GFs within the core-shell structure of fibers seems to be a promising platform for molecules delivery system while they can preserve their bioactivity. Su et al. have fabricated poly(L-lactide-co-caprolactone) PLLACL/collagen fibers by electrospinning a homogeneous solution (BMP-2 and dexamethasone (DEX) embedded in matrix) or fibers by coaxial electrospinning of blended PLLACL/collagen/DEX with BMP-2 solution (BMP-2 in the central core) or by blended PLLACL/collagen with DEX/BMP-2 solution (DEX and BMP-2 in central core). Putting the protein through the voltage gradient did not appear to alter its bioactivity since hMSC seeded on nanofibers with DEX and BMP2 showed higher ALP activity than those seeded on fibers without DEX and BMP-2. In addition, higher ALP activity

was measured by day 21 from cells seeded on core fibers compared to blended fibers due to the slower release rate of BMP-2 by the core fibers (132).

Other approaches aiming on further mimicking ECM functions by modifying carrier's composition to contain naturally derived components which are involved in receptor-ligand interactions in native tissue. The presence of heparin, heparin sulfate, gelatin and fibronectin can provide specific biological sites for BMP-2, BMP-7, PDGF-BB and VEGF immobilization by increasing the electrostatic attractions between the GFs and the matrix. Zhang et al. studied the production of PLCL fibers with heparin added by emulsion or by chitosan hydrogel in the core, for the delivery of bFGF. The studies outcomes showed that the presence of heparin by emulsion reduced the release amount of bFGF around 25% while the presence of chitosan hydrogel core increase the release by 64% in the first week (133).

## **1.8 Scaffolds in Bone Regeneration**

A major focus in bone tissue engineering is the development of implantable scaffolds that will closely imitate the natural tissue. Scaffolds intended for bone should be biocompatible, display controlled biodegradability and appropriate pore size and should provide the right mechanical support. A highly porous scaffold (pore size >90%) has been shown to influence cell adhesion which promotes osteointegration, nutrient/GF transfer and vascularization (134). The mechanical strength is an important consideration, since the scaffold tends to become mechanically fragile over time while undergoing degradation (135). A scaffold can be further modified to mimic physiological aspects (i.e., cell adhesiveness) of native bone tissue matrix. A variety of biomaterials, either synthetic, natural or biomimetic, have been explored as 3D scaffolds for bone tissue repair due to their inherent bioactivity with the ability to promote cell adhesion, proliferation and differentiation with no apparent cytotoxic effects (136–139).

### 1.8.1 Collagen as the Foundation of a Biomimetic Scaffold

Natural biomaterial-based scaffolds (e.g., collagen, gelatin and chitosan) represent promising materials to mimic bone architecture. These scaffolds have been extensively used for bone regeneration due to good biocompatibility and osteogenic capabilities. In general, collagens are formed by three identical polypeptide chains or by two or more different  $\alpha$  chains, described as  $\alpha_1$ ,  $\alpha_2$  and  $\alpha_3$ . Collagens that contain three identical chains are called homotrimers like collagens type II, III, VII, VIII, X and or different to form heterotrimers like collagens type I, IV, V, VI, IX and XI (140). The collagen members can be broadly divided into fibrillar and non-fibrillar collagens. The 90% of the total collagen is represented by the fibril-forming collagens like collagens Type I, II, III, V, XI, XXIV and XXVII.

Collagen type I has been widely examined for scaffolds since it is the primary ECM protein and major component of the organic phase of bone. It can be readily extracted from animal sources like bovine, porcine and lamp as well as human sources like placenta (141), marine sources like shark, grass carp (142) or via recombinant genetic engineering systems (143–147). It consists of two identical  $\alpha_1(I)$  chains encoded by COL1A1 and one  $\alpha_2(I)$  chain encoded by COL1A2, with long (300 nm) and thin (1.5 nm diameter) structure. Collagen based biomaterials can be produced by decellularization of the collagen matrix which retains the original shape and ECM structure or by extraction, purification and polymerization of collagen and then formation of a functional scaffold. Depending on the collagen source, extraction method and post-processing methods used will result in collagen preparations with different properties (148,149). In general, the nature of the crosslinks in different tissues determines the solvent to be used and the corresponding yields. Extraction methods of collagens can be adjusted based on the nature of collagen in the tissue to be extracted: i.e., into salt-soluble, acid soluble and pepsin-soluble collagen(150).

**Acid soluble extraction method** is the most common isolation method of collagen type I from collagen-rich tissues as tendon and dermis, which involves the breaking down of the tissue via enzymatic digestion and/or dissolution in acid. Depending on the application and the desired characteristics of the collagen, the tissues can be immersed in either acidic solvent (e.g., with 0.5 M acetic acid or HCL with pH of 2-3) or enzymatic solution (e.g., Pepsin) or in both of them in some cases (151,152). In general, the isolation procedure varies with the enzyme and acid strength. The use of acetic acid will solubilize the uncrosslinked collagens and will break some interchain crosslinks like aldimine type (bonding between hydroxylysine and lysine aldehyde molecules). The crosslinks are dissociated by the acids when the repulsive repelling charges on the triple-helices will lead to swelling of fibrillar structures. In addition, the telopeptides will be affected with a limited proteolysis, but their structural integrity of the super triple helix will not be affected. In general, the acidic extraction involves the freezing of the tissue, washed with neutral saline to remove soluble proteins and polysaccharides, and the collagen extracted with a low ionic strength.

**Salt-soluble extraction method** can be applied to newly synthesized collagens that are not incorporated yet into tissue networks and can be extracted using a cold neutral salt solution, which leads to receiving a low collagen yield and purity. The most commonly used solvents are pH neutral salt solution (0.15–2 M NaCl) or dilute acetic acid. By modifying the temperature, shaking rate and the volume of extractant to tissue ratio, it is possible to alter the composition of the collagen derived. The majority of tissues have limited or no salt-extractable collagen, so that this is not a large-scale preparation procedure. In case salt-soluble methods are to be used, the animals have to be fed  $\alpha$ -aminopropionitrile, which is an inhibitor of peptidyl lysyl oxidase. However, this procedure is inadequate for larger commercial scale.

The **pepsin-soluble** extraction method is able to disturb the stabilized molecular structure by cleaving the telopeptides on the ends of collagen molecules and therefore increases the efficiency of the dissolution. During the tissue collagen extraction around ~2% is extracted with only salt or acid solutions extraction process. The remaining 98% is referred as insoluble collagen which can further be cleaved with the use of enzymes or strong alkali. The pepsin-soluble collagens have higher cost, longer production time and higher yield compared to acid-soluble collagen (153). By altering variables such as temperature, pH, ionic strength the collagen molecules are able to self-assembly *in vitro* (fibrillogenesis). During fibrillogenesis after acid soluble process, the fibrils are reconstituted and show characteristics of 64 nm banding that is similar to the *in vivo* compared to the fibers formed from proteolytic enzymes since complete removal of the telopeptide region prevents collagen fibril formation *in vitro* (149,154,155).

### **1.8.2 Chemical Crosslinking of Collagen Scaffolds**

Native collagen contains multiple inter and intramolecular crosslinks that provide strength and durability to the tissues. However, studies have demonstrated that extraction and purification during native collagen processing can reduce the native's collagen crosslinking density with consequent impact on mechanical and degradation features of scaffolds (156). The introduction of exogenous crosslinks into the molecular structure of the collagen implants are able to overcome such obstacles. Studies have shown that cross-linkers on collagen may interfere with integrin ligands and cause decrease in cell attachment, proliferation and migration. In addition, the selection of a cross-linker must ensure that cytotoxicity effects are minimized (157). The different crosslinking methods can be classified into chemical, physical or biological in nature and have the ability to form covalent bonds between collagen molecules using chemical or natural moieties that

bind either to the free amine or carboxyl groups of collagen. The most common chemical crosslinkers are the aldehydes reagents such as glutaraldehyde (GA), isocyanates and carbodiimides which are producing scaffolds with high mechanical properties and durability. Most of the reagents including GA form a chemical 'bridge' intermolecularly and intramolecularly (158). However, unwanted cytotoxicity, calcification and foreign body responses are limiting their applications (159,160). Regarding the potential cytotoxicity to chemical crosslinkers, physical crosslinking such as dehydrothermal treatment (DHT) and ultraviolet irradiation (UV) or biological crosslinkers such as enzymes (e.g, transglutaminase) and plant extracts (e.g., genipin) have been expected to reduce cytotoxicity of the biomaterials (**Table 1.5**). Among the physical crosslinkers, the DHT can provide high strength ( $\approx 50$  MPa) but could induce protein denaturation which can lead to rapid degradation of the scaffold *in vivo* by nonspecific proteases. The ultraviolet irradiation (UV) can also provide high strength but the fibers may retain more of their native structure as compared to DHT (161,162). On the other hand, scaffolds that were crosslinked with genipin have shown mechanical properties of  $\sim 250$  Pa and low cytotoxicity as compared to those without chemical crosslinking (163).

Method	Crosslinking reaction	Biological reaction	Ref.
<b>Chemical</b>			
GA	Formation of short aliphatic chains and pyridinium compounds	Produces toxicity & classical agents	(160)
EDC/NHS	Catalysing bindings between amino & carboxylic acid groups	Low toxicity, Zero length cross-links are formed & water soluble by-products	(164)
HMDI	Formation of aliphatic chains containing urea bonds between two adjacent amine group	Produces toxicity	(165)
<b>Physical</b>			
Ion-beam and gamma ray irradiation	Generation of free radicals that is formulating polymer chain scission or crosslinking	Not well controlled, potential irradiation hazard, nonuniformity and heterogeneity of irradiation dose	(166,167)
DHT	Water removal from collagen molecules that forms crosslinking between carboxyl and amino groups of adjacent amino acid side chains	Protein denaturation. No cytotoxicity	(162)
UV irradiation	Generation of free radicals on tyrosine and phenylalanine residues	Lower protein denaturation. No cytotoxicity	(159,162)
<b>Biological</b>			
Transglutaminase	Formation of amide bonds between the glutamine and lysine	Low cytotoxicity	(168)
Genipin	Covalent binding between amino groups, and can bind to other genipin molecules	Low cytotoxicity	(169)

**Table 1.5. Various processing conditions used for generating functional collagen-based scaffolds.**

### 1.8.3 Porosity of collagen scaffolds

Collagens with three-dimensional (3D) porous structures have been extensively applied as scaffolds in the field of tissue engineering. During the design of a new scaffold, the biophysical and biochemical properties of the biomaterial are critical. The pore size, pore size distribution, pore volume, shape, wall roughness and permeability between the interconnecting pores are known regulators that will affect the cell growth, adhesion, proliferation and differentiation. In addition, pores provide the scaffolds with specific structural, morphological and mechanical properties (170). The importance of controlling the pore size has been emphasized by different experiments

since it can affect the phenotype of the bound cells. Cells inside small pore channels ( $>200\ \mu\text{m}$ ) are able to bind over the entire surface of the 3D scaffold and possess a different phenotype than the cells that are inside larger pores. In bone regeneration, the optimum range of pore size was found to be within 200 and 350  $\mu\text{m}$  since scaffold with  $>350\ \mu\text{m}$  porous size was too big for the cells to interact with the scaffold under static conditions (171,172). Pores interconnectivity is also crucial to ensure that all the cells are within 200  $\mu\text{m}$  distance from blood supply. The optimal pore size for bone regenerative scaffolds is still controversial; Akay et al. suggested that osteoblasts populate smaller pores (40  $\mu\text{m}$ ) when osteoblasts were grown in PolyHIPE (i.e., porous emulsion-templated polymers synthesized within high internal phase emulsions) scaffolds with different pore sizes, but pore size larger than 100  $\mu\text{m}$  facilitated cell migration into implants. In general, the total porosity should be higher than 50-60 vol%, the interconnection size should be higher than 50-100  $\mu\text{m}$  and strut porosity should be higher than 20 vol% (170,173). It is crucial to balance the physical and biological properties of the scaffolds since degradation rate should match the formation of the new tissue (174).

Successful regenerative activity of scaffolds mainly depends on the response from the cells with which they are seeded or populated from the tissue that is being targeted. The response of the target tissue to the materials' presence is strongly influenced by the site of implantation, the host species, and the size of the implant. The interactions between the implant and the host organism should not show any harm due to induced cytotoxicity, adverse responses or activation of the blood clotting or complement cascades (175,176). Structural features like identification of the scaffold surface by the cells, the pore size and the duration of scaffolds biodegradability can have an impact on cell-scaffold binding (177). In addition, the surface characteristics of the implants such as wettability, hydrophilicity/hydrophobicity ratio, bulk chemistry, surface charge and charge

distribution, surface roughness and rigidity can alter the behaviour of the adsorption and desorption of adhesion and proliferation of cells on the material (178).

In the case of collagen scaffolds, (i) the periodic banding of the collagen fiber structure must be selectively abolished to prevent platelet aggregation, (ii) the chemical composition must incorporate ligands appropriate for the binding of cells specific to the application area, (iii) the scaffold should possess open pores, with fully interconnected geometry in a highly and controlled biodegradability to allow the scaffold to remain insoluble for a desired period (179). Only a small number of people have shown an allergic reaction in response to collagen-based devices. Collagen can improve the cell migration *in situ* and cell attachment by offering native biochemical signalling to cells. Collagen can interact directly or indirectly with a variety of cell trans-membrane receptors. During the direct cell-collagen interaction, cell receptors recognize specific peptide sequence within collagen molecule. Four different receptors have been identified:

- a) Receptors like glycoprotein VI that can recognize the peptide sequence containing Gly-Pro-Hyp (GPO),
- b) Collagen binding receptor members of integrin family and discoidin domain receptor 1 and 2 (DDR1 and DDR2) which are binding mostly to Gly-Phe-Hyp. Functional integrin contains an alpha ( $\alpha$ ) subunit, which recognizes the ligand in the ECM while beta ( $\beta$ ) subunit sets cellular events in motion. The cell type and the development stage of the cell can influence the integrin subunits present at the cell surface.
- c) Integrin-type receptors that recognize cryptic motifs within the collagen molecule ( $\alpha_1\beta_1$  and  $\alpha_2\beta_1$ ), and
- d) cell receptors that directly bind collagen at the non-collagenous domain.

One of the key molecules during the indirect cell-collagen interactions is fibronectin, which is bounding to integrin that is attached to Arg-Gly-Asp (RGD) sequence. Moreover, many proteins containing RGD or similar sequences can be recognized by integrin and bind to collagen via indirect cell-collagen interactions.

Changes in the structure, chemistry or mechanical microenvironment of collagen used in scaffold preparation can alter the number or conformation of cell adhesion ligands, thus affects scaffold's *in vivo* performance. Preservation of ligands which are communicating with cells during scaffolds formation is extremely important. Various physical forms of collagen type I (sponges, hydrogels, fibers, films) are used clinically due to its physiological compatibility, ready availability and low cost (180,181). A wide number of fabrication techniques like freeze-drying, solvent casting, 3D printing, phase separation, electrospinning, and chemical modification have been used for the production of 3D scaffolds (182–184). Below I describe some of the common fabrication approaches to scaffold preparation.

## **1.8.4 Fabrication of Collagen Scaffolds**

**1.8.4.1 Collagen Scaffolds by Lyophilisation.** In general, collagen sponges are typically formed by lyophilisation (freeze-drying) an aqueous collagen solution. The process includes the solidification (freezing) of the solution at low temperature and then subsequent sublimation of the ice crystals by reducing the environmental pressure, leading to a highly porous structure. The pore structure is a replica of the ice crystal morphology after freezing. During the process, the water is removed that leads to intramolecular cross-linking between the collagen aggregates (185). The use of acetic acid as a solute addition results in dendritic formation of ice and therefore interconnected porosity. In the case of an insoluble collagen type I, the covalent cross-links are irreversible so that a stable collagen sponge is formed. By controlling the volume fraction of the precipitate (collagen)

in the suspension, the freezing temperature and rate of evaporation, one can control the porous structure, size and the mechanical properties of the resulting scaffold. Fast freezing at low temperature may induce cracking, uniform small channels and the production of a fibrous structure. On the other hand, slow freezing at higher temperature results in non-uniformity and large pores with pores collapsed pores than continuous channels.

**1.8.4.2 Collagen Scaffolds by Electrospinning.** Electrospinning have been used for over a decade to create collagen fibers. The principle involves the application of an electric field to draw out a fine thread of charged polymer solution. The polymers solution is ejected from a syringe and is drawn toward a charged collector, producing fibers with diameters ten to hundreds of nanometers. Typically the electrospinning method can produce ultra-fine fibers sheets with special orientation, high surface area and high aspect ratio which can be controlled by various parameters such as applied voltage, viscosity, solution conductivity and temperature (186–188). However, the major challenges of the electrospinning are the fabrication of complex 3D scaffold shapes, poor mechanical properties, low porosity and pores size (189,190).

**1.8.4.3 Collagen Scaffolds by Three-Dimensional (3D) Printing.** The methods presented above has several limitations for fabrication of scaffolds with precise pore size, pore geometry, high levels of interconnectivity and high mechanical strength. 3D printing method allows fabrication of highly property flexible scaffolds. The current 3D printing methods typically involve imaging of a structure by using Computer Aided Design (CAD), Magnetic Resonance imaging (MRI) or Computer Tomography (CT), which is then relayed to a printing system to ‘print’ the desired scaffold. During the printing, the nozzle extrusion system may move side to side and up & down along one plane. The final scaffold structure is a result of a layer-by-layer deposition. The scaffold

can be cross-linked or polymerized through heat, UV or binder solutions. The 3D technique can create scaffolds with complex shapes, controlled pores size and interconnectivity and the resultant scaffolds have the ability to support cell growth and tissue formation. However, the printing technology that will be used can affect the stability and the properties of the scaffold. In addition, the production time of the scaffold is increased as the scaffolds design becomes more precise and intricate (191,192). Wu et al. reported the design of human corneal epithelial cells (HCECs)/ collagen/ gelatin/ alginate hydrogel using 3D printing method. The 3D printing hydrogel had interconnected channels, macroporous structure and achieved cell viability of 90% (193). Lee et al. designed a collagen-based scaffold that was chemically crosslinked and coated with a thin layer of alginate for drug delivery. The scaffolds were highly porous and the drug release was well controlled (194).

### **1.8.5 Presence of Hydroxyapatite**

The ability of creating a stable bond with the host tissue is very important during the scaffold formation. In this regard, the incorporation of hydroxyapatite (HA) which has a similar chemical and crystallographic structure to the bone's inorganic phase, has been extensively used due to the good biocompatibility properties and good osteoconductive and osteoinductive capabilities (88). Studies have shown that the presence of HA which is a good source of calcium and phosphate ions necessary for the survival of the cells enhances cell adhesion sites that result in higher cell attachment (89). In addition, has been shown that supports binding and release of GFs since it is difficult to incorporate therapeutic agents without destroying the biofunctionality of its surface (90). To overcome these shortages, incorporation of HA with collagen in a porous scaffold can mimic the composition and structure of natural bone as well as increase the degradation and mechanical properties (91,92). Lately, studies have focused on the synthesis of

collagen scaffolds that mimic the hierarchical structure of bone at the different length scales. This approach involves self-assembly of collagen fibres and the use of a supersaturated calcium and phosphate-containing solution stabilized by polyelectrolytes like polyaspartic acid, polyacrylic acid, and poly(allylamine) for the formation of intrafibrillar mineralization *in vitro*. This in-well plate mineralization system that allows a spatial control from the top to the bottom mineralization and a control over the mineralized layers and their thickness (195).

### **1.8.5 Mechanical Properties of Scaffolds**

One of the major differences between an *in vitro* culture of cells in scaffolds and an *in vivo* system is the variation in mechanical properties. Mammalian tissues exhibit a vast range of stiffness, such as 10-75 kPa for human skeletal muscle, ~0.76 to 20 GPa for trabecular bone and 0.1-30 kPa for human breast tissue (196,197). By exposing cells to matrices that mimic the mechanical properties of the damaged tissue, a better reflection of the conditions the native cells can be obtained. Controlling the mechanical properties of the material can enhance the successful application of a scaffold. The formation of the new tissue relies on the scaffold's mechanical properties on both the macroscopic and microscopic level. Macroscopically, the scaffold should provide stability during tissue formation and maintain its volume (182,198,199). The mechanical performance of the scaffold depends on specifying, characterizing and controlling the materials mechanical properties including elasticity, compressibility, viscoelastic behaviour, tensile strength, and failure strain. It is essential to retain the mechanical strength of the scaffold after implantation since the scaffold temporarily withstands and conducts the loads and stresses that the new tissue will ultimately bear such as bone and cartilages especially when the healing rate vary with age (182). As an example, at young patients, the fractures normally heal in about 6 weeks,

with complete mechanical integrity and complete recovery in a year (200). Collagen based scaffolds have poor mechanical properties and the crosslinking of the scaffolds in most case is mandatory to enhance the stiffness. However, the range of stiffness that can be achieved in comparison to most other polymer systems is limited. A final consideration for the mechanical properties is the degradation rate of scaffolds. The degradation can involve physical, chemical or biological process. (201). In order to test the mechanical properties of the scaffolds a great development of mechanical tests has been established such as uniaxial extension, compression, indentation and dynamic mechanical. For large scale samples, the uniaxial strain test is the most applicable where the sample is grasped at the two ends and pulled while axial strain ( $\epsilon = \Delta L/L$ , the change in length divided by the initial length) and stress ( $\sigma = F/A$ , where F the force per unit area and A is the area of the cross-section) are simultaneously measured (202). In many cases the use of uniaxial test alone can provide data necessary to fully characterise the mechanical properties of sample; planar biaxial testing provides information similar to those experienced *in vivo* (203).

The less than desirable mechanical properties of collagen scaffolds have been noted and measures were taken during fabrication processes to improve the mechanical properties. Dhand et al. reported the fabrication of electrospun collagen mats doped with catecholamines and  $\text{CaCl}_2$  followed by exposure to ammonium carbonate. The applied methodology resulted in significant enhancement in the mechanical properties of collagen (due to formation of calcium carbonate) without affecting the surface wettability of the composite fibers (204). Kwak et. al. fabricates a micro/nano multi-layered 3D scaffolds of PLGA and collagen by using alternately electrospinning. The incorporation of HA into the Col-PLGA fibrous scaffold improved the bioactive in comparison to the other groups (205).

### **1.8.6 Recombinant Collagen as a Replacement for Purified Collagen**

Collagen products that have been delivered from lived animals are both abundant and inexpensive and have been commonly used for preparation so scaffolds for numerous applications. However, the majority of the preparations may not be highly purified, have the potential to cause harmful inflammatory or immune responses (e.g., collagen allergies) in humans and raise the risk of pathogen transmission, especially potentially life-threatening pathogens (206,207). The use of recombinant protein technology to produce animal component-free collagens holds the key to solving the problems and removing the risks since provides the promise of a safe source and a way to alter several properties of the system by: i) incorporation of non-natural amino acids, (ii) selection of specific domains and their combinatorial design, (iii) functionalization of the sequence, (iv) hybrid designs, (v) production of dynamic stimuli responsive collagens. The use of living organisms as a factory for the production of proteins for biomaterials offers a useful approach to these needs. During recombinant collagen biosynthesis, it is essential to identify the genes that are expressed. So far, mammalian, insect cells, yeast, mice or silk worms, bacterial and transgenic systems have been extensively studied for recombinant collagen production (143,208). Mammalian cells had expressed single procollagen genes that produce homotrimeric type I procollagen, type II procollagen and homotrimetic collagen type V. Recombinant collagen Types I and III are now commercially available and their application can reduce inflammation and immune response. Moreover, bacteria cells are promising candidates as the triple helix can form without post-translational modification. Bacterial collagens have been shown to be non-immunogenic, non-toxic and non-thrombogenic and their potential as vascular grafts is being investigated (209). However, the use of recombinant collagen may lack biocompatibility due to the fact that it does not undergo significant posttranslational modifications (210).

## Thesis Scope

Therapeutic bone regeneration aims to restore normal functions of bone tissue by stimulating the activities of cells and local regenerative milieu; to this end, protein therapies suffer from inherent disadvantages (i.e., due to short half-lives, large doses are needed) that limit their applications. In light of safety concerns with high-dose protein therapies, delivery of pDNA based expression systems have been proposed to deliver proteins at more physiological levels. Gene transfer to bone have been examined for the delivery of BMPs with high weight molecular PEIs which led to low transfection efficacy and high toxicity effects (104). On the other hand, direct injection of expression systems (without a scaffold) can lead to undesired and widespread distribution to other tissues. Several studies have investigated the combined effect of gene delivery via scaffolds to-date. Using this approach, only the cells infiltrating or surrounding the system would be transfected since the scaffold is expected to control the exposure of expression systems to other sites. However, existing delivery systems involve over-simplified scaffolds thus lacking crucial delivery properties since the stiffness, surface chemistry and topography could influence the cell behaviour that will potentially enhance the transfection efficiency as well as induced tissue (211–213). On the contrary, specific binding between the biomaterial and the carrier could provide the opportunity to tune carrier (and complex formulation) affinity for the surface, thereby controlling release and gene delivery.

Based on these knowledge gaps in the field, we hypothesize that the synthesis of low molecular weight PEI carriers for the delivery of BMP-2 plasmid to bone cells will promote osteogenic cell activity. Based on the above hypothesis, we can assume that the delivery of the carriers with modified collagen-based scaffolds, will prolong the duration of transgene expression as well as provide physical support for cell growth and differentiation. In addition, the design of

this two-method scaffold fabrication that we are facilitating, can further affect the outcome of the delivery of the carriers.

This thesis is composed of several chapters, which correspond to studies with different specific aims. Below I summarize the specific aim of each chapter along with methodological details used to reach the specific aim.

We first performed a literature review (**Chapter 1**) to review the most current knowledge around bone regeneration, the available molecular agents for bone regenerative treatments and their limitations as it was a lead target in other chapters. We focused on and presented the relevant aspects of the bone biology as well as the understanding of the bone formation and fracture healing process. We then explored the gene delivery therapies including pDNA, miRNA and siRNA delivery systems via non-viral polymeric carriers and presented the challenges that need to be considered. Finally, we highlighted the importance of incorporating the gene particles into scaffolds and focused on the design properties for efficient particles delivery on the side of the defect. This Chapter identified and presented key considerations required for a gene-based bone regenerative device. This **Chapter** was published in a modified format as E.K. Tsekoura, Remant Bahadur KC, H. Uludağ. Biomaterials to facilitate delivery of RNA agents in bone regeneration and repair. ACS Biomaterials Science and Engineering (2017) 3: 1195–1206.

Fracture repair involves a series of interactions between cells, growth factors and cytokines. Bone marrow stroma cells as well as progenitor cells derived from periosteum layer play an essential role during fracture healing. Therefore, it is critical to understand the osteogenic differentiation of these cells as a result of gene therapy. The aim of **Chapter 2** was to identify an optimal pDNA delivery system from an in-house prepared low MW PEI library by delivering BMP-2 and PDGF genes to induce osteogenic differentiation in rat primary cells derived from

periosteum (so called periosteum derived cells, PDCs) and calvarial bone (so called bone derived cells, BDCs). The transfection comparison studies between the two different primary cells will reveal the transfection effect differences between the two cell types as well as the challenges in transfecting primary cells. The studies involved (i) polymeric library screening, (ii) physicochemical characterization of carriers, (iii) the quantitative characterization of cellular uptake of polyplexes in PDCs and BDCs with flow cytometry, (iv) cellular proliferation by MTT cell assay and (v) osteogenic differentiation based on ALP activity and (vi) matrix mineralization by using a colorimetric calcium assay.

Based on the initial studies in Chapter 2 and challenges faced by working with primary cells, the first aim of **Chapter 3** was to explore the effective delivery of genes to cell lines (C2C12 and MC-3T3 cells) responsive to osteogenic stimuli. The studies involved identification of the most efficient low MW PEI polymer for delivery of pDNA to both cell lines and the impact on the transfection efficiency with an additive during complexation. Next, we explored the influence of a number of different preparation variables of gene complexes, such as polymer:pDNA ratios, pDNA/additive ratios and final concentration of pDNA on: (i) particle size and  $\zeta$ -potential of complexes, (iii) the quantitative cellular uptake of complexes in cell lines with flow cytometry, (iv) cellular proliferation by MTT cell assay and (v) osteogenic differentiation based on RT-PCR and ALP activity for both cell lines.

The identification of the optimal complex conditions for each cell line should acknowledge the importance of focusing as well on the design of the most suitable scaffold for their delivery. So, the second aim of Chapter 3 mainly focused on the design of intrafibrillar mineralized collagen scaffolds and their ability to prolong the duration of transgene expression to C2C12 and MC-3T3 cells. The optimized complexes for each cell line were incorporated in uncrosslinked (native)

collagen scaffolds, crosslinked (x-linked) collagen scaffolds and intrafibrillar mineralized collagen scaffolds which were examined for their efficient delivery of complexes in both cell lines through various experiments.

The electrospinning method that it is proposed in **Chapter 4** was carried out as an alternative for gene delivery. This work was built on my collaborative work with a visiting PhD student (Ms. P. Pankongadisak), who published on the feasibility of employing electrospun mats for gene delivery in osteogenesis (214). The main aim of this Chapter was to explore the impact of collagen and electrospinning process on the delivery of gene complexes to C2C12 and MC-3T3 cells. As the study onset, we explored monolayer mat formulations that contained different volume ratios of gelatine, collagen and PEG on their effective delivery of complexes to both cell lines. We explored the morphology of the formulated Gel-Col-PEG mats by SEM and then we observed the incorporation of complexes into the mats by delivering Cy3 labelled DNA. Next, we investigated by flow cytometer the cellular uptake of polyplexes in both cell lines. The results of these studies revealed the limitations of using this type of configurations and the importance of establishing a new delivery electrospun system. Later, we evaluated the delivery of complexes via double layer Col/ Gel-Col-PEG mats, we repeated the studies and we examined the delivery of BMP-2 via double layered mats to C12C12 and MC-3T3 cells after 1 week.

Finally, we conclude this thesis with **Chapter 5**, where we present a short review about the delivery of expression vector with viral and non-viral carriers, their incorporation into scaffolds and the *in vitro* and *in vivo* outcomes. A summary of this work with the main outcomes from each chapter was presented as well. Finally, we outlined the future studies that are needed for each chapter as well as the importance of continuing research in bone regeneration field.

## **Chapter 2- In Vitro Modification of Rat Skull Periosteum and Bone Derived Cells Using Non-Viral Polyplexes**

**Some results from this chapter were published in:**

Hydrophobe-substituted bPEI derivatives: boosting transfection on primary vascular cells, Pezzoli D., Tsekoura E.K, Bahadur K.C. R, Candiani G., Mantovani D., Uludağ H. Sci. China Mater., 2017, 60: 529

## 2.1 Introduction

Bone regeneration remains an important problem in the field of regenerative medicine. Bone regeneration is required in a wide range of clinical scenarios and may involve narrow anatomical sites as in the case of fracture healing or massive bone defects in the case of blunt-force traumas. Direct delivery of growth factors (GFs) to repair sites has received great attention due to their promising preclinical and clinical results that, through appropriate signalling, GFs may induce or accelerate the healing process (28). However, clinical studies have recently shown that direct delivery of GFs can result in undesirable tissue responses, notably bone resorption and local inflammation and swelling (36,37). To avoid such complications, gene therapy can be an alternative approach; gene therapy involves transferring a genetic material to local tissue to express a therapeutic protein intended for stimulation of bone regeneration (215,216). Proteins delivered via gene transfer are intended for extended expression *in situ*. Several genes have been examined for this purpose, including genes encoding for Bone Morphogenetic Proteins (BMPs), Platelet-Derived Growth Factor (PDGF), Fibroblasts Growth Factors (FGFs) and transcription factors associated with bone/cartilage-related gene expression (217,218).

The critical impediment facing gene therapy is the development of safe and efficient gene delivery systems that are widely applicable for delivery of a range of therapeutic genes. Successful delivery of genes requires carriers that will ensure the entry and expression of the transgenes in target cells. Mesenchymal stem cells (MSCs) are a key importance type of cells in bone regeneration strategies due to their potential to differentiate into various cell types such as osteoblasts, chondrocytes and tenocytes. MSCs are mainly isolated from bone marrow and have been also isolated from tendons, periosteum and trabecular bone. Cells from different origins may show phenotypic heterogeneity and respond differently to gene treatments. In general, the

transfection efficiency of MSCs has been considered as low in comparison to other cell lines (106,219).

Viral vectors are commonly used for gene therapy, but their unpredictable safety and immunological concerns have minimized their use in bone repair. On the other hand, non-viral vectors from cationic lipids and polymers have been considered as relatively safe. They also have the potential to carry large and diverse genetic materials into specific target cells (220). Polyethylenimine (PEI) is a widely used non-viral cationic polymer that is effective with a broad range of target cells (221,222). It is able to form complexes (polyplexes) with the anionic DNA molecules, which creates suitable nanoparticles for cellular uptake. The 'proton sponge' features of PEI further facilitates endosomal escape of the nanoparticles, enabling transgene expression by the transfected cells. However, the high molecular weight (MW; 25 to 800 kDa) PEI displays high toxicity on cells (104), while low MW PEI (< 5 kDa) is not effective due to formation of unstable complexes unable to withstand cell membrane penetration. To enhance endocytosis of DNA nanoparticles by cells and subsequent transfection, lipid-modification of low MW PEIs has been shown to be effective for inducing modification of primary cells as well as *in vivo* expression of reporter genes (106,107).

The objectives of this study were two-fold: (i) to determine if the lipid-modified low MW PEI vector can facilitate transfection of primary cells, and; (ii) to investigate whether BMP-2 or PDGF delivery can enhance the osteogenic differentiation of the primary cells. Specifically, delivery of plasmid DNA (pDNA) was explored in rat primary cells derived from excised periosteum and bone fragments. A comparative analysis of the transfection efficiency was explored in the two cell types by using a variety of low MW lipid-substituted PEI polymers.

## 2.2 Materials and Methods

### 2.2.1 Materials

The PEI1.2 ( $M_n$ :1.1 kDa,  $M_w$ : 1.2 kDa), PEI2 ( $M_n$ :1.8 kDa,  $M_w$ : 2 kDa), PEI25 ( $M_n$ :10 kDa,  $M_w$ : 25 kDa), fetal bovine serum (FBS), (3-(4,5-dimethylthiazol-2-yl)-2,5-diphenyl-tetrazolium bromide) (MTT), alkaline phosphatase (ALP), substrate p-nitrophenol phosphate (p-NPP), 8-hydroxyquinoline, o-cresolphthalein, 2-amino-2-methyl-propan-1-ol (AMP), dexamethasone (Dex), glycerolphosphate (GP), calcium assay kit and ascorbic acid (AA) were from Sigma-Aldrich (St Louis, MO). Dulbecco's Modified Eagles Medium (DMEM; high glucose with *L*-glutamine), Hank's Balanced Salt Solution (HBSS) and penicillin-streptomycin (10,000 U/mL-10,000  $\mu$ g/mL) were from Fisher Scientific (Ottawa, Canada). The gWIZ-GFP (5757 bp) and gWIZ (5100bp) plasmids were purchased from Aldevron (Fargo, ND), while the preparation of gWIZ-BMP-2 (6918bp) plasmid was described before (223). The PDGF plasmid (pPDGF) was obtained from Addgene (Watertown, MA) and expanded at Aldevron. CyQUANT cell proliferation kit for DNA assay was from Molecular Probes (Portland, OR).

### 2.2.2 Isolation of Cells and Cell Culture

Two types of primary cells were used in this study: periosteum-derived cells (PDCs) and bone-derived cells (BDCs) from rat skulls. Periosteum and bone chips were harvested from individual rats and placed separately in 24-well plates with DMEM supplemented with 10% FBS, 100 U/mL penicillin, 100  $\mu$ g/mL streptomycin and 5 ng/mL bFGF-2. Upon ~50% confluence, the cells were transferred to 75 cm<sup>2</sup> tissue culture flask by using 0.25% trypsin. The cells were routinely maintained under humidified atmosphere (95/5% air/CO<sub>2</sub>) at 37°C in the indicated cell

culture medium. Cells were sub-cultured (1:3 dilution) when they reached ~75% confluence. The cells at passage 2 to 5 (P2 to P5) were used in this study.

### **2.2.3 Polymeric Carriers**

PEIs (1.2 and 2.0 kDa) modified with stearic acid (StA), linoleic acid (LA),  $\alpha$ -linoleic acid ( $\alpha$ LA), propionic acid (PrA) and thioester-linked linoleic acid (tLA) were synthesized according to our established protocol and the degree of substitution was determined by the  $^1\text{H-NMR}$  (224–226). The substitution levels are summarized in Fig 1. The commercial 25 kDa PEI (PEI25) was included as a control transfection reagent.

### **2.2.4 Physicochemical Characterization**

Hydrodynamic size (z-average) and surface charge ( $\zeta$ -potential) of the complexes was assayed using Zetasizer Nano-ZS (Malvern, UK). Freshly prepared complexes (polymer/pDNA ratio of 5.0 or 10.0 w/w) were prepared using gWIZ plasmid in ddH<sub>2</sub>O and incubated for 30 min at room temperature before measurements. The complexes were diluted in 1 mL ddH<sub>2</sub>O for measurements at room temperature. Each study group contained two replicates.

### **2.2.5 Carrier Screening for Transfection of Cells and Quantitative Analysis of Transfection**

The transfection efficiencies of several polymers in PDCs and BDCs were initially assessed qualitatively by fluorescent microscopy. The cells were seeded in 48-well plates the day before the transfections. Complexes between pDNA and polymers (polymer/pDNA ratio of 5 w/w) were prepared using gWIZ-GFP with a Green Fluorescent Protein (GFP) reporter gene in oMEM without serum at room temperature for 30 min. Complexes were added to the cells and incubated

for 4 h. After 4 h of incubation, medium was replaced with fresh medium and cells were incubated for an additional 2 days. The extent of transfection was assessed based on a semi-quantitative scale (see Results).

The transfection efficacy of polymers selected from the initial qualitative screen was then investigated quantitatively by flow cytometer using gWIZ-GFP plasmid. Cells were seeded the day before the transfection in 24-well plates. Complexes (polymer/pDNA = 5.0 or 10.0 w/w) were prepared in oMEM and were added to the wells at a final concentration of 1 µg/mL pDNA. After 4 h of incubation, medium was replaced with fresh medium and the cells were incubated for additional 2 days. The cells were treated with PEI25 as a reference carrier. For flow cytometer analysis, the cells were washed (3X) with HBSS, trypsinized with 0.05% trypsin, fixed in 3.7% formalin in HBSS and analysed with BD LSRFortessa (Becton-Dickinson, San Jose, USA). The transfection efficiency was quantified based on GFP-positive population and mean fluorescence intensity/cell with 3 replicates in each group.

### **2.2.6 Cytotoxicity Assay**

*In vitro* cytotoxicity of the complexes was studied in both cell types by the MTT assay. Cells were seeded in 48-well plates the day before the experiment. Complexes of ratios from 2.5 to 20.0 (w/w) were prepared in oMEM using gWIZ plasmid and incubated for 30 min. The complexes were then added to each well at a final concentration of 1 µg/mL pDNA. After 4 h incubation, cell culture medium was replaced with fresh medium (200 µL) and the cells were incubated for another 48 h. The MTT reagent (50 µL; 5 mg/mL in HBSS) was added to the each well to get final concentration of ~1 mg/mL and incubated for 2 h. The medium was replaced with 500 µL DMSO to dissolve the formed MTT formazan crystals. Finally, the absorbance was

measured in universal microplate reader (ELx; Bio-Tech Instrument, Inc.) at  $\lambda=570$  nm. The MTT absorbance of transfected cells was compared to non-treated (NT) controls (taken as 100% viability), and viability of transfected cells was expressed as percentage of non-treated cells.

### **2.2.7 Osteogenic Activity of Transfected Cells**

Specific alkaline phosphatase (ALP) activity and calcification in cells were determined as a measure of osteogenic activity. The cells were seeded in 24-well plates the day before the experiments. Complexes (polymer/pDNA = 5.0) were prepared in oMEM using blank (gWIZ), BMP-2 and PDGF expression plasmid, or combination of BMP-2/PDGF plasmid, and directly added to wells at a final concentration of 1  $\mu\text{g}/\text{mL}$  DNA. After 4 h of incubation, medium was replaced with osteogenic medium (DMEM supplemented with 10% FBS, 10 nM dexamethasone, 10 mM  $\beta$ -glycerolphosphate, and 50 mg/L ascorbic acid). To measure ALP activity, the cells were washed with HBSS (x2) at indicated times (see Results), and lysed with 500  $\mu\text{L}$  ALP buffer (0.5 M 2-amino-2-methylpropan-1-ol and 0.1% Triton-X; pH:10.5) for 2 h at room temperature. 150  $\mu\text{L}$  of lysed cell solution from each well was incubated with 150  $\mu\text{L}$  of 2 mg/mL ALP substrate (p-NPP) and the kinetics of absorbance change (at 405 nm) was determined at 405 nm for up to 15 minutes by using the ELx800 Universal Microplate reader (Bio-Tek Instruments). For DNA content of the cell lysates, the CyQUANT DNA kit was used for DNA analysis according to the manufacturer's instructions ( $\lambda_{\text{abs}} = 480$  nm,  $\lambda_{\text{em}} = 527$  nm). A DNA standard provided by the kit was used to estimate the DNA concentrations, which was also used to normalize the ALP activity obtained above.

For calcification measurements, the cells were rinsed with HBSS (x2) after  $\sim 21$  days of culture and 400  $\mu\text{L}$  of 0.5 N HCl was added to dissolve the mineralized matrix overnight. A 500  $\mu\text{L}$  solution of 2-amino-2-methyl-propan-1-ol (1.5% v/v) and o-cresolphthalein (37 mM) was

mixed with 50  $\mu\text{L}$  8-hydroxyquinoline (28 mM) and sulphuric acid (0.5% v/v) in 48-well plates containing 20  $\mu\text{L}$  of sample. The absorbance was measured by using the ELx800 Universal Microplate reader (Bio-Tek Instruments) at  $\lambda=570$  nm and compared against calcium standards.

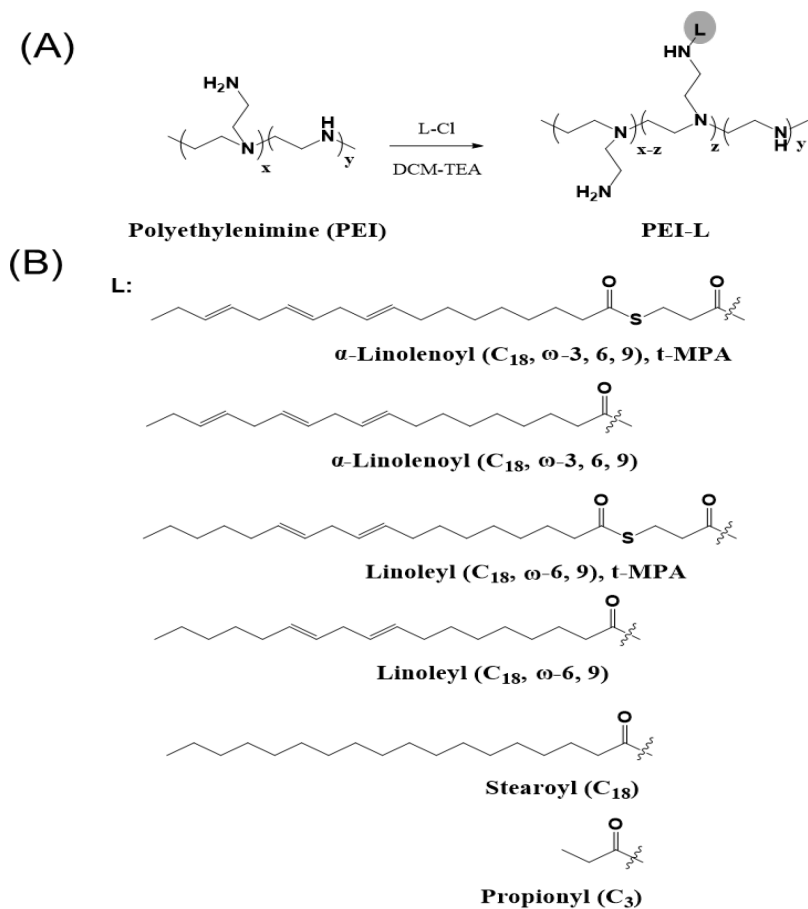
### 2.2.8 Statistical Analysis

All results were expressed and plotted as mean  $\pm$  standard deviation (SD). Data analysis was performed by unpaired Student's  $t$ -test. Statistical significance was considered for  $p$ -values  $<0.05$  and an asterisk (\*) indicated significantly different groups in figures. Statistical analysis was only performed wherever more information from the graphs were needed.

## 2.3 Results

### 2.3.1 Initial Screening of Polymers

Chemical modification of low MW PEIs with lipids is intended to improve the gene delivery of the ineffective parent polymer. The efficacy of polymers is expected to be a function of the nature of lipid used for substitution as well as the conjugation chemistry. We performed a library screening consisting of low MW PEIs modified with short and long aliphatic chains. The substituted lipids included StA, LA,  $\alpha$ LA, PrA and tLA on PEI1.2 and PEI2 (**Scheme 2.1**), and the reporter plasmid gWIZ-GFP was used for initial screens. The identification of the most effective carrier for transgene expression in PDCs and BDCs was determined by fluorescent microscopy and summarized semi-quantitatively as a heat map (**Table 2.1**). Not all polymers tested were effective for the delivery of gWIZ-GFP; among the polymers, PEI2- $\alpha$ LA8, PEI2-PrA0.5 and PEI1.2-tLA2 were chosen for further studies since their transfection efficiencies were higher in both cell types.



**Scheme 2.1.** Reaction scheme for the synthesis of PEI1.2 and PEI2 derivatives substituted with StA, LA,  $\alpha$ LA, PrA and tLA.

Polymer	Substitution (mol/mol)	PDCs	BDCs	Polymer	Substitution (mol/mol)	PDCs	BDCs
PEI1.2-StA3	1.0	-	-	PEI2-StA3	1.02	-	-
PEI1.2-StA6	2.3	-	-	PEI2-StA6	2.14	-	+
PEI1.2-LA4	1.8	-	+	PEI2-LA4	2.17	-	+
PEI1.2-LA6	2.6	-	-	PEI2-LA6	2.55	-	-
PEI1.2- $\alpha$ LA4	2.5	+	+	PEI2- $\alpha$ LA4	2.72	+	+
PEI1.2- $\alpha$ LA6	3.2	+	+	PEI2- $\alpha$ LA6	2.93	-	-
PEI1.2-PrA0.5	0.3	-	+	PEI2- $\alpha$ LA8	3.68	+	++
PEI1.2-PrA1.0	0.8	-	+	PEI2-PrA0.5	0.15	++	++
PEI1.2-tLA2	1.3	+++	++	PEI2-PrA1.0	0.53	-	+
PEI1.2-tLA4	2.8	+	++	PEI2-tLA2	1.3	-	-

**Table 2.1.** Summary of the transfection efficiency of various polymers on PDCs and BDCs.

The degree of lipid substitution (mol/mol) calculated from  $^1\text{H-NMR}$  and the corresponding transfection efficiencies of the modified PEIs are summarized semi-quantitatively. Whereas non-effective polymers were indicated with ‘-’ and the most effective polymers were indicated with ‘+++’.

### 2.3.2 Size and $\zeta$ -potential of pDNA/polymer complexes

The hydrodynamic size (Z-average) and surface charge ( $\zeta$ -potential) of prepared pDNA complexes are shown in Figure 2.1. The comparison between the two examined ratios highlights an increase of the size after the ratio was decreased from 10 to 5 in all cases. In the case of PEI 2-PrA0.5, size was  $\sim 100$  nm for ratio 10, and reached to  $\sim 150$  nm for ratio 5 while, in the cases of PEI 2-aLA8 and PEI1.2-tLA2, size increased from  $\sim 100$  nm and  $\sim 80$  nm for ratio 10 to  $\sim 120$  nm and  $\sim 100$  nm for ratio 5, respectively.

The  $\zeta$ -potential of the complexes formulated with PEI 2-PrA0.5 was  $+35$  mV for ratio 5 but decreased to  $+28$  mV for complexes synthesized at ratio 10. The  $\zeta$ -potential at ratio 5 for both PEI-aLA8 and PEI1.2-tLA2 complexes was in the same range of  $+18$  mV and increased to  $+22$  and  $+25$  mV, respectively when the ratio increased to 10.

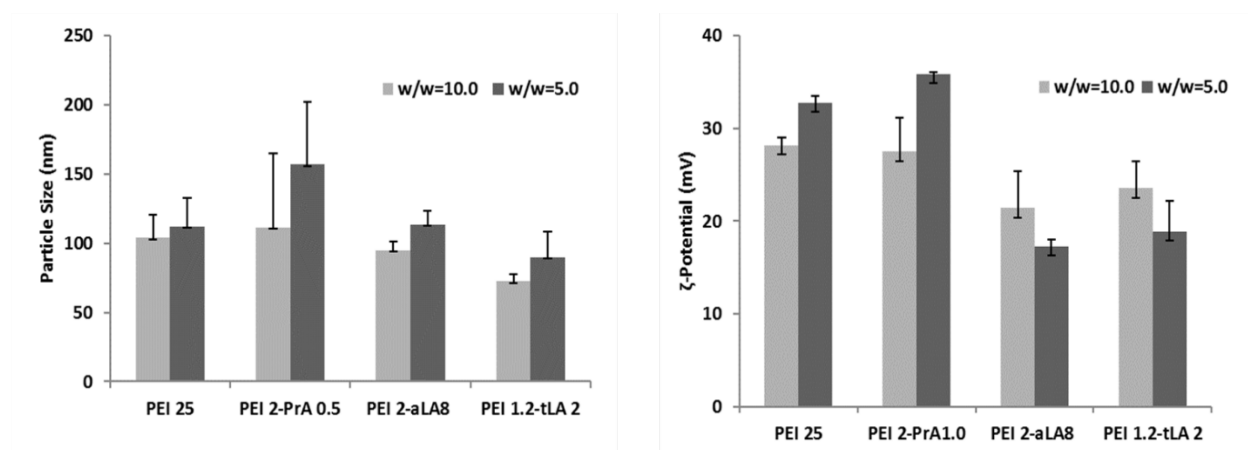


**Figure 2.1.** Size and  $\zeta$ -potential of synthesized complexes at different polymer/pDNA ratios.

### 2.3.2 Cytotoxicity of Polymer/pDNA Complexes

The cytotoxicity of the chosen polymers on PDCs and BDCs was investigated at different concentrations by using the MTT assay (**Fig. 2.2**). Modification of PEI with tLA and  $\alpha$ LA substitution generally maintained viability to greater than 75% for PDCs. Similarly, the viability of BDCs in the presence of PEI1.2-tLA2 remained constant at 75% as the polymer concentration increased, while the viability decreased to 60% or lower for PEI 2- $\alpha$ LA8. It is interesting to note that PEI 2 with PrA substitution showed a significant toxicity in both cell lines. The toxicity increased as the as the polymer:pDNA ratio was increased from 5 to 20. Similar results were also observed with the PEI25.

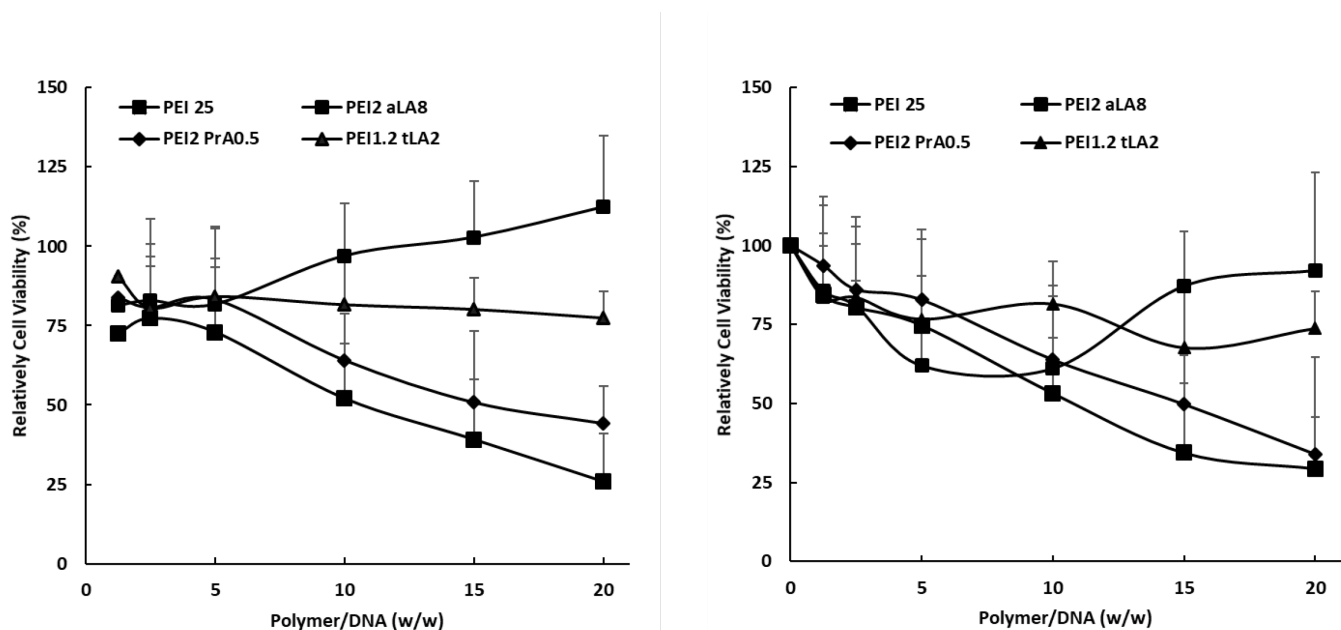


**Figure 2.2.** Cell toxicity of complexes in PDCs (left) and BDCs (right) at different polymer/pDNA ratios as assessed by the MTT assay.

Complexes with PEI2-PrA0.5 and PEI 25 were more cytotoxic as the polymer concentration increased.

### 2.3.3 Transfection Efficiency of Plasmid/Polymer Complexes

We next investigated the transfection efficiencies of PEI2- $\alpha$ LA8, PEI2-PrA0.5 and PEI1.2-tLA2 complexes in PDCs and BDCs by using the gWIZ-GFP and flow cytometry for detailed analysis. The GFP expression was summarized both as the mean GFP fluorescence and GFP positive-cells for PDCs (**Fig 2.2 A-i** and **B-i**) and BDCs (**Fig. 2.2 A-ii** and **B-ii**) derived from 3 different rats. Transfection efficiency in both cell types was dependent on the polymer:pDNA ratio, as higher ratio gave better efficacy compared to lower ratio (10 vs. 5). The maximal transfection for both cell types was obtained with PEI1.2-tLA2. However, differences depending on the origin of the cells were noted. While the performances of PEI2- $\alpha$ LA8 and PEI2-PrA0.5 were equivalent to PEI25, the latter gave inferior results compared to PEI1.2-tLA2 mediated gWIZ-GFP transfection.

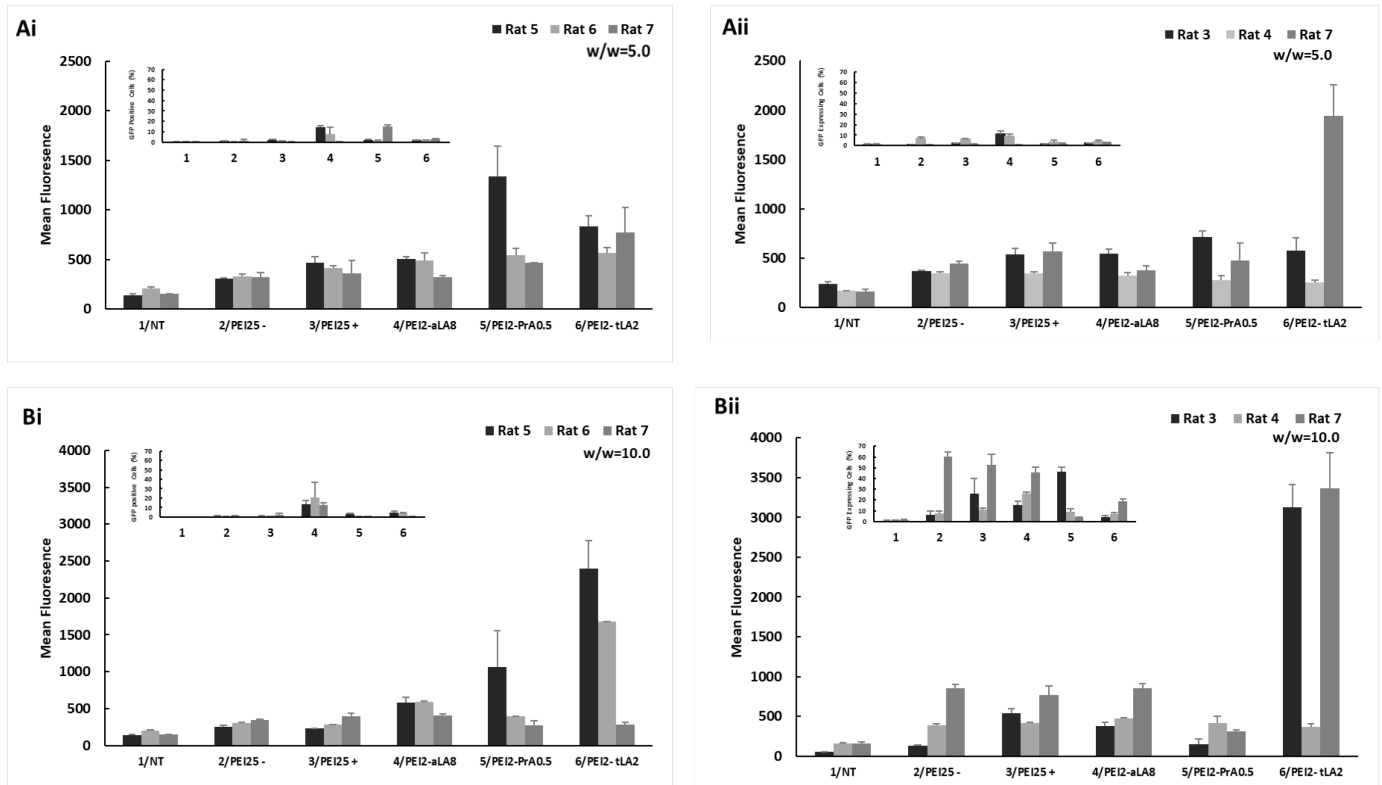


**Figure 2.3. Transfection efficiency of the complexes in PDCs (Ai-Aii) and BDCs (Bi-Bii) as determined by flow cytometry.**

Complexes (polymer/pDNA= 5 and 10, w/w) were prepared by incubating polymers with GFP labeled pDNA and exposed to the cells for 24 h before flow cytometry analysis.

### 2.3.4 ALP Activity of BMP-2 and PDGF Treated Cells

We next explored the ALP activity (as a marker of osteogenic differentiation) of PDCs and BDCs transfected with BMP-2 and PDGF plasmids at 7- and 14-days post-transfection (**Fig. 2.3**). The delivery of functionally active BMP-2 to the cells is expected to increase the ALP activity. However, PDCs treated with BMP-2 plasmid expressed low levels of ALP after 7 days, which did not increase over the 2-weeks culture. Similar results were also observed after treatment with the PDGF plasmid. In the case of BDCs, there was variations in ALP activity depending on the source of the cells; cells from Rat 22 expressed low levels of ALP while cells from Rat 27 expressed relatively high ALP activity. Compared to non-treated cells, cells from Rat 22 did not respond to

BMP-2 and PDGF plasmids, while cells from Rat 23 showed increased ALP activity compared to gWIZ-transfected cells, but not in comparison to non-treated cells. Non-treated cells from Rat 27 showed the highest ALP activity compared to the treated cells with BMP-2 or PDGF (on both day 7 and 14).

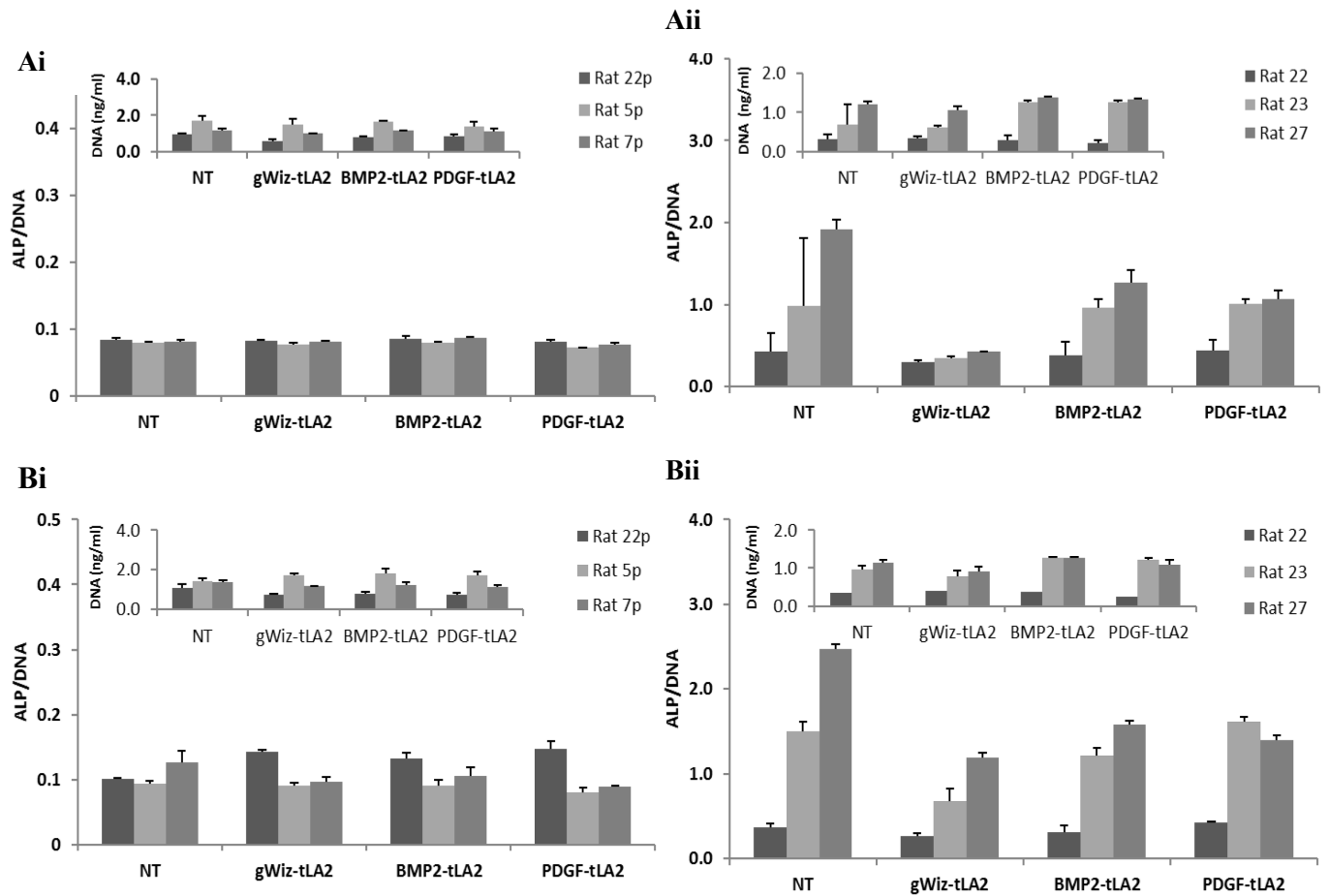


**Figure 2.4. Effect of BMP-2 and PDGF complexes with PEI1.2-tLA2 on osteogenic differentiation.**

ALP activity of PDCs (Ai) and BDCs (Aii) after 1 week of incubation and PDCs (Bi) and BDCs (Bii) after 2 weeks of incubation. ALP was normalized to DNA content.

### 2.3.5 Calcification of BMP-2 and PDGF Treated Cells

Calcium deposition was assessed as an indicator of late stage of osteogenesis. The effects of BMP-2, PDGF and BMP-2/PDGF combination treatment on the mineralization of PDCs and

BDCs were explored after 21 days of incubation (**Fig. 2.4**). Treatment of PDCs with BMP-2 significantly enhance mineralization levels especially cells from Rat 20 while treatment with PDGF or BMP-2/PDGF did not enhance mineralization levels compared to untreated cells. Increased calcification was observed as well in the case of BDCs treated with BMP-2. The calcification levels were higher for Rat 21 and Rat 23 BDCs; whereas cells from Rat 22 did not show any level of mineralization. Lower levels of mineralization compared to BMP-2 were observed after the treatment with PDGF and BMP-2/PDGF combination for both cell types.

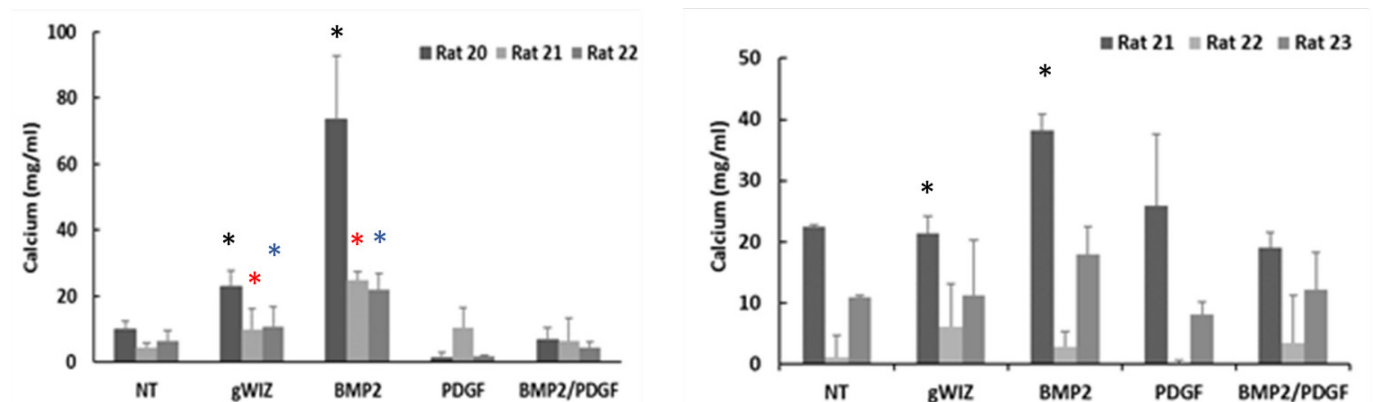


**Figure 2.5. Calcium content of PDCs (left) and BDCs (right) following treatment with gWIZ, BMP-2, PDGF or BMP-2/PDGF complexes formed with PEI1.2-tLA2.**

The cells were treated with the complexes for 4 h, after which the medium was switched to osteogenic medium for incubation for 21 days. Statistical analysis was performed between the groups treated with gWIZ and BMP-2 genes.

## 2.4 Discussion

Bone-resident MSCs have the ability to differentiate into several mesodermal cell lineages including osteoblasts, chondrocytes, adipocytes, tenocytes and myoblasts (227). Bone marrow is the most abundant source of MSCs, although MSCs have been isolated from almost all body compartments, including tendons, periosteum, trabecular bone, adipose tissue, synovial membrane

and muscle. MSCs delivered from periosteum have attracted special interest since they have shown greater *in vitro* osteogenic potential than MSCs derived from other tissues (228,229). In the last decade, the therapeutic potential of MSCs has been extensively investigated *in vitro* and in preclinical settings, with recent successful clinical studies on the treatment of bone and cartilage diseases like osteogenesis imperfecta and osteoarthritis (230,231).

The modification of MSCs at the genomic level can further improve their survival and production of GFs. Therefore, to promote bone regeneration, genetic modification of MSCs with efficient non-viral vectors such as cationic polymers has been explored. PEI based carriers and in particular PEI25 have been widely used *in vitro* and *in vivo* due to high transfection efficacy but its high toxicity had limited its applications in gene therapy (232,233). Alternatively, small MW PEIs with aliphatic lipids substitution have been developed for improved transfection efficiency and, in the current study, we assessed these carriers for the transfection of PDCs and BDCs. Successful delivery of pDNA was observed by three different polymers (PEI1.2-tLA, PEI2-PrA0.5 and PEI2- $\alpha$ LA8) each one modified with a different lipid substitution. This indicated that there were no one ideal lipid substituent to make the low MW PEIs effective on targeted cells and different lipids and conjugation chemistries were compatible with transfection ability of the target cells.

The chemical modification of PEI with lipids is expected to increase the hydrophobicity of polyplexes, facilitating their assembly under aqueous conditions and improving cellular delivery through the hydrophobic plasma membrane (226). Previous studies from our group have shown that modification of small MW PEIs with lipid substitution can increase cellular toxicity due to enhanced polymer interaction with the cells (219,224). The hydrodynamic diameters and surface charges of polymer/pDNA complexes can additionally affect gene delivery efficacy due to the

electrostatic interactions between anionic cell membranes and cationic nanocomplexes. Highly cationic PEI complexes can lead to cell membrane disruption and damage. This phenomenon was confirmed through the viability experiment where high zeta-potential PEI2-Pr0.5 and PEI25 complexes were highly toxic at polymer/pDNA ratios higher than 5. Complexes prepared with PEI2- $\alpha$ LA8 and PEI1.2-tLA2 that displayed lower zeta-potential levels showed that it was still possible to apply a relatively large amount of polymer to cells without severely affecting their viability.

The extent of transfection is one of the key factors for a successful gene delivery system. As expected, transgene expression was increased in both cell lines as the polymer:pDNA ratio was increased. Both cell types expressed high GFP levels after treatment, with PEI1.2-tLA2 delivery with BDCs showing the highest expression. The successful *in vitro* transfection efficiency of PEI1.2-tLA2 have been previously noted in human bone marrow stromal cells (hBMSCs) and this study further emphasized the successful use of this polymer especially in the case of hard-to-transfect MSCs. On the other hand, low transfection efficiencies with  $\alpha$ LA8 and PrA0.5 modified PEIs limited their further use with bone derived cells. However, there are studies that have noted that PrA modified PEIs were effective in delivering pDNA to breast cancer cells (224), so the type of cells that need to be modified appear to be important.

Bone repair is a multistep process that requires specific cellular (inflammatory cells, vascular cells, osteochondral progenitors, and osteoclasts) and molecular (pro-inflammatory cytokines, growth factors, angiogenic and pro-osteogenic factors) activity (58,234,235). BMP-2 is an osteogenic growth factor that was found to play a critical role in bone healing due to the ability to stimulate the differentiation of MSCs to an osteochondroblastic lineage. Similarly, bone healing is enhanced with PDGF, which is a potent chemotactic stimulator for inflammatory cells and the

main stimulator for proliferation and migration of MSCs and osteoblasts (30). The present study found that ALP activity in both cell types, which is important during osteogenic differentiation of MSCs into osteoblasts, was not altered upon treatment with any of the complexes, including BMP-2. The delivery of BMP-2 mainly enhanced the calcium deposition at day 21 compared to treated with PDGF, BMP-2/PDGF and non-treated PDCs and BDCs. Similarly, to our co-delivery outcomes, Wang et al. showed that the co-delivery of PDGF and BMP-2 to periosteum mice cells *in vitro* inhibited the BMP-2 signalling by targeting the BMP-2/Smad 1/5/8 pathway (236). In a separate study, the delivery of only BMP-2 plasmid with PEI-conjugated chitosan (PEI-g-chitosan) nanoparticles to mouse bone marrow cells confirmed our results by showing high BMP-2 activity and calcium deposition after 14 and 21 days post-transfection compared to the control groups (237). Jin et al. also showed high ALP activity and increased calcium deposition after the treatment of MC3T3-E1 cells with PEI-alginate/pBMP-2 nanoparticles *in vitro*. The delivery of those nanoparticles via gelatin scaffolds to a defect site *in vivo* was also able to promote bone regeneration (238).

## 2.5 Conclusions

In this study, we showed that a particular low molecular polymeric vector PEI1.2-tLA2 efficiently delivered pDNA to periosteum and bone derived cells. These complexes were also less toxic in both cell types (based on dose-response relationship with increasing complex concentration) as compared to commonly used PEI25 complexes and a small chain hydrophobe substituted PEI2 and PEI 1.2. In line with successful delivery of GFP-expression pDNA to the cells, our results showed that the delivery of BMP-2 plasmid could increase the calcium deposition of PDCs and BDCs that suggests that this gene transfer system is promising in genetically manipulating periosteum and bone derived cells towards bone regeneration.

**Chapter 3-pDNA Delivery using Polyaspartic Acid  
Supplemented Low MW PEI Polyplexes via Collagen  
Scaffolds**

### 3.1 Introduction

Over the years, significant progress has been made in the development of new technologies for bone regeneration. Due to the unique characteristics of the bone, injuries often end up in non-union and the use of grafts are in need to close the bone defect. Although these technologies have significantly improved the treatment of bone defects as well as the clinical outcomes, there is still a need for further improvement. Recent advances in the delivery of therapeutic agents like proteins and growth factors via biomaterial scaffolds have shown the ability of new bone formation, particularly in large defects (239). While the delivery of recombinant human bone morphogenetic protein-2 (rhBMP-2) via collagen sponges has been approved by FDA for spinal fusion in humans, but the very short half-life and the high amount of needing protein remains a challenge (240).

Gene therapy for bone regeneration can be an alternative since it involves physical entrapment of anionic genes encoding growth factors with cationic non-viral vectors (70). The use of non-viral vectors such as cationic polymers, lipids and peptides have been explored for their effectiveness towards difficult to transfect cells; in particular mesenchymal stem cells (MSCs). The high molecular weight (MW) polyethyleneimine (PEI ~25 kDa) has been characterized as a 'gold standard' as a non-viral vector. Although is highly effective, the high cationic charge density that it is associated with the high molecular weight causes significant damage to cell membranes; therefore high toxicity levels are observed (105,241) At the same time, low molecular weight PEIs (<2 kDa) shows minimal cytotoxicity on cells, but also low transfection efficiency. One solution is the modification of low MW PEI with lipid moieties. Studies have shown that modifications of PEI with linoleic acid (PEI- LA), alpha-linoleic acid (PEI-aLA) or thiolester-linked linoleic acid (tLA) give efficient carriers for the delivery of plasmid DNA (pDNA) to target cells (106,108).

Recently, there have been several studies that explored the concept of incorporating polyanionic polymers as additives during polymer-pDNA complexation. Polyanionic additives like hyaluronic acid (HA) and polyacrylic acid (PA) have shown an increase in the transfection efficiency towards MSCs and cancer cells (226,242,243). In this study, we introduce polyaspartic acid (pASP), another negatively charged, with low cytotoxicity and biodegradable polymer that has drawn a great deal of attention for biomedical and pharmaceutical applications. Nie et al. introduced a series of pseudocomb pASP based supramolecular assemblies for cancer treatment. The pASP-EA-BLA/CD-pASP-DET/pDNA nanocomplexes were synthesized through host-guest interactions between the cyclodextrin (CD)-cored pASP based polycations and the pendant benzene group-containing pASP backbones. The results showed a good biodegradability, low toxicity and high transfection efficiency of the synthesized particles as well as effective antitumor ability after the delivery of 5-FC/ECD to HepG2 cells. Similarly, Krisch et al. synthesized cross-linked nanogels via oxidation of thiol-modified pASP in water-in-oil miniemulsion by ultrasonication and high-pressure homogenization (HPH). By HPH method were able to produce nanogels with narrow size distribution and low drug release measurements appropriate for tumour-targeted drug delivery (244,245).

The most promising approach for localized gene transfer is the delivery of complexes via polymeric scaffolds. Scaffolds capable of securing local distribution, prolonging the release of pDNA, minimizing the immune response to administered non-viral particles and retaining the expression of administered genes are desirable for this end. The presence of a three dimensional polymeric scaffold (natural or synthetic) can further mimic the regenerative microenvironment in order to support cell regeneration, adhesion, proliferation, essentially acting as a temporary extracellular matrix (ECM) template (178). Natural polymers like collagen, which is one of the

main components of the organic phase of the bone, has been well established to act as a scaffold in bone regeneration. As a natural polymer, collagen offers low immune response, good biocompatibility and endogenous biodegradability properties. Also, collagen supports cell adhesion and differentiation, but lacks mechanical strength and structural stability that limits the application in specific tissues (246). In order to overcome such limitations, collagen must be crosslinked by a variety of physical methods (e.g., dehydrothermal treatment) or chemical reagents (e.g., glutaraldehyde or carbodiimides) (160,162,165). The properties of the scaffolds can be further improved by incorporating hydroxyapatite (HA). Studies have shown that the incorporation of HA by using polyelectrolytes such as pASP or PA during collagen scaffolds synthesis can form direct intrafibrillar mineralization (195,247,248). This technique has been found to better mimic the endogenous structure of bone matrix collagen, in comparison to methods that physically incorporate HA particles of various sizes into the scaffolds.

Therefore, the objectives of this study were: (1) to find the optimal pDNA delivery system that will be further improved with the addition of pASP for the delivery of BMP-2 to osteogenic related cell lines and (2) to develop a bioactive collagen based scaffold capable of delivering NPs to the cells and prolong their release while maintaining cell differentiation. The NPs transfection efficiency and optimal physicochemical properties were revealed via *in vitro* studies using C2C12 and MC-3TC-E1 cells. Afterwards, the optimal PEI NPs were incorporated on the surface of three different collagen-based scaffolds: collagen (Col), crosslinked collagen (Xlinked) and collagen polyaspartic acid (Mineralized) scaffolds and tested whether could successfully further promote the osteogenic activity of the cells.

## **3.2 Materials & Methods**

### **3.2.1 Materials**

The 1.2 kDa branched PEI (PEI1.2;  $M_n$ :1.1 kDa,  $M_w$ : 1.2 kDa), 25kDa branched PEI ( $M_n$ :10 kDa,  $M_w$ : 25 kDa), fetal bovine serum (FBS), thiazolyl blue tetrazolium bromide (MTT), alkaline phosphatase (ALP), substrate p-nitrophenol phosphate (p-NPP), 8-hydroxyquinoline, o-cresolphthalein, 2-amino-2-methyl-propan-1-ol (AMP), dexamethasone (Dex), glycerolphosphate (GP) and ascorbic acid (AA) were from Sigma-Aldrich (St Louis, MO). Dulbecco's Modified Eagles Medium (DMEM) /F12 (1:1) (1X) (with L-glutamine and 15mM HEPES), Dulbecco's Modified Eagles Medium (DMEM) (1X) ( with 4.5g/L D-Glucose and L-Glutamine), Minimum Essential Medium (MEM) Alpha (1X) (with L-Glutamine, Ribonucleosides and Deoxyribonucleosides), Hank's Balanced Salt Solution (HBSS) and penicillin-streptomycin (10,000 U/mL-10,000  $\mu$ g/mL), GlutaMax-I (100X) and MEM NEAA (100X) were from Gibco (NY,USA). The gWIZ-GFP and gWIZ plasmids were purchased from Aldevron (Fargo, ND), while the preparation of gWIZ-BMP-2 plasmid was described before (223). The pASP (molecular weight = 14 kDa) was from Alamanda Polymers (AL, USA).

### **3.2.2 Cell Culture**

Mouse myoblast C2C12 and cloned mouse calvarial osteoblasts MC-3TC-E1 used as model cell lines. C2C12 were maintained in DMEM/F:12 (1:1) (1X) supplemented with 10 % FBS, 100 U/mL penicillin, 100  $\mu$ g/mL streptomycin, (0.1%) GlutaMax-I and (0.1 %) MEM NEAA. MC-3TC-E1 were maintained in 50% DMEM/F:12 (1:1) (1X) and 50% (MEM) Alpha (1X) supplemented with 10 % FBS, 100 U/mL penicillin, 100  $\mu$ g/mL streptomycin, (0.1%)

GlutaMax-I and (0.1 %). The cells were routinely maintained under humidified atmosphere (95/5% air/CO<sub>2</sub>) at 37°C in the indicated cell culture medium.

### **3.2.3 Library Screen for Polymeric Carriers**

1.2 kDa PEI modified with linoleic acid (LA),  $\alpha$ -linoleic acid ( $\alpha$ -LA), thioester linoleic acid (t-LA) and thioester  $\alpha$ -linoleic acid ( $\alpha$ t-LA) were synthesized according to our established protocol and the degree of substitution was determined by the <sup>1</sup>H-NMR (224–226). The polymeric carrier PEI25 was included as a positive control carrier. Polyplexes without additive were prepared at room temperature by adding PEI derivatives (1 mg/ml) in serum-free medium (DMEM/F:12) and then an aqueous solution of gWIZ-GFP (0.4  $\mu$ g/ $\mu$ L). Polyplexes with pASP additives were prepared by mixing polyaspartic acid (0.4  $\mu$ g/ $\mu$ L) with gWIZ-GFP (0.4  $\mu$ g  $\mu$ L<sup>-1</sup>) and then added to the polymer solution. The final ratio polymer:pDNA was 10:1, the final ratio of pDNA/pASP was (1:1) and the final pDNA concentration in the complex's suspension was 1  $\mu$ g/mL. Polyplexes were incubated for 30 min at room temperature prior to use.

### **3.2.4 Transfection Experiments on Tissue Culture Plastic**

Twenty-four hours prior to transfection experiments, C2C12 and MC3TC cells were seeded in 48-well cell culture plates at a density of 10<sup>4</sup> cells. For polymer screening studies, the prepared polymer:gWIZ-GFP complexes were added to the wells and cells were assessed for transgene expression 48 hours post transfection using fluorescence microscopy. The transfection efficacy of the successful polymers was investigated in C2C12 and MC-3TC-E1(MC-3T3) by flow cytometer using gWIZ-GFP plasmid. Complexes (polymer:pDNA ratios of 2.5, 5 or 10) and the (pDNA/pASP ratios of 0.5 or 1) were prepared as was described above and were added to the wells at a final concentration of 0.25, 5 or 1  $\mu$ g/mL pDNA. Control cells were treated with complexes

of gWIZ plasmid at the same conditions. For flow cytometer analysis; the cells were washed (3X) with HBSS, trypsinized with 0.05% trypsin, and fixed in 3.7% formalin in HBSS. The transfection efficiency was quantified based on GFP positive population and the mean fluorescence intensity of the cells using a BD LSRFortessa instrument (Becton-Dickinson, San Jose, USA). Each study group contained three replicates.

### **3.2.5 Cytotoxicity Assay**

*In vitro* cytotoxicity of the complexes was studied in both cell types by the MTT (3-(4,5-dimethylthiazol-2-yl)-2,5-diphenyl-tetrazolium bromide) assay. Cells were seeded in 48-well plates the day before the experiment. Complexes of with polymer:pDNA ratios of 2.5, 5 and 10 and pDNA/pASP 0.5 for MC-3T3 and 1 for C2C12 cells were prepared using gWIZ plasmid and incubated for 30 min. The complexes were then added to each well at a final concentration of 0.25, 5 and 1  $\mu\text{g}/\text{mL}$  DNA. The MTT reagent (50  $\mu\text{L}$ , 5 mg/mL in HBSS) was added to the each well to get a final MTT concentration of 1 mg/mL and incubated for 2 hours. The medium was replaced with 200  $\mu\text{L}$  DMSO to dissolve the formed MTT formazan crystals. Finally, the absorbance was measured with a universal microplate reader (ELx; Bio-Tech Instrument, Inc.) at  $\lambda=570$  nm. The MTT absorbance of transfected cells was compared to non-treated (NT) controls (~100% viability), and viability of transfected cells was expressed as percentage of non-treated cells.

### **3.2.6 Alkaline Phosphatase (ALP) Activity**

Specific alkaline phosphatase (ALP) activity in C2C12 and MC3TC cells were determined as a measure of osteogenic activity. The cells were seeded in 24-well plates the day before the experiments. Complexes (polymer:pDNA ratios of 2.5, 5 and 10) and (pDNA/pASP ratios of 0.5 for MC-3T3 cells and 1 for C2C12 cells) were prepared using blank gWIZ and BMP-2 expression

plasmids, and directly added to wells at a final concentration of 0.25, 5 and 1 µg/mL of pDNA. For the ALP activity, the cells were washed with HBSS (x2) at indicated times (see Results), and lysed with 200 µL ALP buffer (0.5 M 2-amino-2-methylpropan-1-ol and 0.1% Triton-X; pH:10.5) for 2 h at room temperature and under constant shaking. 200 µL of lysed cell solution from each well was incubated with 200 µL of 2 mg/mL ALP substrate (p-NPP) and the absorbance change was determined after 30 minutes at 405 nm by using the ELx800 Universal Microplate reader (Bio-Tek Instruments).

### **3.2.7 Polymerase Chain Reaction (RT-qPCR) Analysis**

The MC-3T3 cells were transfected by PEI1.2-tLA10 and pBMP-2 (Pol:pDNA ratio 5, pDNA 0.25 µg/mL and pDNA/pASP ratio 0.5). Total RNA was extracted from cells after 1 and 2 weeks of treatment using TRIzol reagent (Invitrogen, Carlsbad, CA). After identifying the purity and the concentration, RNA from each sample was transcribed to cDNA using SYBR Green qPCR Mastermix (Molecular Biology Service Unit, Department of Biological Sciences, University of Alberta, Edmonton, AB). Real-time PCR amplification was performed using StepOne Real-Time PCR System (Applied Biosystems, Foster City, CA). The expression of osteogenic marker genes, including osteocalcin (OCN), osteopontin (OPN), ALP, RUNX 2 and Collagen type 1 (COL1A1) were analyzed. GAPDH and Act β were used as reference genes.

## **3.2.8 Delivery of Polyplexes from Collagen Scaffolds**

### **3.2.8.1 Scaffolds preparation**

Collagen, crosslinked collagen and collagen polyaspartic acid (Mineralized) scaffolds investigated in this study were prepared using a technique developed by Dr. E. Sone at the University of Toronto (195). Briefly, type I collagen was extracted from rat tail tendons via acid dissolution. Collagen scaffolds were produced by gel casting in 48-well plates. Collagen was dissolved in 0.5 M acetic acid at 3 mg/mL. Acid soluble collagen was pipetted into each well and the plates were placed in an ammonia environment for 30–45 min for gelation to occur. Then the gels were washed with dH<sub>2</sub>O for 2 days and crosslinked with 0.6% glutaraldehyde for 2 h at RT. The mineralization solution contained 125 µg/mL pASP and buffered to pH 7.4 at 37 °C with  $50 \times 10^{-3}$ M Tris. Ion concentrations were as follows:  $133 \times 10^{-3}$ M Na<sup>+</sup>,  $2.5 \times 10^{-3}$ M K<sup>+</sup>,  $1.7 \times 10^{-3}$ M Ca<sup>2+</sup>,  $123 \times 10^{-3}$ M Cl<sup>-</sup>, and  $9.1 \times 10^{-3}$ M Pi. Mineralization solution was filtered through 0.2 µm syringe filters prior to use to remove any prematurely formed mineral. The gels were mineralized on a shaker at 37 °C and 100% relative humidity. Mineralization solution was changed twice during the first 24 h and once per day for 3 and 6 days. After mineralization, the gels were washed, froze at -80°C and lyophilized overnight.

### **3.2.8.2 Evaluation of Cell Growth in Collagen scaffolds**

The cytotoxicity of the scaffolds was assessed by the MTT assay. The desired cells were harvested and seeded on the top of the scaffolds and incubated at room temperature for 20 min. Afterwards, media was added to the scaffolds and incubated for 3, 5 and 7 days. At the end of the incubation period, the MTT reagent (50 µL, 5 mg/mL in HBSS) was added to the each well to get a final MTT concentration of 1 mg/mL and incubated for 2 hours. The medium was replaced with

200  $\mu$ L DMSO to dissolve the formed MTT formazan crystals inside the scaffold. Finally, the absorbance was measured in universal microplate reader (ELx; Bio-Tech Instrument, Inc.) at  $\lambda=570$  nm. The MTT absorbance of seeded cells inside of the crosslinked and mineralized scaffolds were compared to pure collagen-based scaffolds (~100% viability), and viability of seeded cells was expressed as percentage.

### **3.2.8.3 Observation genes in Collagen scaffolds**

In order to observe the presence of complexes on the scaffolds. The complexes solution was added on top of the scaffolds and then were alcohol dehydrated from 50%-75%-80%-90%-100% alcohol leaving the samples for 5 min at 4°C at each step. Then, 100% hexamethyldisizane (HMDS) was added for 30 min at room temperature. Finally, the scaffolds were air dried. The scaffolds with and without complexes were examined by a Sigma 300VP Field Emission SEM (ZEISS, Germany) with an accelerator voltage 15kV.

### **3.2.8.4 Transfection with Gene-activated Collagen Scaffolds**

The incorporation of complexes into scaffolds and their ability to deliver pGFP into both cell lines was determined using fluorescence microscopy. The scaffolds were manufactured as described in Section 2.7.1 and the pDNA complexes were prepared as previously described in section 2.4. The pDNA complexes for transfection of C2C12 cells were formulated at the polymer:pDNA ratio of 10, pDNA/pASP ratio of 1, with a final pDNA concentration 1, 2 or 4  $\mu$ g/mL of gWIZ-GFP. For transfection of MC-3T3 cells, the complexes were formulated at polmer:pDNA ratio of 5, pDNA/pASP ratio of 0.5, final pDNA concentration of 0.25, 2 or 4  $\mu$ g/ml of GFP-pDNA. The formulated pDNA complexes were added on top of the scaffolds for 20 min. Next, the media containing  $2 \times 10^4$  cells was added on top of the scaffold. After 20 min, 500  $\mu$ L

of media was added again and the scaffolds have been incubated at 37°C. Forty-eight hours post transfection the scaffolds were assessed for transgene expression using fluorescence microscopy.

### **3.2.8.5 Osteogenic Activity from Gene Activated Collagen Scaffolds**

The gWIZ-GFP complexes for C2C12 transfection were formulated at a polymer:pDNA ratio of 10 with pDNA/pASP ratio of 1. The concentration of the pDNA in transfection solution was 1, 2 or 4 µg/mL. For MC-3T3 cells, the complexes were formulated at polymer:pDNA ratio of 5 with pDNA/pASP ratio of 0.5. The concentration of the pDNA in transfection solution was 0.25, 2 or 4 µg/mL. The complexes were added on top of the scaffolds for 20 min in 48 -well plates. Next, media containing  $2 \times 10^4$  cells was added on top of the scaffold. After 20 min, 500 µL of media was added further into the wells and the scaffolds have been incubated at 37°C. An additional set of transfections were conducted using gWIZ-BMP-2 complexes (polymer:pDNA ratio of 10 and pDNA/pASP ratio 1 for C2C12 and polymer:pDNA ratio of 5 and pDNA/pASP ratio 0.5 for MC-3T3 cells were directly added to the top of the scaffolds for 20 min (final pDNA concentration of 1, 2 or 4 µg/mL for C2C12 and 0.25, 2 or 4 µg/mL for MC-3TC). Media containing  $2 \times 10^4$  cells were then added on top of the scaffold and allowed to incubate at 37 °C. After 20 min, 500 µL of media was added and the scaffolds have been incubated at 37 °C for 7, 14 and 21 days. For the ALP activity, the cells attached to the scaffolds were washed with HBSS (x2) and lysed with 200 µL ALP buffer (0.5 M 2-amino-2-methylpropan-1-ol and 0.1% Triton-X; pH:10.5) for 2 h at RT with constant shaking. 200 µL of lysed cell solution from each well was incubated with 200 µL of 2 mg/mL ALP substrate (p-NPP) and the absorbance was determined at 405 nm after 24h by using the ELx800 Universal Microplate reader (Bio-Tek Instruments).

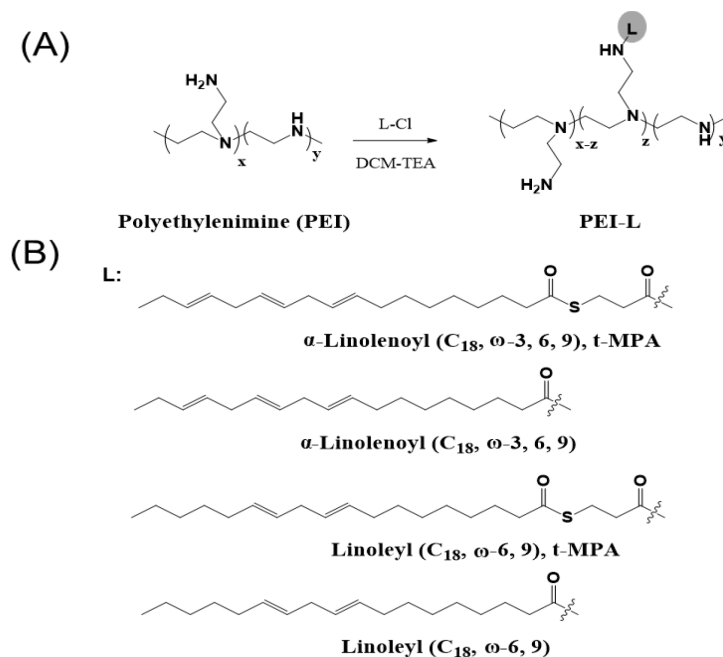
### 3.2.9 Statistical Analysis

All results were expressed and plotted as mean  $\pm$  standard deviation (SD). Data analysis was performed by unpaired Student's *t*-test. Statistical significance was considered for *p*-values  $<0.05$  and an asterisk (\*) indicated significantly different groups in figures. Statistical analysis was only performed wherever more information from the graphs were needed.

## 3.3 Results

### 3.3.1 Polymer Screening

In this study, we investigated the transfection efficiency of hydrophobic-substituted PEI derivatives with and without the presence of a polyanionic additive. A polymer library with fatty acid-based substitutes (Scheme 3.1) such as linoleic acid (LA),  $\alpha$ -linoleic acid ( $\alpha$ -LA), thioester linoleic acid (t-LA) and thioester  $\alpha$ -linoleic acid ( $t\alpha$ -LA) have been synthesized and examined for the transfection of C2C12 and MC3T3 cells. The polymers that have been shortlisted for further exploration were PEI1.2-tLA4, PEI1.2-tLA10, PEI1.2-taLA4, PEI1.2-taLA5, PEI1.2-taLA6, and PEI1.2-taLA6-3. The number value (e.g., 1.2) after the PEI (e.g., PEI1.2) indicates the MW of the polymer, the tLA and taLA are the substituents and the number at the end indicates the lipid:polymer amine feed ratio that was used during the synthesis.



**Scheme 3.1. (A) Reaction scheme for the synthesis of lipid-substituted PEIs.**

Acid chlorides of the lipids were added to the amine groups of PEI in dichloromethane (DCM). Extent of substitution was controlled by the lipid:polymer ratio during synthesis. (B) Nature of lipid substituents used in this study: linoleic acid (C<sub>18</sub>,  $\omega$ -6,9; LA),  $\alpha$ -linoleic acid (C<sub>18</sub>,  $\omega$ -3,6,9;  $\alpha$ LA), thioester linoleic acid (C<sub>18</sub>,  $\omega$ -6,9; tLA), thioester  $\alpha$ -linoleic acid (C<sub>18</sub>,  $\omega$ -3,6,9;  $\alpha$ tLA).

In this project, we introduced the polyanionic polyaspartic acid (pASP) polymer as an additive during complexation and we compared the GFP transfection with and without this additive 48 h after transfection (Fig. 3.1. A and B). In general, the presence of pASP in complexes was able to improve the GFP transfection compared to the complexes without it. The transfection of C2C12 cells (Fig. 3.1 A) was more effective as compared to MC-3T3 cells (Fig. 3.1 B). The general trends, however, was equivalent with both cell types. Among the examined carriers, the most effective polymers (without pASP) additive was found to be PEI1.2-tLA10 and PEI1.2-taLA5 but, after the addition of the pASP, PEI1.2-tLA10 polymer complexes were found to be most effective. Based on this initial screen, this carrier was selected for more detailed investigation.

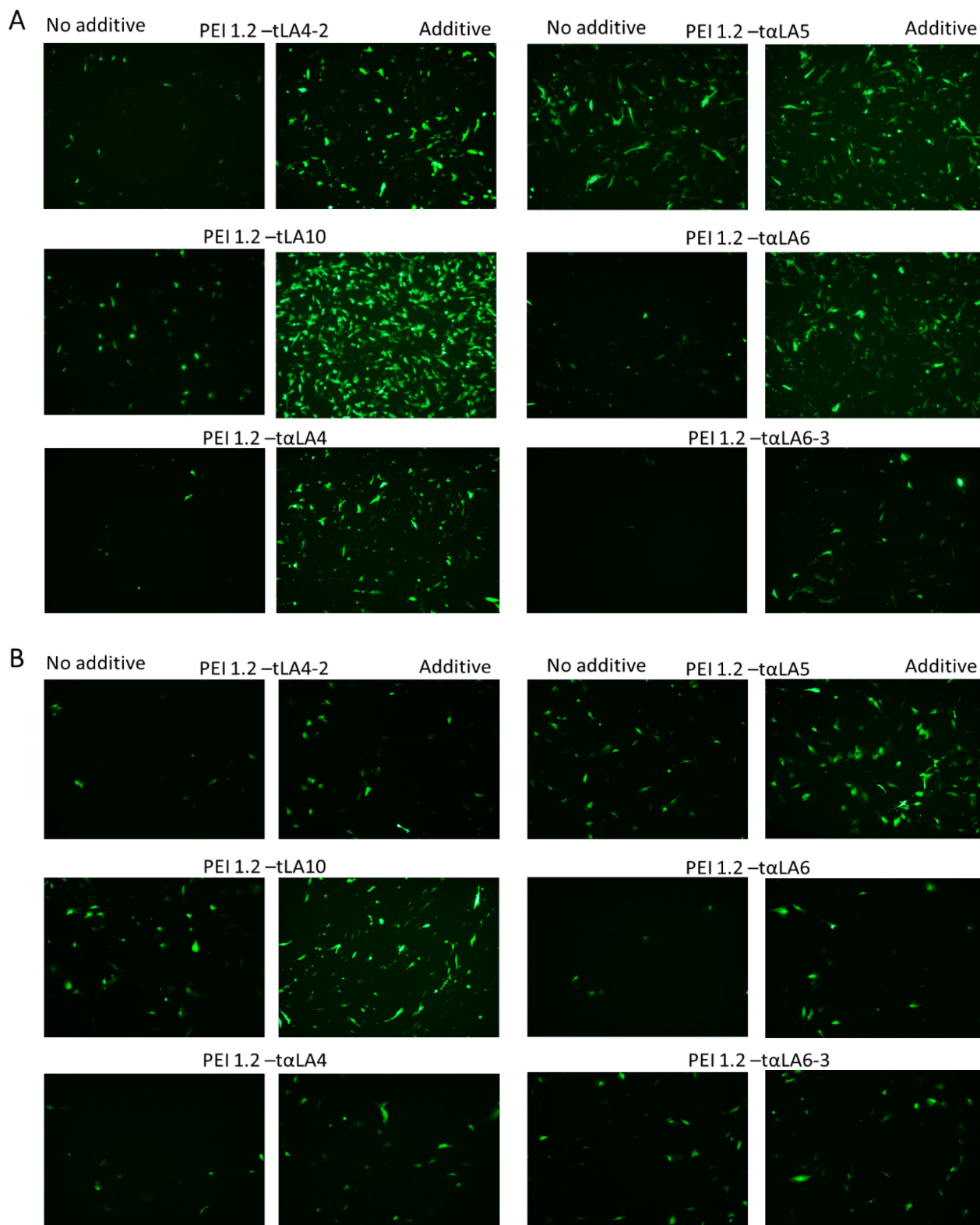


**Figure 3.1. Polymer library screening for GFP transfection.**

Delivery of gWIZ-GFP complexes with and without the presence of pASP was investigated in C2C12 (A) and MC-3T3 (B) cells. GFP expression was qualitatively assessed 48 hours after transfection using fluorescent microscopy. The micrographs show typical GFP expression among

the confluent cell populations. The specific polymer used for transfection is indicated on top of the micrographs while the left micrograph was generated without pASP and right micrograph by addition of pASP.

### 3.3.2 Effect of Polymer:pDNA Ratio and pASP on Polyplex Size and Zeta-potential

The pDNA complexes were analyzed for hydrodynamic size (Z-average) and surface charge ( $\zeta$ -potential) using a Zetasizer Nano ZS system (Table 3.1). pDNA complexes with PEI1.2-tLA10 (without pASP) at polymer:pDNA ratios of 5 and 10 were 153 nm and 185nm, respectively. The size of the same formulations (polymer:pDNA ratios of 5 and 10) with the presence of an additive at ratio of 0.5 was reduced to ~110 and ~136 nm, respectively. In the case of polymer:pDNA ratio 10, the size of the complexes was decreased even more reaching the value of 106 nm when the ratio of pDNA/pASP was increased from 0.5 to 1. Differently, in the case of formulated complexes with polymer:pDNA ratio of 5 and pDNA/pASP ratio 1, the size increased to 155 nm. Overall, the particles containing the pASP additive were smaller than the nanoparticles without.

The zeta potential values in the case of polymer:pDNA ratio of 5 dropped from positive to negative by increasing the pDNA/pASP ratio. By increasing the polymer:pDNA ratio from 5 to 10, the  $\zeta$ -potential remained in the positive range even after the addition of pASP with no obvious pattern.

Groups	DNA:pASP	Diameter (nm)	$\zeta$ -Potential (mV)
<b>PEI 1.2-tLA10 (polymer:pDNA 5:1)</b>	1:0	153 ± 5	13.1 ± 1.1
	1:0.5	110 ± 4	1.8 ± 1.6
	1:1	155 ± 1	-9.6 ± 2.4
<b>PEI 1.2-tLA10 (polymer:pDNA 10:1)</b>	1:0	185 ± 17	7.8 ± 1.9
	1:0.5	136 ± 1	7.2 ± 2.1
	1:1	106 ± 1	14.3 ± 1.2

**Table 3.1. Size and  $\zeta$ -potential of pDNA/PEI1.2-tLA10 complexes with and without pASP additive.**

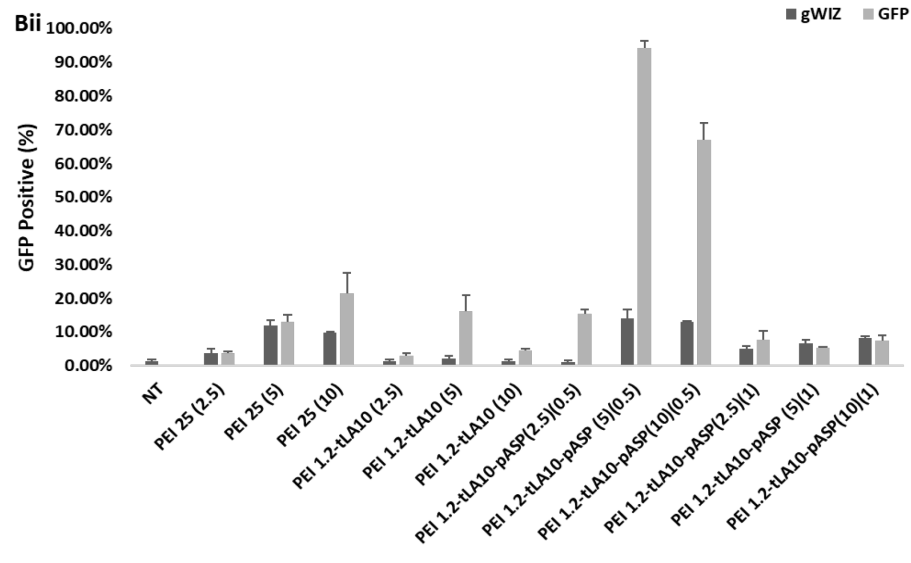
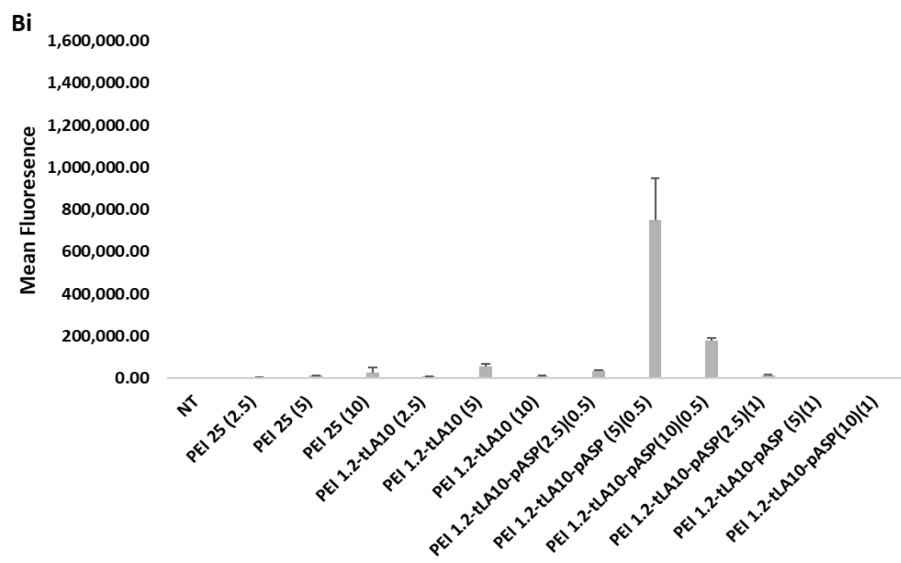
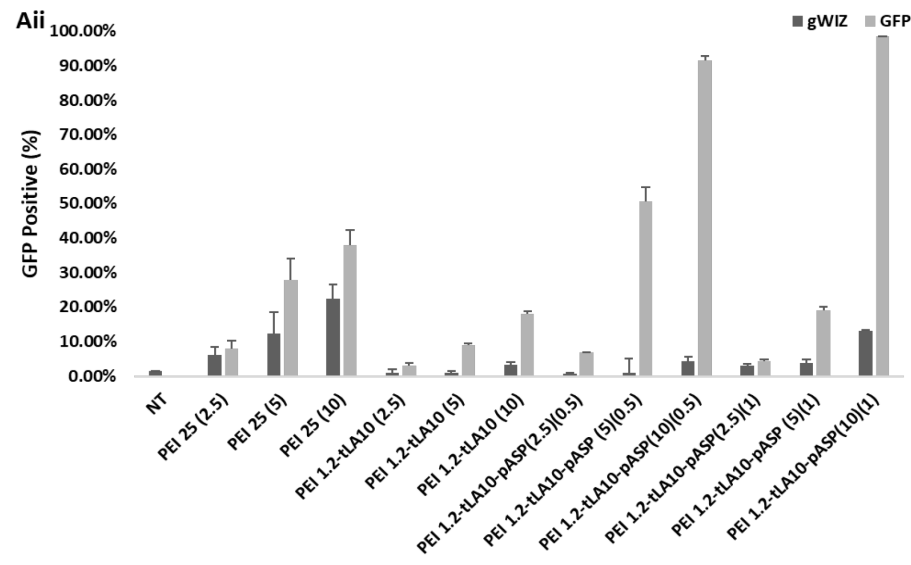
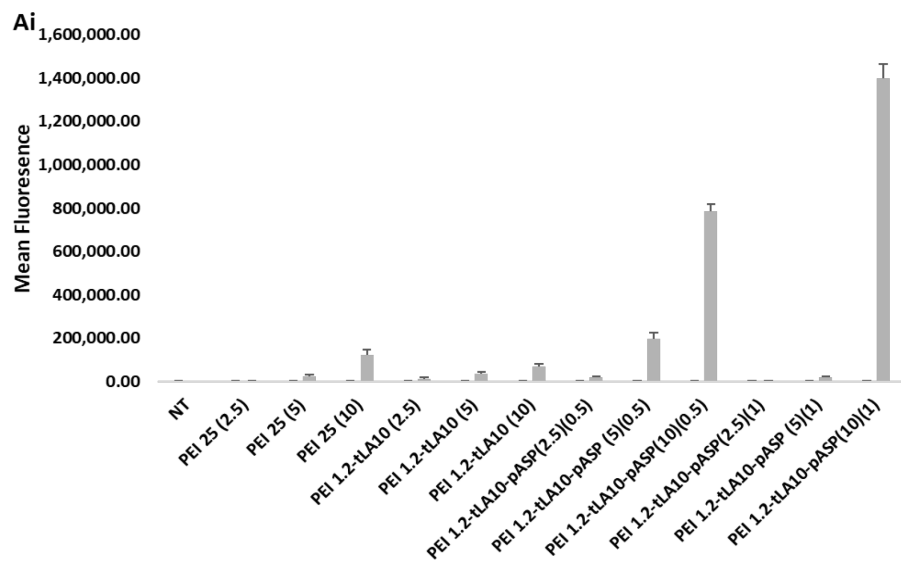
The examined polymer:pDNA ratios were 5 and 10, while the pDNA/pASP ratios were 1:0, 1:0.5 and 1:1.

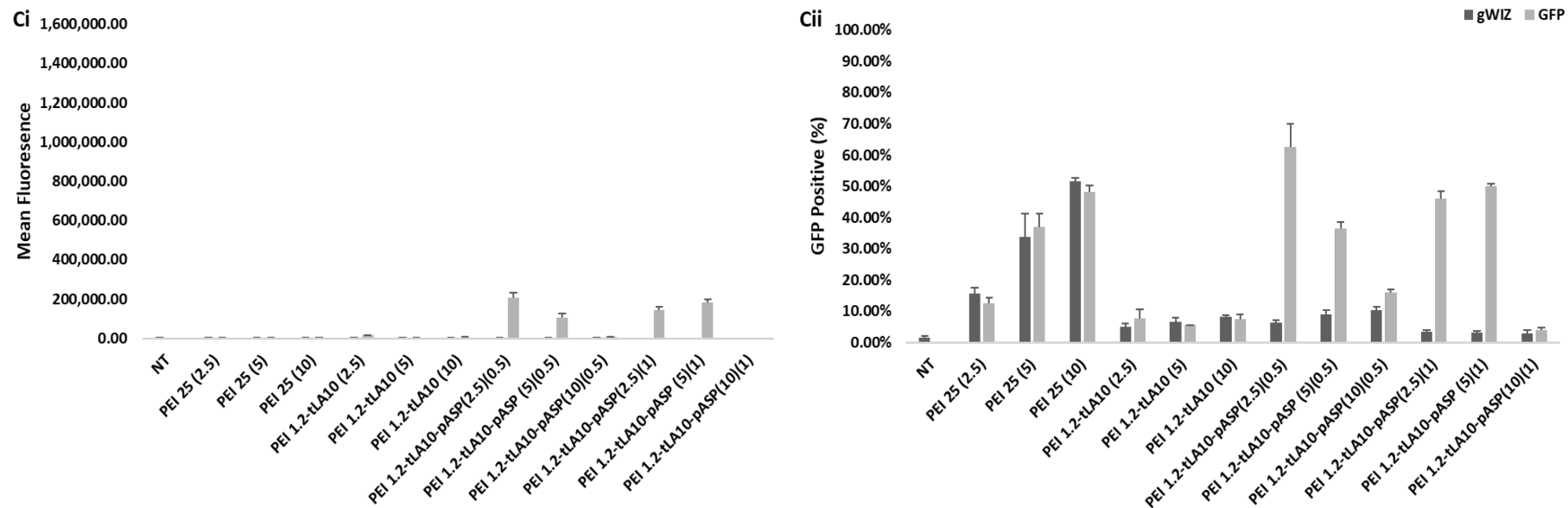
### 3.3.3 Transfection Efficiency with C2C12 & MC-3TC cells

To quantitatively determine the *in vitro* gene transfection efficiency in C2C12 (Fig 3.2 A–D) and MC3TC (Fig 3.2 A-D) cells, PEI1.2-tLA10 complexes with and without pASP were delivered to the cells for 48 h. The GFP expression levels in both cell lines were analyzed using flow cytometer. The polymer/pDNA complexes were prepared at ratios of 2.5, 5 or 10, with pDNA/pASP ratios (0.5 or 1). The mean fluorescence intensity and the percentage of GFP expression were plotted against the different conditions.

In C2C12 cells, the reference carrier used, PEI 25, gave little transfection as evident by the low levels of mean GFP fluorescence in the cell population. Only at polymer:pDNA ratio of 10, some transfection was evident with the PEI25 complexes. Based on the analysis of GFP positive cell population, no apparent difference between the gWIZ and gWIZ-GFP was evident for PEI complexes, indicating a non-specific effect of treatment in this analysis. The PEI1.2-tLA10 polymer alone also did not give a high GFP transfection efficiency but the addition of pASP clearly enhanced the transfection efficiency; (a) at 1 µg/mL pDNA concentration (Fig 3.2 A), polymer:pDNA ratio of 10 and pDNA/pASP ratio of 0.5 and 1 were the most effective, giving as much as 80-90% GFP positive cell population; (b) at 0.5 µg/mL pDNA concentration (Fig 3.2 B), polymer:pDNA ratio of 5 and pDNA/pASP ratio of 0.5 was the most effective, giving as much as 80% GFP positive cell population, and; (c) at 0.25 µg/mL pDNA concentration (Fig 3.2 C), polymer: pDNA ratio of 2.5 and 5 and pDNA/pASP ratio of 0.5 and 1 were the most effective, giving a lower percentage of 40-50% GFP positive cell population. Although the highest pDNA concentration (1mg/mL) gave the most effective transfection, the successful group for each concentration was variable,

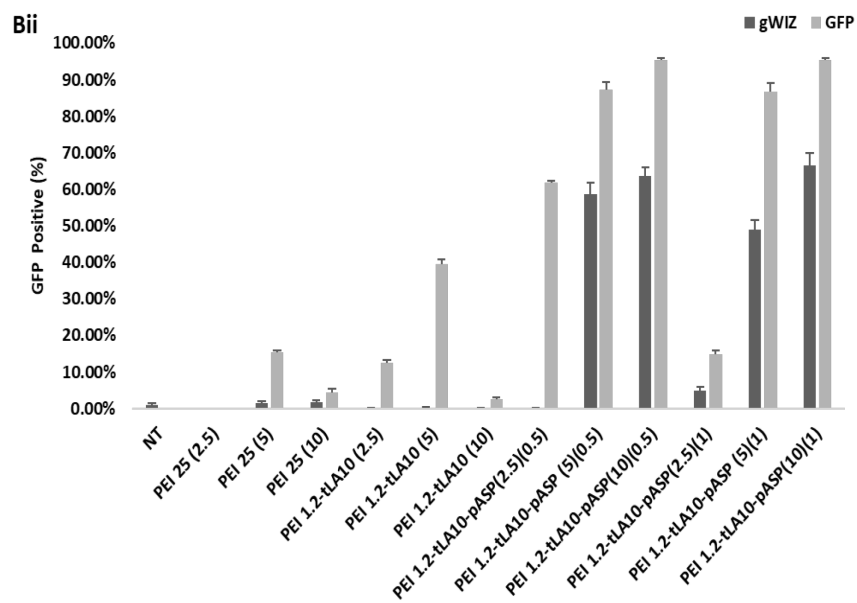
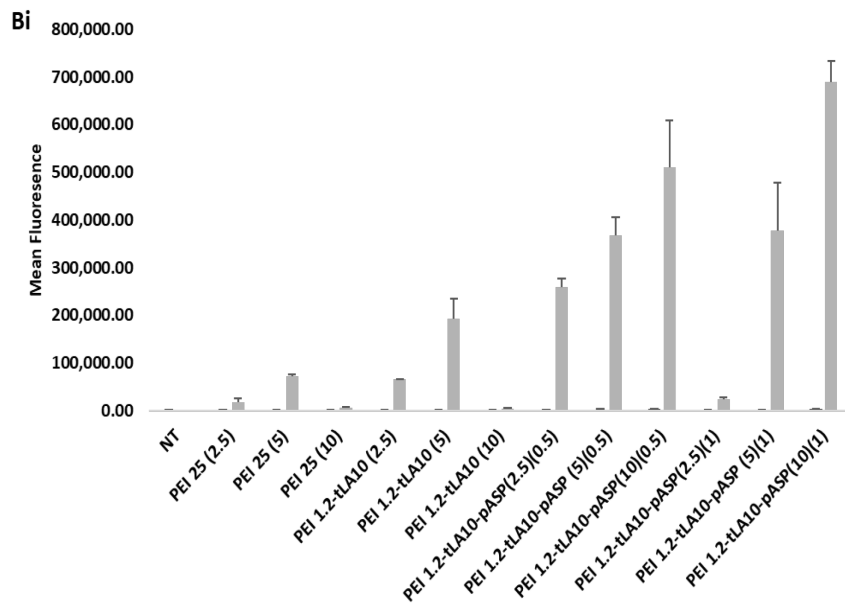
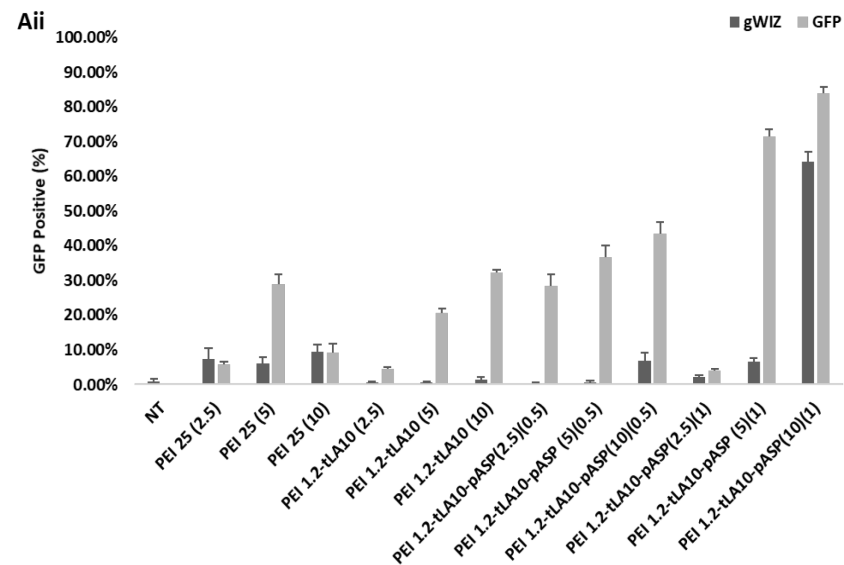
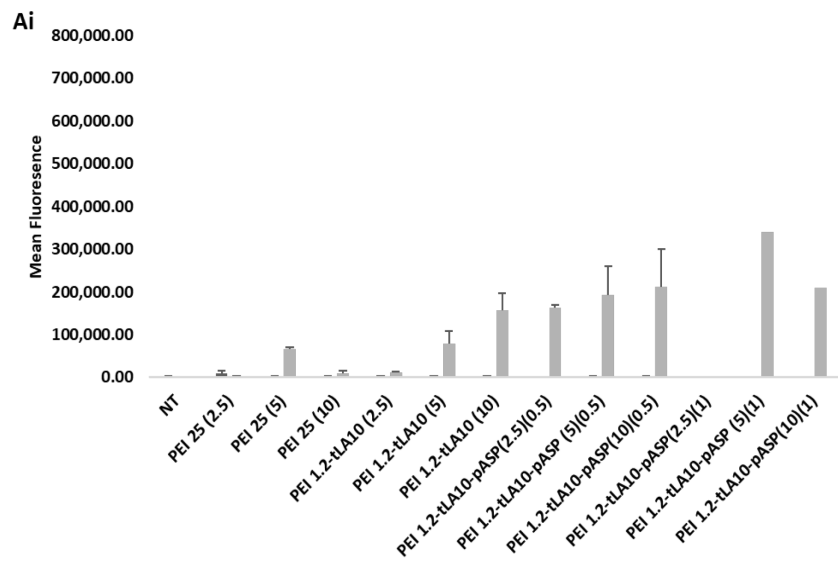
indicating the need to optimize reagent composition to obtain optimal effects under a variety of conditions.





**Figure 3.2. The mean fluorescence intensity/cell (i) and GFP-positive population (ii) in C2C12 as analyzed 48 h post-transfection.** The pDNA concentrations in cell culture medium carried by the complexes were 1 (A), 0.5 (B) and 0.25(C)  $\mu\text{g}/\text{mL}$ . The polymer:pDNA ratio and pDNA/pASP ratio used for the complex formation was 2.5, 5 and 10, and 0.5 and 1, respectively. Complexes were prepared with either the blank (control) gWIZ plasmid or GFP-expressing gWIZ-GFP plasmid. Labeling of different examined groups: Name of polymer (polymer:DNA ratio) and name of polymer (polymer:pDNA ratio) (pDNA:pASP ratio), NT: Non Treated cells.

The data from the similar treatment groups for MC-3T3 cells are summarized in Fig 3.3 A-C. Interestingly, the mean GFP fluorescence and GFP-positive cell population values were notable higher ( $\sim 700.000$  and  $\sim 90\%$  respectively) in the cases where the final pDNA concentration was 0.5 or 0.25  $\mu\text{g}/\text{mL}$  compared to the 1  $\mu\text{g}/\text{mL}$  group. For the 0.5  $\mu\text{g}/\text{mL}$  pDNA concentration, the most effective groups contained polymer:pDNA ratio 10 and pDNA:pASP ratio 0.5 or 1. In the case of 0.25  $\mu\text{g}/\text{mL}$  pDNA concentration, the most successful complexes contained polymer:pDNA ratio 5 and pDNA:pASP ratio 0.5 or 1. We again noted that PEI 25 was not a successful carrier in these cells as well.



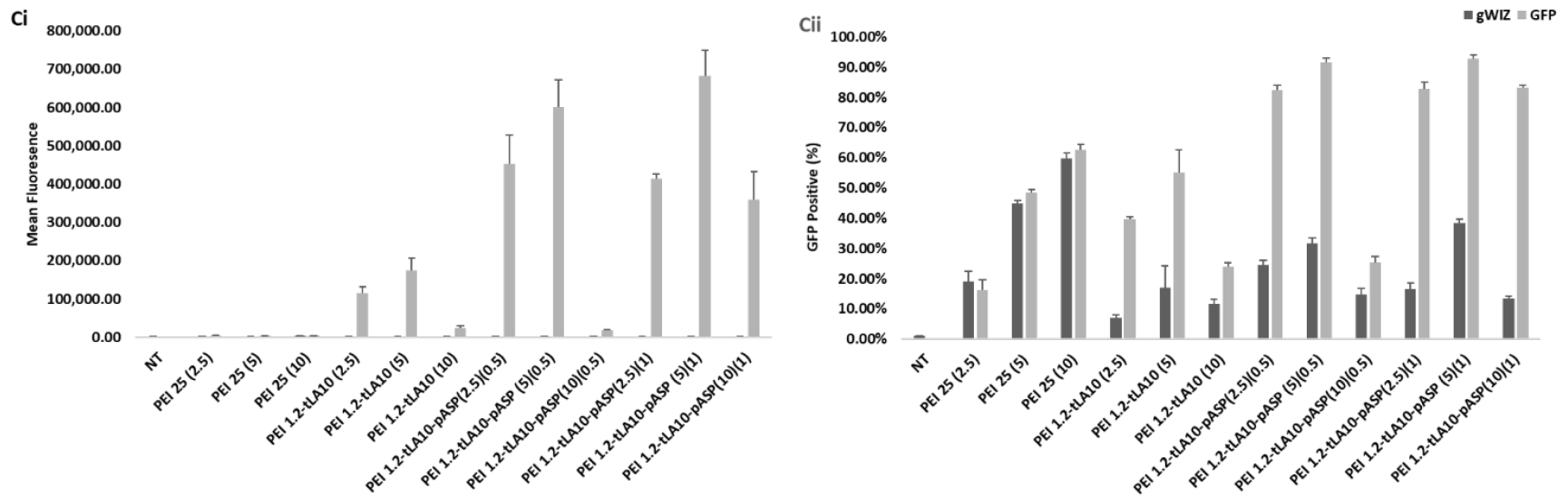


**Figure 3.3. The mean fluorescence intensity per cell (i) and GFP-positive population (ii) in MC-3T3 as analyzed 48 h post transfection.**

The DNA concentration carried by the complexes was 1 (A), 0.5 (B) and 0.25 (C)  $\mu$ g/ml. The polymer:pDNA ratio and pDNA/pASP ratio used for the complex formation was 2.5, 5 and 10 and 0.5 and 1, respectively. Labeling of different examined groups: Name of polymer (polymer:DNA ratio) and name of polymer (polymer:pDNA ratio) (pDNA:pASP ratio), NT: Non Treated cells.

### 3.3.4 Assessment of Cytotoxicity of Complexes

The MTT cell viability assay was performed to evaluate the cytotoxicity of complexes with both cell lines. The potential cytotoxic effects of complexes with different formulations were examined after 3, 5 and 7 days. The results for C2C12 cells (Fig 3.4 A-D) showed that in almost all the examined conditions, the cells exhibited 80-100% cell viability after a 7 days incubation period with the complexes.

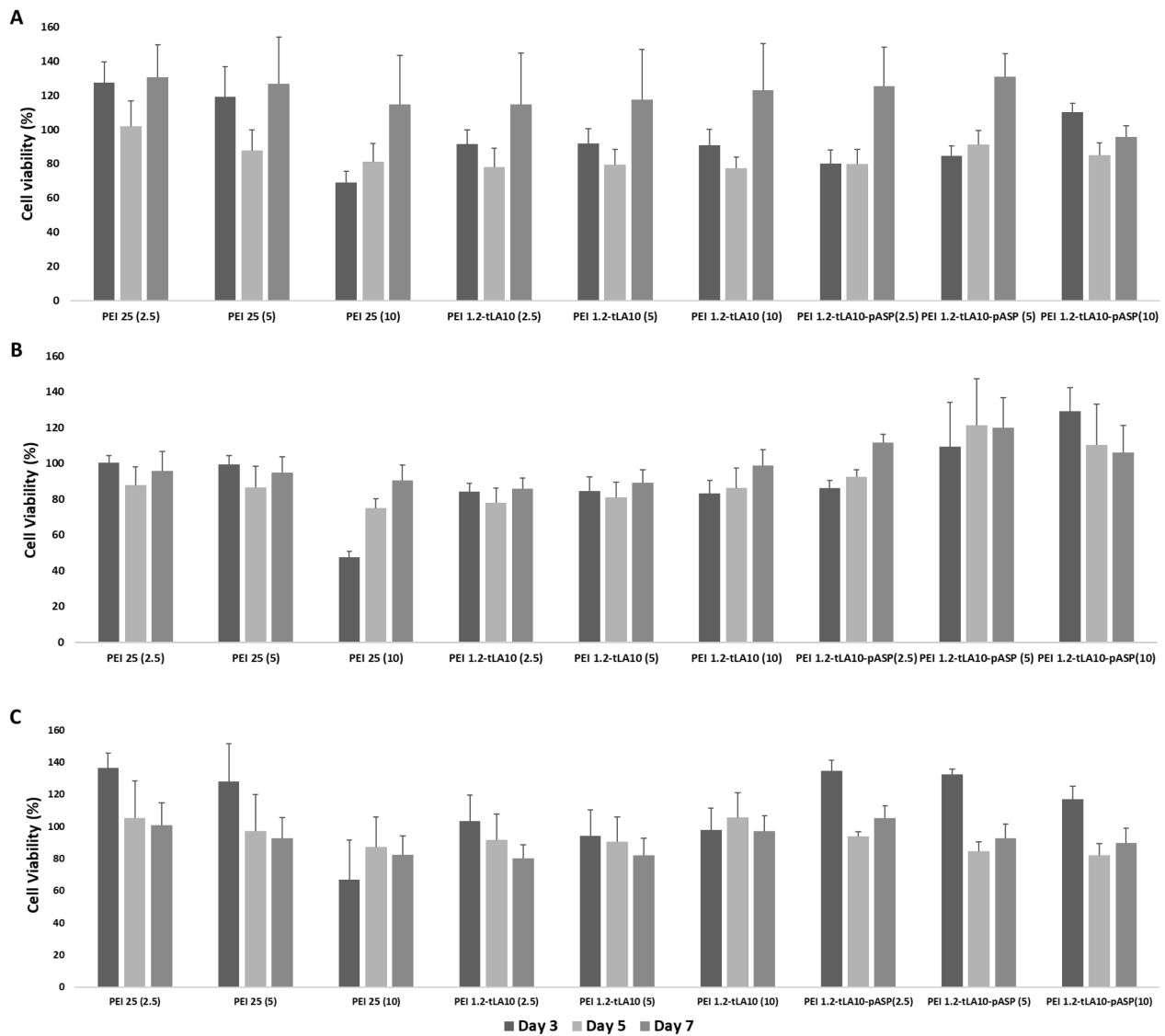


**Figure 3.4. Viability of C2C12 cells incubated with complexes containing different pDNA concentrations.**

The examined DNA concentrations were 1 (A), 0.5 (B) and 0.25 (C)  $\mu\text{g/ml}$ . Labeling of different examined groups: Name of polymer (polymer:pDNA ratio) and pDNA:pASP ratio of 1.

Significantly higher cytotoxicity was observed with the MC-3T3 cells (Fig 3.5 A-D) under similar conditions. After 3 days, the cells suffered an 80% decrease after being treated with complexes caring 1 $\mu\text{g/ml}$  of DNA, polymer:DNA ratio 10 and pDNA/pASP ratio 0.5 were unable to recover by day 7. In most of the other tested groups containing pASP the cells were able to recover after day 3 and reach 100% viability by day 7.

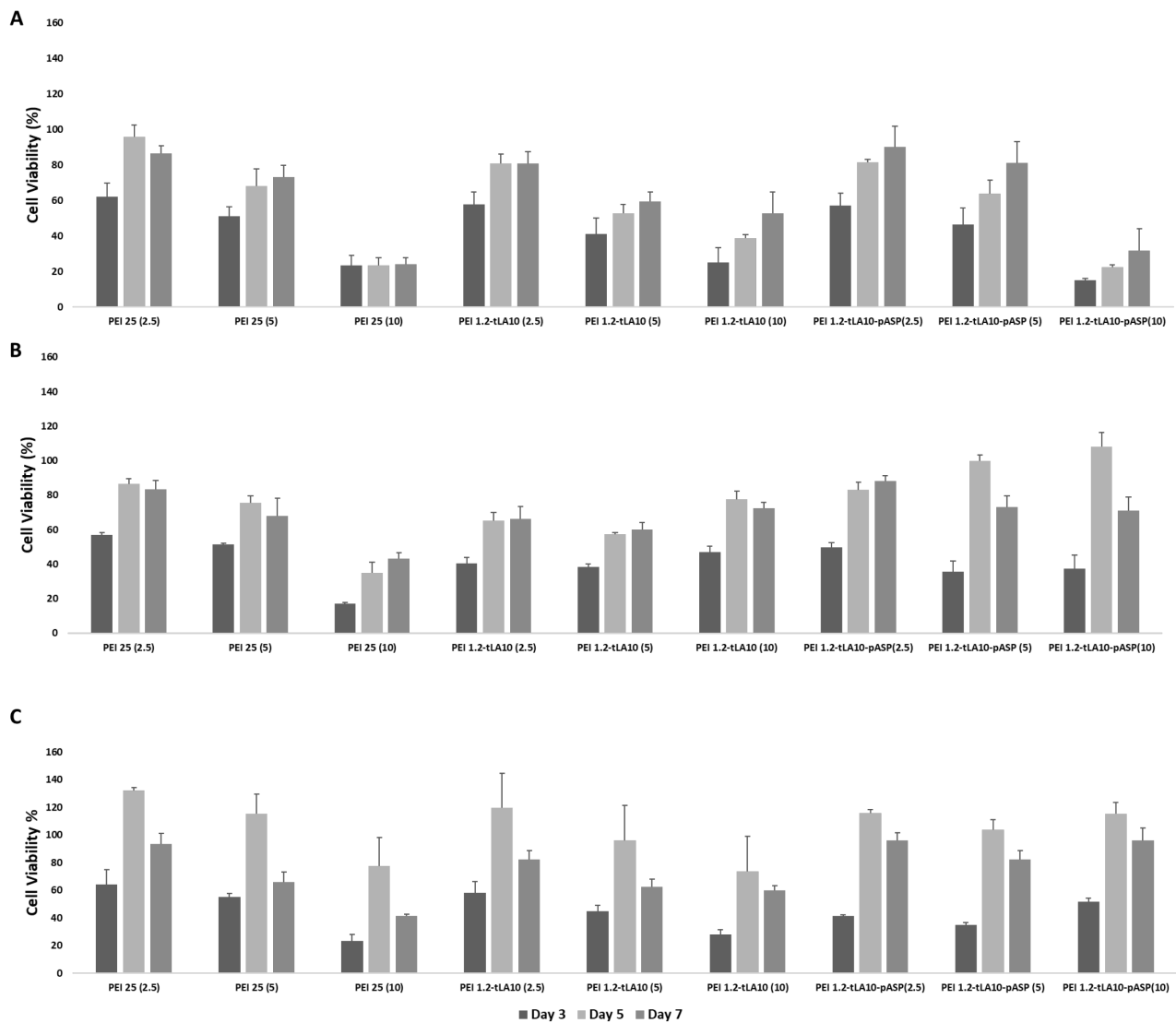


**Figure 3.5. Viability of MC-3T3 cells incubated with complexes containing different DNA concentrations.**

The examined DNA concentrations were 1 (A), 0.5 (B) and 0.25 (C)  $\mu\text{g/ml}$  and pDNA:pASP ratio of 0.5. Labeling of different examined groups: Name of polymer (polymer:DNA ratio).

### 3.3.5 ALP Activity on Tissue Culture Polystyrene

The induced osteogenic activity was evaluated by quantifying the alkaline phosphatase (ALP) activity over 21 days. The cells were treated with the complexes bearing control plasmid gWIZ and BMP-2 expressing gWIZ-BMP-2. The carriers were PEI25 and PEI1.2-tLA10 (polymer:pDNA ratios of 2.5, 5 and 10), where the latter were formulated without or with pASP additive (pDNA/pASP ratios of 1 for C2C12 and ratio 0.5 for MC-3T3 cells). The results are summarized based on the three pDNA concentrations of 1.0, 0.5 and 0.25  $\mu\text{g/ml}$  that have been tested. As shown in Fig. 3.6 A-B, the C2C12 cells treated with the higher concentrations of pDNA (1 and 0.5  $\mu\text{g/ml}$ ) and at polymer:pDNA ratio of 10 and 5, respectively, expressed the highest ALP levels. The cells that have been treated with PEI25 complexes did not induce ALP activity which was similar to the complexes formulated with PEI1.2-tLA10 without additive. With the addition of pASP (ratio 1) to the complexes, significant ALP induction was seen with PEI1.2-tLA10 bearing gWIZ-BMP-2, while the gWIZ complexes did not display any ALP induction. The obtained ALP induction was generally highest on day 7, after which it gradually decreased by day 21.

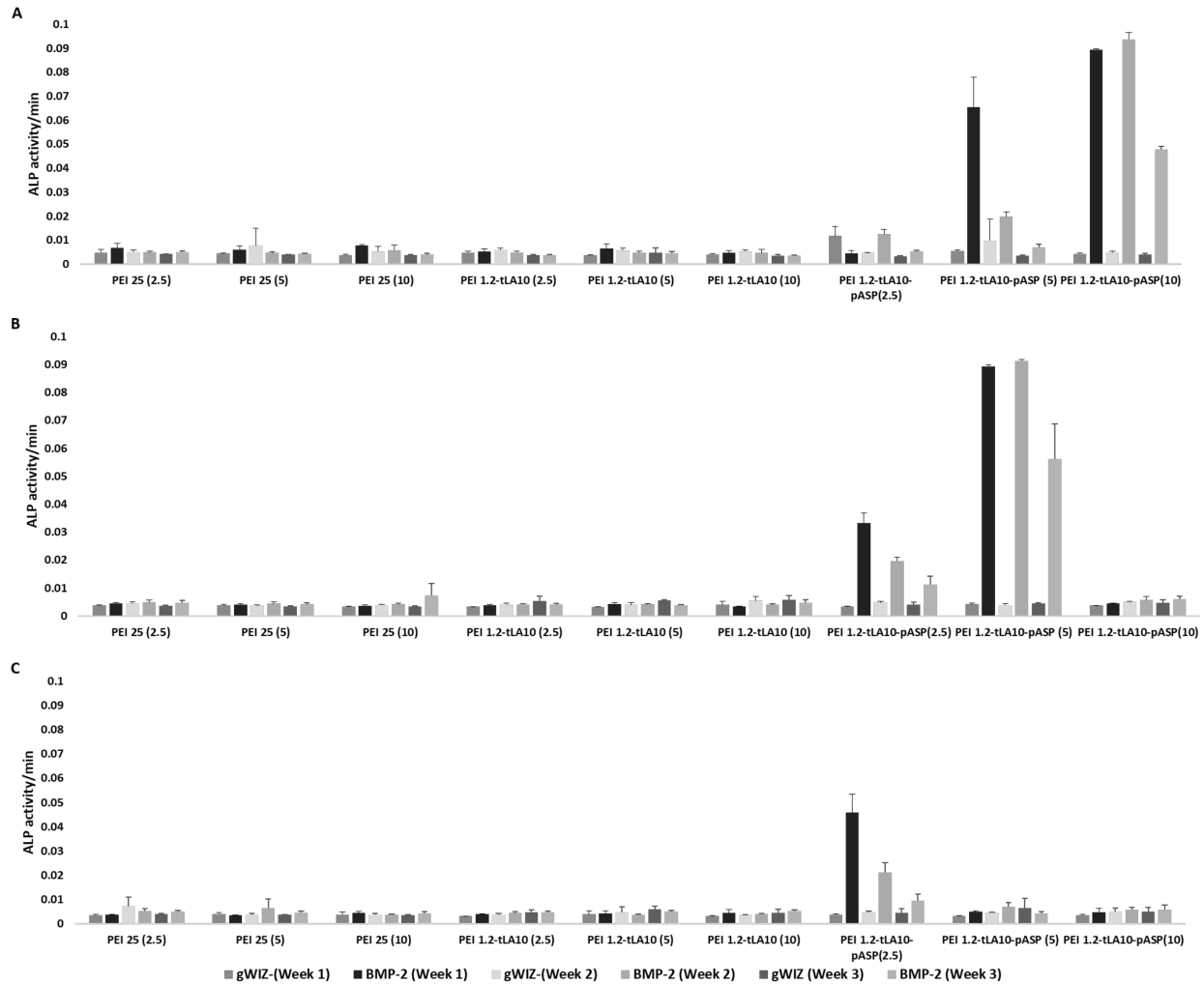


**Figure 3.6. Osteogenic activity (ALP induction) in C2C12 cells after delivery of gWIZ and gWIZ-BMP-2 complexes.**

The pDNA concentrations in cell culture were 1 (A), 0.5 (B) and 0.25 (C)  $\mu\text{g/ml}$  and pDNA:pASP ratio of 1. The ALP activity was measured 30 mins after the addition of the substrate on 1, 2 and 3 weeks post-transfection. Labeling of different examined groups: Name of polymer (polymer:DNA ratio)

In the case of MC-3T3 cells, the ALP activity during the first week was low in all the examined groups (Fig 3.7 A-C). In the next 2 weeks, the ALP activity increased and remained high up to 3 weeks. The fact that the non-treated group also displayed similar changes in ALP activity was indicative of spontaneous induction of osteogenic activity in these cells (as expected). It was interesting to note that even the gWIZ complexes caused some increase in ALP activity, so that to determine ‘net’ ALP induction for gWIZ-BMP-2 treated cells, we calculated the difference in ALP

activity between the gWIZ and gWIZ-BMP-2 treated cells at each time point. Based on this analysis, which is summarized in Fig 3.8 A-C, it was apparent that cells treated with PEI25 complexes did not indicate any ‘Net’ ALP activity. Complexes formed with PEI1.2-tLA10 without the presence of an additive gave significant ‘NET’ ALP activity in the cases of polymer:pDNA ratio of 10 and pDNA concentrations of 1 and 0.5  $\mu\text{g}/\text{mL}$ . Similarly, the complexes formed with the addition of pASP (ratio 0.5) also gave significant ‘Net’ ALP activity at various polymer:pDNA ratios at all time points assessed.

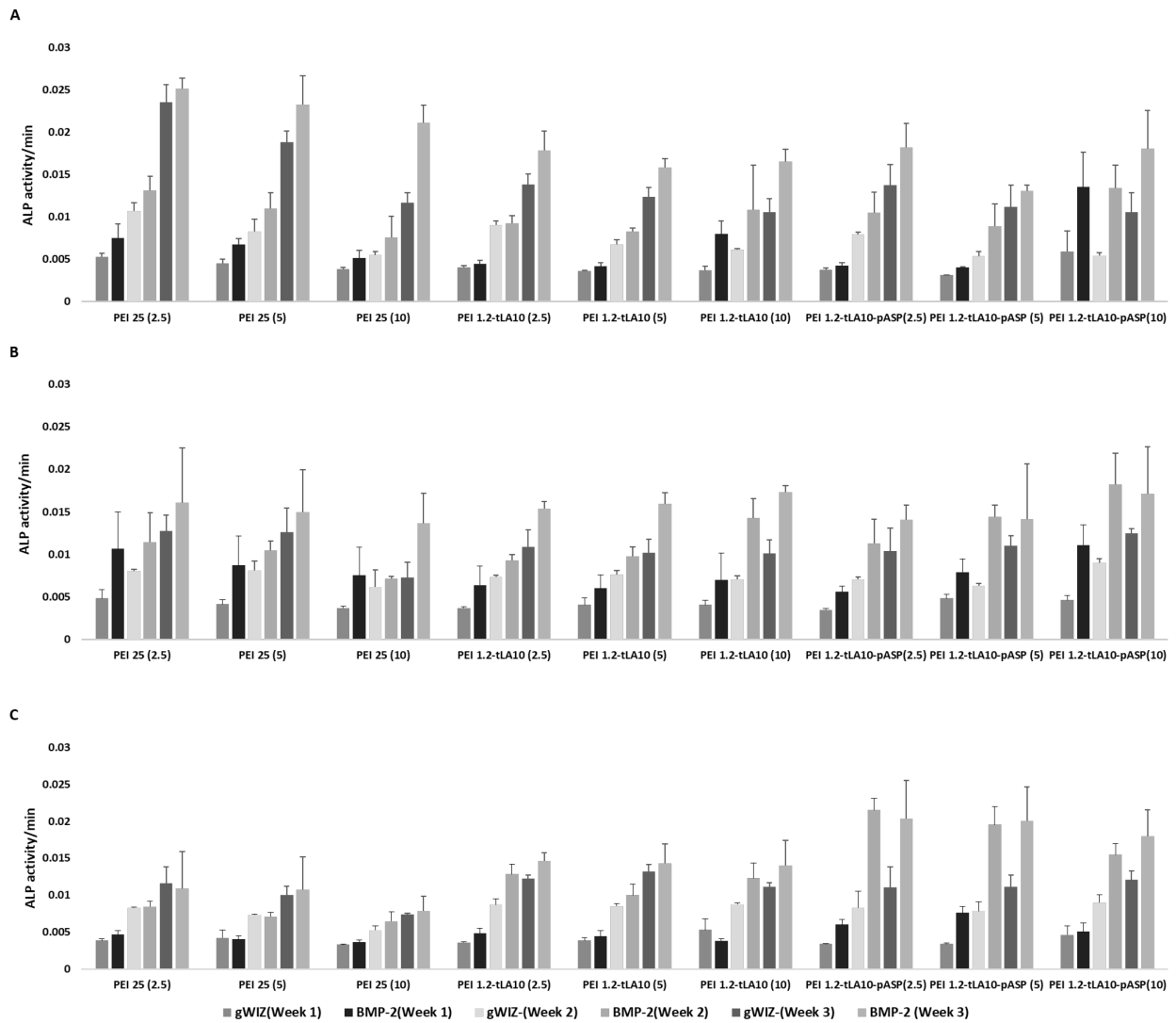


**Figure 3.7. ALP induction in MC-3T3 cells after delivery of gWIZ and gWIZ-BMP-2 complexes.**

The pDNA concentrations in cell culture were 1 (A), 0.5 (B) and 0.25 (C)  $\mu\text{g}/\text{ml}$  and pDNA:pASP ratio of 0.5. The ALP activity was measured 30 mins after the addition of the substrate on 1, 2 and 3 weeks post-transfection. Labeling of different examined groups: Name of polymer (polymer:DNA ratio).

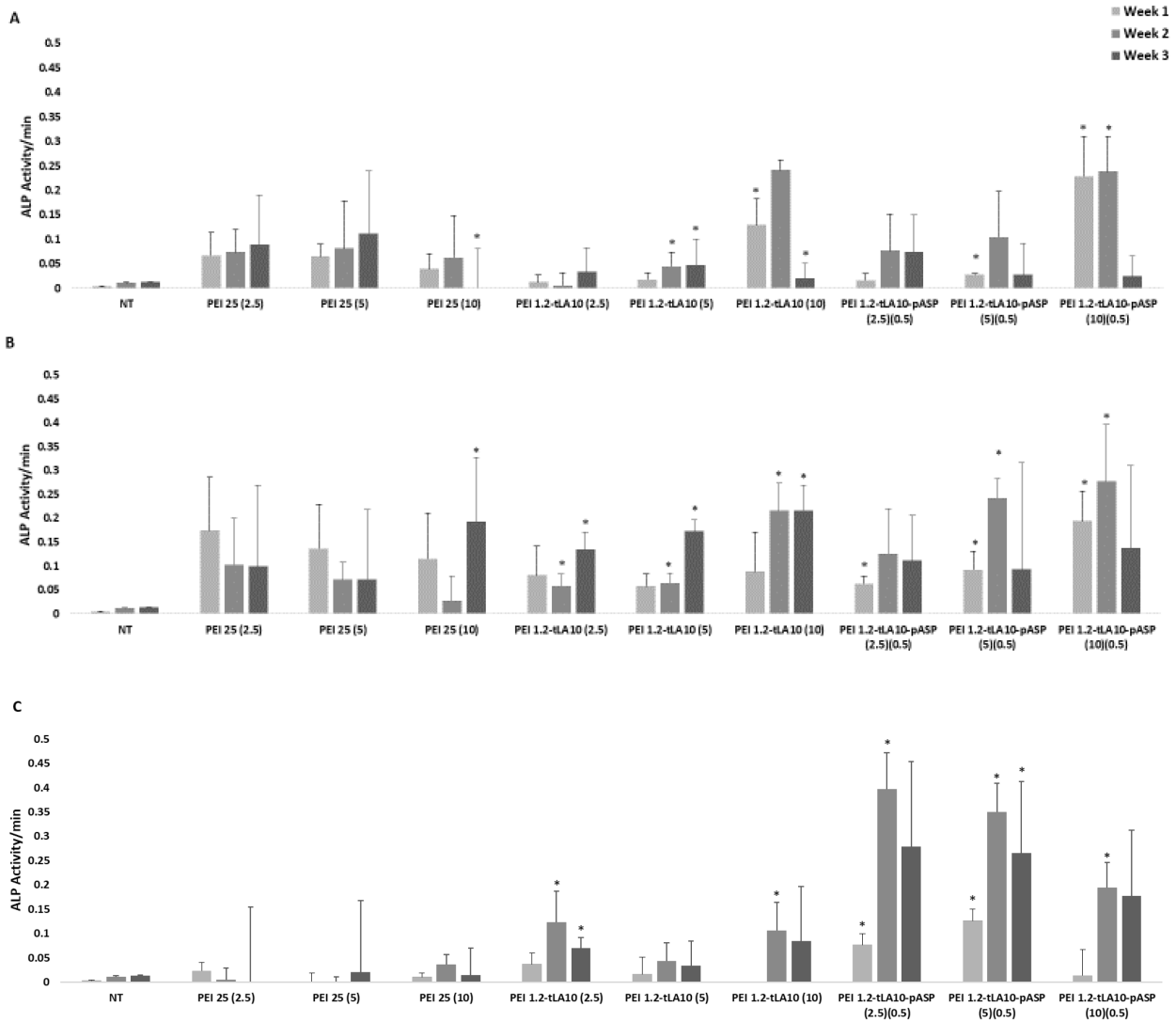


**Figure 3.8. 'Net' ALP induction in MC-3T3 cells after delivery of gWIZ and gWIZ-BMP-2 complexes.**

The pDNA concentrations in cell culture were 1  $\mu\text{g}/\text{mL}$  (A), 0.5  $\mu\text{g}/\text{mL}$  (B) and 0.25 (C)  $\mu\text{g}/\text{mL}$  and pDNA:pASP ratio of 0.5. The ALP activity was measured 30 min after the addition of the substrate on 1, 2- and 3-weeks post-transfection. Labeling of different examined groups: Name of polymer (polymer:DNA ratio). 'Net' ALP activity was calculated by subtracting ALP activity obtained from pBMP-2 treated cells from that of gWIZ-treated cells. Statistical analysis was performed between those groups as well.

### 3.3.6 qPCR for Osteogenic Markers in MC-3T3

The expression levels of osteogenesis associated genes (ALP, Col1A1, OCN, OPN and Runx2) in MC-3T3 cells was analyzed by PCR after 1 (Fig. 3.9 A) and 2 (Fig. 3.9 B) weeks for the complexes containing PEI1.2-tLA10 carrying 0.25  $\mu\text{g/ml}$  pBMP-2 and pgWIZ, polymer:pDNA ratio 2.5, 5 and 1 and pDNA/pASP 0.5. After week 1, there was no difference between the expression levels of ALP, COL1A1, OCN, OPN and Runx2 compared to the non treated cells. On week 2, the expression levels of COL1A1 and Runx2 were upregulated by the complexes containing polymer:pDNA ratio 2.5 and 5 compared to the control groups, but no significant differences were observed by the complexes containing polymer:pDNA ratio 10.

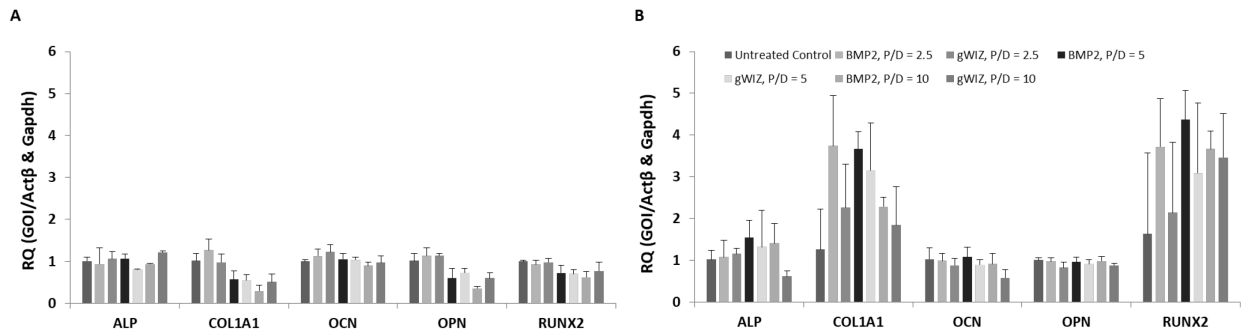


**Figure 3.9. The expression levels of osteogenic marker genes in MC-3T3 was analyzed by PCR.**

The expression was measured on week 1 (A) and week 2(B). The complexes delivered to the cells 0.25  $\mu\text{g/ml}$  pBMP-2 and pgWIZ, polymer:pDNA ratio 2.5, 5 and 1 and pDNA/pASP 1

### 3.3.7 Growth of cells in mineralized collagen scaffolds

The MTT assay was used to measure the metabolic activity of the cells and could be used as a measure of total cell number or viability in scaffolds. Both cell lines were cultured for 3, 5 and 7 days with 0 (un-mineralized), 3- and 6-day mineralized scaffolds. The results of MTT assay revealed a similar response by both C2C12 cells and MC-3T3 cells (Fig 3.10 A and B); the cell

number was highly variable among different scaffolds and the difference was clear from the first assessment point (day 3). The total activity generally remained the same as a function of time in all three types of scaffolds, with 6d mineralized scaffolds yielding lower cell activities throughout the study period.

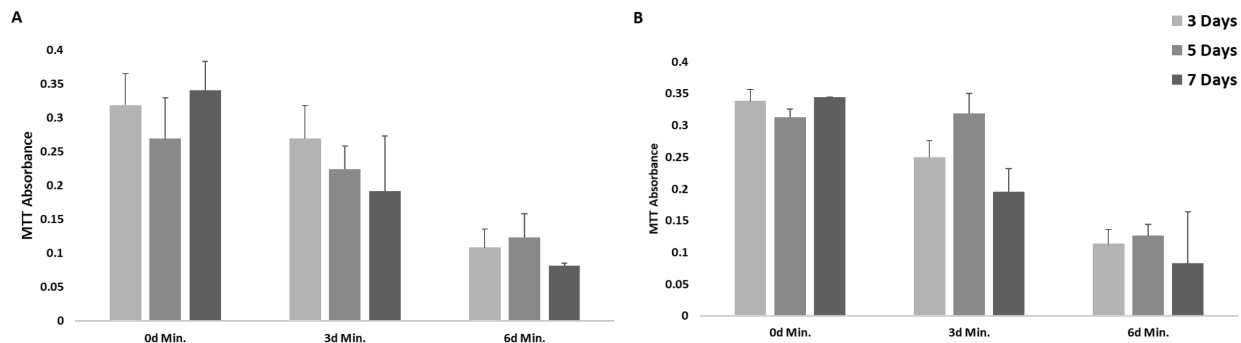


**Figure 3.10. The viability of C2C12 (A) and MC-3T3 (B) cells cultured on mineralized collagen scaffolds.**

The scaffolds were mineralized for 0 (i.e., no mineralization), 3 and 6 days. The viability was assessed by the MTT assay at 3, 5- and 7-days post cell-seeding.

### 3.3.7.1 Observation of genes in Collagen scaffolds

SEM analysis following loading of polyplexes confirmed the presence of polyplexes in scaffold surfaces. Figure 3.11 shows the even distribution of the complexes throughout the scaffolds but the complexes appeared not to be very embedded in the collagen scaffolds compared to x-linked and 3d Mineralized scaffolds.

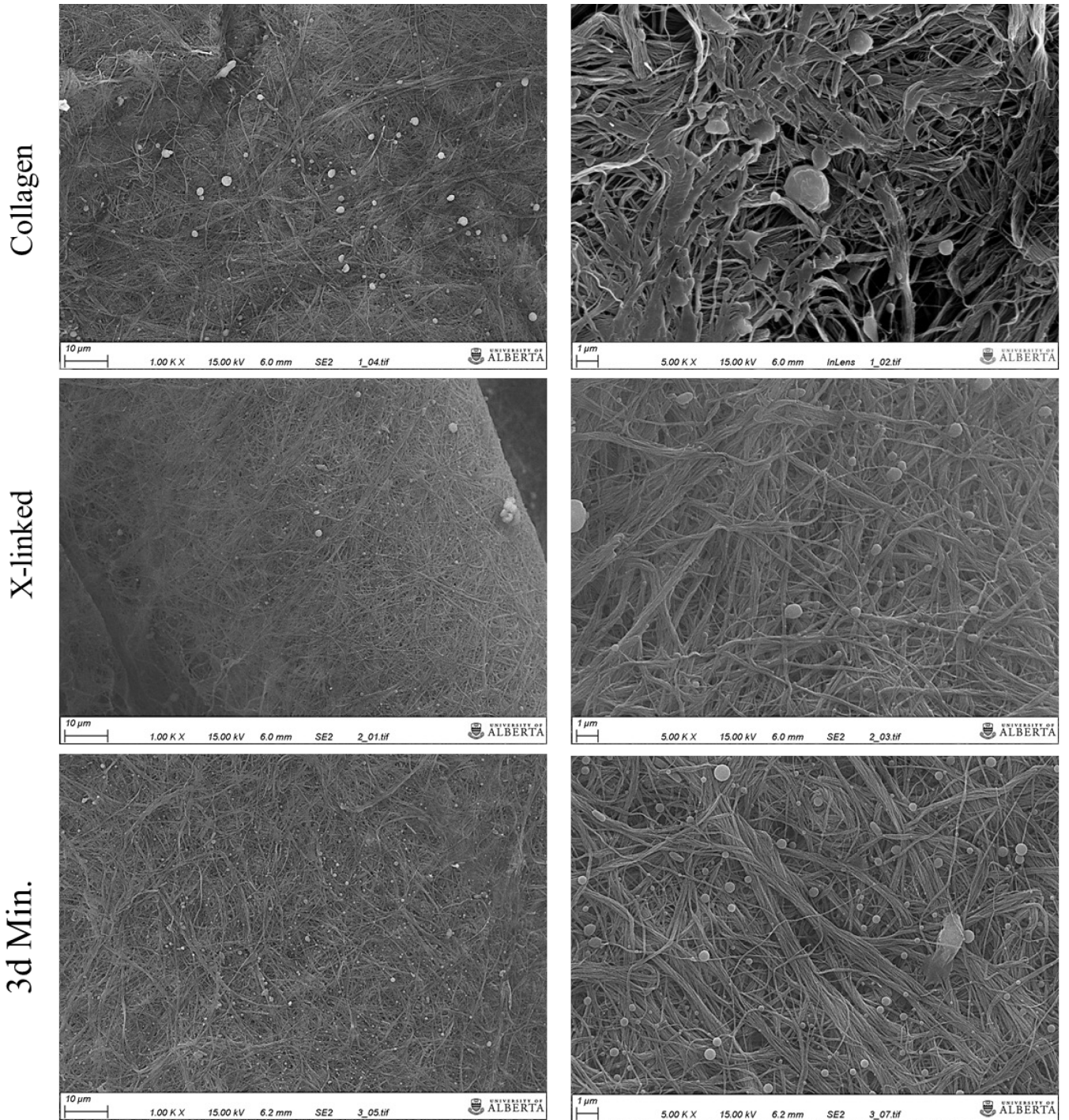


**Figure 3.11.** The presence of complexes in collagen, X-linked collagen and 3d Mineralized scaffolds was determined with SEM (scale bars 10 and 1 μm).

### 3.3.7.2 Transfection efficiency in gene-activated scaffolds

Fluorescent images were taken 48h post transfection showing that the cells expressed GFP; which indicates the successful delivery of pDNA to cells via scaffolds. C2C12 (Fig. 3.12) were successfully transfected after being seeded on collagen activated scaffolds compared to x-linked and 3d Mineralized scaffolds in all the examined concentrations. On the other hand, GFP expression was not able to be determined in MC3TC cells in all the examine conditions.

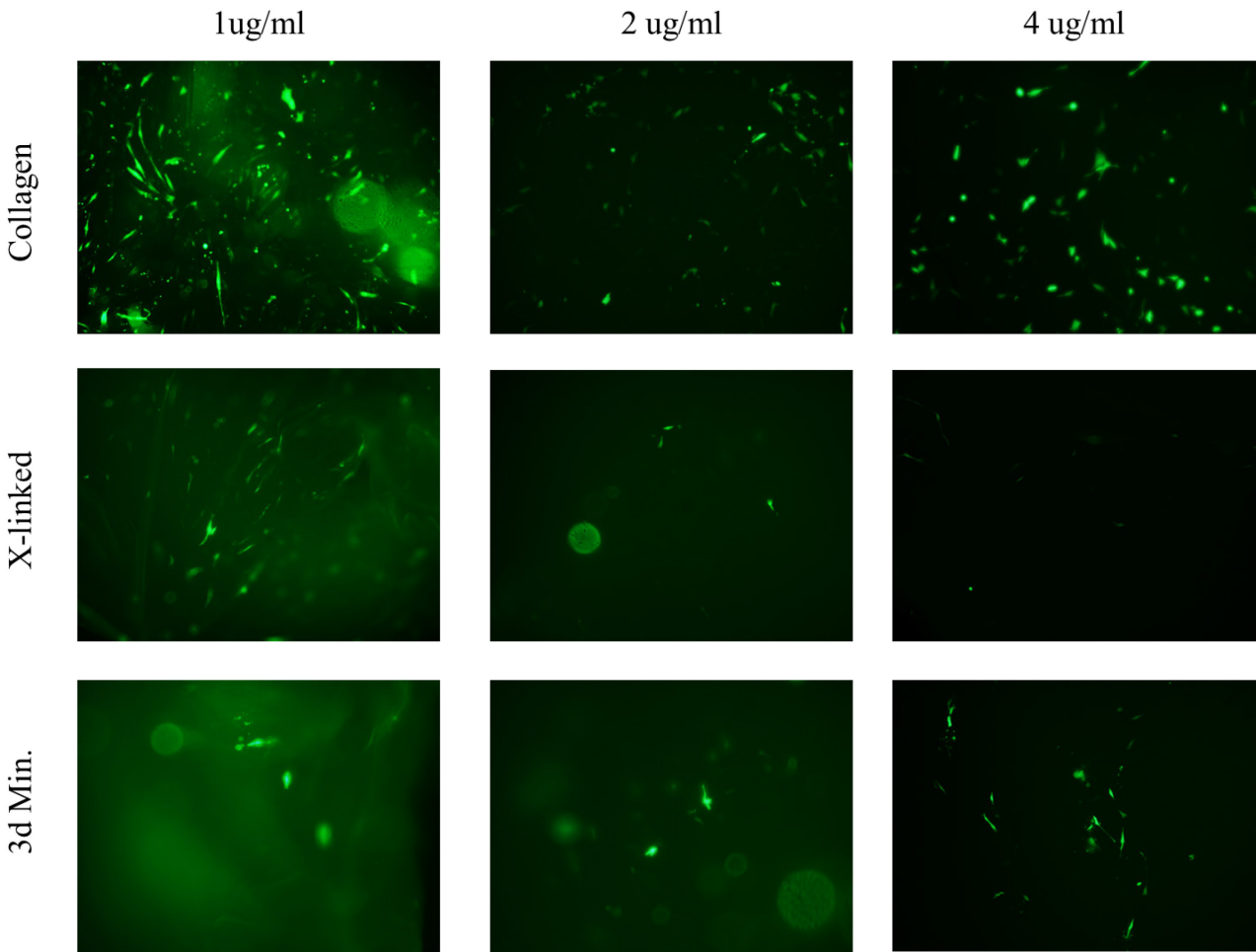


**Figure 3.12. Transfection efficiency of PEI 1.2-tLA10-pGFP delivered to C2C12 cells via collagen, X-linked collagen and 3d mineralized scaffolds.**

The pGFP concentration used were 0, 1, 2 and 4 µg/ml. The images were taken 48h post transfection. Green cells signify positive transfection.

### 3.3.7.3 ALP activity in gene activated scaffolds

The ability of gene-activated scaffolds for inducing ALP activity in C2C12 and MC-3T3 cells was quantified by delivering different pBMP-2 concentrations (0, 1, 2 and 4  $\mu\text{g/ml}$ ) in collagen, X-linked collagen and mineralized collagen scaffolds (3 day Mineralized) over a period of 3 weeks. As shown in Fig. 3.13 A, C2C12 cells displayed ALP activity after prolonged culture (3 weeks) in X-collagen and 3d Mineralized scaffolds even in the absence of pBMP-2 treatment. The ALP activity was low among the study groups on week 1, but significant differences among the groups became evident after week 2. Some of the C2C12 treatment groups displayed less ALP activity than the untreated cells (i.e., 0  $\mu\text{g/mL}$  pBMP-2 group) in corresponding scaffolds (e.g., 1 and 2  $\mu\text{g/mL}$  groups in X-linked collagen groups), indicating a detrimental effect on the ALP activity by polyplex treatment. Among the cells treated with 1  $\mu\text{g/mL}$  pBMP-2, there was no beneficial effect of the pBMP-2 treatment as compared to untreated cells. Among the scaffolds receiving 2  $\mu\text{g/mL}$  pBMP-2, only the unprocessed collagen scaffolds showed an increased ALP activity especially 3 weeks after cell seeding. The highest ALP activity was observed for cells cultured in 3d mineralized scaffolds carrying 4  $\mu\text{g/ml}$  pBMP-2 (on both week 2 and week 3).

For MC-3T3 cells (Fig. 3.13 B), relatively high ALP activity was only observed by the 3d mineralized scaffolds that did not receive pBMP-2 at 1- and 2-weeks post-transfection, which was declined after 3 weeks. The MC-3T3 cells in collagen scaffolds bearing 4  $\mu\text{g/ml}$  pBMP-2 sustained the ALP activity even after 3 weeks, which led to significantly increased ALP activity at that time point. Polyplexes delivered with 3D Mineralized collagen scaffolds did not sustain high ALP activity, as the control (non-treated) MC-3T3 cells in 3D Mineralized scaffolds.

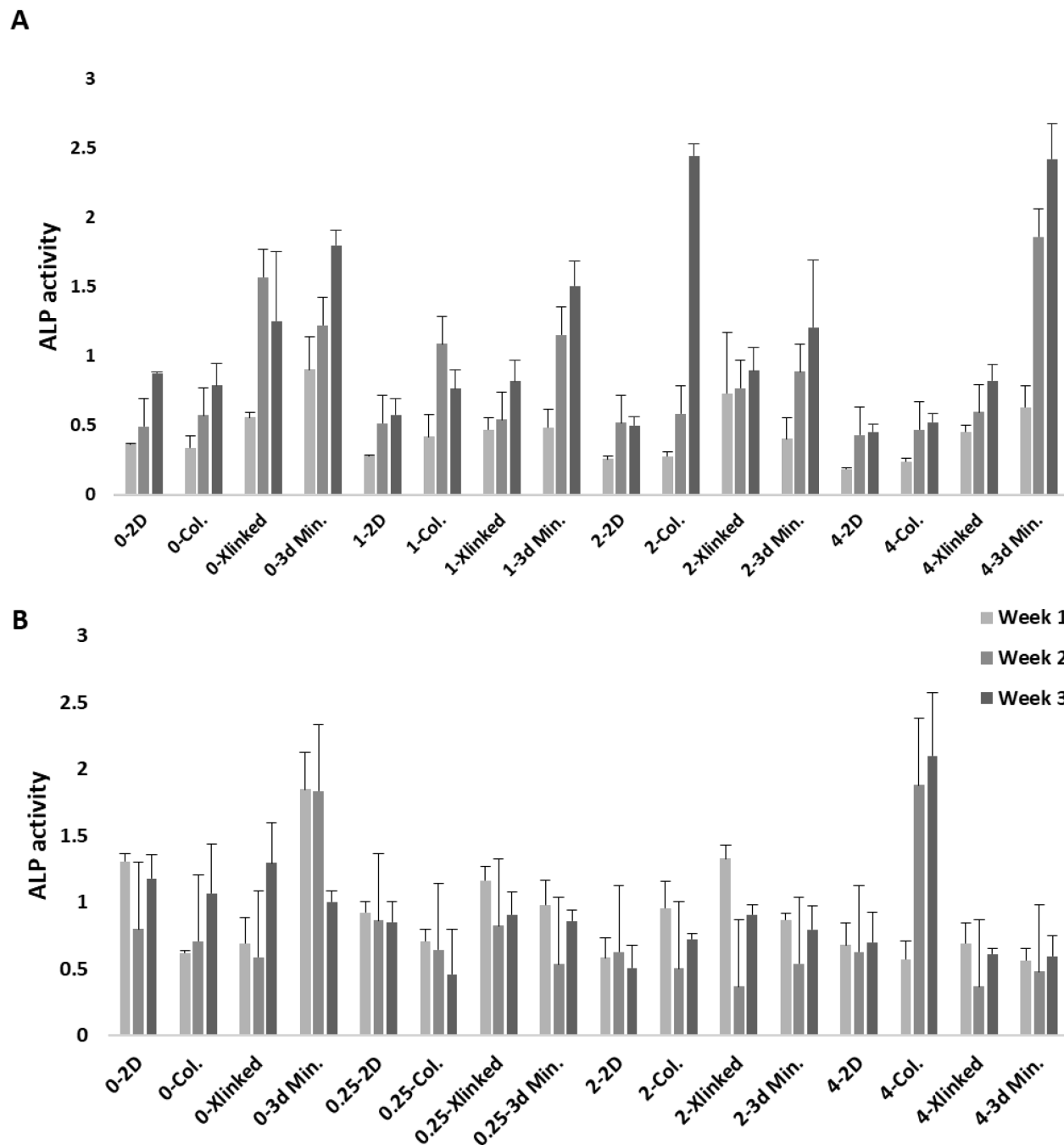


**Figure 3.13.** The ALP activity was evaluated by delivering pBMP-2 to C2C12 (A) and MC-3T3 (B) cells via collagen, X-linked collagen and 3d mineralized scaffolds for 1, 2 and 3 weeks. The pBMP-2 concentrations used were 0, 1, 2 and 4  $\mu\text{g/ml}$  for C2C12 and 0, 0.25, 2 and 4  $\mu\text{g/ml}$  for MC-3T3 cells. The polymer:pDNA and pDNA/pASP conditions were ratio 10 and ratio 1 respectively for C2C12, and ratio 5 and 0.5 respectively for MC-3T3 cells. The ALP activity was measured 24 h after the addition of the substrate and was based on the optimal density values obtained.

### 3.4 Discussion

Gene therapy involves the introduction of therapeutic genes into cells via non-viral and viral vectors. Non-viral vectors are generally considered relatively safe and highly effective. High MW PEI has been touted as a broad-spectrum cationic polymer for non-viral gene delivery since it shows high transfection efficiency in numerous cell types, but its use is limited due to high toxicity levels (104). Our results (based on flow cytometer and cell viability) highlighted PEI 25 as a non-suitable polymer for gene delivery in both cell lines.

On the other hand, low MW PEI shows a relatively low toxicity but lower transfection efficiency. Previous studies have shown that the performance of low MW PEI (e.g., 1.2 kDa PEI) could be improved by being modified with lipid moieties. To this end, we developed a library of lipid-modified low MW PEI carriers and as it has been reported before, we found that the presence of a cleavable thioester linkage between the lipid and the polymer (i.e., PEI-tLA) to be the most effective for delivering pDNA to the cells. A previous study from our group suggested that the delivery of pDNA with PEI-tLA to MSCs can be further improved by using hyaluronic acid (HA) as an additive during the complex formulation (226). The presence of polyanionic additives during complexation is possible to affect the transfection efficiency since the molecular weight of the polymeric additives can have an impact on the complexes packing, charge and size. In this study, we introduce the 14 kDa polyaspartic acid as an additive and by visual examination, we found that the introduction of pASP into the complexation process further increased the delivery efficiency of pDNA to C2C12 and MC-3T3 cells when we used PEI 1.2-tLA10 as the carrier.

Changes on some of the variable involving pDNA complex formulations, such as the polymer:pDNA or pDNA/pASP ratios, may affect the electrostatic interactions between the positively charged cationic polymers and the negatively charged pDNA. Thus, the

physicochemical properties and the transfection efficiency levels may change. The influence of polymer:pDNA and pDNA/pASP ratios on both hydrodynamic sizes and surface charges showed that the polymer:pDNA ratio as well as the presence of polyanionic pASP during complex formation has an impact on the NPs properties. Notably, the size of the complexes became smaller with the addition of pASP at polymer:pDNA ratio 10. The zeta potential was also evaluated and found to increase from 7.8 to 14.3 mV along with the increase in the weight ratio of pASP for the polymer:pDNA ratio 10 while for ratio 5 decreased from 13.1 to -9.6 mV. Usually, highly cationic complexes can easily bind and disrupt the anionic cell membrane and improve gene transfection but can also cause cytotoxicity if the disruption is excessive. Later in our experiments, we observed the positive effect of high surface charges on the transfection efficiency and cell viability against C2C12, but the negative effect against MC-3T3 cells.

To ascertain the influence of the pASP on the transfection efficiency, we examined on both cell lines a series of complexes synthesized by various DNA concentrations, polymer:pDNA and pDNA/pASP ratios in comparison with PEI 1.2-tLA10 no additive and PEI25. Interestingly, the presence of pASP in the complex formation in every examined condition enhanced the transfection efficiency in both cell lines compared to the controls. It was found that polymer:pDNA ratio of 10, pDNA/pASP ratio of 1 and pDNA concentration of 1  $\mu\text{g}/\text{ml}$  was required for efficient transfection (~85%) of C2C12 cells, while the same conditions were not applicable for MC-3T3 cells since under the same conditions high cytotoxicity was observed. The data revealed that for C2C12 cells, a decrease in the DNA concentration and polymer:pDNA ratio led to a significant decrease on transfection efficiency while for MC-3T3 cells led to an increase. The MC-3T3 cells, being more sensitive than the C2C12 cells, benefited from the decreased pDNA concentration (hence polyplex concentration), which was not the case for C2C12 cells. The transfection efficiency of MC-3T3

cells was enhanced to the same levels of C2C12 cells by delivering complexes at polymer:pDNA ratio of 5, pDNA/pASP ratio of 0.5 and DNA concentration 0.25 µg/ml.

High cytotoxicity can limit the use of non-viral vectors for gene therapy. Lipid modified low MW PEIs were shown in general to increase the toxicity of the polymers. In our case, none of the optimised formulations of PEI1.2-tLA10 with or without pASP tested in C2C12 cells caused a decrease in cell viability at any time-point up to 7 days post transfection. On the other hand, the effect of high surface charges due to pASP on the toxicity was confirmed on MC-3T3 since a significant drop (80%) in cell viability was recorded compared to the toxicity manifested on C2C12 under the same conditions (Fig. 3.5 A).

In bone tissue engineering, delivery of encoded growth factors such as BMP-2 protein to osteogenic cells can promote osteogenic activity. Expression of ALP is an important assessment criterion regarding to osteogenic activity, being the enzyme responsible for mineralization of deposited extracellular matrix (249). Throughout this study, we tested two different cell types as realistic models for the measurement of induction of osteogenic activity. C2C12 cells are known for their ability to convert from their clonal myoblast pathways into cells displaying osteoblastic features when treated with BMP-2 protein (250). The MC-3T3 cells, on the other hand, are a well-known preosteoblastic model isolated from mouse calvaria and it has been used extensively for studying differentiation of osteoblasts (251). The delivery of BMP-2 significantly induced the ALP activity on both cell lines under specific conditions. The induction was more obvious in C2C12 cells, which lacked an endogenous ALP activity under normal conditions and the cells displayed an ALP peak over the first week of the cells being exposed to pBMP-2 polyplexes. In some cases, the ALP activity remained high during the 3-week study duration, while in other cases the ALP was significantly lower after 3 weeks. A high ALP activity in MC-3T3 was observed in most of

the cases after week 2 and remained high up to 3 weeks. Comparing cell lines, generally MC-3T3 cells expressed lower ALP activity compared to C2C12 even when they were exposed to optimal for MC-3T3 complex conditions.

The non-viral polyplexes of pDNA found effective for 2D modification of C2C12 and MC3T3 cells were further evaluated for their ability to modify cells under 3D conditions. The use of a scaffold as a delivery system for localizing genes at the defect site usually requires a biocompatible matrix that will enhance cell attachment and differentiation while promoting the slow long-term release of polyplexes for enhanced gene transfection efficiency. Collagen-based scaffolds were initially used as a system for the delivery of a human parathyroid hormone (hPTH 1-34) gene on the site of a bone fracture, where a bony union was observed after the period of 8 weeks (252). Similarly, Chen et al. promoted the osteochondral tissue formation via delivering TGF- $\beta$ 1 and BMP-2 plasmids via chitosan-gelatin and hydroxyapatite/chitosan-gelatin scaffolds over a period of 12 weeks (253). However, the efficient delivery of the genes in the presence of a scaffold remains a challenge. In this study, we proposed the incorporation of PEI 1.2-tLA10-pASP/pDNA complexes into intrafibrillar mineralized collagen-based scaffolds in order to control their effective and prolonged delivery to the cells. The presence of a crosslinker as well as the presence of hydroxyapatite can change the scaffolds biocompatibility and mechanical properties. Polyelectrolytes such as pASP have been found to direct intrafibrillar mineralization *in vitro*. The proposed intrafibrillar mineralized collagen scaffolds that have been fabricated by Dr. Sone's group at the University of Toronto are showing interconnectivity, mineralized-unmineralized layers as well as better spatial control over mineralization. In addition, they show porosity with pore sizes ranging from 20-60  $\mu$ m, which may inhibit cell infiltration (Appendix Fig 3.S 1). Zero, three- and six-days mineralized scaffolds have been fabricated and been used for investigating cell

viability. Cell culture experiments suggested that the presence of a crosslinker (zero days of mineralization) did not affect the cell viability in comparison to the presence of mineralization. Especially, the 6 days mineralized scaffolds were highly toxic to both cell lines and only the 3 days mineralized scaffolds were chosen for further applications. Later, we examined the development of delivery of the optimal polyplex formulations, delivery of higher pDNA concentration via 3D mineralized scaffolds caused significantly higher prolonged ALP activity in C2C12 cells in comparison to the scaffolds without mineralization. In comparison, MC-3T3 cells seeded on 3D mineralized scaffolds without the pBMP-2 treatment gave much higher ALP activity as compared to cells in mineralized scaffolds and treated with pBMP-2 polyplexes. This may be due to stronger surface bonds being created between the particles surface and hydroxyapatite that may reduce their uptake from the cells. Furthermore, prolonged ALP expression occurred from MC-3T3 on collagen scaffolds that delivered high DNA concentration.

### **3.5 Conclusions**

The low MW PEIs polymers has become a viable approach to develop carriers for successful delivery of pDNA to cells. Our first objective was the development of low MW lipid modified PEI based nanoparticles (NPs) with pASP as an additive that will facilitate C2C12 and MC-3T3 transfection efficiency. The optimal formulations for C2C12 and MC-3T3 were found to be PEI1.2-tLA10, polymer:pDNA ratio 10, pDNA/pASP ratio 1 carrying 1  $\mu\text{g}$  of pDNA and PEI1.2-tLA10, polymer:pDNA ratio 5, pDNA/pASP ratio 0.5 carrying 0.25  $\mu\text{g}$  of pDNA respectively. These formulations showed transfection efficiency of  $\sim 85\%$  in monolayer causing limited cytotoxicity. The incorporation of the optimized complexes into three different collagen scaffolds showed that 3d mineralized scaffolds prolonged the ALP activity in C2C12 cells while the same scaffolds without complexes and collagen scaffolds carrying complexes prolonged the

ALP activity in MC-3T3 cells. These different complex and scaffold variations can produce successful delivery systems based on the cell type for bone regeneration applications.

## **Chapter 4- Delivery of particles via collagen/gelatin fibers in C2C12 and MC-3T3 cells**

## 4.1 Introduction

Over the last decade, gene therapy has gained powerful attention in the fields of bone regeneration and tissue engineering (254). The alteration of genetic information over protein delivery has been an alternative method for the expression or deactivation of a desired protein from target cells or tissues (255). A variety of viral and non-viral vectors has been developed and used for the safe delivery of plasmid DNA to the cells. Among these, synthetic non-viral vectors and especially cationic polymer-based vectors like polyethyleneimine (PEI) has been receiving great deal of attention (256). However, the transfection efficiency and toxicity levels are significant and related to molecular weight (MW) and type of the polymer structure. The low MW linear or branched structures have low cytotoxicity compared to the high MW PEIs but suffer from poor transfection efficiency (257). To overcome these limitations, previous studies (Chapter 4) revealed that a chemical modification of low MW PEI (<2 kDa) with lipid moieties like thioester-linoleic acid (tLA) can effectively serve as a vehicle for the delivery of pDNA to C2C12 and MC-3T3 cells. Our results further showed an enhanced transfection with the presence of poly(aspartic acid), pASP, as an additive in the complexes, with or without the presence of a 3D mineralized collagen scaffold.

Gene activated matrices (GAMs) have been developed for effective delivery of pDNA in an anatomical area of interest while simultaneously can offer a structural support for new matrix deposition (258,259). The selection of the most appropriate natural or synthetic scaffold polymer along with the method of processing should be chosen considering the type of interactions between the complexes and the scaffold. The stability of the complexes during scaffold fabrication as well as the controlled release rate during scaffold degradation are additional considerations to be addressed (33,260). A variety of GAM systems, including nanoparticles, hydrogels, and freeze

dried scaffolds and electrospun membranes have been investigated with the aim of the successful delivery of complexes to cells of interest (261–264). Electrospun fibers have become increasingly attractive due to their structural similarities to that of extracellular matrix (ECM) (265). The electrospinning process involves several important parameters, including polymer properties such as MW, solution properties such as viscosity, process parameters such as applied voltage, flow rate and drying time, and environmental conditions such as temperature and humidity. All of these parameters can have an impact on the final nanofiber properties and the release/presentation profile of the genes (266,267).

Gelatin (Gel) has been successfully used as a natural polymer for scaffolds fabrication due to its biocompatible and biodegradable properties (268). As a natural polymer, Gel is water-soluble but for the formation of electrospun fibers, organic solvents such as 2,2,2-Trifluoroethanol (TFE) and 1,1,1,3,3,3-Hexafluoro-2-propanol (HFP) are usually needed (269,270). Gel has been previously investigated as drug, protein and plasmid DNA (pDNA) delivery carrier. Pankongadisak et al. proposed Gel-PEG (Polyethylene Glycol) electrospun fibers for the delivery of pDNA complexes for bone regeneration. The study showed a robust ALP induction by delivering pBMP-2/PEI 1.2-tLA complexes to C2C12 and MC-3T3 cells via the Gel-PEG fibers (214). However, gelatin's high degradation rates under physiological conditions (i.e., it dissolves readily if un-crosslinked) eliminate its use for long-term use that is typically needed for bone tissue engineering. The degradation (or resiliency) of gelatin can be altered by changing the gelatine source, its MW, the degree of crosslinked or by adding another synthetic/natural polymer to the Gel formulation depending on the final application (271,272).

In this work, we aimed to improve resiliency of electrospun Gel fibers by incorporating collagen Type I into the mats. Collagen Type I is the main structural component of the ECM. Two

different methods of collagen incorporation into the Gel-PEG electrospun mats have been examined. We prepared (a) Gel-Col-PEG mats that contained different volumes of Gel, collagen and PEG, in addition to complexes, and b) two-layered mats that contained collagen fibers without complexes as the first layer and Gel-PEG/complexes as the second layer. The mats bearing gene complexes were evaluated for osteogenic activity in vitro using the well established C2C12 and MC3T3 cell models.

## **4.2 Materials & Methods**

### **4.2.1 Materials**

The 1.2 kDa branched PEI (PEI1.2;  $M_n$ :1.1 kDa,  $M_w$ : 1.2 kDa), fetal bovine serum (FBS), ALP substrate p-nitrophenol phosphate (p-NPP), gelatin Type A (300 Bloom; porcine skin), and 2,2,2-Trifluoroethanol (TFE) (N99.0%) were purchased from Sigma-Aldrich (St Louis, MO). The PEG ( $M_n$  = 20 kDa) was obtained from Fluka (Buchs, Switzerland). The polyaspartic acid (pASP) was purchased from Alamanda Polymers (Huntsville, Alabama, US). Dulbecco's Modified Eagles Medium (DMEM) /F12 medium (1:1) (1X, with L-glutamine and 15mM HEPES), Hank's Balanced Salt Solution (HBSS), penicillin-streptomycin (10,000 U/mL-10,000  $\mu$ g/mL), GlutaMax-I (100X) and MEM NEAA (100X) were from Gibco (NY, USA). The gWIZ-GFP and gWIZ plasmids were purchased from Aldevron (Fargo, ND). Type I collagen was extracted from rat tail tendons via acid dissolution. Prior to use, the rat tails have been disinfected with 70% ethanol by submerging and remained stored at -20°C. During the procedure, the tendons were removed from the rat tails and washed with Tris buffered saline (0.9% NaCl, 10 mM Tris). Then, have been weighted and dehydrated with a serial concentration of ethanol (50%, 75%, 95% and 100%, ~30 min each). Afterwards, they were added into pre-cooled 0.5 M acetic acid (100 ml

per 1 g wet tendon) and stirred at 4°C for 48-72 hours. After the incubation time with acetic acid, the tendons solution has been centrifuged and supernatant has been added to an equal volume of pre-cooled 10% NaCl for precipitation overnight at 4°C. The next day, the floated collagen, has been harvested and centrifuged. The collagen pellets have been collected and resuspend in 0.25 M acetic acid at 4°C (100 ml per 1 g initial tendons). Later, the collagen-acetic acid solution has been dialyzed against 0.025 M acetic acid at 4°C for three days and the buffer has been changed twice a day. For the last two changes the buffer has been replaced with ddH<sub>2</sub>O. Finally, the resulting dialyzed collagen solution has been freeze-dried for 48h and the obtained powder has been stored at 4 °C prior to any further use.

#### **4.2.2 Preparation of complexes**

PEIs 1.2 kDa modified with thioester-linked linoleic acid (tLA) was synthesized according to our established protocol and the degree of substitution was determined by the <sup>1</sup>H-NMR (224–226). The polyplexes were prepared at room temperature by adding PEI 1.2-tLA10 (1mg/ml) in serum-free medium (DMEM/F:12) and then an aqueous solution containing pASP (0.4 µg/µL) with GFP-pDNA (0.4 µg/µL) was added. The final ratio of polymer:pDNA was 10:1, and the final ratio of pDNA:pASP was 1:1. Polyplexes were incubated for 30 min at room temperature prior to use.

#### **4.2.3 Fabrication of gene-activated electrospun mats**

##### **4.2.3.1 Monolayer mats**

The gene-activated mats were prepared using a similar approach as Pankongadisak et al. (214). Briefly, gelatin (100 mg/ml) and collagen (50 mg/ml) were dissolved in TFE solution and

PEG (10 mg/ml) was dissolved in dH<sub>2</sub>O. For the fabrication of the mats, different volume ratio Gel-Col-PEG mixtures were prepared at 100-0-100, 75-25-100, 50-50-100 and 0-100-0. For the mats loaded with complexes, the complexes were prepared prior to electrospinning as described in Section 2.2 and dispersed in the different volume ratio Gel-Col-PEG solutions at a volume ratio of 1:3 respectively and mixed well before electrospinning. The final solution was transferred into a 1-mL plastic syringe with a 20-gauge needle. The mats were electrospun onto an aluminium foil by using an AL-4000 programmable syringe-pump. The conditions that the mat production were: (i) flow rate of 350  $\mu$ L/h, (ii) applied voltage 19 kV and (iii) working distance to foil of 10 cm. The final mats were collected and dried under a biological safety cabinet for 30 min and disinfected under UV light for 15 min prior to any further use.

#### **4.2.3.2 Double-layered mats**

For the first layer, 50  $\mu$ g/ml collagen Type I in TFE was spanned first by using the same electrospinning parameters described in 2.3.1 section. For the second layer, a solution containing Gel-Col-PEG (100-0-100 or 75-25-100) with complexes at a volume ratio 1:3 respectively was spanned onto the collagen mat by using the same parameters. The final mats were collected and dried under a biological safety cabinet for 30 min and disinfected under UV light for 15 min prior to any further use.

#### **4.2.4. Characterization of gene-activated electrospun mats**

The morphology of the electrospun mats with and without complexes was observed by SEM operated at an acceleration voltage of 10 kV. Before observation, the mats were cut into 1 cm  $\times$  1 cm pieces and coated with gold to increase conductivity. Fiber diameters were measured

by using Image J 1.52 V software. The presence of complexes in mats was determined by preparing the mats as described in Section 2.3 except that the complexes were carrying Cy3-labeled pDNA as described in Pankongadisak et al. (214). The mats were collected and then observed under Olympus FSX100 Fluorescence Microscope. The particle size and surface charge of the polyplexes used for electrospinning was determined by using a Litesizer 500 system (Anton Paar, Austria) with dynamic light scattering and zeta potential measurements, respectively. The mats with and without complexes were dissolved with 0.05% trypsin and incubated in a water bath for 5 min at 37 °C. Next, equal amount of DMEM/F12 was added and finally the solution was diluted with free RNA water. Freshly free complexes were also prepared as controls at room temperature. Prior to measurements all the samples have been filtered.

#### **4.2.5 Cell culture**

Mouse myoblast C2C12 cells and cloned mouse calvarial osteoblast MC3TC-E1 cells were used as model cell lines. C2C12 cells were maintained in DMEM/F:12 (1:1) supplemented with 10% FBS, 100 U/mL penicillin, 100 µg/mL streptomycin, 0.1% GlutaMax-I and 0.1% NEAA. The MC3TC-E1 were maintained in 50% DMEM/F:12 (1:1) and 50% AMEM supplemented with 10% FBS, 100 U/mL penicillin, 100 µg/mL streptomycin, 0.1% GlutaMax-I and 0.1% NEAA. The cells were routinely maintained under humidified atmosphere (95/5% air/CO<sub>2</sub>) at 37 °C in the indicated cell culture medium.

#### **4.2.6 Transfection efficiency of gene activated matrices**

Twenty-four hours prior to transfection experiments, the cells were seeded in 48-well cell culture plates at a density of 10<sup>4</sup> cells/cm<sup>2</sup>. The mats fabricated as described in Section 2.3.1

carrying the gWIZ-GFP complexes were first incubated in 200  $\mu$ L of 0.05% trypsin and incubated for 5 min at 37 °C water bath. Then, 200  $\mu$ L of DMEM/F12 were added to stop the reaction. A predetermined volume of the final solution was added to the cells to give final pDNA concentrations of 0.5 and 1  $\mu$ g/ml in tissue culture medium. Free complexes were also prepared and mixed with trypsin and DMEM/F12 solution (as above) prior to adding them into the cells. Free complexes without any treatment were also prepared and added directly to the cells to serve as a positive control treatment. The transfection efficacy was investigated 48 h post-transfection by Olympus FSX100 Fluorescence Microscope and by flow cytometer. For flow cytometer analysis, the cells were washed (3X) with HBSS, trypsinized with 0.05% trypsin, and fixed with 3.7% formalin in HBSS. The transfection efficiency was quantified based on GFP positive population and the mean fluorescence intensity of the cells by BD LSRFortessa (Becton-Dickinson, San Jose, USA). Each study group contained three replicates.

#### **4.2.7 Delivery of BMP-2 plasmid from gene activated matrices**

The cells were seeded in 24-well plates the day before the experiments. Gene activated mats were prepared as described in Sections 2.3.1 and 2.3.2 and added to the cells as was explained in Section 2.6. One-week post-transfection, the cells were washed with HBSS (x2 times) and lysed with 200  $\mu$ L ALP buffer (0.5 M 2-amino-2-methylpropan-1-ol and 0.1% Triton-X; pH:10.5) for 2 h at room temperature under constant shaking. 200  $\mu$ L of lysed cell solution from each well was incubated with 200  $\mu$ L of 2 mg/mL ALP substrate (p-NPP) for 30 min. Afterwards, the ALP activity was determined by measuring the absorbance at 405 nm by using the ELx800 Universal Microplate reader (Bio-Tek Instruments).

#### **4.2.8 Statistical analysis**

All results were expressed and plotted as mean  $\pm$  standard deviation (SD). Data analysis was performed by one-way analysis of variance (ANOVA). Statistical significance was considered for p-values  $<0.05$ . Statistical analysis was only performed wherever more information from the results were needed.

## 4.3. Results

### 4.3.1 SEM imaging of gene-activated matrices

The morphology and average diameter of the electrospun fibers are shown in Fig. 4.1 and Table 4.1, respectively. Four different volume ratio Gel-Col-PEG mats with and without complexes were characterized through SEM observation. As shown in Fig. 4.1 A-B, the 100-0-100 Gel-Col-PEG mat with and without complexes showed poor quality of fibers containing a large number of beads. The average fiber diameter without complexes was  $90 \pm 20$  nm and the bead size was  $663 \pm 215$  nm. For the electrospun fibers carrying complexes, the fibers diameter increased to  $97 \pm 6$  nm and the bead size to  $770 \pm 111$  nm. Similar fibers quality was observed from 75-25-100 Gel-Col-PEG mats (Fig. 4.1 C-D); the presence of collagen in the electrospun mixture increased the fiber diameter to  $140 \pm 10$  nm and beads size  $706 \pm 95$  nm without complexes, while the fiber diameter decreased to  $126 \pm 32$  nm and the bead size to  $330 \pm 27$  nm in the presence of complexes. Further increasing the collagen content in the case of 50-50-100 Gel-Col-PEG mat (Fig 4.1 E-F), the quality of fibers was even lower given by much higher number and size of beads in the mats. This was the case for both with and without complexes added to the electrospun mats. In contrast, uniform fibers without the presence of beads and an average diameter of  $146 \pm 38$  nm were observed by electrospinning collagen (0-100-0 Gel-Col-PEG mats) without complexes as illustrated in Fig. 4.1 G. In the presence of complexes (Fig. 4.1 H), good quality fibers were obtained but the fiber size increased to  $177 \pm 31$  nm and the size of the observed beads was  $770 \pm 99$  nm.

Samples	Average diameter (nm)			
	Without polyplexes		With polyplexes	
	Fiber	Beat	Fiber	Beat
Gel-Col-PEG (100-0-100)	90 ± 20	663 ± 215	97 ± 5.8	770 ± 111
Gel-Col-PEG (75-25-100)	140 ± 10	706 ± 95	126 ± 32.1	330 ± 27
Gel-Col-PEG (50-50-100)	103 ± 6	867 ± 343	87 ± 21	1080 ± 329
Gel-Col-PEG (0-100-0)	146 ± 38	-	177 ± 31	770 ± 99

**Table 4.1. Average fiber diameters and bead size of electrospun mats without and with pDNA complexes.**

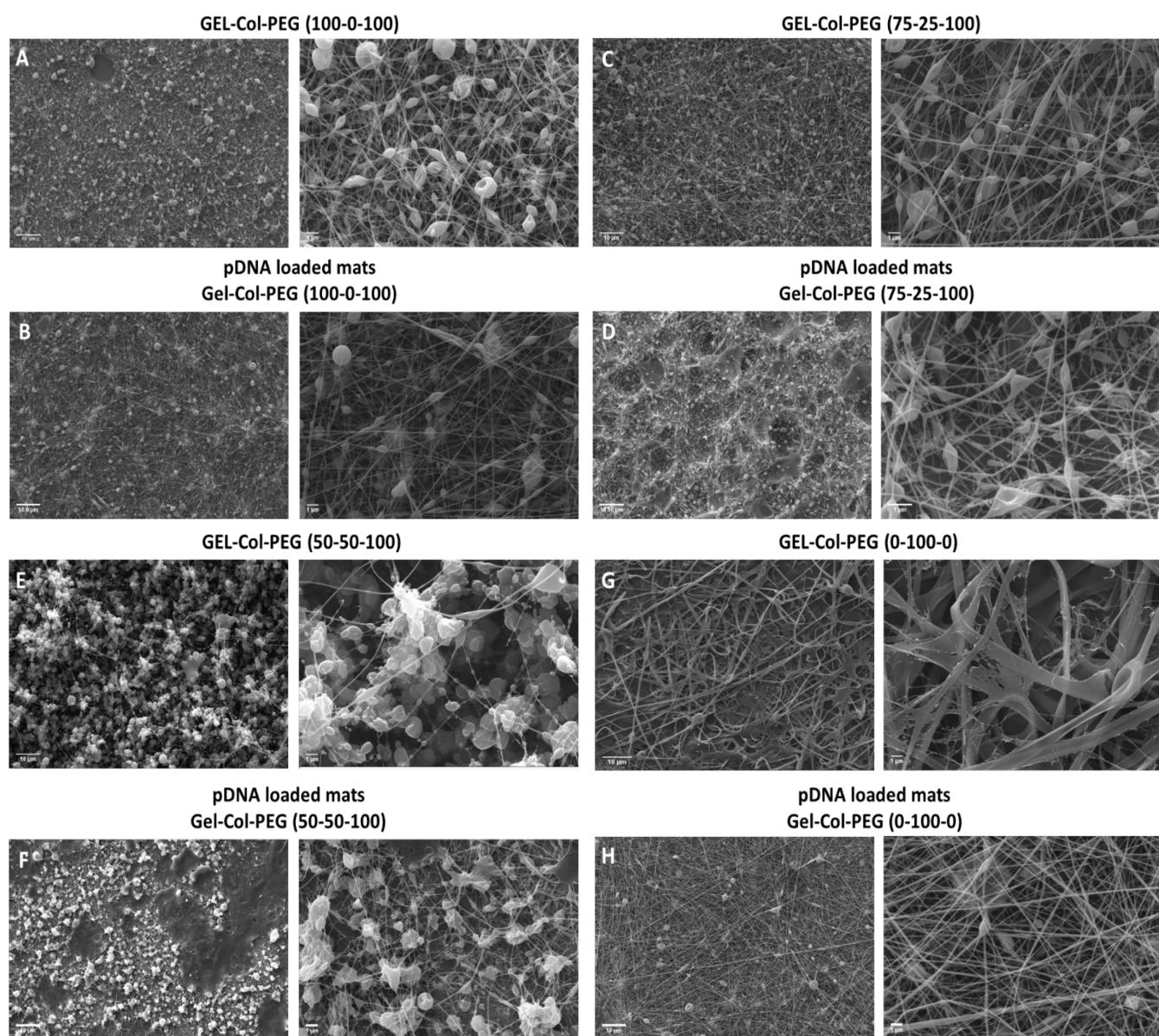


**Figure 4.1. SEM images of different volume ratio Gel-Col-PEG electrospun fibers with and without complexes (scale bars 10 and 1  $\mu\text{m}$ ).**

### **4.3.2 Delivery of Cy3 loaded complexes via mats**

To evaluate the presence and distribution of pDNA complexes in the fiber mats, the electrospun monolayer mats were prepared by using Cy3-labeled pDNA complexes, whose presence and distribution were examined by fluorescence microscopy. As shown in Figure 4.2, the entrapment of Cy3-complexes in collagen-free 100-0-100 Gel-Col-PEG mats showed the strongest red signal, which confirmed the successful entrapment of complexes in the mat. The presence of the red Cy3-complexes was fading out in the next set of mats, as the collagen content in the mats was increasing and the gelatin content was decreasing.

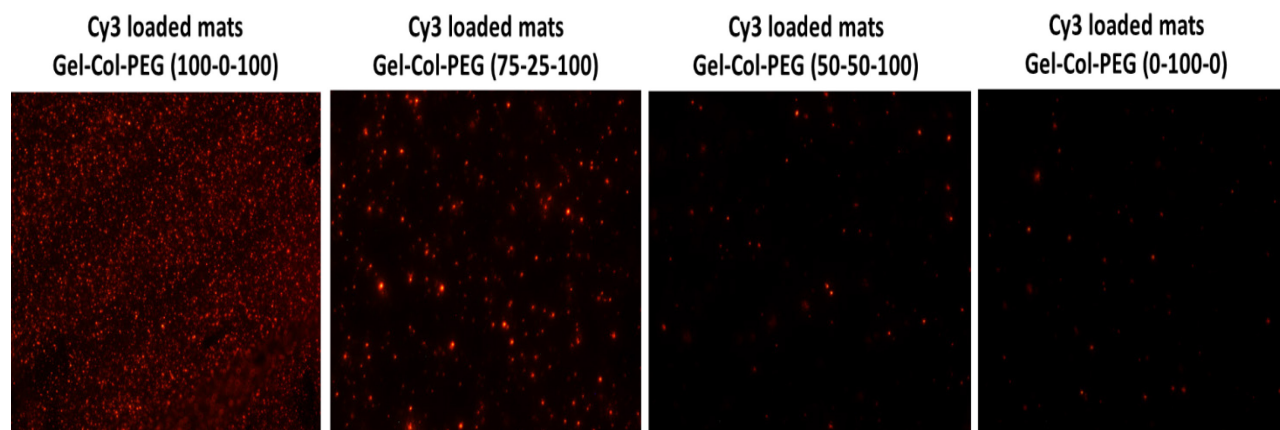


**Figure 4.2. Fluorescence microscopy images of mats with Cy3 labeled pDNA complexes.**

### **4.3.3 Particle size and charge analysis**

The pDNA complexes released from the monolayer fibers mats were analyzed for hydrodynamic size (Z-average) and surface charge ( $\zeta$ -potential) (Table 4.2). The mean size of the PEI1.2-tLA10/pDNA complexes without pASP at polymer:pDNA ratios of 10:1 was 101.3 nm, while the mean size of the formulation with the additive (pDNA/pASP ratio of 1) was 90.0 nm.

The mean size of the PEI1.2-tLA10/pDNA/pASP complexes released from 100-0-100 Gel-Col-PEG mat was 113.3 nm and it was further decreased to 42.0 nm in the case of 0-100-0 Gel-Col-PEG mat. Overall, the particles incorporated into the mats with high collagen volume ratio were smaller than the particles in the mats without collagen. Fig 4.S1. shows the correlation function and size distribution of dissolved mats with and without complexes. The  $\zeta$ -potential values decreased from 38.0 to 35.5 mV after the addition of pASP during complexes formation. After the encapsulation of the complexes in 100-0-100 and 75-25-100 Gel-Col-PEG mats, the release particles showed  $\zeta$ -potential values that was half the value of the original particles.

	Particle size (nm)		$\zeta$ -potential (mV)	
PEI1.2- tLa10/pDNA	101.3 $\pm$ 2.0		38.0 $\pm$ 2.6	
PEI1.2- tLa10-/pDNA/pASP	90.0 $\pm$ 1.2		35.5 $\pm$ 0.5	
Mats	no complexes	with complexes	no complexes	with complexes
Gel-Col-PEG (100-0-100)	ND	113.3 $\pm$ 0.9	ND	16.1 $\pm$ 1.4
Gel-Col-PEG (75-25-100)	ND	85.8 $\pm$ 2.3	ND	16.8 $\pm$ 0.5
Gel-Col-PEG (50-50-100)	ND	45.7 $\pm$ 1.5	ND	11.9 $\pm$ 5.0
Gel-Col-PEG (0-100-0)	ND	42.0 $\pm$ 3.2	ND	10.5 $\pm$ 2.7

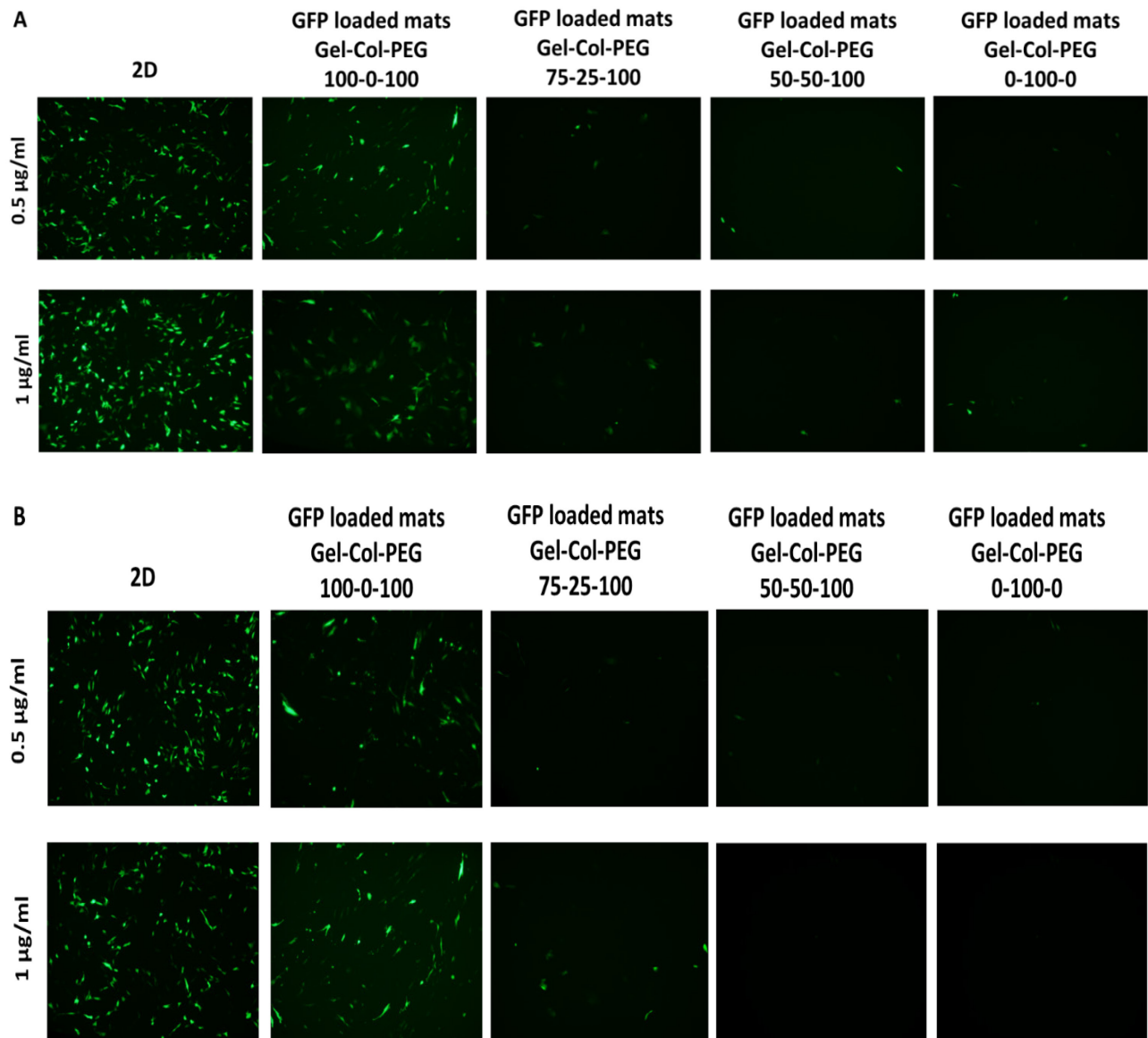
**Table 4.2. Size and  $\zeta$ -potential of original free particles and particles released from the different Gel-Col-PEG mats.**

ND: Non detected

#### 4.3.4 Transfection efficiency

The delivery of pDNA complexes to C2C12 and MC-3T3 cells from different monolayer mats was evaluated by fluorescent microscopy (Fig. 4.3 A - B) and flowcytometer (Fig. 4.4 A-B) 48 h post-transfection. Two concentrations of the pDNA complexes were used, where the concentration from the mats were estimated by assuming 100% encapsulation efficiency. Transfection by free (un-electrospun) complexes on cells on tissue culture plastic served as the positive reference treatment, which indicated strong transfection in both cell types (Fig 4.3 A and

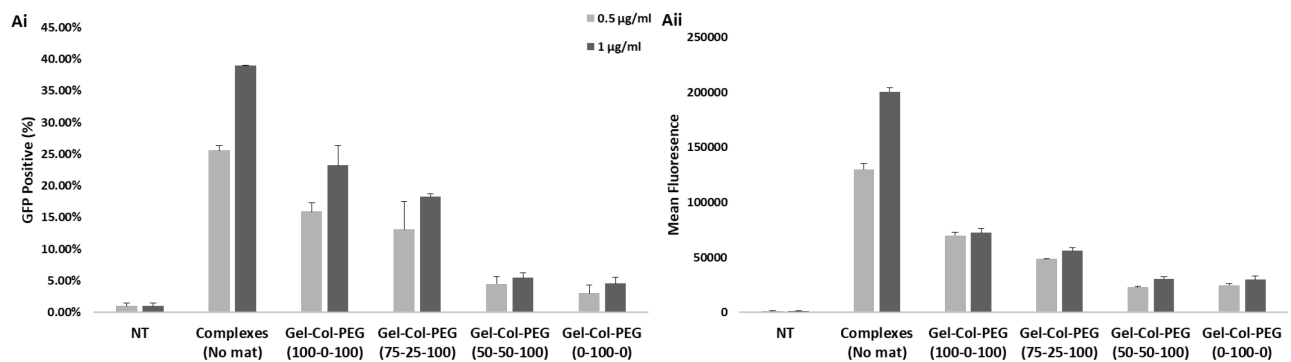
B – left micrographs). In both cell lines, the presence of collagen in the mats showed a negative effect on the transfection efficiency, where the transfection efficiency was decreased as the collagen volume in the mats was increased. In addition, a significant difference in transfection efficiency was observed between the delivery of free pDNA complexes and the complexes encapsulated into the different monolayer mats.



**Figure 4.3. Delivery of gWIZ-GFP complexes via different volume ratio Gel-Col-PEG mats to C2C12 (A) and MC-3T3 (B) cells.**

GFP expression was qualitatively assessed 48 hours after transfection using fluorescent microscopy. The different volume monolayer mats used are indicated on top of the micrographs where on the left is the pDNA concentrations (1 and 0.5  $\mu\text{g}/\text{mL}$ ) in cell culture medium carried by the complexes.

To quantitatively analyze the GFP expression levels in C2C12 (Fig 4.4 Ai-ii) and MC-3T3 (Fig 4.4 Bi-ii) cells, the PEI1.2-tLA10 complexes with pASP were encapsulated in different Gel-Col-PEG mats and used to treat the cells and the GFP expression levels in both cell lines were analyzed using flow cytometer. The mean fluorescence intensity and the percentage of GFP expression were plotted against the different volume ratio Gel-Col-PEG mats. In C2C12 cells, based on the GFP positive cell population (Fig 4.4 Ai), an increase in GFP expression was observed after increasing the pDNA concentration from 0.5 to 1.0  $\mu\text{g}/\text{mL}$ ; 25% to 40%, 16% to 23% and 13% to 18% for free complexes (no mat), 100-0-100 Gel-Col-PEG and 75-25-100 Gel-Col-PEG, respectively, while for 50-50-100 and 0-100-0 Gel-Col-PEG mats, GFP expression remained at  $\sim 5\%$  for both pDNA concentrations. The mean fluorescence results (Fig 4.4 Aii) also showed a similar pattern for the free complexes and the delivered with different mats.



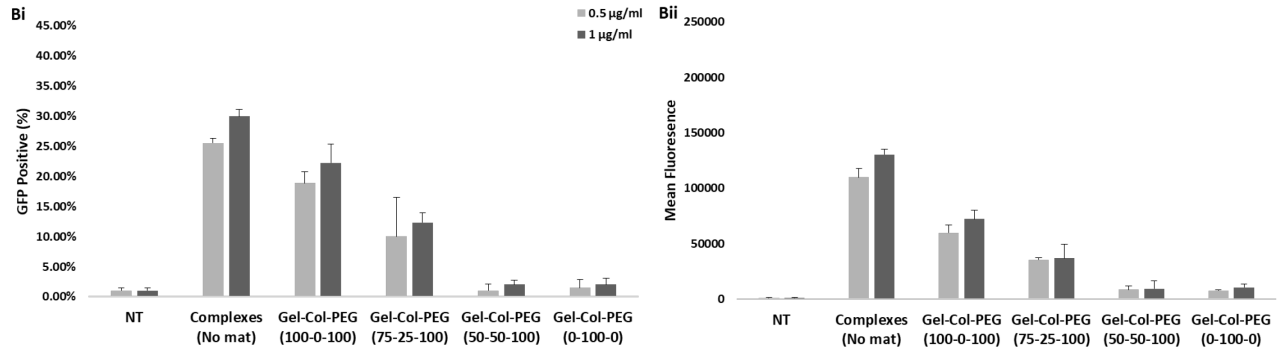


**Figure 4.4. The GFP-positive population and mean fluorescence intensity/cell in C2C12 (Ai-ii) and MC3T3 (Bi-ii) cells analyzed 48 h post-transfection by flow cytometry.** The pDNA concentrations in cell culture medium were 1.0 and 0.5 µg/mL.

The data from the delivery of complexes to MC-3T3 cells are summarized in Fig. 4.4 Bi-ii. In general, the incorporation of complexes in the different volume ratio mats reduced the GFP expression and mean fluorescence compared to the free complexes independent of the examined pDNA concentration. The delivery of free complexes (no mat) increased the GFP expression from 26% to 30% following the increase of pDNA concentration from 0.5 to 1.0 µg/mL, while for complexes delivered via mats, the GFP expression increased from 19% to 22% for 100-0-100 Gel-Col-PEG and from 10% to 12% for 75-25-100 Gel-Col-PEG mats, respectively. Finally, in the cases of 50-50-100 and 0-100-0 Gel-Col-PEG mats, the presence of higher collagen content had significantly decreased the mean GFP values with under 3% of the cell population displaying GFP fluorescence.

#### 4.3.5 Double-layer vs. Monolayer Mats

To evaluate the effect of collagen as a first layer of a multilayer structure, the electrospun double-layered mats were prepared by electrospinning first pure collagen solution (i.e., Gel-Col-PEG of 0-100-0) and then Gel-Col-PEG (100-0-100) or Gel-Col-PEG (75-25-100) fibers in order

to produce Col/PEG (100-0-100) and Col/Gel-Col-PEG (75-25-100) double-layer mats. The morphology of the double-layered electrospun fibers was characterized by SEM (Fig. 4.5 A-B). Both mats with complexes showed fibers containing a large number of beads similar to the monolayered mats. The Gel-ColPEG (100-0-100) and Col/Gel-Col-PEG (75-25-100) double-layer mats had fibers diameter of  $98.2 \pm 3$  nm and  $138.6 \pm 6$  nm and bead size of  $769 \pm 85$  nm and  $705 \pm 110$  nm, respectively. The presence of pDNA complexes in mats was evaluated by using Cy3-labeled pDNA. Identical to the monolayered mats, the double layered Col/Gel-Col-PEG (100-0-100) mats showed the strongest red signal and the Col/ Gel-Col-PEG (75-25-100) displayed lower amount of the complexes.

The delivery of pGFP complexes to C2C12 (4.5 Ei-ii) and MC-3T3 (4.5 Fi-ii) cells was also quantitatively evaluated by flow cytometer. The mean fluorescence intensity and the percentage of GFP expression were plotted against the different volume ratio Col/ Gel-Col-PEG mats. In C2C12 cells, based on the mean fluorescence and GFP positive cell population results (Fig 4.5 Ei.), an increase was observed after increasing the pDNA concentration from 0.5 to 1.0  $\mu\text{g/mL}$  for free complexes and complexes delivered by Col/Gel-Col-PEG (100-0-100). No difference in mean fluorescence and GFP results was observed between the two examined concentrations for Col/Gel-Col-PEG (75-25-100). In addition, similar values were recorded between monolayered and double layered mats, where the mats having collagen electrospun with complexes (i.e., Gel-Col-PEG of 75-25-100) led to lower delivery of complexes to the cells. Finally, for MC-3T3 a similar pattern with C2C12 cells was observed with the mean fluorescence and GFP expression results. Taken together, the delivery of complexes to the cells was equivalent between the single-layer and double-layer format, and the presence of the first layer of collagen did not significantly affect the delivery of complexes to the cells.

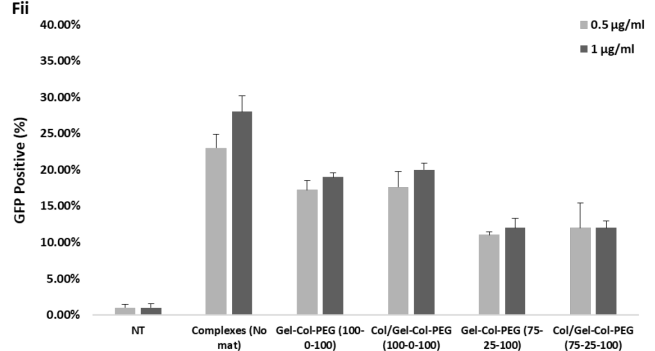
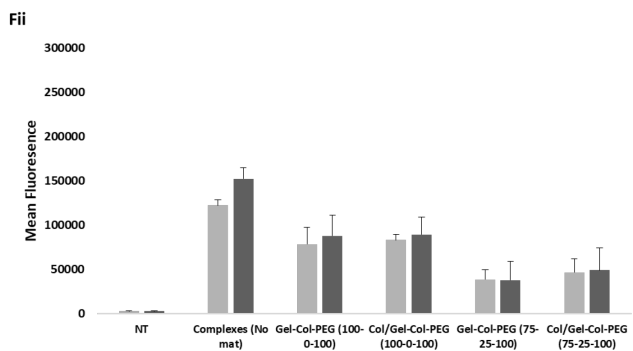
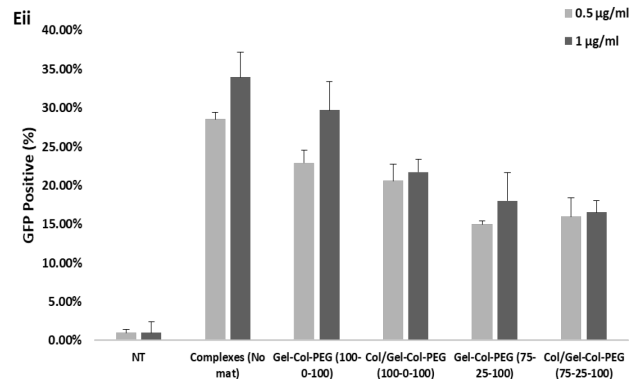
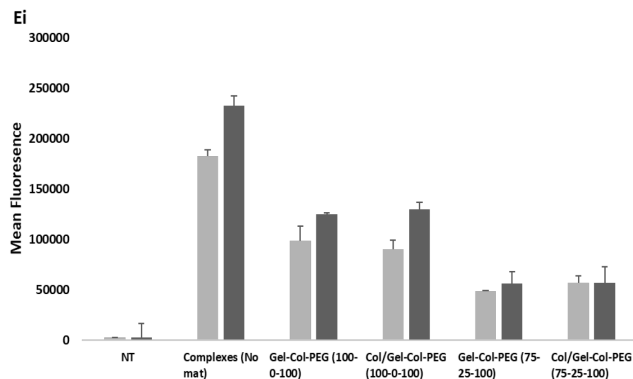
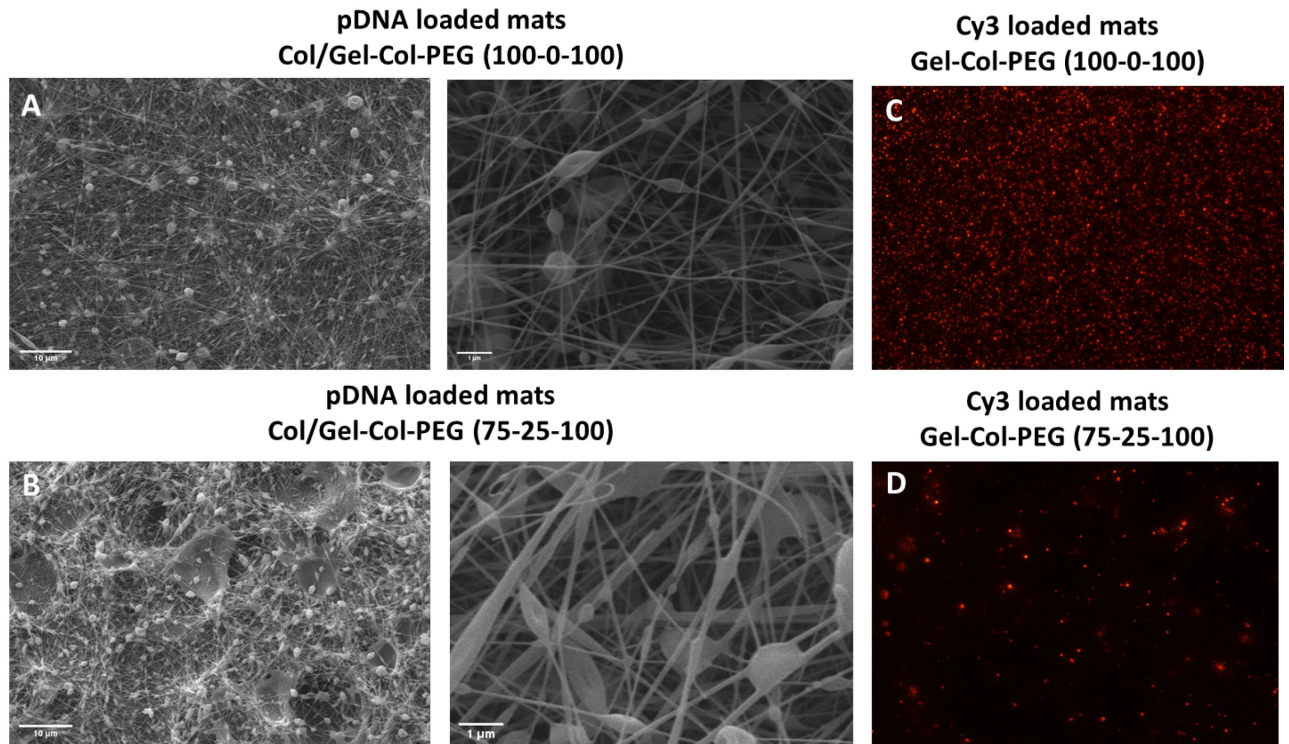


**Figure 4.5.** Experimentally observed the morphology of double layered fibers and the delivery of Cy3 and GFP labeled DNAs by them.

SEM (A-B) images of multilayered Col/GEL-Col-PEG mats with complexes (scale bars 10 and 1  $\mu\text{m}$ ). Fluorescence microscopy images (C-D) of mats with Cy3 labeled pDNA complexes. Delivery of pGFP in C2C12 (Ei-ii) and MC3T3 (Fi-ii) cells. Analysis of GFP-positive population and mean fluorescence intensity/cell, 48h post transfection by flow cytometry.

#### **4.3.6 ALP activity from double vs. mono-layer mats**

The successful delivery of BMP-2 expression plasmid to the cells was evaluated by quantifying the ALP activity in transfected cells. The complexes were incorporated into 4 different Gel-Col-PEG mats and delivered to the cells over 7 days. The estimated pDNA concentrations were 1.0 and 0.5  $\mu\text{g/mL}$ , but the ALP induction results were equivalent at both concentrations. As shown in Fig. 4.6 A - B, the delivery of free complexes increased the ALP levels in both cell lines, as expected. In both cell types, the cells that were treated with complexes released from the 0-100-0 and 50-50-100 Gel-Col-PEG mats were not effective for ALP induction (i.e., similar to untreated cells). On the other hand, the cells treated with complexes in mats without collagen (100-0-100 Gel-Col-PEG) showed a relatively high ALP activity compared to the other examined mats. The presence of Col in monolayer mats again decreased the ALP induction by the complexes. Lastly, the C2C12 cells that have been treated with Col/Gel-Col-PEG (100-0-100) and Col/Gel-Col-PEG (75-25-100) double-layered scaffolds increased the ALP activity compared to the mono-layered mats. In the case of MC-3T3 cells, there was no difference in the ALP activity values between the multilayered and monolayered mats.

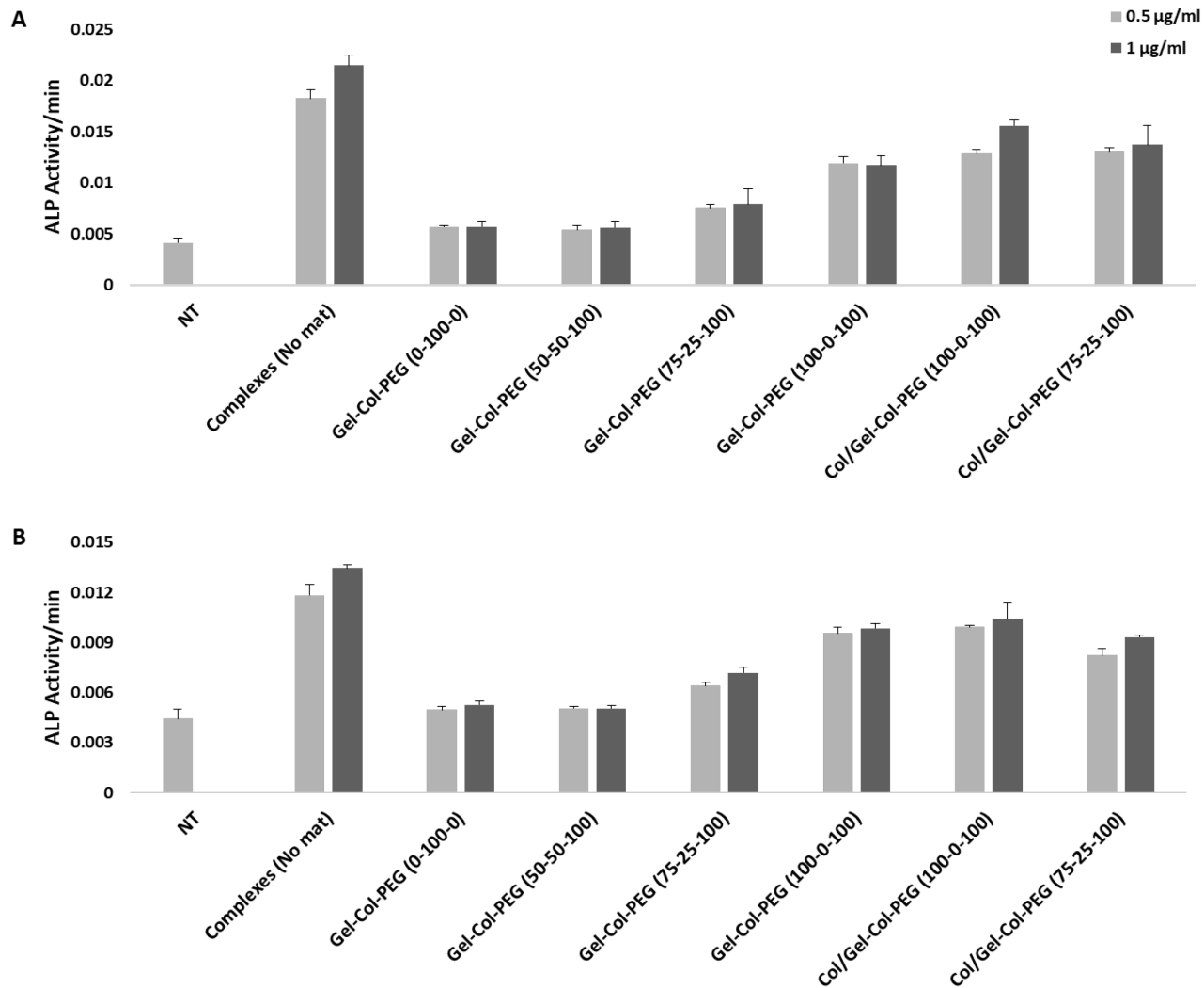


**Figure 4.6. ALP induction in C2C12 cells (A) and in MC3T3-E1 (B) cells after delivery of gWIZ-BMP-2 complexes from different Gel-Col-PEG monolayer mats and double-layered mats 7 days post transfection.**

The pDNA concentrations in cell culture were 0.5 and 1.0 µg/mL. The ALP activity was measured 30 mins after the addition of the substrate in triplicate.

#### 4.4. Discussion

The evolution of gene activated matrices in medicine have opened a new era in effective delivery of expression vectors via non-viral and viral carriers in the area of interest. Producing nanofibers via electrospinning technique is considered a suitable method for the delivery of nanoparticles even though problems associated with interactions between the nanoparticles and the scaffold are still unsolved (273). To overcome these limitations, the selection of the right fabrication method as well as the most suitable polymers for the application is critical. Electrospinning method of fabrication has attracted significant attention since good control over the solution properties of the starting materials, process parameters and environmental conditions is possible to influence the final nanofiber properties and the release profile of any entrapped bioactive agents (266,267)

Gelatin is derived from controlled hydrolysis of fibrous insoluble collagen and has been widely used in the form of hydrogels, fibers and microspheres in numerous biomedical applications. However, its poor mechanical properties and low thermal stability limits remain a challenge (274). The modification of gelatin including blending with other natural or synthetic polymers has been explored by researchers (275,276). In our previous study, the incorporation of PEG as a modifier into gelatin solution significantly improved the spinnability of the gelatin and enabled successful delivery of complexes prepared with low molecular weight PEIs to C2C12 and MC-3T3 cells (214). In the present work, in order to further improve the limiting features of gelatin-PEG composite fibers, collagen Type I was incorporated into spinning process with two different ways; (i) by incorporating collagen in the gelatin-PEG solution to create homogenous (monolayer) mats or (ii) by first spinning a first layer of mat, followed by deposition of a second layer of Gel-PEG mat as a double-layered scaffold. Collagen type I, as the main ECM protein of

many tissues, closely mimics the native ECM tissue and is highly desirable for improved tissue regeneration (277).

When the morphology of the fibers with and without complexes was examined using SEM, a large number of beads was intertwined in all the mats that contained Gel and PEG, which indicates the poor electrospinnability of the solutions. With an increase in the collagen content, the quality and the diameter of the composite nanofibers changed, and a dramatically larger numbers of beads were found. This was most likely due to the decrease in the solution viscosities and thus an increase in the number of beads occurred (278). In contrast, as was expected the electrospinning of pure collagen without complexes created uniform fibers with average diameter 146 nm without beads, demonstrating high electrospinnability. The good quality of collagen fibers was also confirmed after the encapsulation of complexes, where the diameter of fibers increased to 176.6 nm with the appearance of a small number of beads. Our studies proved once more that electrospinning can produce uniform and good quality collagen fibers with diameter from 50 to 1200 nm as reported in the literature (279).

Changes in the way of delivering the pDNA complexes to the cells, such as the complexes encapsulated in fibers produced by electrospinning, may affect the physicochemical properties of the complexes and affect the transfection efficiency (29). The influence of blending different volumes of Gel, collagen and PEG with complexes had an impact on the NPs properties. Notably, the size of the complexes released from the 100-0-100 and 75-25-100 Gel-Col-PEG mats were similar to the free polyplexes, but the  $\zeta$ -potential appeared to be lower. Both the size and  $\zeta$ -potential dropped further as the volume of collagen increased and Gel decreased, showing the negative effect of adding high volume amount of collagen into the gelatine-PEG-complexes solution. It is likely that the collagen was involved in coating the polyplexes and reducing the  $\zeta$ -potential.

Electrospinning Cy3-labeled pDNA complexes into the mats confirmed the successful entrapment of complexes, but in line with size measurements, less abundant and smaller fluorescent particles were evident especially in collagen containing Gel-Col-PEG mats. In subsequent experiments, we confirmed the negative effect of delivering complexes via mats with large collagen content on the transfection efficiency and ALP activity against both cell lines.

In order to ascertain the influence of collagen on the transfection efficiency, we examined the delivery of gWIZ-GFP complexes from the different monolayer mats to C2C12 and MC-3T3 cells. The experimental procedure used here involved extraction of the complexes with trypsin and exposure of the cells to the complexes. This was considered necessary, since unlike Gel-PEG mats, mats with collagen did not dissolve right away in tissue culture medium, which would have complicated assessment of transfection efficiency due to possible slower release profile of complexes. Initial studies indicated that incubation of complexes (free) in the employed trypsin concentration/time did not affect the transfection efficiency of the complexes (not shown). The data from our experimental system revealed that the transfection efficiency was higher with 100-0-100 and 75-25-100 Gel-Col-PEG mats than with those containing higher volume of collagen, suggesting that the presence of collagen in the fibers did not enhance transfection. Small amount of collagen appeared to be tolerated but not higher amounts. The reduced transfection efficiency was evident in both cell lines, and we attributed this to (i) decreases in the amount of pDNA entrapped and released from the mats (based on entrapment efficiency of Cy3-labeled pDNA) and (ii) smaller and less charged complexes with reduced sedimentation and possibly binding to anionic cell surfaces. Similar results have been observed in other controlled release studies, suggesting that a high matrix density can imprison bioactive molecules (280,281). In addition, we observed a significant effect on the transfection efficiency between the free and entrapped

complexes. This is not un-expected given the possible adverse effects from the process or entrapping matrix; however, typically >50% of the bioactivity of the complexes were preserved in the electrospun matrices with small amount of collagen, providing encouraging results to further optimize the transfection efficiency of gene-activated electrospun mats.

The BMPs and in particular BMP-2 play an important role during osteogenesis since they can promote osteogenesis by up-regulating ALP during the process of calcification (282). For this study, the induction of osteogenic activity was measured by delivering BMP-2 expressing pDNA to C2C12 and MC-3T3 cells. The delivery of BMP-2 protein to C2C12 cells has the ability to convert their myoblast phenotype into cells displaying osteoblastic features (250). On the other hand, MC-3T3 cells, is a preosteoblasts cell line with the capacity for enhanced differentiate into osteoblast and osteocytes upon the right stimulation. The delivery of BMP-2 complexes significantly induced the ALP activity in both cell lines after 7 days of incubation, further confirming the bioactivity of the entrapped complexes as observed with gWIZ-GFP plasmids. As in latter complexes, results with the BMP-2 plasmid transfection also indicated a detrimental role of excess collagen incorporation in the Gel-Col-PEG mats.

To create more effective electrospun mats, we considered another strategy to produce a mat by multilayered electrospinning, where different polymeric solutions were spinning individually, and each layer contributes in the overall outcome (205). The multilayered scaffold proposed here was intended to address the main challenge of monolayer mats, where the high volume of collagen prevented effective transfection. Based on the results from monolayer mats, we decided to first fabricate a collagen layer without complexes and then overlay a second layer of Gel-Col-PEG (100-0-100 or 75-25-100) bearing the complexes. We observed no difference between the monolayered and double-layered mats from the SEM as well as the Cy3 images.

Similarly, no differences were observed from the delivery of GFP complexes from double-layered mats to C2C12 and MC-3T3 cells. Finally, we demonstrated that significant ALP activity was induced in C2C12 cells after the delivery of complexes from double-layered mats. The ALP induction was equivalent to monolayer counterparts as long as the Col was electrospun separately from the complexes. This presumably reduces undesirable interactions between the collagen and the complexes. On the other hand, the difference in the ALP levels for BMP-2 complex treated cells were not as high as in the MC-3T3 cells after one week of incubation. As seen in Chapter 4, on three weeks post transfection the MC-3T3 cells expressed lower ALP activity compared to C2C12 cells even when the cells have been exposed to optimal for MC-3T3 complex conditions. It is possible that this difference might in incubation time might not have allowed for the differences to be relieved. A more systematic study is warranted in this regard. Nevertheless, one can still see an induction of ALP activity in MC-3T3 cells for the most optimal mat, Gel-Col-PEG of 100-0-100 (Figure 4.6B; i.e., twice the background). In these cells, having a Col layer in addition to the mats fabricated with Gel-Col-PEG of 100-0-100 and pDNA complexes supported the osteogenic activity of the complexes. Clearly separating the Col from complexes during electrospinning helped to preserve the activity of the complexes.

## 4.5. Conclusions

Electrospun fiber mats were prepared by mixing different volumes of Gel, collagen and PEG solutions with and without complexes generated from low MW PEIs. SEM images revealed that high volume of collagen in Gel-PEG mats affected the quality and the structure of the electrospun fibers. The incorporation of the complexes into different Gel-Col-PEG mats showed the negative effect of collagen on the transfection efficiency of gWIZ-GFP complexes and ALP activity induction activity of BMP-2 complexes as compared to free complexes. All results showed a consistently negative effect of high collagen concentration on the bioactivity of complexes when the mats were fabricated from a mixture of complexes and Col material. To overcome this limitation, we have fabricated double-layered scaffolds that contained a collagen mat as a first layer and Gel-Col-PEG/complexes as a second layer, which prevented the contact of Col with complexes. Such scaffolds were successfully able to increase the ALP activity in C2C12 and MC-3T3 cells compared at a level equivalent to the mono-layer mats without Col. These multilayered scaffolds can be applied for bone regeneration and other gene delivery applications.

## **Chapter 5- Overall Conclusions and Future Considerations**

## 5.1 Overall Thesis Conclusions and Discussion

The concept of transferring genes and gene-regulatory molecules to cells and tissues has seen many advances in recent years in areas where current therapies fail. In the last decade, researchers, including Dr. Uludag’s group, have exerted great effort in developing novel gene delivery systems that has shown potential in addressing critical issues linked to the field of bone regeneration. Through a lengthy review on bone regeneration and the recent therapies, Chapter 1 highlights the introduction of specific plasmids (pDNA) or RNAs (micro or siRNA) via non viral carriers that may enhance the osteogenic activity of the target cells.

In the last five years, numerous studies have focused on synthesizing non-viral and viral based vectors for the delivery of therapeutic molecules that will improve osteogenic activity *in vitro* and new bone formation *in vivo*. Exploring more recent literature on the viral vectors (**Table 5.1**), it is demonstrated that adenoviruses are the most widely explored systems. The delivery features of these systems are well characterized; they do not integrate into host genome (i.e., lower chance of mutagenicity) and they have been leading the vectors in high effectiveness of gene expression in various animal models. Despite their promising results, toxicity and severe immune responses resulted in limiting their clinical applications.

Gene	Virus	Scaffold	Model	Study details and outcome	Ref.
<b>BMP-2</b>	Tet-on adenoviral (AdTetBMP-2)	Biphasic calcium phosphate ceramic (MBCP®) granules	Femoral defect in rat	Direct application of AdTetBMP-2 or pre coating MBCP granules with AdTetBMP-2 and hMSCs were implanted on the day of the surgery. In all AdTetBMP-2 groups, new bone formation was observed which was vascularized and fully integrated with nascent tissue and scaffold. Delivery of MSCs, pre-coated MBCP with AdTetBMP-2 and fibrin enhanced bone regeneration after 12 weeks.	(283)

	Lentiviral	Gelatin	Intramuscular in SCID mice	Efficient transgene expression and high osteogenic activity <i>in vitro</i> by hBMCs encapsulated in scaffolds. Effective bone formation 3.5 months post implantation.	(284)
	Serotype 5 adenovirus	$\beta$ -TCP	Femoral defect in rat	With 24h prior seeding on scaffolds, MSCs were infected with Ad-BMP-2. Bone defect was closed 12 weeks post-surgery.	(285)
	Adenovirus	Nano-calcium sulfate disc with platelet-rich plasma fibrin (PRP) gel	Calvarial bone defect in rat	Transplantation of BMP2-modified MSCs with nCS and PRP fibrin gel increased new bone regeneration <i>in vivo</i> in 8 weeks.	(286)
<b>pCAG-BMP-2</b> <b>Pcytomegalovirus BMP-2/7</b> <b>Pcytomegalovirus BMP2-Advanced</b> <b>Pelongationfactor1<math>\alpha</math> BMP2-Advanced</b>	Chitosan NPs	Collagen hydroxyapatite	Calvarial bone defect in rat	The delivery of pCMVBMP-2-Adv via scaffolds produced around 2500 $\mu$ g calcium per scaffolds <i>in vitro</i> while <i>in vivo</i> induced the differentiation of osteoprogenitor cells to mature osteoblasts which improved healing in bone defect.	(287)
<b>VEGF-A BMP-2</b>	Adenovirus	Poly (LLA-co-CL)	Subcutaneous in mouse	Combined delivery of VEGF-A and BMP-2 (ad-BMP2 + VEGFA) upregulated osteogenic and angiogenic activity <i>in vitro</i> and <i>in vivo</i> .	(288)
<b>BMP-4</b>	Adenovirus	No	Skeletal muscle pocket in mice	Large ectopic bone tissue formation 12 weeks post treatment.	(289)

**Table 5.1. Delivery of gene therapeutics via viral carriers in animal models in the last 5 years.**

Several therapeutic genes have been explored with the indicated viral delivery systems. Abbreviations used are:  $\beta$ -TCP: Beta-tricalcium phosphate; Poly(LLA-co-CL): Poly(lactide-co- $\epsilon$ -caprolactone)

In this context, the development of non-viral carriers with the ability to deliver genetic material like viral vectors still hold great promise. Natural biomaterials like hydroxyapatite and chitosan, or synthetic biomaterials like polyethylenamine (PEI) and Lipofectamine<sup>TM</sup> continued to offer promising results in recent years both in *in vitro* (Table 5.2.) and *in vivo* (Table 5.3.) models. High molecular weight (~25 kDa) PEI, despite concerns of excessive toxicity, remains to be a commonly used carrier in these studies. On the other hand, much work has been done on exploring low molecular weight PEI (<2 kDa) carriers since they have been recognized as safe due to their low immune response, but their applications to most of primary cells is often inefficient due to low

transfection efficiency levels. A potential chemical modification with lipids such as with linoleic acid,  $\alpha$ -linoleic acid, thioester-linoleic acid, stearic acid and propionic acid seems promising as it may result in more effective carriers. In Chapter 2, a library of chemically modified low MW PEI polymers was prepared and tested for efficient delivery of GFP plasmid to rat periosteum and calvarial bone derived cells. Microscopic images suggested that PEI1.2-tLA2, PEI2-PrA0.5 and PEI2- $\alpha$ LA8 achieved similar levels of GFP expression in both cell types and were chosen for further investigation. Comparative experiments showed that both cell types expressed high GFP levels after treatment, with PEI1.2-tLA2 delivery to BDCs showing the highest expression while low GFP levels were recorded with  $\alpha$ LA8 and PrA0.5 modified PEIs.

Numerous *in vitro* and *in vivo* studies up to date have shown the successful delivery of BMP-2 or the co-delivery of BMP-2 with VEGF, TGF- $\beta$ 1, TGF- $\beta$ 3 and FGF-2 in the form of plasmid with viral (Table 5.1.) and non-viral vectors (Table 5.2. and 5.3.). Only limited number of studies had studied the beneficial effect of other growth factor like hBMP-4, hBMP-7, FGF-2 and PDGF-BB. Having ascertained that PEI1.2-tLA2 was the polymer that successfully deliver GFP plasmid to both cell types, we sought to investigate whether a combination of therapeutic molecules (BMP-2 and PDGF) could be a promising system to the enhance of osteogenic activity. The results showed that the delivery of BMP-2 boost calcium deposition in both PDCs and BDCs cells while the delivery of PDGF or the co-delivery of BMP-2/PDGF impaired the desired results observed with BMP-2. In the case of PDCs, the co-delivery of BMP-2/PDGF plasmids had a negative impact since the presence of PDGF inhibited the BMP-2/Smad 1/5/8 signaling pathway. On the other hand, *in vivo* studies have shown that the delivery of PDGF may stimulate bone formation in animal models (290). A reason for this limitation is perhaps the alternative

mechanisms that were in play to obtain this outcome and the limited *in vitro* system used in our studies were not sufficient to reveal (or recruit) this mechanism.

pDNA	Carrier	Scaffold	Study description and outcome	Ref.
<b>BMP-2</b>	Chitosan-g-PEI (PEI 1.8 kDa)	No	Gene transfer gave 17% transfection efficiency and 80% of cell viability in MSCs. The delivery of BMP-2 gene enhanced osteogenic differentiation.	(237)
	Lipofectamine 2000	Hyaluronic acid hydrogel	Transfection of hBMSCs with BMP-2 prior to encapsulation into hydrogels gave high RUNX2 but not SOX9 expression for up to 3 weeks.	(291)
	PEI (25 kDa)	PLGA	hPDLSCs showed high transfection efficiency. Delivery of BMP-2 via electrospun PLGA scaffolds showed high BMP-2 expression for more than 28 days.	(292)
	PEI-tLA (1.2 kDa) pASP	No	Entrapment of BMP-2 plasmid in electrospun collagen/PEG mats gave effective transfection and ALP induction in C2C12 cells	(214)
<b>TGF-β1 BMP-2</b>	Lipofectamine 2000	Mineral-hydroxyapatite MPs	Localized delivery of single or combination of genes to porcine BMSCs enhanced the expression of bioactive protein levels.	(293)
<b>TGF-β3 BMP2</b>	nHA NPs	Alginate hydrogel	The delivery of TGF-β3, BMP-2 plasmids or the combination via alginate hydrogels supported the transfection of encapsulated MSCs and directed their phenotype toward either a chondrogenic (with TGF-β3) or osteogenic phenotype (with BMP-2).	(294)
	nHA NPS Amphipathic peptide (RALA peptide) PEI 25 kDa	No	Delivery of both therapeutic genes to MSCs via nHA promoted the osteogenesis in monolayer and endochondral phenotype in pellet culture. The co-delivery via RALA promoted a more stable hyaline cartilage-like phenotype in pellet culture (high expression of ACAN and SOX9 and strong staining for GAG and COL II deposition) while the delivery via PEI did not induce osteogenic or chondrogenic activity of MSCs in both types of cells culture.	(295)
<b>BMP-7</b>	Niosomes (2,3-di (tetradecyloxy) propan-1-amine and polysorbate 80)	No	Transfected MSCs showed increased growth rate, ALP activity and extracellular matrix deposition <i>in vitro</i> .	(296)
<b>FGF-2</b>	25 kDa PEI	Collagen	Delivery of complexes with or without scaffolds promoted FGF-2 expression in BMSCs.	(297)

**Table 5.2. Delivery of gene therapeutics via non-viral carriers *in vitro* in the last 5 years.**

Abbreviations used are: Runx2: runt-related transcription factor; PLGA: poly (lactic-co-glycolic acid); hPDLSCs: human periodontal ligament stem cells; ACAN:aggrecan; GAG: glycosaminoglycan.

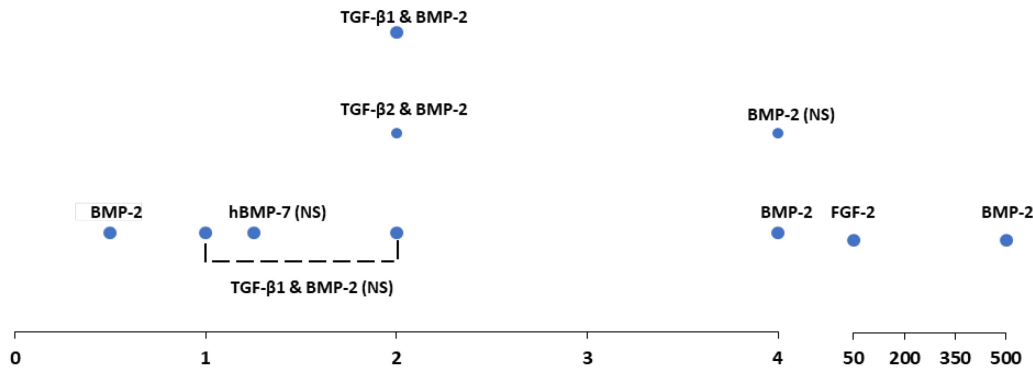
pDNA	Carrier	Scaffold	<i>In vivo</i> model	Study description and outcome	Ref.
<b>BMP-2</b>	25 kDa PEI	PDLLA coated titanium discs	Mandible bone defect in rat	Partial bridging of the defect within 14 days and completion within 112 days when the DNA dose per implant did not exceed 2.5µg.	(298)
	Chitosan NPs	Chitosan thermosensitive hydrogel	Calvarial bone defect in rat  Periodontitis model in beagle dog	Enhanced bone formation in both examined models 8 weeks post-surgery.	(261)
	Bioactive glass NPs	Collagen gel	Calvarial bone defect in rat	NPs had high loading capacity with 2 weeks release period. Transfection of rat MSCs with BMP-2 prior to their encapsulation into gels improved bone formation <i>in vivo</i> in 6 weeks.	(299)
	Lipofectamine 2000	PEG-PLLA hydrogel with periosteum	Femoral diaphysis defect in rat	Transfection of BMSCs with BMP-2 prior to their encapsulation into scaffolds with periosteum promoted bone regeneration in 12 weeks.	(300)
	PEI (25 kDa)/PEG	PCL/ Pluronic F127 membrane	Calvarial bone defect in rat  Mandible bone defect in miniature pig model	<i>In vitro</i> and <i>in vivo</i> results showed that encapsulated BMP-2 complexes were continuously released from membranes and transfected surrounding cells and increase osteogenic differentiation <i>in vitro</i> and bone regeneration <i>in vivo</i> after 12 weeks in both models.	(301)
	pACEMam1	Silica coated nHA-gelatine reinforced with fibers	Segmental defect in rat	Scaffolds with transfected MSCs showed high viability, proliferation & osteogenic differentiation <i>in vitro</i> and augmented union and new bone formation <i>in vivo</i> in 12 weeks.	(302)
	TransIT-2020	Corning Matrigel Matrix (HC)	Calvarial bone defect in rat	High transfection and high osteopontin/osteocalcin expression <i>in vitro</i> . Bone healing <i>in vivo</i> in 12 weeks.	(303)
	pcDNA3.1	Chitosan film	Calvarial bone defect in rat	Improved proliferation and RUNX2 expression of MC-3T3 and new bone formation <i>in vivo</i> in 12 weeks.	(304)
	pEGFP-N1 (with upstream CAG promoter & downstream IRES)	Gelatin gel, atelocollagen gel & atelocollagen pellets	Calvarial bone defect in rat	Gelatin gel was more efficient than atelocollagen for delivery of plasmids both <i>in vitro</i> and <i>in vivo</i> .	(305)
	Alginate hydrogel	Biphasic calcium phosphate cylinders	Iliac crest model in goat	pBMP-2 in combination with MSCs resulted in prolonged gene expression and bone formation <i>in vivo</i> .	(306)
Calcium phosphate transfection kit	PLGA microspheres	Tibialis anterior muscles in rat	The PLGA-pBMP-2/CaPi microspheres promote ectopic osteogenesis in non-bone tissue in 8 weeks.	(307)	

	pEGFP-N1 pVAX1	Alginate-biphasic calcium phosphate scaffold	Subcutaneous and paraspinal intramuscular model in rat	Non-viral delivery of BMP-2 plasmid <i>in vitro</i> induced BMP-2 expression in MSCs while fibroblasts produced a substantial amount. 8 weeks post- surgery, BMP-2 expression by cells was more obvious in scaffolds containing MSCs and 100 µg/mL pBMP-2 and in unseeded scaffolds containing 500 µg/mL pBMP-2 <i>in vivo</i> . No bone formation was observed in groups with pBMP-2 while rhBMP-2 gave bone formation.	(308)
<b>VEGFA BMP-2</b>	PEI dual nHA dual mix dual	Collagen-nHA	Calvarial bone defect in rat	Delivery of both genes with of nHA and scaffolds improved vascularization and bone repair in 4 weeks.	(309)
<b>BMP-2 BMP-2</b>	25 kDa PEI and protective copolymer P6YE5C	PDLLA titanium discs	Mandible bone defect in rat	Local controlled physiological bone formation by pBMP-2, whereas delivery of rhBMP-2 triggered rapid and ectopic, but insufficient bone formation.	(310)
<b>FGF-2 BMP-2</b>	25 kDa PEI	Collagen	Diaphyseal long bone radial defect in diabetic rabbits	Co-delivery of FGF-2 and BMP-2 via scaffolds improved bone regeneration <i>in vivo</i> .	(218)
<b>TGF-β3 BMP-2</b>	RGD-γ-irradiated alginate & nHA	PCL	Subcutaneous in mice	Co-deposition of PCL solution and gene activated bioink mixture containing RGD-γ-irradiated alginate/nHA/TGF-β3 and BMP-2 complexes gave robust osteogenesis of encapsulated MSCs <i>in vitro</i> and supported vascularization and mineralization after 12 weeks <i>in vivo</i> .	(311)
<b>PDGF-BB</b>	25 kDa PEI	Collagen	Periodontal defect in rat	Delayed bone healing from PEI groups compared to controls.	(312)

**Table 5.3. Delivery of gene therapeutics via non-viral carriers in animal models.**

Abbreviations used are: PDLLA: Poly(DL-lactide); PLLA: Poly (l-lactic acid); PCL: Polycaprolactone; PLGA: poly(lactic-co-glycolic acid).

(A) *In vitro*



(B) *In vivo*

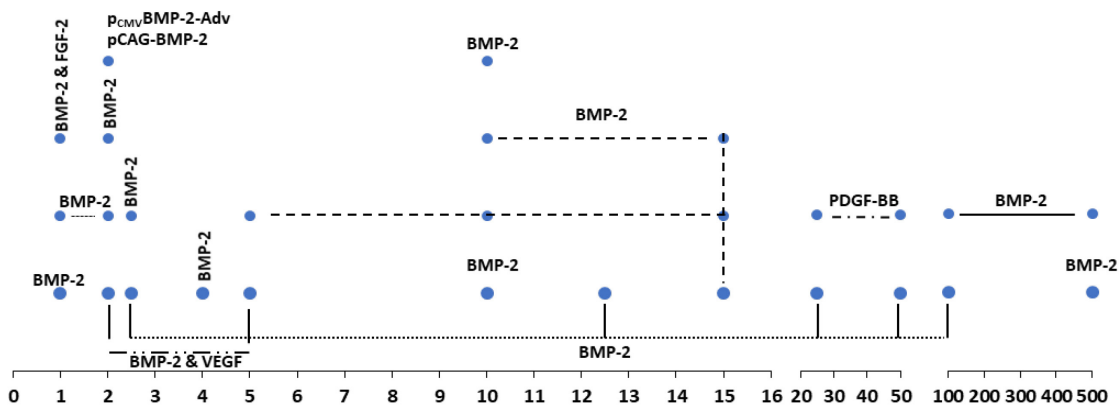


**Figure 5.1. Schematic diagram of non-viral delivery of pDNA related to bone formation and the concentrations (µg/scaffold in horizontal axis) that have been used in the *in vitro* (A) and *in vivo* (B) studies.**

The data was derived from the studies in Tables 5.2. and 5.3. The dashed lines between points indicates the range of different concentrations of one or more proteins tested in the same study. The NS indicates that there was no use of a scaffold in this study.

Cell lines, in contrast to primary cells, have been chosen by many researchers as they are in general easier to culture and transfect. In **Chapter 3**, a new polymeric library of low MW PEI polymers was prepared in the Uludag Lab and has been examined for their potential on C2C12 and MC-3T3 cells. Both cell lines have been previously selected for assessing transfection parameters in bone studies. Our results clearly demonstrated that thioester-linked linoleic acid (tLA, PEI 1.2-tLA10) PEI polymer as the most promising system. In this chapter, we established

a new polymeric pDNA delivery system which was further improved with the presence of polyaspartic acid (pASP) during complexation. Comparative experiments between both cell lines showed that various polymer:pDNA ratios, DNA concentrations as well as pDNA:pASP ratios are playing a significant role on transfection efficiency. It was surprising to find that the same conditions were not applicable in these two cell lines in order to achieve high transfection efficiency, GFP positive expression, cell viability levels and ALP activity. The identification of the right conditions for each cell line played an essential role on translating these 2D cultures (on tissue culture plastic) to 3D cultures (in scaffolds).

The material selection, fabrication method, structure, porosity and degradation rate of the 3D scaffolds along with the concentration of biomolecules loaded in the them can have an impact on the delivery process of the biomolecules to the target cells or tissues. Most of the studies in Tables 5.2 and 5.3 reported a single application of BMP-2 formulation in concentrations between 0.5 to 500 ug/scaffold while the co-delivery of BMP-2 with TGF- $\beta$ 1 or  $\beta$ 2, FGF-2 or VEGF was between 1 to 5  $\mu$ g/scaffold (Figure 5.1). A large variation in the applied dose of the gene expression system was evident for individual therapeutic genes (e.g., BMP-2) as well as among various genes. This may be related to the specific animal or cell model chosen for osteogenesis assessment or related to the efficiency of the delivery system.

In order to validate the importance of designing scaffolds that will control the duration of transgene expression, we synthesized uncrosslinked (native) scaffolds, crosslinked (x-linked) and intrafibrillar mineralized collagen scaffolds for the delivery of the optimum complexes for each cell line. In the 3D cultures, from the ALP values we observed that the delivery of BMP-2 complexes from mineralized scaffolds to C2C12 cells increased ALP activity up to 3 weeks while for MC-3T3 cells the delivery of complexes from collagen scaffolds was more appropriate. Taken

together, the results from this chapter point toward the importance of identifying the right complex conditions and the proper scaffold characteristics for each cell line but shows the limitation of synthesizing a system that will target multiple cell types.

In **Chapter 4**, we formulated a series of different monolayer volume ratio Gel-Col-PEG electrospun mats and examine their capability of delivering the new polymeric pDNA systems, established in Chapter 3, on C2C12 and MC-3T3 cells. The mats with high content of collagen had a negative effect on the delivery of complexes to both cell lines, affecting the transfections efficiency and ALP activity. On the other hand, the delivery was improved by formulating double layer mats where collagen without complexes serve as first layer and then overlay a second layer of Gel-Col-PEG (100-0-100 or 75-25-100) bearing the complexes. The double layered mats played a role in increasing the ALP activity after one week in C2C12 cells, but that did not appear to be applicable for MC-3T3 cells; this could be further examined by extending the incubation time. Even though, delivery of complexes via electrospinning is an interesting approach for better delivery control; the interactions between the polymer solution and the bioactive molecules can be affected by the physicochemical properties of the polymers. For this reason, should be an equilibrium between the hydrophilic and hydrophobic properties of the chosen polymers and molecules because these characteristics may have an impact in the encapsulation efficiency, dispersity of the complexes and the release profile (313). Overall, this thesis contributed in the field by (i) evaluating a pDNA-low MW PEI delivery system for the successful delivery of BMP-2 in rat primary PDCs and BDCs derived cells; ii) developing a new delivery system using low MW PEI with polyanionic polymer during complexation and optimizing the right transfection conditions in two different cell line; iv) exploring the delivery of complexes via 3D systems and optimize the most suitable system for each cell line; and (v) exploring the impact on complexes

release profile from different electrospun mats and optimize the most suitable system for each cell line.

## **5.2 Further Discussion and Future Considerations**

### **5.2.1 Scaffolds characterization and improvement.**

In Chapters 3 and 4, we mainly focused on investigating the gene delivery properties of the proposed bioactive scaffolds. A more extensive research should be performed on the degradation, physical and mechanical properties since each of these characteristics directly affect the biological response as well as the gene release profile. As an example, the biodegradation profile and the mechanical properties as well as an analysis on the physicochemical interactions between the genes and the scaffolds should be performed for the scaffolds in Chapter 3. Further research should be performed on the improvement of the proposed bioactive matrices in Chapter 4 as well; like the synthesis of alternative collagen-based electrospun mats (multilayer or core shell electrospinning), the introduction of a chemical or physical crosslinker and investigating methods that would not negatively affect the release profile of the proposed mats.

### **5.2.2 Enhanced osteogenic activity of primary cells through a 3D system**

We applied polymer:pDNA complexes extensively to cell line models in order to understand the impact of several experimental variables, such as the nature of polymer, polymer to pDNA ratios in nanoparticle formulations, DNA concentrations and pDNA to additive ratios on transfection efficiency and osteogenic activity. Our results showed how important it was to determine these parameters for each cell type prior to any further refined studies. The use of primary hBMSCs may provide an even better model for assessing these parameters since they have been characterized as difficult to transfect and are most relevant for clinical applications. A few preliminary studies I conducted, after applying the optimal conditions identified for MC-3T3 cells (Chapter 3) to hBMSCs and assessing osteogenesis by qPCR (Appendix 5.S1) and ALP (Appendix 5.S2) activity showed the need for further evaluation/optimization of these parameters.

More extensive research on suitable 3D culture conditions as they were investigated in **Chapters 3 and 4** for cell lines is needed since the composition of the 3D scaffolds may affect the delivery of the complexes to the cells, thus their osteogenic activity. In **Chapter 3**, we compared three collagen-based scaffolds, i.e. collagen, crosslinked collagen and mineralized, as carriers for pBMP-2 to C2C12 and MC3TC cells. The results indicated that 3d mineralized scaffolds could facilitate on the transduction of the pBMP-2 complexes (4 $\mu$ g pDNA dose, polymer:pDNA ratio 10 and pDNA/pASP ratio 1) to C2C12 than the other two types while the transduction to MC-3T3 cells was more efficient with collagen scaffolds for the same amount of pDNA (4 $\mu$ g pDNA dose) but for polymer:pDNA ratio of 5 and pDNA/pASP ratio 0.5. In a similar study, Tierney et al. proposed a delivery system for bone regeneration by fabricating PEI 25 kDa-pDNA complexes (2  $\mu$ g pDNA dose and polymer:pDNA ratio 7) and loading them onto collagen, collagen-glycosaminoglycan and collagen-nHA scaffolds. They found that the collagen-nHA scaffolds showed the most prolonged and elevated gene expression levels over 14 days when seeded with rat MSCs (263). In another study, Raftery et al. proposed the delivery of pDNA via two types of chitosan nanoparticles to MSCs, polymeric (PCS-160 kDa) and oligomeric chitosan (OCS 7.3 kDa) particles. The incorporation of those particles into collagen, collagen-nHA and collagen-hyaluronic acid scaffolds showed high gene expression from MSCs seeded on collagen scaffolds carrying PCS particles (2  $\mu$ g pDNA dose and polymer:pDNA ratio 10) or OCS particles (2 $\mu$ g pDNA dose and polymer:pDNA ratio 20) up to 21 and 14 days respectively(314). In addition, high expression levels by cells were observed from collagen hyaluronic acid scaffolds after 28 days. Therefore, our scaffolds should be further characterized on the long term, or a more suitable scaffold should be synthesized for the delivery of the complexes to the cells of interest (primary or cell lines).

### **5.2.3 Treatment of bone defects in animal models**

In this thesis, we have mainly performed *in vitro* studies and determined the outcomes of delivering polymer/pBMP-2 complexes in 2D and 3D systems. The promising *in vitro* outcomes will allow us in the future to apply our systems to animal models and assess whether the proposed 3D scaffolds designed induce tissue that resemble the physiological bone. There are many animal models being tested to evaluate the proposed treatments, but the calvarial and mandible are the most tested in the literature (Table 5.3). A calvarial defect would have been our model to consider for applying our bioactive scaffolds since reconstruction of the calvarium in general is related with the protection of the brain. The calvarial bone consists of two layers of compact bone and in between is lining a layer of spongy bone. Depending on the scaffold the healing of a standardised calvarial defect can be between 8-12 weeks. In addition, calvarial models do not require a special mechanical integrity of the scaffold since the site is not weight bearing.

As an example, in the study of Hsieh et al., the healing of the calvarial defect occurred 12 weeks after the implantation of Matrigel (constituted by approximately 60% laminin, 30% collagen IV and 8% entactin) carrying TransIT-2020/BMP-2 complexes and BMSCs (303). In a similar study from Oh et al., the delivery of PEI/PEG complexes carrying BMP-2 via PCL/ Pluronic F127 membranes increased osteogenic differentiation *in vitro* and bone regeneration *in vivo* 12 weeks after implantation in both calvarial bone defect in rat and mandible bone defect in miniature pig model.

### **5.2.4 RNA delivery as an alternative to pDNA therapy for bone regeneration**

Both *in vitro* and *in vivo* studies have shown the strong connection between the BMP-2 and the osteoinductive activity, for this reason the delivery of BMP-2 in the form of plasmid has been

our first choice instead of other proteins related to bone formation. Our studies clearly showed the increase of osteogenic activity after the delivery of pBMP-2 in various cell types. But, even though we mainly focused on pDNA, other RNA therapeutics also have a great potential and can be additionally considered for future research. The delivery of miRNA as an alternative approach for the treatment of bone fractures have been described in Chapter 1. So far, multiple potential miRNAs have been identified to play an important role on up-regulating osteogenic genes or down-regulating adverse (inhibiting) genes. Among them, miRNA-26a has been applied in multiple studies since simultaneously can promote osteogenesis and angiogenesis in BMSCs (87). miRNA-26a is an interesting regulator since it targets different signaling pathways; for instance, it enhances the osteogenic differentiation of BMSCs by targeting GSK3 $\beta$  to activate Wnt signaling while, in the case of ADSCs, it can target Smad1 that suppresses BMP signaling (315). Recently, Zhang et al. were able to promote new bone formation in 8 weeks by delivering PLGA microspheres that encapsulated PEG-H<sub>2</sub>O-PEI/miR-26a complexes from PLLA scaffolds to a calvarial bone defect in mouse (88). Wang et al. also proposed transfection of ADSCs with Lipofectamine 2000/miRNA-26a complexes and then their incorporation into HA scaffolds. The insertion of the scaffolds into a critical tibia defect in rats improved new bone formation within the defective area within 12 weeks (316). miRNA-148b is another potential candidate, it targets Noggin to enhance the expression of BMP in BMSCs (317). The study by Mariner et al. showed a rapid and robust induction of bone-related markers after the transfection of hBMSCs with miRNA-148b using a human MSC nucleofection kit (i.e., electroporation) in 2D and 3D cultures (86). Finally, Li et al. prepared complexes by using baculovirus Bac-Cre that expressed Cre recombinase and BMP-2/miRNA128b. The transfection of hASCs prior to their incorporation into PLGA scaffolds resulted in new bone formation *in vivo* within 12 weeks (317).

In addition to the miRNA delivery, a small number of publications are proposing delivery of chemically modified ribonucleic acids (cmRNA; a form of messenger RNA, mRNA, capable to translating specific proteins) as a novel delivery system that can overcome the barriers associated with the current mRNA therapy approaches for bone regeneration. Elanovan et al. reported the delivery of cmRNA-BMP-2 via PEI (25 kDa) to BMSCs *in vitro* and their delivery from collagen-based scaffolds to a calvarial defect in rats. The results shown that the incorporation of PEI-cmRNA-BMP-2 into collagen scaffold promoted significantly the new bone formation compared to the scaffolds containing PEI-pBMP-2 over a period of 4 weeks (318). Similarly, the same group proposed the delivery of PEI-BMP-9-cmRNA and PEI-BMP-2-cmRNA from collagen scaffolds into a calvarial bone defect shown that BMP-9-cmRNA was more efficient compared to BMP-2-cmRNA over 4 weeks (319). These studies are also attesting to the promise of mRNA in improving bone repair and regeneration in a clinical setting and could be deployed with the suitable delivery system in the future.

## References

1. Brydone AS, Meek D, Maclaine S. Bone grafting, orthopaedic biomaterials, and the clinical need for bone engineering. *Proc Inst Mech Eng H*. 2010;224:1329–43.
2. Carofino BC, Lieberman JR. Gene therapy applications for fracture-healing. *J Bone Joint Surg Am*. 2008;90(1):99–110.
3. U.S. Department of Health and Human Services, Public Health Services. Bone health and osteoporosis: a report of the Surgeon General. *US Dep Heal Hum Serv Off Surg Gen*. 2004;1–437.
4. Amini AR, Laurencin CT, Nukavarapu SP. Bone Tissue Engineering: Recent Advances and Challenges. *Crit Rev Biomed Eng*. 2012;40(5):363–408.
5. Giannoudis P V, Dinopoulos H, Tsiridis E. Bone substitutes: an update. *Injury*. 2005;36S:S20–7.
6. Conway JD. Autograft and Nonunions: Morbidity with Intramedullary Bone Graft versus Iliac Crest Bone Graft. *Orthop Clin North Am*. 2010;41(1):75–84.
7. Rose FRAJ, Oreffo ROC. Bone tissue engineering: hope vs hype. *Biochem Biophys Res Commun*. 2002;292:1–7.
8. Zimmermann G, Moghaddam A. Allograft bone matrix versus synthetic bone graft substitutes. *Injury*. 2011;42(2):16–21.
9. Bruder SP, Jaiswal N, Haynesworth SE. Growth kinetics, self renewal, and the osteogenic potential of purified human mesenchymal stem cells during extensive subcultivation and following cryopreservation. *J Cell Biochem*. 1997;64:278–94.
10. Bennett CN, Longo KA, Wright WS, Suva LJ, Lane TF, Hankenson KD, et al. Regulation of osteoblastogenesis and bone mass by Wnt10b. *Proc Natl Acad Sci U S A*. 2005;102(9):3324–9.
11. Long F. Building strong bones: molecular regulation of the osteoblast lineage. *Nat Rev Mol Cell Biol*. 2011;13(1):27–38.
12. Shapiro F. Bone development and its relation to fracture repair. The role of mesenchymal osteoblasts and surface osteoblasts. *Eur Cells Mater*. 2008;15:53–76.
13. Ducy P, Zhang R, Geoffroy V, Ridall AL, Karsenty G. *Osf2/Cbfa1*: A Transcriptional Activator of Osteoblast Differentiation. *Cell*. 1997;89(5):747–54.
14. Olsen BR, Reginato AM, Wenfang Wang. Bone Development. *Annu Dev Biol*. 2000;16:191–220.
15. Bart Clarke. Normal Bone Anatomy and Physiology. *Clin J Am Soc Nephrol*. 2008;3:S131–9.
16. Bonewald LF. Establishment of an Osteocyte-like Cell Line , MLO-Y4. *Bone Miner Metab*. 1999;17:61–5.
17. Plotkin LI, Manolagas SC, Bellido T. Transduction of cell survival signals by connexin-43 hemichannels. *J Biol Chem*. 2002;277(10):8648–57.
18. Nisato RE, Tille J, Jonczyk A, Goodman SL, Pepper MS.  $\alpha$  V  $\beta$  3 and macrophage colony-stimulating factor: partners in osteoclast biology. *Tetrahedron*. 2001;42(10):2787–90.
19. Little N, Rogers B, Flannery M. Bone formation, remodeling and healing. *Surgery*. 2011;29(4):141–5.
20. Akrouf R, Bendjemaa S, Fourati H, Ezzeddine M, Hachicha I, Baklouti S. Hypertrophy of the feet and ankles presenting in primary hypertrophic osteoarthropathy or pachydermoperiostosis: a case report. *J Med Case Rep*. 2012;6(31):1–4.
21. Barrère F, Blitterswijk CA Van. Bone regeneration : molecular and cellular interactions

- with calcium phosphate ceramics. *Int J Nanomedicine*. 2006;1(3):317–32.
22. Alford AI, Kozloff KM, Hankenson KD. Extracellular matrix networks in bone remodeling. *Int J Biochem Cell Biol*. 2015;65:20–31.
  23. Li J, Liu X, Zuo B, Zhang L. The Role of Bone Marrow Microenvironment in Governing the Balance between Osteoblastogenesis and Adipogenesis. *Aging Dis*. 2016;7(4):514–25.
  24. Chang MK, Raggatt L-J, Alexander KA, Kuliwaba JS, Fazzalari NL, Schroder K, et al. Osteal Tissue Macrophages Are Intercalated throughout Human and Mouse Bone Lining Tissues and Regulate Osteoblast Function In Vitro and In Vivo. *J Immunol*. 2008;181(2):1232–44.
  25. Pazzaglia UE, Zarattini G, Giacomini D, Rodella L, Menti AM, Feltrin G. Morphometric analysis of the canal system of cortical bone: An experimental study in the rabbit femur carried out with standard histology and micro-CT. *J Vet Med Ser C Anat Histol Embryol*. 2010;39(1):17–26.
  26. Allen MR, Hock JM, Burr DB. Periosteum: Biology, regulation, and response to osteoporosis therapies. *Bone*. 2004;35(5):1003–12.
  27. Roberts SJ, van Gestel N, Carmeliet G, Luyten FP. Uncovering the periosteum for skeletal regeneration: The stem cell that lies beneath. *Bone*. 2015;70:10–8.
  28. Devescovi V, Leonardi E, Ciapetti G, Cenni E. Growth factors in bone repair. *Chir Organi Mov*. 2008;92(3):161–8.
  29. Dimitriou R, Tsiridis E, Giannoudis P V. Current concepts of molecular aspects of bone healing. *Injury*. 2005;36(12):1392–404.
  30. Lieberman JR, Daluiski A, Einhorn T a. The Role of Growth Factors in the Repair of Bone. *J bone Jt surgery*. 2002;84:1032–44.
  31. Barnes GL, Kostenuik PJ, Gerstenfeld LC, Einhorn TA. Growth factor regulation of fracture repair. *J Bone Miner Res*. 1999;14(11):1805–15.
  32. Cahill KS, Chi JH, Day A, Claus EB. Prevalence, complications, and hospital charges associated with use of bone-morphogenetic proteins in spinal fusion procedures. *JAMA*. 2009;302(1):58–66.
  33. Vo T, Kasper K, Mikos AG. Strategies for controlled delivery of growth factors and cells for bone regeneration. *Adv Drug Deliv Rev*. 2012;64(12):1292–309.
  34. Ali IH a, Brazil DP. Bone morphogenetic proteins and their antagonists: Current and emerging clinical uses. *Br J Pharmacol*. 2014;171(15):3620–32.
  35. O’Keefe RJ, Mao J. Bone Tissue Engineering and Regeneration: From Discovery to the Clinic—An Overview. *Tissue Eng Part B Rev*. 2011;17(6):389–92.
  36. Tannoury C a, An HS. Complications with the use of bone morphogenetic protein 2 (BMP-2) in spine surgery. *Spine J*. 2014;14(3):552–9.
  37. Woo EJ. Adverse events after recombinant human BMP2 in nonspinal orthopaedic procedures general. *Clin Orthop Relat Res*. 2013;471:1707–11.
  38. Woo EJ. Recombinant human bone morphogenetic protein-2: Adverse events reported to the Manufacturer and User Facility Device Experience database. *Spine J*. 2012;12(10):894–9.
  39. Fu R, Selph S, Mcdonagh M, Peterson K, Tiwari A, Chou R. Annals of Internal Medicine Effectiveness and Harms of Recombinant Human Bone Morphogenetic. *Am Coll Physicians Downloaded*. 2012;158(12):890–902.
  40. Van Gestel N, Stegen S, Stockmans I, Moermans K, Schrooten J, Graf D, et al. Expansion of murine periosteal progenitor cells with fibroblast growth factor 2 reveals an intrinsic

- endochondral ossification program mediated by bone morphogenetic protein 2. *Stem Cells*. 2014;32(9):2407–18.
41. Bluteau G, Julien M, Magne D, Mallein-Gerin F, Weiss P, Daculsi G, et al. VEGF and VEGF receptors are differentially expressed in chondrocytes. *Bone*. 2007;40(3):568–76.
  42. Beamer B, Hettrich C, Lane J. Vascular endothelial growth factor: An essential component of angiogenesis and fracture healing. *HSS J*. 2010;6(1):85–94.
  43. Martino MM, Briquez PS, Maruyama K, Hubbell JA. Extracellular matrix-inspired growth factor delivery systems for bone regeneration. *Adv Drug Deliv Rev*. 2015;94:41–52.
  44. Kaipel M, Sch??tzenberger S, Schultz A, Ferguson J, Slezak P, Morton TJ, et al. BMP-2 but not VEGF or PDGF in fibrin matrix supports bone healing in a delayed-union rat model. *J Orthop Res*. 2012;30(10):1563–9.
  45. Hollinger JO, Onikepe AO, MacKrell J, Einhorn T, Bradica G, Lynch S, et al. Accelerated Fracture Healing in the Geriatric, Osteoporotic Rat with Recombinant Human Platelet-Derived Growth Factor-BB and an Injectable Beta-Tricalcium Phosphate/Collagen Matrix. *J Orthop Res*. 2007;11:83–90.
  46. Bruder SP, Jaiswal N, Haynesworth SE. Growth Kinetics , Self-Renewal , and the Osteogenic Potential of Purified Human Mesenchymal Stem Cells During Extensive Subcultivation and Following Cryopreservation. *J Cell Biochem*. 1997;64:278–94.
  47. Qin Y, Guan J, Zhang C. Mesenchymal stem cells: mechanisms and role in bone regeneration. *Postgrad Med J*. 2014;90:643–7.
  48. Rozalia Dimitriou, Tsiridi E, V.Giannoudis P. Current concepts of molecular aspects of bone healing. *Inj Int J Care Inj*. 2005;36:1392–404.
  49. Gilbert SF. *Developmental biology* /. 9th ed. Sunderland, Mass. : Sinauer Associates,; 2010.
  50. OpenStax. *Anatomy-and-Physiology*. OpenStax CNX; 2016.
  51. 6.4 Bone Formation and Development | *Anatomy and Physiology*.
  52. Waddington RJ, Roberts HC, Sugars R V., Schönherr E, Plenck H, Daculsi G, et al. Differential roles for small leucine-rich proteoglycans in bone formation. *Eur Cells Mater*. 2003;6(0):12–21.
  53. Mackie EJ, Ahmed YA, Tatarczuch L, Chen KS, Mirams M. Endochondral ossification: How cartilage is converted into bone in the developing skeleton. *Int J Biochem Cell Biol*. 2008;40(1):46–62.
  54. Crockett JC, Rogers MJ, Coxon FP, Hocking LJ, Helfrich MH. Bone remodelling at a glance. *J Cell Sci*. 2011;124(7):991–8.
  55. Hadjidakis DJ, Androulakis II. Bone remodeling. *Ann N Y Acad Sci*. 2006;1092:385–96.
  56. Li J, Liu X, Zhang L. The Role of Bone Marrow Microenvironment in Governing the Balance between Osteoblastogenesis and Adipogenesis. *Aging Dis*. 2016;7(4):514–25.
  57. W.Westerman R, E.Scammel B. Principles of bone and joint injuries and their healing. *Surg*. 2012;30(2):54–60.
  58. Schindeler A, McDonald MM, Bokko P, Little DG. Bone remodeling during fracture repair : The cellular picture. *Semin Cell Dev Biol*. 2008;19:459–66.
  59. Kolar P, Katharina Schmidt-Bleek HS, Gaber T, Toben D, Gerhard Schmidmaier CP, Buttgerit F, et al. The early fracture hematoma and its potential role in fracture healing. *Tissue Eng Part B Rev*. 2010;16(4):427–34.
  60. Chima SM, Jennifer Tickner, Chow ST, Kuek V, Guo B, Zhang G, et al. Angiogenic factors in bone local environment. *Cytokine Growth Factor Rev*. 2013;24(3):297–310.
  61. Dirckx N, Hul M Van, Maes C. Osteoblast recruitment to sites of bone formation in skeletal

- development, homeostasis, and regeneration. *Birth Defects Res Part C - Embryo Today*. 2013;99(3):170–91.
62. Cameron JA, Milner DJ, Lee JS, Cheng J, Fang NX, Jasiuk IM. Employing the biology of successful fracture repair to heal critical size bone defects. *Stocum, DL. New Perspectives in Regeneration*; 2012. 113–132 p.
  63. Santos MI, Reis RL. Vascularization in Bone Tissue Engineering : Physiology , Current Strategies , Major Hurdles and Future Challenges. *Macromol Biosci*. 2010;10:12–27.
  64. Merceron C, Vinatier C, Portron S, Masson M, Amiaud J, Guigand L, et al. Differential effects of hypoxia on osteochondrogenic potential of human adipose-derived stem cells. *Am J Physiol Physiol*. 2010;298(2):355–64.
  65. Carlier A, Geris L, Gastel N van, Carmeliet G, Oosterwyck H Van. Oxygen as a critical determinant of bone fracture healing — A multiscale model. *J Theor Biol*. 2015;365:247–64.
  66. Mountziaris PM, Mikos AG, Ph D. Modulation of the Inflammatory Response for Enhanced Bone Tissue Regeneration. *Tissue Eng Part B*. 2008;14(2):179–86.
  67. Nauth A, Ristiniemi J, Mckee MD, Schemitsch EH. Bone morphogenetic proteins in open fractures : past , present , and future. *Inj Int J Care Inj*. 2009;40:27–31.
  68. Franceschi RT, Yang S, Rutherford RB, Krebsbach PH, Zhao M, Wang D. Gene Therapy Approaches for Bone Regeneration. *Cells Tissues Organs*. 2004;176(1–3):95–108.
  69. Evans CH. Gene delivery to bone. *Adv Drug Deliv Rev*. 2012;64(12):1331–40.
  70. Balmayor ER, Griensven M Van. Gene therapy for bone engineering. *Front Bioeng Biotechnol*. 2015;3(February):1–7.
  71. Rose L, Uludağ H. Realizing the potential of gene-based molecular therapies in bone repair. *J Bone Miner Res*. 2013;28(11):2245–62.
  72. Elsabahy M, Nazarali A, Foldvari M. Non-viral nucleic acid delivery: key challenges and future directions. *Curr Drug Deliv*. 2011;8(3):235–44.
  73. Verma IM, Somia N. Gene therapy – promises , problems and prospects. *Nature*. 1997;389:239–42.
  74. Mintzer MA, Simanek EE. Nonviral Vectors for Gene Delivery. *Chem Rev*. 2008;109(2):259–302.
  75. Godbey WT, Mikos a G. Recent progress in gene delivery using non-viral transfer complexes. *J Control Release*. 2001;72(1–3):115–25.
  76. Han S. Development of Biomaterials for Gene Therapy. *Mol Ther*. 2000;2(4):302–17.
  77. Wagner E. Biomaterials in RNAi therapeutics: quo vadis? *Biomater Sci*. 2013;1:804–9.
  78. Kanasty R, Dorkin JR, Vegas A, Anderson D. Delivery materials for siRNA therapeutics. *Nat Mater*. 2013;12:967–77.
  79. Lam JKW, Chow MYT, Zhang Y, Leung SWS. siRNA Versus miRNA as Therapeutics for Gene Silencing. *Mol Ther acids*. 2015;4:e252.
  80. Peng B, Chen Y, Leong KW. MicroRNA delivery for regenerative medicine. *Adv Drug Deliv Rev*. 2015;88:108–22.
  81. Franceschetti T, M.Delany A. Chapter 25: miRNAs in Bone repair. In: *MicroRNA in Regenerative Medicine*. 2014. p. 653–83.
  82. Tsekoura EK, Bahadur KC R, Uludag H. Biomaterials to Facilitate Delivery of RNA Agents in Bone Regeneration and Biomaterials to Facilitate Delivery of RNA Agents in Bone Regeneration and Repair. *ACS Biomater Sci Eng*. 2017;3:1195–206.
  83. Eskildsen T, Taipaleenmäki H, Stenvang J, Abdallah BM, Ditzel N, Nossent AY, et al.

- MicroRNA-138 regulates osteogenic differentiation of human stromal (mesenchymal) stem cells in vivo. *Proc Natl Acad Sci U S A*. 2011;108:6139–44.
84. Nguyen MK, Jeon O, Krebs MD, Schapira D, Alsberg E. Sustained localized presentation of RNA interfering molecules from in situ forming hydrogels to guide stem cell osteogenic differentiation. *Biomaterials*. 2014;35(24):6278–86.
  85. Mencía Castaño I, Curtin CM, Duffy GP, O'Brien FJ. Next generation bone tissue engineering: non-viral miR-133a inhibition using collagen-nanohydroxyapatite scaffolds rapidly enhances osteogenesis. *Sci Rep*. 2016;6(27941):1–10.
  86. Mariner D.M, E J, Anseth KS. Manipulation of miRNA activity accelerates osteogenic differentiation of hMSCs in engineered 3D scaffolds. *J Tissue Eng Regen Med*. 2012;6:314–24.
  87. Li Y, Fan L, Liu S, Liu W, Zhang H, Zhou T, et al. The promotion of bone regeneration through positive regulation of angiogenic-osteogenic coupling using microRNA-26a. *Biomaterials*. 2013;34(21):5048–58.
  88. Zhang X, Li Y, Chen YE, Chen J, Ma PX. Cell-free 3D scaffold with two-stage delivery of miRNA-26a to regenerate critical-sized bone defects. *Nat Commun*. 2016;7:1–15.
  89. Deng Y, Bi X, Zhou H, You Z, Wang Y, Gu P, et al. Repair of critical-sized bone defects with anti-miR-31-expressing bone marrow stromal stem cells and poly(glycerol sebacate) scaffolds. *Eur Cell Mater*. 2014;27:13–25.
  90. Chen L, Holmstrøm K, Qiu W, Ditzel N, Shi K, Hokland L, et al. MicroRNA-34a inhibits osteoblast differentiation and in vivo bone formation of human stromal stem cells. *Stem Cells*. 2014;32:902–12.
  91. Xie Q, Wang Z, Zhou H, Yu Z, Huang Y, Sun H, et al. The role of miR-135-modified adipose-derived mesenchymal stem cells in bone regeneration. *Biomaterials*. 2016;75:279–94.
  92. Liao YH, Chang YH, Sung LY, Li KC, Yeh CL, Yen TC, et al. Osteogenic differentiation of adipose-derived stem cells and calvarial defect repair using baculovirus-mediated co-expression of BMP-2 and miR-148b. *Biomaterials*. 2014;35(18):4901–10.
  93. Li H, Li T, Fan J, Li T, Fan L, Wang S, et al. miR-216a rescues dexamethasone suppression of osteogenesis, promotes osteoblast differentiation and enhances bone formation, by regulating c-Cbl-mediated PI3K/AKT pathway. *Cell Death Differ*. 2015;22:1935–45.
  94. Kowalczewski CJ, Saul JM. Surface-mediated delivery of siRNA from fibrin hydrogels for knockdown of the BMP-2 binding antagonist noggin. *Acta Biomater*. 2015;25:109–20.
  95. Fan J, Park H, Tan S, Lee M. Enhanced Osteogenesis of Adipose Derived Stem Cells with Noggin Suppression and Delivery of BMP-2. *PLoS One*. 2013;8(8):1–10.
  96. Zhou Y, Guan X, Yu M, Wang X, Zhu W, Wang C, et al. Angiogenic/osteogenic response of BMMSCs on bone-derived scaffold: effect of hypoxia and role of PI3K/Akt-mediated VEGF-VEGFR pathway. *Biotechnol J*. 2014;9(7):944–53.
  97. Cui Z-K, Fan J, Kim S, Bezouglaia O, Fartash A, Wu BM, et al. Delivery of siRNA via cationic Sterosomes to enhance osteogenic differentiation of mesenchymal stem cells. *J Control Release*. 2015;217:42–52.
  98. Jeon SY, Park JS, Yang HN, Lim HJ, Yi SW, Park H, et al. Co-delivery of Cbfa-1-targeting siRNA and SOX9 protein using PLGA nanoparticles to induce chondrogenesis of human mesenchymal stem cells. *Biomaterials*. 2014;35(28):8236–48.
  99. Liang C, Guo B, Wu H, Shao N, Li D, Liu J, et al. Aptamer-functionalized lipid nanoparticles targeting osteoblasts as a novel RNA interference-based bone anabolic

- strategy. *Nat Med*. 2015;21(3):288–94.
100. Jia S, Yang X, Song W, Wang L, Fang K, Hu Z, et al. Incorporation of osteogenic and angiogenic small interfering RNAs into chitosan sponge for bone tissue engineering. *Int J Nanomedicine*. 2014;9(1):5307–16.
  101. Kim J-Y, Min J-Y, Baek JM, Ahn S-J, Jun HY, Yoon K-H, et al. CTRP3 acts as a negative regulator of osteoclastogenesis through AMPK-c-Fos-NFATc1 signaling in vitro and RANKL-induced calvarial bone destruction in vivo. *Bone*. 2015;79:242–51.
  102. Putnam D. Polymers for gene delivery across length scales. *Nat Mater*. 2006;5(6):439–51.
  103. Akinc A, Thomas M, Klivanov A, Langer R. Exploring polyethylenimine-mediated DNA transfection and the proton sponge hypothesis. *J Gene Med*. 2005;7:657–63.
  104. Kunath K, Von Harpe A, Fischer D, Petersen H, Bickel U, Voigt K, et al. Low-molecular-weight polyethylenimine as a non-viral vector for DNA delivery: Comparison of physicochemical properties, transfection efficiency and in vivo distribution with high-molecular-weight polyethylenimine. *J Control Release*. 2003;89(1):113–25.
  105. Godbey WT, KK W, AG M. Size matters: molecular weight affects the efficiency of poly(ethylenimine) as a gene delivery vehicle. *J Biomed Mater Res*. 1999;268–75.
  106. Neamark A, Suwantong O, Bahadur RK, Hsu CY, Supaphol P, Uludag H. Aliphatic lipid substitution on 2 kDa polyethylenimine improves plasmid delivery and transgene expression. *Mol Pharm*. 2009;6(6):1798–815.
  107. Liu Z, Zhang Z, Zhou C, Jiao Y. Hydrophobic modifications of cationic polymers for gene delivery. *Prog Polym Sci*. 2010;35(9):1144–62.
  108. Pezzoli D, Tsekoura EK, C RBK, Candiani G, Mantovani D. Hydrophobe-substituted b PEI derivatives: boosting transfection on primary vascular cells. *Sci China Mater*. 2017;60(6):529–42.
  109. Allen TM, Cullis PR. Liposomal drug delivery systems: From concept to clinical applications. *Adv Drug Deliv Rev*. 2013;65(1):36–48.
  110. Tam YYC, Chen S, Cullis PR. Advances in lipid nanoparticles for siRNA delivery. *Pharmaceutics*. 2013;5(3):498–507.
  111. Kane RC, Farrell AT, Saber H, Tang S, Williams G, Jee JM, et al. Sorafenib for the treatment of advanced renal cell carcinoma. *Clin Cancer Res*. 2006;12(24):7271–8.
  112. Zhang G, Guo B, Wu H, Tang T, Zhang B-T, Zheng L, et al. A delivery system targeting bone formation surfaces to facilitate RNAi-based anabolic therapy. *Nat Med*. 2012;18(2):307–14.
  113. Matsuda N, Shimizu T, Yamato M, Okano T. Tissue engineering based on cell sheet technology. *Adv Mater*. 2007;19(20):3089–99.
  114. Yan J, Zhang C, Zhao Y, Cao C, Wu K, Zhao L, et al. Non-viral oligonucleotide anti-miR-138 delivery to mesenchymal stem cell sheets and the effect on osteogenesis. *Biomaterials*. 2014;35(27):7734–49.
  115. Fomby P, Cherlin AJ. Noggin regulation of bone morphogenetic protein (BMP) 2/7 heterodimer activity in vitro. *Bone*. 2011;72(2):181–204.
  116. Ungureanu C, Kroes R, Petersen W, Groothuis TAM, Ungureanu F, Janssen H, et al. Light interactions with gold nanorods and cells: Implications for photothermal nanotherapeutics. *Nano Lett*. 2011;11(5):1887–94.
  117. Remant Bahadur KC, Thapa B, Bhattarai N. Gold nanoparticle-based gene delivery: Promises and challenges. *Nanotechnol Rev*. 2014;3(3):269–80.
  118. Kim TH, Kim M, Eltohamy M, Yun YR, Jang JH, Kim HW. Efficacy of mesoporous silica

- nanoparticles in delivering BMP-2 plasmid DNA for in vitro osteogenic stimulation of mesenchymal stem cells. *J Biomed Mater Res - Part A*. 2013;101 A(6):1651–60.
119. Wang S, Gao X, Gong W, Zhang Z, Chen X, Dong Y. Odontogenic differentiation and dentin formation of dental pulp cells under nanobioactive glass induction. *Acta Biomater*. 2014;10(6):2792–803.
  120. Kim WS, Kim HJ, Lee ZH, Lee Y, Kim HH. Apolipoprotein E inhibits osteoclast differentiation via regulation of c-Fos, NFATc1 and NF- $\kappa$ B. *Exp Cell Res*. 2013;319(4):436–46.
  121. Kim T, Singh RK, Sil M, Kim J, Kim H. Inhibition of osteoclastogenesis through siRNA delivery with tunable mesoporous bioactive nanocarriers. *Acta Biomater*. 2015;
  122. Lacey DL, Tan HL, Lu J, Kaufman S, Van G, Qiu W, et al. Osteoprotegerin ligand modulates murine osteoclast survival in vitro and in vivo. *Am J Pathol*. 2000;157(2):435–48.
  123. Wang Y, Tran KK, Shen H, Grainger D. Selective local delivery of rank siRNA to bone phagocytes using bone augmentation biomaterials. *Biomaterials*. 2012;33(33):8540–8547.
  124. Pissuwan D, Niidome T, Cortie MB. The forthcoming applications of gold nanoparticles in drug and gene delivery systems. *J Control Release*. 2011;149(1):65–71.
  125. Zhao X, Huang Q, Jin Y. Gold nanorod delivery of LSD1 siRNA induces human mesenchymal stem cell differentiation. *Mater Sci Eng C Mater Biol Appl*. 2015;54:142–9.
  126. Yin F, Lan R, Zhang X, Zhu L, Chen F, Xu Z, et al. LSD1 regulates pluripotency of embryonic stem/carcinoma cells through histone deacetylase 1-mediated deacetylation of histone H4 at lysine 16. *Mol Cell Biol*. 2014;34(2):158–79.
  127. Liang D, Luu YK, Kim K, Hsiao BS, Hadjiargyrou M, Chu B. In vitro non-viral gene delivery with nanofibrous scaffolds. *Nucleic Acids Res*. 2005;33(19):1–10.
  128. Y.K.Luu, K.Kim, B.S.Hsiao, B.Chu, M.Hadjiargyrou. Development of a nanostructured DNA delivery scaffold via electrospinning of PLGA and PLA-PEG block copolymers. *J Control Release*. 2003;89:341–53.
  129. Wang Z, Zhefeng Wang, William Weijia Lu, Wanxin Zhen, Dazhi Yang, Peng S. Novel biomaterial strategies for controlled growth factor delivery for biomedical applications. *NPG Asia Mater*. 2017;9:1–16.
  130. ZS H, Hamdy RC, Tabrizian M. Delivery of recombinant bone morphogenetic proteins for bone regeneration and repair. Part B: Delivery systems for BMPs in orthopaedic and craniofacial tissue engineering. *Biotechnol Lett*. 2009;31(12):1825–35.
  131. Lee SS, BJ H, SR K, S S, CJ N, SR S, et al. Bone regeneration with low dose BMP-2 amplified by biomimetic supramolecular nanofibers within collagen scaffolds. *Biomaterials*. 2013;34(2):452–9.
  132. Su Y, Su Q, Liu W, Lim M, Venugopal JR, Ramakrishna S, et al. Controlled release of bone morphogenetic protein 2 and dexamethasone loaded in core-shell PLLACL-collagen fibers for use in bone tissue engineering.pdf. *Acta Biomater*. 2012;8:763–71.
  133. Zhang H, Liang J, Ding Y, Li P. The controlled release of growth factor via modified coaxial electrospun fibres with emulsion or hydrogel as the core.pdf. *Mater Lett*. 2016;181:119–22.
  134. Gibson LJ. Modelling the mechanical behavior of cellular materials. *Mater Sci Eng A*. 1989;110:1–36.
  135. Gerhardt L-C, Boccaccini AR. Bioactive Glass and Glass-Ceramic Scaffolds for Bone Tissue Engineering. *Materials (Basel)*. 2010;3(7):3867–910.
  136. Ngan F, Huang, Li S. Regulation of the matrix microenvironment for stem cell engineering

- and regenerative medicine. *Ann Biomed Eng.* 2013;18(9):1199–216.
137. Hutmacher DW. Scaffolds in tissue engineering bone and cartilage. *Biomaterials.* 2000;21(24):2529–43.
  138. Leong KF, Cheah CM, Chua CK. Solid freeform fabrication of three-dimensional scaffolds for engineering replacement tissues and organs. *Biomaterials.* 2003;24(13):2363–78.
  139. Wei G, Ma PX. Nanostructured biomaterials for regeneration. *Adv Funct Mater.* 2009;18(22):3566–82.
  140. Birk DE, Bruckner P. *The Extracellular Matrix: an Overview.* Vol. 1, ed Mecham R. P. (Academic Press, Orlando, FL). New York: Springer-Verlag; 2011. 77–115 p.
  141. Spira M, Liu BC, Xu ZL, Harrell R, Chahadeh H. Human Amnion Collagen for Soft-Tissue Augmentation - Biochemical Characterizations and Animal Observations. *J Biomed Mater Res.* 1994;28(1):91–6.
  142. Muralidharan N, Jeya Shakila R, Sukumar D, Jeyasekaran G. Skin, bone and muscle collagen extraction from the trash fish, leather jacket (*Odonus niger*) and their characterization. *J Food Sci Technol.* 2013;50(6):1106–13.
  143. Olsen D, Yang C, Bodo M, Chang R, Leigh S, Baez J, et al. Recombinant collagen and gelatin for drug delivery. *Adv Drug Deliv Rev.* 2003;55(12):1547–67.
  144. Ramshaw JAM. Biomedical applications of collagens. *J Biomed Mater Res - Part B Appl Biomater.* 2016;104(4):665–75.
  145. Carmichael DJ LR. Bovine collagen I changes in collagen solubility with animal age. *Int J Food Sci Technol.* 1967;2:299–311.
  146. Chang MC, Ikoma T, Kikuchi M, Tanaka J. Preparation of a porous hydroxyapatite/collagen nanocomposite using glutaraldehyde as a crosslinkage agent. *J Mater Sci Lett.* 2001;20(13):1199–201.
  147. Pacak C a, MacKay A a, Cowan DB. An improved method for the preparation of type I collagen from skin. *J Vis Exp.* 2014;(83):1–4.
  148. Shoulders MD, Raines RT. Collagen Structure and Stability. *Annu Rev Biochem.* 2010;78:929–58.
  149. Walton RS, Brand DD, Czernuszka JT. Influence of telopeptides, fibrils and crosslinking on physicochemical properties of Type i collagen films. *J Mater Sci Mater Med.* 2010;21(2):451–61.
  150. Gilbert TW, Sellaro TL, Badylak SF. Decellularization of tissues and organs. *Biomaterials.* 2006;27(19):3675–83.
  151. Lia D., Lin Y., Chen M. Optimum Conditions of Extracting Collagen from Chicken Feet and its characteristics. *Asian Australas J Anim Sci.* 2001;14(11):1638–43.
  152. Francis G, Thomas J. Isolation and chemical characterization of collagen in bovine pulmonary tissues. *Biochem J.* 1975;145(2):287–97.
  153. Heu MS, Lee JH, Kim HJ, Jee SJ, Lee JS, Jeon YJ, et al. Characterization of acid- and pepsin-soluble collagens from flatfish skin. *Food Sci Biotechnol.* 2010;19(1):27–33.
  154. Zeugolis DI, Paul RG, Attenburrow G. Factors influencing the properties of reconstituted collagen fibers prior to self-assembly: Animal species and collagen extraction method. *J Biomed Mater Res - Part A.* 2008;86(4):892–904.
  155. Capaldi MJ, Chapman JA. The C-terminal extrahelical peptide of type I collagen and its role in fibrillogenesis in vitro. *Biopolymers.* 1982;21(11):2291–313.
  156. Davidenko N, Schuster CF, Bax DV, Raynal N, Fardale RW, Best SM, et al. Control of crosslinking for tailoring collagen-based scaffolds stability and mechanics. *Acta Biomater.*

- 2015;25:131–42.
157. Meshel AS, Wei Q, Adelstein RS, Sheetz MP. Basic mechanism of three-dimensional collagen fibre transport by fibroblasts. *Nat Cell Biol.* 2005;7(2):157–64.
  158. Yang HT, Tan Q, Zhao H. Progress in various crosslinking modification for acellular matrix. *Chin Med J (Engl).* 2014;127(17):3156–64.
  159. Lew D-H, Liu PH-T, Orgill DP. Optimization of UV cross-linking density for durable and nontoxic collagen GAG dermal Substitute. *J Biomed Mater Res B Appl Biomater.* 2006;51–6.
  160. Braile MCVB, Carnevalli NC, Goissis G, Ramirez VA, Braile DM. In vitro properties and performance of glutaraldehyde-crosslinked bovine pericardial bioprostheses treated with glutamic acid. *Artif Organs.* 2011;35(5):497–501.
  161. Weadock KS, Miller EJ, Bellincampi LD, Zawadsky JP, Dunn MG. Physical Cross-Linking of Collagen-Fibers - Comparison of Ultraviolet-Irradiation and Dehydrothermal Treatment. *J Biomed Mater Res.* 1995;29(11):1373–9.
  162. Weadock KS, Miller EJ, Keuffel EL, Dunn MG. Effect of physical crosslinking methods on collagen-fiber durability in proteolytic solutions. *J Biomed Mater Res.* 1996;32(2):221–6.
  163. Willits RK, Skornia SL. Effect of collagen gel stiffness on neurite extension. *J Biomater Sci.* 2004;15(12):1521–31.
  164. Duan X, Sheardown H. Dendrimer crosslinked collagen as a corneal tissue engineering scaffold: Mechanical properties and corneal epithelial cell interactions. *Biomaterials.* 2006;27(26):4608–17.
  165. Rault I, Frei V, Herbage D, Abdul-Malak N, Huc a. Evaluation of different chemical methods for cross-linking collagen gel, films and sponges. *J Mater Sci Mater Med.* 1996;7(4):215–21.
  166. Tanaka T, Ujiie R, Yajima H, Mizutani K, Suzuki Y, Sakuragi H. Ion-beam irradiation into biodegradable nanofibers for tissue engineering scaffolds. *Surf Coatings Technol.* 2011;206(5):889–92.
  167. Srinivas A, Ramamurthi A. Effects of gamma-irradiation on physical and biologic properties of crosslinked hyaluronan tissue engineering scaffolds. *Tissue Eng.* 2007;13:447–59.
  168. Chen RN, Ho HO, Sheu MT. Characterization of collagen matrices crosslinked using microbial transglutaminase. *Biomaterials.* 2005;26(20):4229–35.
  169. Yunoki S, Ohyabu Y, Hatayama H. Temperature-responsive gelation of type I collagen solutions involving fibril formation and genipin crosslinking as a potential injectable hydrogel. *Int J Biomater.* 2013;2013.
  170. Perez RA, Mestres G. Role of pore size and morphology in musculo-skeletal tissue regeneration. *Mater Sci Eng C.* 2016;61:922–39.
  171. Lim TC, Chian KS, Leong KF. Cryogenic prototyping of chitosan scaffolds with controlled micro and macro architecture and their effect on in vivo neo-vascularization and cellular infiltration. *J Biomed Mater Res - Part A.* 2010;94(4):1303–11.
  172. Lee JW, Ahn G, Cho DW, Kim JY. Evaluating cell proliferation based on internal pore size and 3D scaffold architecture fabricated using solid freeform fabrication technology. *J Mater Sci Mater Med.* 2010;21(12):3195–205.
  173. Hing KA. Bioceramic bone graft substitutes: Influence of porosity and chemistry. *Int J Appl Ceram Technol.* 2005;2(3):184–99.

174. O'Brien FJ, Harley B a, Yannas I V, Gibson LJ. The effect of pore size on cell adhesion in collagen-GAG scaffolds. *Biomaterials*. 2005 Feb;26(4):433–41.
175. Kyongbum Lee DK. *Tissue Engineering I: Scaffold Systems for Tissue Engineering*. 2006. 243 p.
176. JamesMAnderson. BIOLOGICAL RESPONSES TO MATERIALS. *Annu Rev Mater Res*. 2001;31:81–110.
177. Ghasemi-Mobarakeh L, Prabhakaran MP, Tian L, Shamirzaei-Jeshvaghani E, Dehghani L, Ramakrishna S. Structural properties of scaffolds: Crucial parameters towards stem cells differentiation. *World J Stem Cells*. 2015;7(4):728–44.
178. Dhandayuthapani B, Yoshida Y, Maekawa T, Kumar DS. Polymeric Scaffolds in Tissue Engineering Application : A Review. *Int J Polym SWcience*. 2011;1–19.
179. Smith I, Liu XH, Smith L, Ma P. Nano-structured polymer scaffolds for tissue engineering and regenerative medicine. *Wiley Interdiscip Rev Nanomedicine Nanobiotechnology*. 2009;1(2):226–36.
180. Salgado AJ, Coutinho OP, Reis RL. Bone tissue engineering: State of the art and future trends. *Macromol Biosci*. 2004;4(8):743–65.
181. Browne S, Zeugolis DI, Pandit A. Collagen: finding a solution for the source. *Tissue Eng A*. 2013;13–14:1491–4.
182. Drury JL, Mooney DJ. Hydrogels for tissue engineering: Scaffold design variables and applications. *Biomaterials*. 2003;24(24):4337–51.
183. Wang L, Stegemann JP. Thermogelling chitosan and collagen composite hydrogels initiated with [beta]-glycerophosphate for bone tissue engineering. *Biomaterials*. 2011;31(14):3976–85.
184. Dori F, Huszar T, Nikolidakis D, Arweiler NB, Gera I, Sculean A. Effect of platelet-rich plasma on the healing of intra-bony defects treated with a natural bone mineral and a collagen membrane. *J Clin Periodontol*. 2007;34(3):254–61.
185. Schoof H, Bruns L, Fischer A, Heschel I, Rau G. Dendritic ice morphology in unidirectionally solidified collagen suspensions. *J Cryst Growth*. 2000;209(1):122–9.
186. Srouji S, Kizhner T, Suss-Tobi E, Livne E, Zussman E. 3-D Nanofibrous electrospun multilayered construct is an alternative ECM mimicking scaffold. *J Mater Sci Mater Med*. 2008;19(3):1249–55.
187. Subia B, Kundu J, Kundu S. Biomaterial scaffold fabrication techniques for potential tissue engineering applications. *Tissue Eng*. 2010;(3):141–59.
188. Pham QP, Sharma U, Mikos AGE. Electrospinning of polymeric nanofibers for tissue engineering applications: a review. *Tissue Eng*. 2006;12:1197.
189. Heydarkhan-Hagvall S, Schenke-Layland K, Dhanasopon AP, Rofail F, Smith H, Wu BM, et al. Three-dimensional electrospun ECM-based hybrid scaffolds for cardiovascular tissue engineering. *Biomaterials*. 2008;29(19):2907–14.
190. Annabi N, Nichol JW, Zhong X, Ji C, Koshy S, Khademhosseini A, et al. Controlling the porosity and microarchitecture of hydrogels for tissue engineering. *Tissue Eng Part B Rev*. 2010;16(4):371–83.
191. Do A, Khorsand B, Geary SM, Salem AK. 3D Printing of Scaffolds for Tissue Regeneration Applications. *Adv Heal Mater*. 2015;4(12):1742–62.
192. Murphy S V, Atala A. 3D bioprinting of tissues and organs. *Nat Biotechnol*. 2014;32(8):773–85.
193. Wu Z, Su X, Xu Y, Kong B, Sun W, Mi S. Bioprinting three-dimensional cell-laden tissue

- constructs with controllable degradation. *Sci Rep.* 2016;6:1–10.
194. Lee HJ, Ahn SH, Kim GH. Three-dimensional collagen/alginate hybrid scaffolds functionalized with a drug delivery system (DDS) for bone tissue regeneration. *Chem Mater.* 2012;24(5):881–91.
  195. Lausch AJ, Chong LC, Uludag H, Sone ED. Multiphasic Collagen Scaffolds for Engineered Tissue Interfaces. *Adv Funct Mater.* 2018;28:1804730 (1-9).
  196. Bajpai S, Kim NY, Reinhart-King CA. Approaches to manipulating the dimensionality and physicochemical properties of common cellular scaffolds. *Int J Mol Sci.* 2011;12(12):8596–609.
  197. Young JAE, Ashman RB, Turner CH. Young ' S Modulus of Trabecular and Cortical Bone Material : Ultrasonic and Microtensile Measurements. *Biomechanics.* 1993;26(2):111–9.
  198. Yoshito Ikada. *Tissue Engineering: Fundamentals and Applications.* 2011. 490 p.
  199. Guilak F. Functional Tissue Engineering The Role of Biomechanics in Reparative Medicine. *J Biomech Eng.* 2000;122:553–69.
  200. Brien FJO. Biomaterials & scaffolds for tissue engineering. *Mater Today.* 2011;14(3):88–95.
  201. West J, Hubbell J. Polymeric biomaterials with degradation sites for protease involved in cell migration. *Macromolecules.* 1999;32:241–4.
  202. Robles-Vásquez O, Orozco-Avila I, Sánchez-Díaz JC, Hernandez E. An Overview of Rheological Models for Polymeric Biomaterial scaffolds Used in Tissue Engineering. *J Res Updat Polym Sci.* 2015;4(4):168–78.
  203. Macrae RA, Miller K, Doyle BJ. Methods in Mechanical Testing of Arterial Tissue: A Review. *Strain.* 2016;
  204. Dhand C, Ong ST, Dwivedi N, Diaz SM, Venugopal JR, Navaneethan B, et al. Bio-Inspired in situ crosslinking and mineralization of electrospun collagen scaffolds for bone tissue engineering. *Biomaterials.* 2016;104:323–38.
  205. Kwak S, Haider A, Gupta KC, Kim S, Kang I-K. Micro/Nano Multilayered Scaffolds of PLGA and Collagen by Alternately Electrospinning for Bone Tissue Engineering. *Nanoscale Res Lett.* 2016;11(323):1–16.
  206. Lynn AK, Yannas I V., Bonfield W. Antigenicity and immunogenicity of collagen. *J Biomed Mater Res - Part B Appl Biomater.* 2004;71(2):343–54.
  207. Hiruma H, Toida H, Hanawa T, Sakuragi H, Suzuki Y. Biocompatibility control of recombinant collagen by ion beam modification. *Surf Coatings Technol.* 2011;206(5):911–5.
  208. Liu W, Merrett K, Griffith M, Fagerholm P, Dravida S, Heyne B, et al. Recombinant human collagen for tissue engineered corneal substitutes. *Biomaterials.* 2008;29(9):1147–58.
  209. An B, Kaplan DL, Brodsky B. Engineered recombinant bacterial collagen as an alternative collagen-based biomaterial for tissue engineering. *Front Chem.* 2014;2(June):40.
  210. Koide T. Designed triple-helical peptides as tools for collagen biochemistry and matrix engineering. *Philos Trans R Soc Lond B Biol Sci.* 2007;362(1484):1281–91.
  211. Kong HJ, Liu J, Riddle K, Matsumoto T, Leach K, Mooney DJ. Non-viral gene delivery regulated by stiffness of cell adhesion substrates. *Nat mate.* 2005;4(June):460–4.
  212. Adler AF, Leong KW. Emerging links between surface nanotechnology and endocytosis: impact on nonviral gene delivery. *Nano Today.* 2010;5(6):553–69.
  213. Jang J-H, Rives CB, Shea LD. Plasmid Delivery in Vivo from Porous Tissue-Engineering Scaffolds: Transgene Expression and Cellular Transfection. *Mol Ther.* 2005;12(3):475–83.

214. Pankongadisak P, Tsekoura EK, Suwantong O, Uludag H. Electrospun gelatin matrices with bioactive pDNA polyplexes. *Int J Biol Macromol*. 2020;149:296–308.
215. C.H. Evans, F.-J. Liu, V. Glatt, J.A. Hoyland, C. Kirker-Head, A. Walsh, O. Betz, J.W. Wells, V. Betz, R.M. Porter, F.A. Saad, L.C. Gerstenfeld, T.A. Einhorn, M.B. Harris and MSV. Use of genetically modified muscle and fat grafts to repair defects in bone and cartilage. *Eur Cell Mater*. 2015;(18):96–111.
216. Zhang W, Tsurushima H, Oyane A, Yazaki Y, Sogo Y, Ito A, et al. BMP-2 gene-fibronectin-apatite composite layer enhances bone formation. *J Biomed Sci*. 2011;18(62):1–11.
217. Kempen DHR, Lu L, Heijink A, Hefferan TE, Creemers LB, Maran A, et al. Effect of local sequential VEGF and BMP-2 delivery on ectopic and orthotopic bone regeneration. *Biomaterials*. 2009;30(14):2816–25.
218. Khorsand B, Nicholson N, Do AV, Femino JE, Martin JA, Petersen E, et al. Regeneration of bone using nanoplex delivery of FGF-2 and BMP-2 genes in diaphyseal long bone radial defects in a diabetic rabbit model. *J Control Release*. 2017;248:53–9.
219. Remant Bahadur KC, Landry B, Aliabadi HM, Lavasanifar A, Uludağ H. Lipid substitution on low molecular weight (0.6-2.0 kDa) polyethylenimine leads to a higher zeta potential of plasmid DNA and enhances transgene expression. *Acta Biomater*. 2011;7(5):2209–17.
220. Guillot-Nieckowski M, Eisler S, Diederich F. Dendritic vectors for gene transfection. *New J Chem*. 2007;31(7):1111.
221. Huh SH, Do HJ, Lim HY, Kim DK, Choi SJ, Song H, Kim NH, Park JK, Chang WK, Chung HM KJ. Optimization of 25 kDa linear polyethylenimine for efficient. *Biologicals*. 2007;35:165–71.
222. Wang W, Li W, Ou L, Flick E, Mark P, Nesselmann C, et al. Polyethylenimine-mediated gene delivery into human bone marrow mesenchymal stem cells from patients. *J Cell Mol Med*. 2011;15(9):1989–98.
223. Wang Y, Mostafa NZ, Hsu CYM, Rose L, Kucharki C, Yan J, et al. Modification of human BMSC with nanoparticles of polymeric biomaterials and plasmid DNA for BMP-2 secretion. *J Surg Res*. 2013;183(1):8–17.
224. Thapa B, Plianwong S, Remant Bahadur K, Rutherford B, Uludağ H. Small hydrophobe substitution on polyethylenimine for plasmid DNA delivery: Optimal substitution is critical for effective delivery. *Acta Biomater*. 2016;33:213–24.
225. Hugh JC, Uludağ H, Kucharski C, Parmar MB, Aliabadi HM, Mahdipoor P, et al. Targeting Cell Cycle Proteins in Breast Cancer Cells with siRNA by Using Lipid-Substituted Polyethylenimines. *Front Bioeng Biotechnol*. 2015;3(February):1–14.
226. Remant BK, Kucharski C, Uludag H. Additive nanocomplexes of cationic lipopolymers for improved non-viral gene delivery to mesenchymal stem cells. *J Mater Chem B*. 2015;3(19):3972–82.
227. Volle DH, Babajko S, Bunnell BA, Bateman ME, Strong AL, Mclachlan JA, et al. The effects of endocrine Disruptors on Adipogenesis and Osteogenesis in Mesenchymal Stem Cells: A Review. *Front Endocrinol*. 2017;7(7):1713389–171.
228. You-Kyoung Kim, Hidemi Nakata, Maiko Yamamoto, Munemitsu Miyasaka, Shohei Kasugai and SK. Osteogenic Potential of Mouse Periosteum-Derived Cells Sorted for CD90 In Vitro and In Vivo. *Stem Cells Transl Med*. 2016;5:227–34.
229. Arnsdorf EJ, Jones LM, Carter DR, Jacobs CR. The Periosteum as a Cellular Source for Functional Tissue Engineering. *Tissue Eng Part A*. 2009;15(9):2637–42.
230. Pers YM, Rackwitz L, Ferreira R, Pullig O, Delfour C, Barry F, Sensebe L, Casteilla L,

- Fleury S, Bourin P, Noël D, Canovas F, Cyteval C, Lisignoli G, Schrauth J, Haddad D, Domergue S, Noeth U JCAC. Adipose Mesenchymal Stromal Cell-Based Therapy for Severe Osteoarthritis of the Knee :A Phase I Dose-Escalation Trial. *Stem Cells Transl Med.* 2016;847–56.
231. Götherström C, Westgren M, Shaw SW, Aström E, Biswas A, Byers PH, Mattar CN, Graham GE, Taslimi J, Ewald U, Fisk NM, Yeoh AE, Lin JL, Cheng PJ, Choolani M, Le Blanc K CJ. Pre- and postnatal transplantation of fetal mesenchymal stem cells in osteogenesis imperfecta: A two-center experience. *Stem Cells Transl Med.* 2014;3(2):255–64.
  232. Moghimi SM, Symonds P, Murray JC, Hunter AC, Debska G, Szewczyk A. A two-stage poly(ethylenimine)-mediated cytotoxicity: Implications for gene transfer/therapy. *Mol Ther.* 2005;11(6):990–5.
  233. Peng Q, Zhong Z, Zhuo R. Disulfide cross-linked polyethylenimines (PEI) prepared via thiolation of low molecular weight PEI as highly efficient gene vectors. *Bioconjug Chem.* 2008;19(2):499–506.
  234. Marsell Richard, Einhorn TA. The biology of fracture healing. *Injury.* 2012;42(6):551–5.
  235. Marsell R, Einhorn TA. The role of endogenous bone morphogenetic proteins in normal skeletal repair. *Inj Int J Care Inj.* 2009;40(S3):S4–7.
  236. Wang X, Matthews BG, Yu J, Novak S, Grcevic D, Sanjay A, et al. PDGF Modulates BMP2-Induced Osteogenesis in Periosteal Progenitor Cells. *JBMR Plus.* 2019;3(5):e10127.
  237. Yue J, Wu J, Liu D, Zhao X, Lu WW. BMP2 gene delivery to bone mesenchymal stem cell by chitosan-g-PEI nonviral vector. *Nanoscale Res Lett.* 2015;10(203):1–11.
  238. Jin H, Liu Z, Li W, Jiang Z, Zhang B. Polyethylenimine-alginate nanocomposites based bone morphogenetic protein 2 gene-activated matrix for alveolar bone regeneration. *RCS Adv.* 2019;(46):26598–608.
  239. Witte T De, Fratila-apachitei LE, Zadpoor AA, Peppas NA. Bone tissue engineering via growth factor delivery : from scaffolds to complex matrices. *Regenerative Biomater.* 2018;197–211.
  240. Khan SN, Lane JM. The use of recombinant human bone morphogenetic protein-2 ( rhBMP-2 ) in orthopaedic applications The use of recombinant human bone morphogenetic protein-2 ( rhBMP-2 ) in. *Expert Opin Biol Ther.* 2004;4(5):741–8.
  241. Dagmar Fischer, Bieber T, Li Y, Elsässer H-P, Kissel T. A novel non-viral vector for DNA delivery based on low molecular weight, branched polyethylenimine effect of molecular weight on transfection efficiency and cytotoxicity.pdf. *Pharm Reserach.* 1999;16(8):1273–9.
  242. Parmar MB, K.C RB, Löbenberg R, Uludag H. Additive Polyplexes to Undertake siRNA Therapy against CDC20 and Survivin in Breast Cancer Cells. *Biomacromolecules.* 2018;19:4193–206.
  243. Online VA, Wang H, Zhang J, Liu Y, Luo T, He X, et al. Hyaluronic acid-based carbon dots for efficient gene delivery and cell imaging. *R Soc Chem.* 2017;7:15613–24.
  244. Krisch E, Messenger L, Gyarmati B, Ravaine V, Szilágyi A. Redox- and pH-Responsive Nanogels Based on Thiolated Poly ( aspartic acid ). *Macromol Mater Eng.* 2015;301:260–6.
  245. Nie J, Dou X, Hu H, Yu B, Wang R, Xu F. Poly(aspartic acid)-based Degradable Assemblies for Highly Efficient Gene Delivery. *Appl Mater interfaces.* 2015;7:533–62.
  246. Zhang D, Wu X, Chen J, Lin K. The development of collagen based composite scaffolds

- for bone regeneration. *Bioact Mater.* 2018;3:129–38.
247. Lausch AJ, Quan BD, Miklas JW, Sone ED. Extracellular Matrix Control of Collagen Mineralization In Vitro. *Ad.* 2013;23:4906–12.
  248. Liu Y, Kim Y, Dai L, Li N, Khan S, Pashley DH, et al. Hierarchical and non-hierarchical mineralisation of collagen Franklin. *Biomaterials.* 2011;32(5):1291–300.
  249. Parvizi J, FRCS, Gregory K.Kim, Editor A. Osteoblasts. In: *High Yield Orthopaedics.* 2010. p. 331–2.
  250. Katagiri T, Yamaguchi A, Komaki M, Abe E, Takahashi N, Ikeda T, et al. Bone Morphogenetic Protein-2 Converts the Differentiation Pathway of C2C12 Myoblasts into the Osteoblast Lineage. *J Cell Biol.* 1994;127(6):1–5.
  251. Hwang PW, Horton JA. Variable osteogenic performance of MC3T3-E1 subclones impacts their utility as models of osteoblast biology. *Sci Rep.* 2019;9:1–9.
  252. Onadio JEB, Miley ELS, Atil PRP, Oldstein STG. Localized , direct plasmid gene delivery in vivo : prolonged therapy results in reproducible tissue regeneration. :753–9.
  253. Jiangning C, HuanChena, Pei L, Huajia D, Shiyu Z, Lei D, et al. Simultaneous regeneration of articular cartilage and subchondral bone in vivo using MSCs induced by a spatially controlled gene delivery system in bilayered integrated scaffolds.pdf. *Biomaterials.* 2011;32:4793–805.
  254. Shapiro G, Lieber R, Gazit D, Pelled G. Recent Advances and Future of Gene Therapy for Bone Regeneration. *Curr Osteoporos Rep.* 2018;16(4):504–11.
  255. Bleich NK, Kallai I, Lieberman JR, Schwarz EM, Pelled G, Gazit D. Gene therapy approaches to regenerating bone. *Adv Drug Deliv Rev [Internet].* 2012;64:1320–30. Available from: <http://www.ncbi.nlm.nih.gov/pubmed/22429662>
  256. Zakeri A, Kouhbanani MAJ, Beheshtkhoo N, Beigi V, Mousavi SM, Hashemi SAR, et al. Polyethylenimine-based nanocarriers in co-delivery of drug and gene: a developing horizon. *Nano Rev Exp.* 2018;9:1–14.
  257. Taranejoo S, Liu J, Verma P, Hourigan K. A review of the developments of characteristics of PEI derivatives for gene delivery applications. *J Appl Polym Sci.* 2015;132(25):42096 (1 of 8).
  258. D’Mello S, Atluri K, Geary SM, Hong L, Satheesh Elangovan AKS. Bone regeneration using gene-activated matrices. *AAPS J.* 2017;19(1):43–53.
  259. Tierney EG, Duffy GP, Cryan S, Curtin CM, J.O’Brien F. Non-viral gene-activated matrices: Next generation constructs for bone repair. *Organogenesis.* 2013;9(1):22–8.
  260. Chan BP, Leong KW. Scaffolding in tissue engineering: General approaches and tissue-specific considerations. *Eur Spine J.* 2008;17(SUPPL. 4):S467–79.
  261. Li H, Ji Q, Chen X, Sun Y, Xu Q, Deng P, et al. Accelerated bony defect healing based on chitosan thermosensitive hydrogel scaffolds embedded with chitosan nanoparticles for the delivery of BMP2 plasmid DNA. *Biomed Mater Res A.* 2017;105A(1):265–73.
  262. Needham CJ, Shah SR, Dahlin RL, Kinard LA, Lam J, Watson BM, et al. Osteochondral tissue regeneration through polymeric delivery of DNA encoding for the SOX trio and RUNX2. *Acta Biomater.* 2014;10(10):4103–12.
  263. Erica G. Tierney, Duffy GP, Hibbitts AJ, Cryan S-A, O’Brien FJ. The development of non-viral gene-activated matrices for bone regeneration using polyethyleneimine (PEI) and collagen-based scaffolds. *J Control Release.* 2012;158:304–11.
  264. Wang C, Hou W, Guo X, Li J, Hu T, Qiu M, et al. Two-phase electrospinning to incorporate growth factors loaded chitosan nanoparticles into electrospun fibrous scaffolds for

- bioactivity retention and cartilage regeneration. Vol. 79, *Materials Science and Engineering C*. 2017. p. 507–15.
265. Rajesh Mishra JM. Electrospun Nanofibers. In: *Nanotechnology in Textiles: Theory and Application*. Matthew Deans; 2018. p. 1–389.
  266. Shahriar SMS, Mondal J, Hasan MN, Revuri V, Lee DY, Lee YK. Electrospinning nanofibers for therapeutics delivery. *Nanomaterials*. 2019;9(532):1–32.
  267. Pillay V, Dott C, Choonara YE, Tyagi C, Tomar L, Kumar P, et al. A review of the effect of processing variables on the fabrication of electrospun nanofibers for drug delivery applications. *J Nanomater*. 2013;1–22.
  268. Foox M, Zilberman M. Drug delivery from gelatin-based systems. *Expert Opin Drug Deliv*. 2015;12(9):1547–63.
  269. Choktaweessap N, Arayanarakul K, Aht-Ong D, Meechaisue C, Supaphol P. Electrospun gelatin fibers: Effect of solvent system on morphology and fiber diameters. *Polym J*. 2007;39(6):622–31.
  270. Erencia M, Cano F, Tornero JA, Macanás J, Carrillo F. Preparation of electrospun nanofibers from solutions of different gelatin types using a benign solvent mixture composed of water/PBS/ethanol. *Polym Adv Technol*. 2016;27:382–92.
  271. Echave MC, Hernández-Moya R, Iturriaga L, Pedraz JL, Lakshminarayanan R, Dolatshahi-Pirouz A, et al. Recent advances in gelatin-based therapeutics. *Expert Opin Biol Ther*. 2019;19(8):773–9.
  272. Vázquez N, Sánchez-Arévalo F, MacIel-Cerda A, Garnica-Palafox I, Ontiveros-Tlachi R, Chaires-Rosas C, et al. Influence of the PLGA/gelatin ratio on the physical, chemical and biological properties of electrospun scaffolds for wound dressings. *Biomed Mater*. 2019;14:045006.
  273. Zhang CL, Yu SH. Nanoparticles meet electrospinning: Recent advances and future prospects. *Chem Soc Rev*. 2014;43(13):4423–48.
  274. Chanchal A, Vohra R, Elesela S, Bhushan L, Kumar S, Kumar S, et al. Gelatin Biopolymer: A Journey from Micro to Nano. *J Pharm Res*. 2014;8(10):1387–97.
  275. Janani G, Pillai MM, Selvakumar R, Bhattacharyya A, Sabarinath C. An in vitro 3D model using collagen coated gelatin nanofibers for studying breast cancer metastasis. *Biofabrication*. 2017;9:015016.
  276. Li M, Mondrinos MJ, Chen X, Lelkes PI. Electrospun blends of natural and synthetic polymers as scaffolds for tissue engineering. *Annu Int Conf IEEE Eng Med Biol Soc*. 2005;5858–61.
  277. Cen L, Liu W, Cui L, Zhang W, Cao Y. Collagen tissue engineering: Development of novel biomaterials and applications. *Pediatr Res*. 2008;63(5):492–6.
  278. Nezarati RM, Eifert MB, Cosgriff-hernandez E. Effects of Humidity and Solution Viscosity on Electrospun Fiber Morphology. *Tissue Eng Part C*. 2013;19(10):810–9.
  279. Shih Y-R V., Chen C-N, Tsai S-W, Wang YJ, Lee OK. Growth of Mesenchymal Stem Cells on Electrospun Type I. *Stem Cells*. 2006;24:2391–7.
  280. Saraf A, Baggett LS, Raphael RM, Kasper FK, Mikos AG. Regulated non-viral gene delivery from coaxial electrospun fiber mesh scaffolds. *J Control Release*. 2010;143:95–103.
  281. Saraf A, Baggett LS, Raphael RM, Kasper FK, Mikos AG. Regulated non-viral gene delivery from coaxial electrospun fiber mesh scaffolds. *J Control Release*. 2010;143(1):95–103.

282. Golub EE, Boesze-Battaglia K. The role of alkaline phosphatase in mineralization. *Curr Opin Orthop.* 2007;18:444–8.
283. Bara JJ, Dresing I, Zeiter S, Anton M, Daculsi G, Eglin D, et al. A doxycycline inducible , adenoviral bone morphogenetic protein-2 gene delivery system to bone. *J Tissue Eng Regenwratve Med.* 2018;12(June 2017):106–18.
284. Lin H, Tang Y, Lozito TP, Oyster N, Kang RB, Madalyn R, et al. Projection Stereolithographic Fabrication of BMP-2 Gene- activated Matrix for Bone Tissue Engineering. *Nature:Scientific Reports.* 2017;7(11327):1–11.
285. Müller CW, Hildebrandt K, Gerich T, Krettek C, Griensven M Van, Balmayor ER. BMP-2-transduced human bone marrow stem cells enhance neo-bone formation in a rat critical-sized femur defect. *J Tissue Eng Regen Med.* 2017;11:1122–31.
286. Liu Z, Yuan X, Fernandes G, Dziak R, Ionita CN, Li C, et al. The combination of nano-calcium sulfate / platelet rich plasma gel scaffold with BMP2 gene-modified mesenchymal stem cells promotes bone regeneration in rat critical- sized calvarial defects. *Stem Cell Res Ther.* 2017;8(122):1–9.
287. R M Raftery, Mencía-Castaño I, Sperger S, Chen G, Cavanagh B, Feichtinger GA, et al. Delivery of the improved BMP-2-Advanced plasmid DNA within a gene-activated scaffold accelerates mesenchymal stem cell osteogenesis and critical size defect repair. *J Control Release.* 2018;283:20–31.
288. Sharma S, Sapkota D, Xue Y, Rajthala S, Yassin MA, Finne-wistrand A. Delivery of VEGFA in bone marrow stromal cells seeded in copolymer scaffold enhances angiogenesis , but is inadequate for osteogenesis as compared with the dual delivery of VEGFA and BMP2 in a subcutaneous mouse model. *Stem Cell Res Ther.* 2018;9(23):1–13.
289. Tian K, Qi M, Wang L, Li Z, Xu J, Li Y, et al. Two-stage therapeutic utility of ectopically formed bone tissue in skeletal muscle induced by adeno-associated virus containing bone morphogenetic protein-4 gene. *J Orthop Surg Res.* 2015;10(86):1–5.
290. Chen W, Baylink DJ, Brier-Jones J, Neises A, Kiroyan JB, Rundle CH, et al. PDGFB-based stem cell gene therapy increases bone strength in the mouse. *Proc Natl Acad Sci U S A.* 2015;112(29):E3893–900.
291. Paidikondala M, Kadekar S, Varghese OP. Innovative Strategy for 3D Transfection of Primary Human Stem Cells with BMP-2 Expressing Plasmid DNA : A Clinically Translatable Strategy for Ex Vivo Gene Therapy. *Int J Mol Sci.* 2019;20(56):1–13.
292. Xie Q, Jia L, Xu H, Hu X, Wang W, Jia J. Fabrication of Core-Shell PEI / pBMP2-PLGA Electrospun Scaffold for Gene Delivery to Periodontal Ligament Stem Cells. *Stem Cells Int.* 2016;2016:1–11.
293. McMillan A, Khanh Nguyen M, Gonzalez-Fernandez T, Ge P, Yu X, L.Murphy W, et al. Dual non-viral gene delivery from microparticles within 3D high-density stem cell constructs for enhanced bone tissue engineering. *Biomaterilas.* 2018;161:240–55.
294. Gonzalez-fernandez T, Tierney EG, Cunniffe GM, O'Brien FJ, Kelly DJ. Gene Delivery of TGF-  $\beta$ 3 and BMP2 in an MSC-Laden Alginate Hydrogel for Articular Cartilage and Endochondral Bone Tissue Engineering. *Tissue Eng Part A.* 2016;22(9–10):776–87.
295. T. Gonzalez-Fernandez B. S, Hobbs C, Cunniffe G., McCarthy H., Dunne N., Nicolosi V, et al. Mesenchymal stem cell fate following non-viral gene transfection strongly depends on the choice of delivery vector. *Acta Biomater.* 2017;55:226–38.
296. Attia N, Mashal M, Grijalvo S, Eritja R, Zarate J, Puras G, et al. Stem cell-based gene delivery mediated by cationic niosomes for bone regeneration. *Nanomedicine*

- Nanotechnology, *Biol Med.* 2018;14:521–31.
297. Mello SD, Elangovan S, Salem AK. FGF2 gene activated matrices promote proliferation of bone marrow stromal cells. *Arch Oral Biol.* 2015;60(12):1742–9.
  298. Kolk A, Tischer T, Koch C, Vogt S, Haller B, Smeets R, et al. A novel nonviral gene delivery tool of BMP-2 for the reconstitution of critical-size bone defects in rats. *Biomed Mater Res A.* 2016;104A(10):2441–55.
  299. Kim T, Singh RK, Kang MS, Kim J, Kim H. Gene delivery nanocarriers of bioactive glass with unique potential to load BMP2 plasmid DNA and to internalize into mesenchymal stem cells for osteogenesis and bone regeneration. *R Soc Chem.* 2016;8:8300–11.
  300. Hsiao H-Y, Yang S-R, Brey EM, Chu I-M, Cheng M-H. Hydrogel Delivery of Mesenchymal Stem Cell-Expressing Bone Morphogenetic Protein-2 Enhances Bone Defect Repair. *PRS Global Open.* 2016;4(8):1–7.
  301. Oh SH, Byun J, Chun SY, Jang Y, Lee H, J-ho B, et al. Plasmid DNA-loaded asymmetrically porous membrane for guided bone regeneration. *Mater Sci Technol.* 2020;
  302. Kuttappan S, A.Anitha, M.G.Minsha, M.Menon P, T.B.Sivanarayanan, Vijayachandran LS, et al. BMP2 expressing genetically engineered mesenchymal stem cells on composite fibrous scaffolds for enhanced bone regeneration in segmental defects. *Mater Sci Eng C.* 2018;85:239–48.
  303. Hsieh M-K, Chia-Junghun W, Chen C-C, Tsai T-T, Niu C-C, Wu S-C, et al. BMP-2 gene transfection of bone marrow stromal cells to induce osteoblastic differentiation in a rat calvarial defect model. *Mater Sci Eng C Mater Biol Appl.* 2018;91:806–16.
  304. Li J, Lin J, Yu W, Song X, Hu Q, Xu J-H, et al. BMP-2 plasmid DNA-loaded chitosan films - A new strategy for bone engineering. *J Cranio-Maxillo-Facial Surg.* 2017;45:2084–91.
  305. Komatsu K, Shibata T, Shimada A, Ideno H, Nakashima K, Tabata Y, et al. Cationized gelatin hydrogels mixed with plasmid DNA induce stronger and more sustained gene expression than atelocollagen at calvarial bone defects in vivo induce stronger and more sustained gene expression than. *J Biomater Sci Polym Ed.* 2016;27(5):419–30.
  306. Loozen LD, Helm YJM Van Der, Dhert WJA, Kruyt MC, Alblas J. Bone Morphogenetic Protein-2 Nonviral Gene Therapy in a Goat Iliac Crest Model for Bone Formation. *Tissue Eng Part A.* 2015;21(9):1672–9.
  307. Qiao C, Zhang K, Sun B, Liu J, Song J, Hu Y, et al. Sustained release poly ( lactic-co-glycolic acid ) microspheres of bone morphogenetic protein 2 plasmid / calcium phosphate to promote in vitro bone formation and in vivo ectopic osteogenesis. *Am J Transl Res.* 2015;7(12):2561–72.
  308. Croes M, Oner CF, Dhert WJA, Alblas J. BMP-2 gene delivery in cell-loaded and cell- free constructs for bone regeneration. *PLoS One.* 2019;1–16.
  309. Curtin CM, Tierney EG, Mcsorley K, Cryan S, Duffy GP, Brien FJO. Combinatorial Gene Therapy Accelerates Bone Regeneration : Non-Viral Dual Delivery of VEGF and BMP2 in a Collagen-Nanohydroxyapatite Scaffold. *Adv Healthc Mater.* 2015;4:223–7.
  310. Kolk A, Boskov M, Haidari S, Tischer T, Griensven M Van, Bissinger O, et al. Comparative analysis of bone regeneration behavior using recombinant human BMP-2 versus plasmid DNA of BMP-2. *J Biomed Mater Res Part A.* 2018;107A(1):163–73.
  311. Cunniffe GM, Gonzalez-Fernandez T, Daly A, Sathy BN, Jeon O, Alsberg E, et al. Three-Dimensional Bioprinting of Polycaprolactone Reinforced Gene Activated Bioinks for Bone Tissue Engineering. *Tissue Eng Part A.* 2017;23(17–18):891–900.
  312. Plonka AB, Khorsand B, Yu N, Sugai J V, Salem AK, Giannobile W V, et al. Effect of

- sustained PDGF nonviral gene delivery on repair of tooth-supporting bone defects. *Gene Ther.* 2017;24:31–9.
313. Zamani M, Prabhakaran MP, Ramakrishna S. Advances in drug delivery via electrospun and electrosprayed nanomaterials. *Int J Nanomedicine.* 2013;8:2997–3017.
  314. Raftery RM, Tierney EG, Curtin CM, Cryan SA, O'Brien FJ. Development of a gene-activated scaffold platform for tissue engineering applications using chitosan-pDNA nanoparticles on collagen-based scaffolds. *J Control Release.* 2015;210:84–94.
  315. Su X, Liao L, Shuai Y, Jing H, Liu S, Zhou H, et al. MiR-26a functions oppositely in osteogenic differentiation of BMSCs and ADSCs depending on distinct activation and roles of Wnt and BMP signaling pathway. *Cell Death Dis.* 2015;6:1–12.
  316. Wang Z, Zhang D, Hu Z, Cheng J, Zhuo C, Fang X, et al. MicroRNA-26a-modified adipose-derived stem cells incorporated with a porous hydroxyapatite scaffold improve the repair of bone defects. *Mol Med Rep.* 2015;12:3345–50.
  317. Li K, Lo S, Sung L, Liao Y, Chang Y, Hu Y. Improved calvarial bone repair by hASCs engineered with Cre / loxP-based baculovirus conferring prolonged BMP-2 and MiR-148b co-expression. *J Tissue Eng Regen Med.* 2017;11:3068–77.
  318. Elangovan S, Khorsand B, Do A, Hong L, Kormann M, Ross RD, et al. Chemically Modified RNA Activated Matrices Enhance Bone Regeneration. *J Control Release.* 2015;22–8.
  319. Behnoush Khorsand SE, Hong L, Dewerth A, Kormann M, Salem AK. A comparative study of the bone regenerative effect of chemically modified RNA encoding BMP-2 or BMP-9. *AAPS J.* 2017;19(2):438–46.

# Appendix

## Supplementary information for Chapter 3

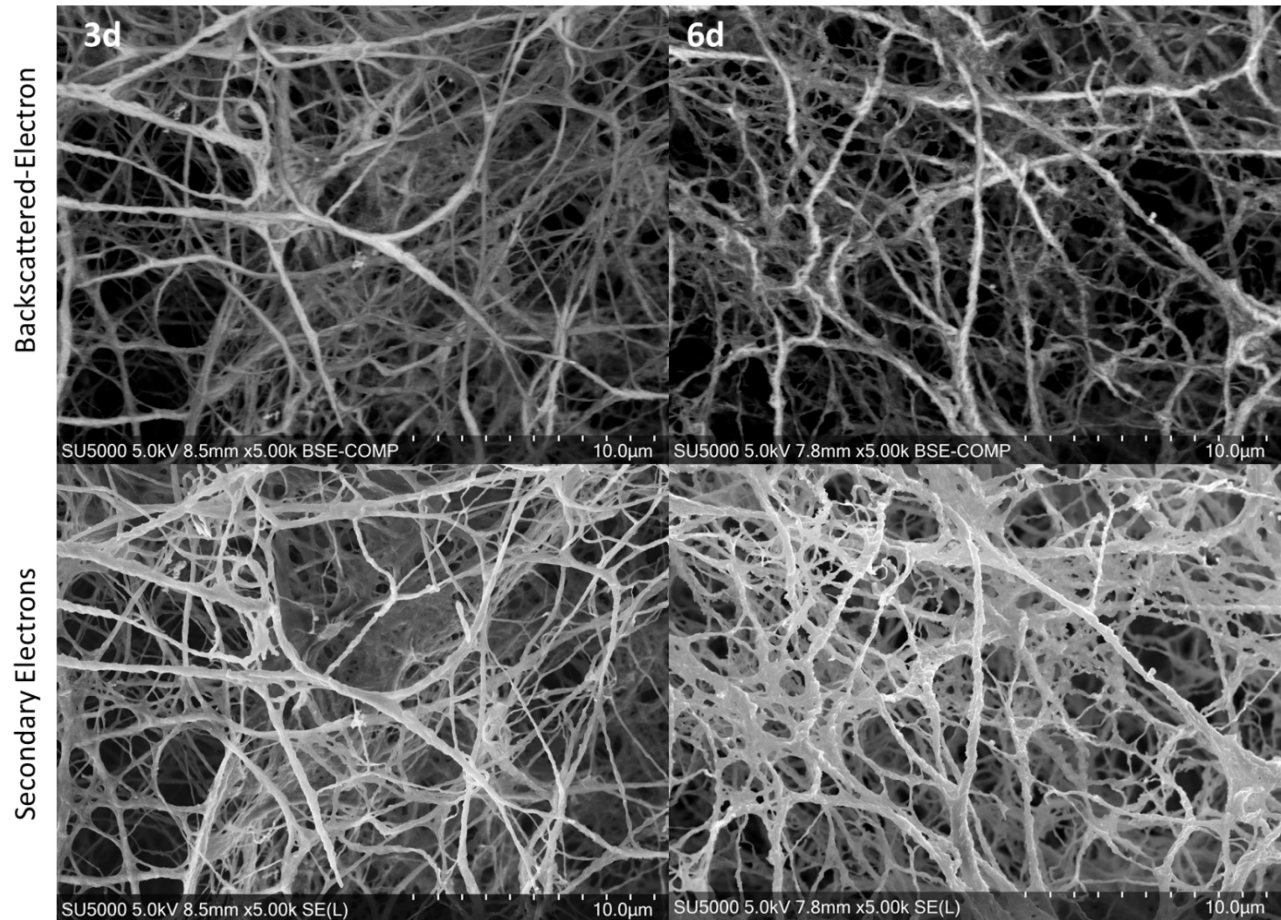
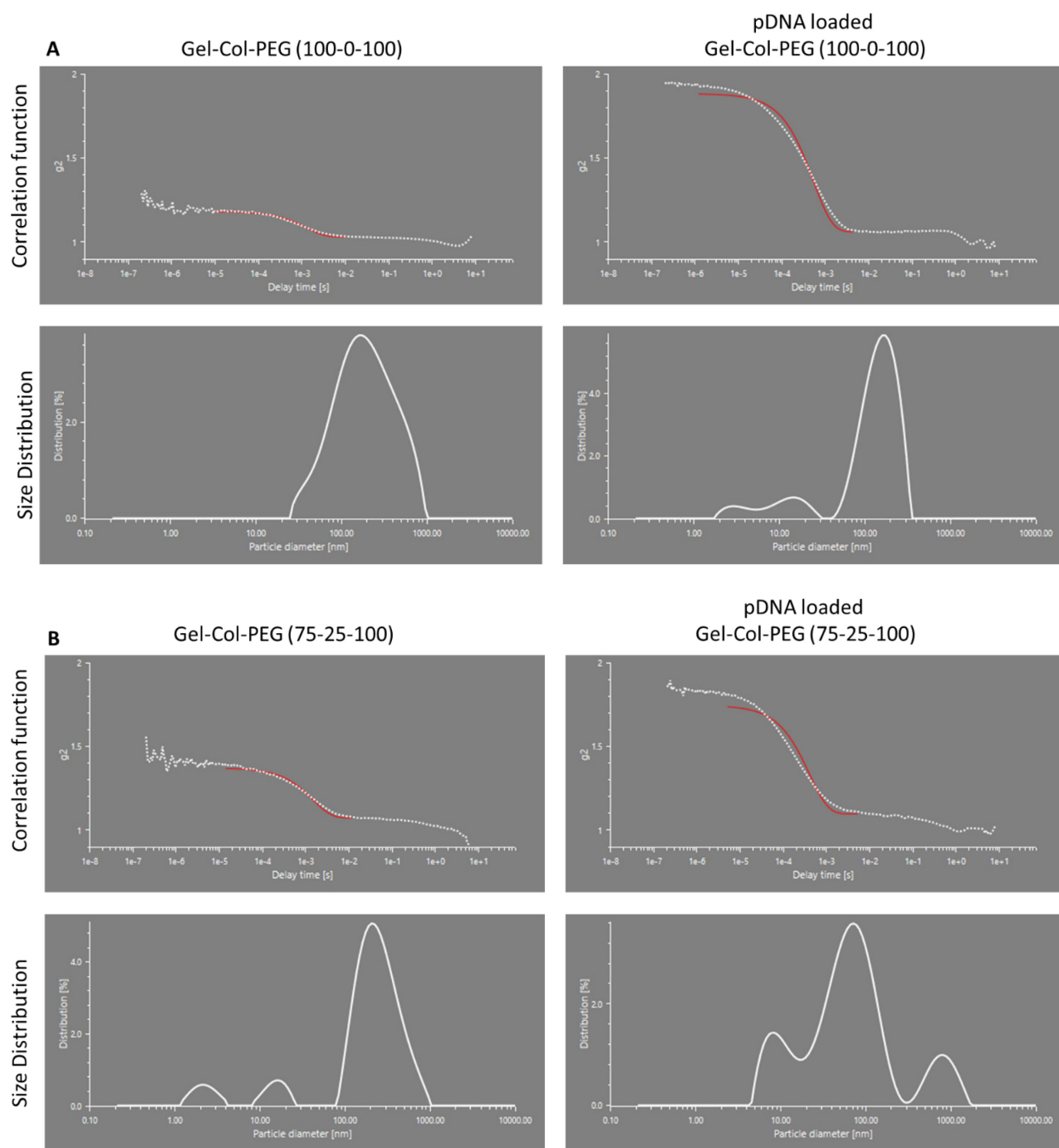
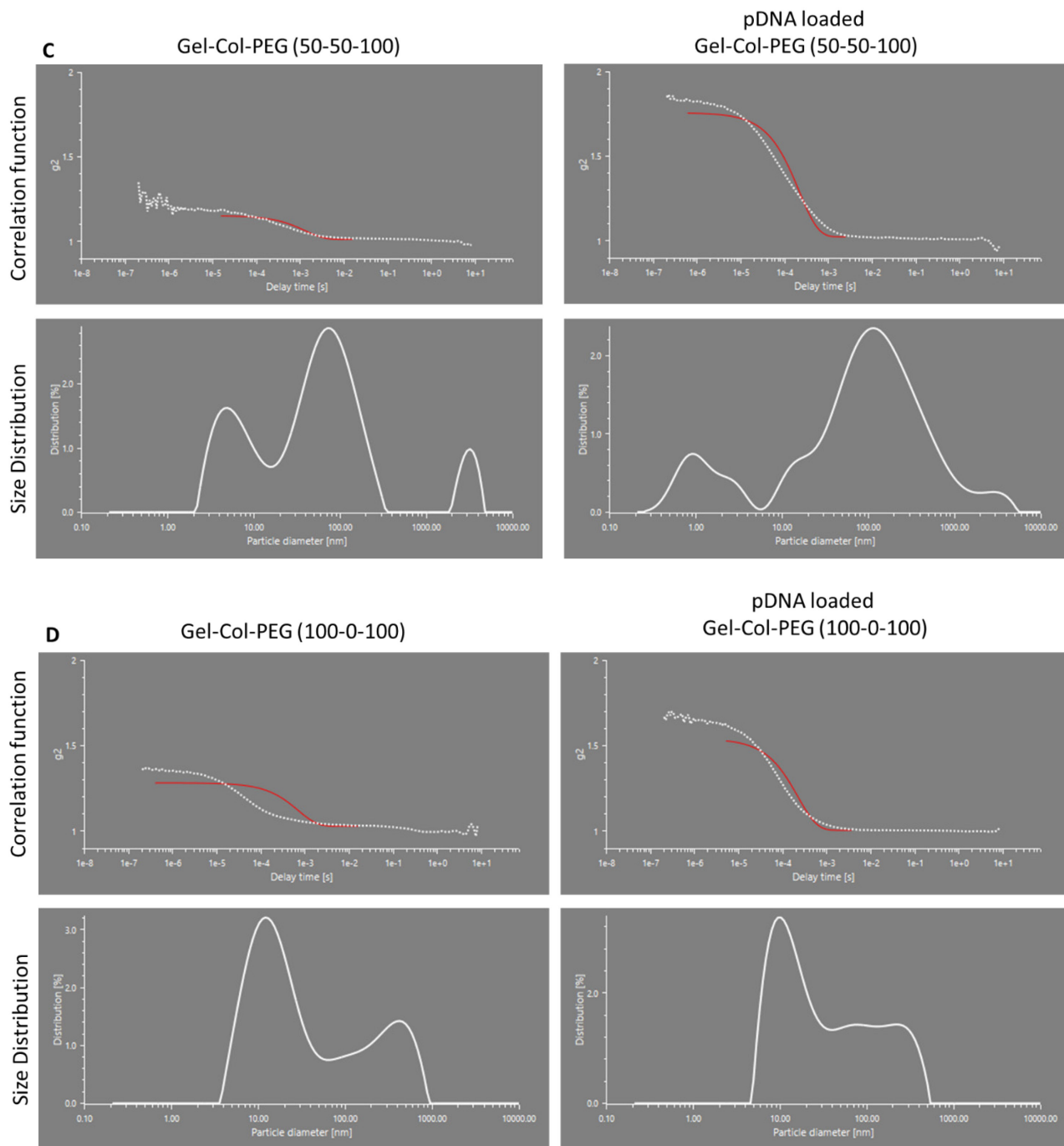


Figure 3.S 1. SEM images of 3 days and 6 days intrafibrillar mineralized scaffolds.

## Supplementary information for Chapter 4





**Figure 4.S 2. Correlation function and size distribution of particles released from different volume ratio Gel-Col-PEG mats (A-D) in comparison to mats without particles**

## Supplementary information for Chapter 5

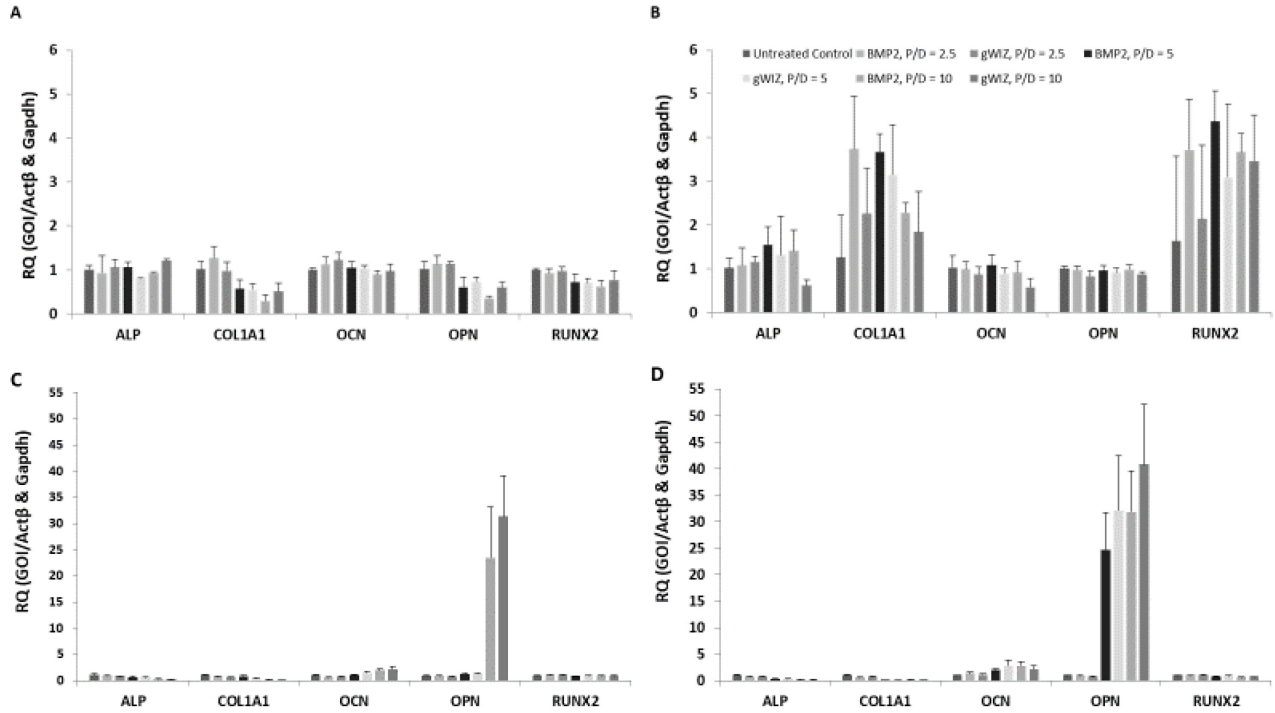


**Figure 5.S 1.** The expression levels of osteogenic genes in MC-3T3 and hBMSCs were analyzed by PCR.

The expression was measured on week 1 (A) and week 2 (B) for MC-3T3 and week 1 (C) and week 2 (D) for hBMSCs. The complexes delivered 0.25  $\mu\text{g/ml}$  pBMP-2 and pgWIZ, Pol:DNA ratio 2.5, 5 and 1 and pASP:DNA 1 to the cells.

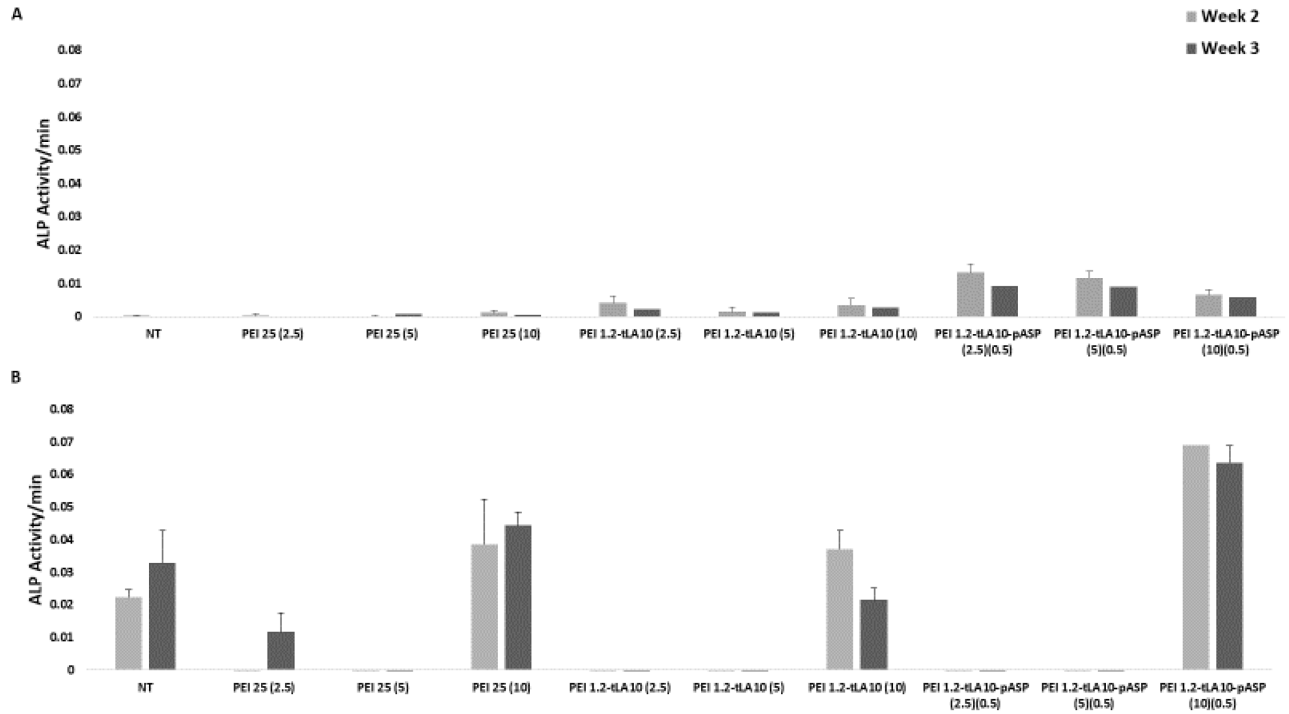


**Figure 5.S 2. ‘Net’ ALP induction in MC-3T3 (A) and hBMSCs (B) cells after delivery of gWIZ and gWIZ-BMP-2 complexes.**

The pDNA concentrations in cell culture was 0.25 (C)  $\mu\text{g}/\text{mL}$ . The ALP activity was measured 30 min after the addition of the substrate on 2- and 3-weeks post-transfection. ‘Net’ ALP activity was calculated by subtracting ALP activity obtained from pBMP-2 treated cells from that of gWIZ-treated cells.